



HAL
open science

Dissecting the role of the homeoprotein engrailed and line elements in the physiopathology of midbrain dopaminergic neurons

Eugénie Pezé-Heidsieck

► **To cite this version:**

Eugénie Pezé-Heidsieck. Dissecting the role of the homeoprotein engrailed and line elements in the physiopathology of midbrain dopaminergic neurons. *Neurons and Cognition [q-bio.NC]*. Sorbonne Université, 2019. English. NNT : 2019SORUS308 . tel-03348739

HAL Id: tel-03348739

<https://theses.hal.science/tel-03348739>

Submitted on 20 Sep 2021

HAL is a multi-disciplinary open access archive for the deposit and dissemination of scientific research documents, whether they are published or not. The documents may come from teaching and research institutions in France or abroad, or from public or private research centers.

L'archive ouverte pluridisciplinaire **HAL**, est destinée au dépôt et à la diffusion de documents scientifiques de niveau recherche, publiés ou non, émanant des établissements d'enseignement et de recherche français ou étrangers, des laboratoires publics ou privés.

Sorbonne Université

ECOLE DOCTORALE CERVEAU-COGNITION-COMPORTEMENT

CIRB – Collège de France / Équipe Alain Prochiantz

**DISSECTING THE ROLE OF THE HOMEOPROTEIN
ENGRAILED AND LINE ELEMENTS IN THE
PHYSIOPATHOLOGY OF MIDBRAIN DOPAMINERGIC
NEURONS**

Par Eugénie PEZÉ-HEIDSIECK

Thèse de Doctorat de Biologie

Dirigée par Alain PROCHIANTZ

Présentée et soutenue publiquement le 18 septembre 2019

Devant un jury composé de :

Pr Alain TREMBLEAU

Pr Didier TRONO

Dr Andrea WIZENMANN

Pr Wolfgang WURST

Dr Pascale LESAGE

Dr Julia FUCHS

Pr Alain PROCHIANTZ

Président

Rapporteur

Rapporteuse

Examineur

Examinatrice

Examinatrice

Directeur de Thèse

*“ On n’a pas deux cœurs, un pour les animaux et un pour les humains. On a un
Cœur ou on n’en a pas.”*

Lamartine

A notre planète qui brûle

REMERCIEMENTS

Je tiens à remercier mon entourage pour son aide et soutien au cours de ces trois dernières années et plus précisément :

Les membres du jury pour leur implication dans l'examen de mon travail de Thèse et plus particulièrement les rapporteurs, Didier Trono et Andrea Wizenmann pour m'avoir accordé leur temps pour la relecture et la correction de mon manuscrit.

Alain, tu m'as accueillie dans un contexte difficile et je t'en resterai toujours reconnaissante. Toujours disponible, à l'écoute, je ne connais aucun autre directeur de thèse qui accorde autant de temps pour échanger avec ses étudiants, et cela, en dépit de toutes tes responsabilités par ailleurs. Tu as toujours été là, sans faille, pendant trois ans, pour transmettre ton excellence scientifique, tes conseils et je t'en remercie infiniment. Si je suis bien armée pour la suite, c'est grâce à toi !

Je souhaite remercier Michael Shelanski qui m'a ouvert les portes du monde des neurosciences, qui m'a aiguillée, donné des conseils comme un mentor et grâce à qui j'ai rencontré Alain en catastrophe : MERCI ! Meilleur transfert (paracrine celui-là !) à ce jour.

Je n'aurais pas pu travailler autant en douceur au cours de ces trois ans sans la gentillesse, la patience et l'accompagnement scientifique de Julia. Je sais que le projet que tu développes est passionnant et que tu le porteras au mieux avec ta jeune équipe. Je te souhaite tout le succès que tu mérites : à toi les plus beaux articles !

Olivia, tu es pour nous tous, jeunes thésards, comme une deuxième maman, un puit sans fond de connaissances et de techniques. Tu as bien sûr énormément contribué aux travaux de cette thèse, à chacune de nos questions tu as toujours la réponse ! Par ailleurs, que la logistique du laboratoire Prochiantz roule si bien, est en grande partie grâce à toi.

Rajou, je tiens à te remercier pour tes mails presque quotidiens de veille bibliographique et la transmission de ta curiosité scientifique.

Enfin, les autres membres PD (huhu Julia c'est pour toi) passés et en cours : FX et Hocine qui m'ont formée – Hocine tu m'as même psychanalysée au CROUS de nombreuses fois -- Mélanie, on a commencé presque en même temps et c'était de super mois à travailler ensemble, ta force de caractère argentine bien trempée et ton entrain insufflent un esprit dynamique au labo, Camille pour ta motivation à boire des verres tous ensemble, Marguerite merci pour ta fraîcheur tout juste arrivée : à toi la relève !

Jess, tu auras été là du début à la fin de ma thèse et nous avons fait tant de choses ensemble. Notamment, tu m'as suivie dans quelques uns de mes plans foireux, activités sportives et ce toujours avec une gentillesse inégalable. Nous nous sommes, plus particulièrement serrées les coudes tous ces derniers mois à rédiger ensemble, je suis tellement heureuse que tu aies été là, cela aurait été bien plus difficile sans toi. Ne nous perdons pas de vue par la suite !

Les autres jeunes du labo Prochiantz: Clémentine (pour nos apéros au Chat Ivre), Damien (pour ta capacité à boire de l'eau), Hadhémi (tu t'es entraînée avec nous avant de devenir réellement maman), Rachel (pour nos débats parfois enflammés et dont on rigole bien maintenant), Vanessa (pour ta détermination sans faille), Angélique (courage ce n'est que le début!), Javier (ta sagesse de post-doc nous fait tant de bien), Bilal (avec ta chaise pour mon maillot de bain – huhu je blague), Stéphanie puis naturellement les moins jeunes du laboratoire Prochiantz : Yoko (fidèle voisine de bureau avec tes bonbons en intraveineuse – pour info tout le monde t'en pique et je sais qui sont les plus gros mangeurs, si tu veux je peux cafter !) Ken, Ariel, Navy, Chantal, Pat, Vincent (dont l'aide au quotidien est tellement précieuse). Une petite mention spéciale pour Francine qui nous décharge de l'administratif ☺. Enfin tous les membres de l'Equipe Joliot Vriz, Ed, Jojo, Michel, Sophie, Marion.

Irène, tu as été ma copine du 2ème étage, petit refuge au calme, promis, je ne dirai à personne que tu as une bonne descente bien décoiffante après le labo chez Bon Vivant ainsi qu'au Cod House ! Soutien constant, scientifique mais aussi culturel, j'ai eu tant de chance de t'avoir juste là au dessus de moi pour veiller sur moi. Sans oublier nos pyjamas parties.... <3

Merci à tout le CIRB en général, spécialement la Gestion, les Animaliers (Maya MERCI MERCI MERCI) ainsi que la Plateforme d'Imagerie (Philippe pour les conseils de macro, Julien et Estelle pour le TIRF ainsi que Tristan qui pilote le tout). Anahi, merci pour ta sagesse d'ancienne qui me guide et qui m'aide à prendre confiance en moi pour me lancer !

Je souhaite remercier ma famille : Marguerite avec qui j'ai habité pendant tout le début de ma thèse, tu m'as souvent nourrie, Colombe grâce à qui j'ai pu voyager et m'aérer (Palestine, Maroc...), Hector parce que tu ajoutes toujours un peu de remue-ménage rigolo dans la famille, les parents qui même partis si loin depuis 8 ans prennent soin de nous et veillent au grain. Merci d'avoir supporté ma mauvaise humeur parfois PEZante.

J'aimerais aussi remercier le sport comme soutien moral ou plutôt les compagnons de chocs associés : Yoyo de t'être extirpé du lit de si bonne heure pour nager dans l'eau froide et faire nos 5 km nage (désormais Irène), Hocine pour la course à pied et nos 20km de Paris ainsi que le triathlon (relève par David), le conservatoire de danse avec Marie puis nos innombrables verres qui suivent en général jusqu'à un peu trop tard et enfin, la salle de muscu de l'ENS avec tous les jeunes Prochiantz. Stefan, j'ai hâte qu'on s'y mette ensemble et ton soutien à distance m'a tellement tirée vers le haut.

A tous mes amis qui m'ont aidée de près ou de loin avec nos conversations absurdes : Conversations de filles (mention pour Pauline qui a lu mon intro), surfeuses revival, Blanche Neige et les 7 nains, Mariage Tania, SL Diner, Tinder Surprise, Roscoff, Panam' et Bourg, Danseuses, Clé Finder, et puis enfin, les singletons : Solenne, BA, JoJo, Kraj.

Antoine, je ne trouverai pas les mots pour te remercier d'être la quotidiennement à mes côtés et de me donner ton amour, si vital quand je ne vois pas le bout.

Table of Contents

REMERCIEMENTS	iii
Table of Contents	v
Abstract	ix
Table of Figures	xi
Table of Abbreviations	xiii

INTRODUCTION

Chapter I: Functions and Transfer of Homeoproteins	3
I.1 The discovery of homeoproteins in <i>Drosophila</i>	3
I.2 Homeoproteins control Brain Morphogenesis	4
I.3 Focus on ENGRAILED Homeoprotein	6
I.3.a ENGRAILED: a repressive transcription factor.....	6
I.3.b Role of <i>Engrailed</i> during development	6
I.3.c Expression of ENGRAILED in the adult midbrain	7
I.3.d mDA neurons and Parkinson disease.....	9
I.3.e ENGRAILED protects mDA neurons in Parkinson Disease models	10
I.4. Homeoproteins can transfer between cells through unconventional pathways	13
I.4.a Discovery and mechanism.....	13
I.4.b The difficulty to distinguish cell autonomous from non-cell autonomous functions	15
I.4.c Non-cell autonomous functions of PAX6 and OTX2	16
I.4.d Non-cell autonomous functions of ENGRAILED	19
Working Hypothesis of Chapter I:.....	23
Chapter II: From Engrailed protective abilities to transposable elements	25
II.1 ENGRAILED protects mDA neurons against oxidative stress through the reduction of DNA strand breaks and heterochromatin maintenance	25
II.1.a. Oxidative stress, genomic instability and epigenetic alteration in Parkinson Disease and aging 25	
II.1.b ENGRAILED guarantees proper heterochromatin maintenance and reduces DSBs	27
II.2 Transposable elements: purely “parasitic” elements alive in our genome?	28
II.2.a. Discovery and classification of transposable elements (TEs)	28
II.2.b. The structure of L1 elements and Life Cycle	30
II. 3 Dynamics of L1 elements in the genome.....	32
II.3.a L1: a potential genomic threat.....	32

II.3.b The Genome’s defence tactics	32
II. 3 L1 elements in the CNS or age related diseases	34
II. 4 L1 elements: regulatory roles and evolutionary co-option?	36
Working Hypothesis Chapter II:	41

RESULTS

Non-cell autonomous ENGRAILED regulates dendritic growth and maintenance	45
Introduction	47
Results	48
Non-cell autonomous ENGRAILED regulates dendrite maintenance and survival of mDA neurons <i>in vivo</i> and dendritic growth in midbrain primary culture <i>in vitro</i>	48
Discussion	53
Materials and Methods	55
Supplementary material	57
ENGRAILED homeoprotein blocks degeneration in adult dopaminergic neurons through LINE-1 repression	61
Exploring the physiological significance of L1 expression	85
Introduction	85
Results	87
fL1 are enriched in Long Genes	87
Down regulation of L1 expression impacts gene expression and respective protein levels	91
Mapping the L1 protein interactome in neurons	94
SFPQ, an RNA-binding protein implicated in long gene transcription, potentially interacts with ORF1p	96
Plan of action to ascertain current preliminary results	98
Materials and Methods	99
Supplementary material	101

DISCUSSION

Part I: ENGRAILED, a multi-faceted protein, more than just a transcription factor during development.....	105
What are the direct targets of ENGRAILED following internalisation?	105
Does Non-cell autonomous ENGRAILED regulate dendritic maintenance via physiological eustress?	106
ENGRAILED as a potential therapeutic protein for Parkinson disease.....	109
Non-cell autonomous ENGRAILED signalling: questions on regulation and specificity	111
Part II: Overactive L1 elements: drivers of neurological disorders?	113
L1 elements in the brain: false positives or real physiological phenomenon	113
L1 expression: drivers of local inflammation	114
Reverse transcriptase inhibitors as potential medication?.....	117
Part III: Physiological roles of L1	119
What are the different levels of regulation by TE elements?	119
Physiological role of L1 elements: breaking the strand to better transcribe?	121
How do L1 elements regulate specific genes?	123
How did fL1 elements get enriched in long genes?	124
On neural diversity and somatic mosaicism: Darwinian selection at the cell population level?	126
L1 elements: environmental and stress sensors for adaptive response?	127
General Conclusion:.....	128
References	131

Abstract

ENGRAILED homeoprotein controls the development of ventral midbrain dopaminergic (mDA) neurons and, in the adult, remains expressed assuring their survival. In Parkinson disease (PD), it is these mDA neurons that degenerate. Their loss is responsible for the classical motor symptoms due to reduced levels of the neurotransmitter dopamine.

We first questioned the importance of the transfer of ENGRAILED from cell to cell. We demonstrated that blocking the transfer of ENGRAILED reduces dendritic length and induced the death of mDA neurons. This and other data from the lab in PD models suggest a potential use of ENGRAILED in the therapy for PD. Indeed, in an oxidative stress context, mDA neurons of the *substantia nigra* exhibit an increased number of DNA strand breaks, changes in nuclear and nucleolar heterochromatin marks and abnormally high expression of repressed genes, in particular LINE-1 (L1) retrotransposons. L1 elements are repeated elements distributed within the genome and were long thought to be entirely repressed as they represent a threat to genome integrity. Indeed, they “move” throughout the genome using a “copy-paste” mechanism and in doing so, they induce breaks in the DNA. We have shown that an injection of recombinant ENGRAILED can revert the altered heterochromatin marks and repress L1 elements, rescuing the neurons from cell death following an acute oxidative stress. We then pursued further investigations in order to better understand by which mechanisms ENGRAILED exerts its protective activity. Our studies, published in EMBO Journal, demonstrate that L1 inhibition, through three distinct means (i) an siRNA approach (ii) stavudine, a reverse transcriptase inhibitor (iii) a viral gain of function of the PIWI protein, a repressor of L1 elements, is protective in a PD mouse model and in an acute oxidative stress condition.

As L1 are expressed at basal level in adult neurons, we are now currently exploring its potential physiological role. We propose a threshold model in which L1 may participate to normal neuronal function until a certain expression threshold which, when reached, will damage the cell by DNA breaks. In order to test this, we are using the described anti-L1 strategies and assessing expression of important neuronal genes. We are also identifying molecular partners of L1 elements in dopaminergic neurons to decipher the mechanisms by which it could regulate gene expression. This will provide very original and new insights on physiological roles of evolutionary conserved and long considered “parasitic” sequences in adult neurons.

Table of Figures

FIGURE 1: HOX GENE EXPRESSION IN THE DROSOPHILA ALONG THE ANTERIOR-POSTERIOR BODY AXIS CORRESPONDS TO THEIR 3'-5' ORDER IN THE GENOME ALONG THE ANTERO-POSTERIOR AXIS. TAKEN FROM GILBERT ET AL,1990.	3
FIGURE 2: SCHEMATIC DRAWING OF THE ANTENNAPEDIA HOMEODOMAIN-DNA COMPLEX. TAKEN FROM GEHRING ET AL.,1994	4
FIGURE 3: EXAMPLES OF BOUNDARIES DEFINED BY THE EXPRESSION OF ABUTTING HOMEOPROTEINS WITH SELF-ACTIVATING AND RECIPROCAL INHIBITORY PROPERTIES. TAKEN FROM PROCHIANTZ AND DI NARDO, 2015.	5
FIGURE 4: SUMMARY OF INTRINSIC GENETIC MECHANISMS OF AREA PATTERNING AND MUTANT PHENOTYPES. TAKEN FROM O'LEARY ET AL., 2007	6
FIGURE 5: EXPRESSION (PINK) OF ENGRAILED IN THE ADULT. TAKEN FROM PROCHIANTZ ET DI NARDO 2015.	7
FIGURE 6: DETECTION OF EN1 MRNA IN DENDRITES (ARROWS) OF MDA NEURONS IN THE SNPC. TAKEN FROM DI NARDO ET AL., 2007	8
FIGURE 7: THE DOPAMINERGIC SYSTEM. TAKEN FROM MONEY AND STANWOOD, 2013	8
FIGURE 8: THE MAIN IDENTIFIED MECHANISM OF DEGENERATION. TAKEN FROM DAUER AND PRSEDBORSKI, 2003.	10
FIGURE 9: EN1+/- MICE EXHIBIT A LOSS OF DOPAMINERGIC NEURONS. TAKEN FROM SONNIER ET AL., 2007	11
FIGURE 10: EN1+/- MICE EXHIBIT MOTOR AND NON-MOTOR SYMPTOMS CHARACTERISTIC OF PARKINSON'S DISEASE. RESULTS EXTRACTED FROM SONNIER ET AL., 2007	11
FIGURE 11: ENGRAILED PROTECTS FROM MPTP AND ROTENONE BY INCREASING NDUFS1/3 TRANSLATION. TAKEN FROM SANDERS AND GREENAMEYRE, 2011.	12
FIGURE 12: TOP) HOMEOPROTEINS DOMAINS AND ASSOCIATED FUNCTIONS. TAKEN FORM PROCHIANTZ ET DI NARDO 2015 BOTTOM) ALIGNMENT OF HDS FOR 10 HP VERIFIED FOR INTERCELLULAR TRANSPORT. THE HELICES ARE INDICATED BY BOLD DARK LINES. OF NOTE, INTERNALIZATION AND SECRETION SEQUENCES CONTAIN HYDROPHOBIC AND BASIC RESIDUES CHARACTERISTIC OF NUCLEAR IMPORT AND EXPORT SEQUENCES.	14
FIGURE 13: THE SCFV STRATEGY WITH OTX2 AND THE REOPENING OF VISUAL PLASTICITY IN THE ADULT (ON AGAIN).	16
FIGURE 14: EYE MORPHOLOGY OF THE ZEBRAFISH IN LESAFFRE ET AL, 2007.	17
FIGURE 15: STUDIES OF NON-CELL AUTONOMOUS FUNCTIONS OF HOMEOPROTEINS.	18
FIGURE 16: TEMPORAL AXONS ARE REPELLED BY EN2 (BLUE GRADIENT) WHILE NASAL AXONS ARE ATTRACTED. TAKEN FROM BRUNET ET AL, 2005	19
FIGURE 17: EN SIGNALLING AT THE GROWTH CONE. EN IS INTERNALIZED BY THE GROWTH CONE. WITHIN THE GROWTH CONE IT STIMULATES THE TRANSLATION OF NDUFS3, A COMPLEX I MITOCHONDRIA PROTEIN. THIS ACTIVATES ATP SYNTHESIS, WHICH IS EXTERNALIZED INTO THE EXTRACELLULAR MATRIX	

HYDROLYSED TO ADENOSINE. ADENOSINE ACTIVATES THE A1R RECEPTOR, WHICH ACTS SYNERGISTICALLY WITH EPHRINA5SIGNALLING PERHAPS VIA ADENYLATE CYCLASE TO CAUSE GROWTH CONE COLLAPSE AND ARREST. TAKEN FROM WIZENMANN ET AL., 2015	21
FIGURE 18: THE SCFV AB TOOL TO BLOCK ENGRAILED'S TRANSFER.	23
FIGURE 19: INJECTION OF ENGRAILED PROTECTS MDA NEURONS (TH+) FROM DEGENERATION IN 6-OHDA MODEL. TAKEN FROM REKAIK ET AL., 2015.	27
FIGURE 20: 6-OHDA INJECTION INDUCES DSBS (STAINED BY γ -H2AX -RED) AND ALTERED H3K27ME3 STAINING (CYAN) - TOP PANNEL - THAT ARE REVERSED FOLLOWING ENGRAILED INJECTION - BOTTOM PANNEL- TAKEN FROM REKAIK ET AL., 2015.	28
FIGURE 21 : THE COMPOSITION OF THE HUMAN GENOME. L1 ELEMENTS REPRESENT AROUND 21% OF THE GENOME.	29
FIGURE 22: TRANSPOSABLE ELEMENTS FAMILIES. TAKEN FROM BECK ET AL., 2001	30
FIGURE 23 : STRUCTURE OF L1 ELEMENTS	30
FIGURE 24 : LIFE CYCLE OF L1 ELEMENTS IN THE CELL	31
FIGURE 25: PIWI REPRESS TE ELEMENTS THROUGH HETEROCHROMATINIZATION AND PIRNA INTERFERENCE.	33
FIGURE 26: MODEL FOR SIRT6-MEDIATED AGE-RELATED ACTIVATION OF L1 EXPRESSION. TAKEN FROM VAN METER ET AL., 2014	36
FIGURE 27: GRAPHICAL ABSTRACT FROM PERCHARDE ET AL. (2018) DEPICTING THE IMPORTANCE OF L1 ELEMENTS IN ESC IDENTITY.	38
FIGURE 28: ENGRAILED INDUCES FILOPODIA DEPENDANT OF ROS INCREASE. FROM AMBLARD ET AL., IN PREP	108
FIGURE 29: ENGRAILED MULTI-MODAL PROTECTIVE ACTIVITY IN MDA NEURONS. TAKEN FROM DI NARDO ET AL., 2018.	109
FIGURE 30: L1 EXPRESSION IS A DRIVER OF INFLAMMATION IN ASTROCYTES INDUCING IFN RESPONSE AND NEURONAL DEGENERATION. TAKEN FROM THOMAS ET AL., 2017	116
FIGURE 31: DNA SUPERCOILING ALONG TRANSCRIPTION. TAKEN FROM DORMAN ET AL., 2016	121
FIGURE 32: MAKING BREAKS TO INDUCE TRANSCRIPTION. TAKEN FROM MADABHUSHI ET AL, 2015	122
FIGURE 33: SFPQ REGULATES LONG GENE EXPRESSION. TAKEN FROM TAKEUCHI ET AL, 2018.	123

Table of Abbreviations

A-T	Ataxia telangiectasia
ATM	Ataxia telangiectasia mutated protein
AD	Alzheimer disease
AGS	Aicardi-Goutieres syndrome
ALS	Amyotrophic lateral sclerosis
ASD	Autism spectrum disorder
ASO	Antisense oligonucleotides
AUB	Aubergine protein
Cb	Cerebellum
dbGaP	Database of Genotypes and Phenotypes
DMB	Diencephalic-mesencephalic boundary
DSB	DNA double strand breaks
DG	Dentate gyrus
DIV	Day in vitro
ECM	Extracellular matrix
En	Engrailed
ERVs	Endogenous retrovirus
ESC	Embryonic stem cells
FIL1	Full length LINE-1
FTLD	Fronto-temporal dementia
GO	Gene ontology
HD	Homeodomain
HP	Homeoprotein
IC	Inferior colliculus
IFN	Interferon
KRAP-ZFPs	Krüppel associated box containing zinc finger proteins
L1	Line-1
mDA	Mesencephalic dopaminergic
MHB	Midbrain-hindbrain boundary
MS	Mass spectrometry
NOX	NADPH oxidases
OPC	Oligodendrocyte precursor cell
PD	Parkinson disease
PSB	pallial-subpallial boundary
PV	Parvalbumine
RNP	Ribonucleoprotein
ROS	Reactive oxygen species
scFv	Single chain antibody
SNpc	Substantia nigra pars compacta
SO	Superior olive
TE	Transposable elements
TH	Tyrosine hydroxylase
Top1	Topoisomerase 1 protein
TPRT	Target primer reverse transcription

VTA
ZLI

Ventral tegmental area
Zona limitans intrathalamica

INTRODUCTION

Chapter I: Functions and Transfer of Homeoproteins

I.1 The discovery of homeoproteins in *Drosophila*

In 1967, Walter Jakob Gehring, studying cell fate and determination, undertook segmental gene interchange along chromosomes in the *Drosophila*. This induced “odd” looking *Drosophila*, for example with legs instead of antennas on their head (Garber et al., 1983; Gehring, 1987). This is how the first homeogene *Antennapedia* was identified.

Homeoproteins (HPs) are a class of transcription factors that control gene expression thanks to their DNA-binding homeodomain (HD). The HD is a 60 amino acid-long sequence encoded by a 180 nucleotide-long sequence called “homeobox” (McGinnis et al., 1984). The conservation of this feature was used to identify a large set of developmental homeotic genes in the *Drosophila* as well as in vertebrates.

As depicted in Figure 1, the site and time of expression of homeotic genes along the *Drosophila* anterior-posterior body is controlled by their positioning along the chromosome. This colinearity rule (Lewis, 1978) explains why interchanging homeogene position could induce morphological changes during development. Not only the timing and the site of expression but also the concentration of homeoproteins is crucial in tissue patterning, determination of cell fate and other developmental events.

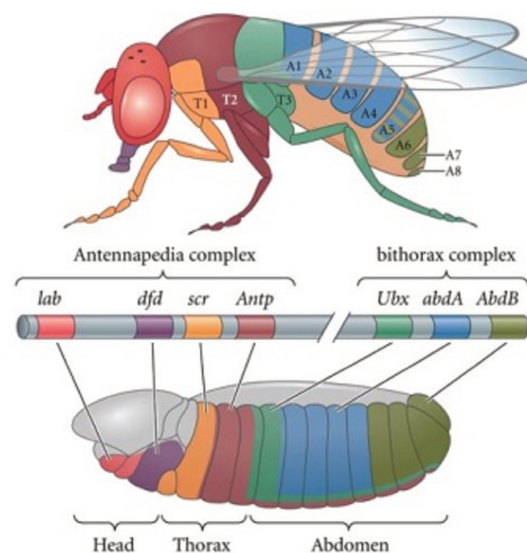


Figure 1: Hox gene expression in the *Drosophila* along the anterior-posterior body axis corresponds to their 3'-5' order in the genome along the anterior-posterior axis. Taken from Gilbert et al, 1990.

The structure of the homeodomain was first described for ANTENNAPEDIA by nuclear magnetic resonance spectroscopy. Homeodomains are composed of three alpha helices arranged in a helix-turn-helix motif. The third helix, also called the recognition helix, is able to bind target sequences in the large groove of double-stranded DNA (Billeter et al., 1990). This DNA-HD contact reinforced by the interaction of the HD N-terminus with the double-stranded DNA minor groove enables the HP to exert its regulatory functions. However, not all HPs participate in development and now the consensual definition is that to be named “homeoprotein”, a protein must only possess a homeodomain within its sequence.

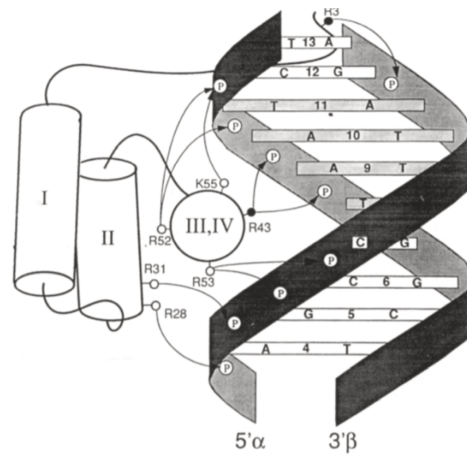


Figure 2: Schematic drawing of the ANTENNAPEDIA Homeodomain-DNA Complex. The helices of the homeodomain are represented by cylinders and the amino acid residues contacting the DNA are shown by circles. Arrows indicate specific contacts with the DNA bases. The bars representing the core basepairs (TAAT/A A) are shaded. Taken from Gehring et al., 1994.

1.2 Homeoproteins control Brain Morphogenesis

The HD is highly conserved across species and this enabled the identification, across vertebrates and all eukaryotic species, of numerous HPs that often share sequence homologies (Derelle et al., 2007; Joyner et al., 1985).

Mice make no exception and the development of the mouse brain is also controlled by HPs (Bishop et al., 2000; Di Bonito et al., 2013; Nédélec et al., 2004; O’Leary et al., 2007; Simeone, 2000; Simon et al., 2001; Wurst et al., 1994). As can be appreciated in Figure 3, several HPs participate in the establishment of brain compartments. Indeed, the pattern of

expression of different HPs determines boundaries and gives rise to different brain areas endowed with different brain functions (Prochiantz and Di Nardo, 2015).

For instance, the OTX2/GBX2 boundary defines the midbrain-hindbrain boundary (MHB) (Joyner et al., 1985; Simeone, 2000; Wurst et al., 1994) .

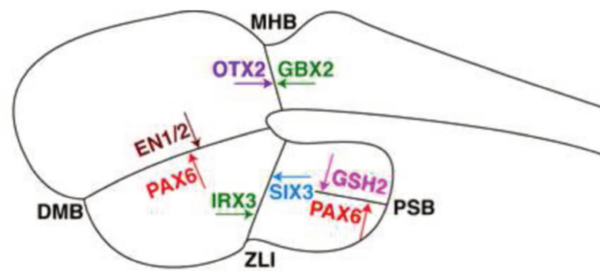


Figure 3: Examples of boundaries (MHB: Midbrain-hindbrain boundary, PSB: pallial-subpallial boundary, DMB: diencephalic-mesencephalic boundary, ZLI: zona limitans intrathalamica) defined by the expression of abutting homeoproteins (in colors) with self-activating and reciprocal inhibitory properties. Taken from Prochiantz and Di Nardo, 2015.

Interestingly, HPs cross-interact to create those boundaries. On each side of the boundary, the HPs are both self-activating and reciprocal inhibitors, thus creating a dynamic gradient of expression.

- Figure 4 A shows the **graded expression** of four different HPs along the antero-posterior and medial-lateral axes. For instance, *Emx2* is more expressed posteriorly while *Pax6* is more expressed anteriorly.
- Figure 4 B illustrates the **activation/inhibition relationship between HPs**: EMX2 inhibits *Pax6* expression and is reciprocally inhibited by PAX6.

The importance of the pattern of expression of HPs can be demonstrated by loss or gain of functions. Indeed, dysregulation of this pattern displaces boundaries and strongly impacts brain structure (O’Leary et al., 2007).

- Figure 4 C illustrates **boundary displacements** following changes in HP expression. In this example *Emx2* loss of function induces an increase in the somato-sensory cortical area, while a gain of function induces an increase of the visual cortex area.

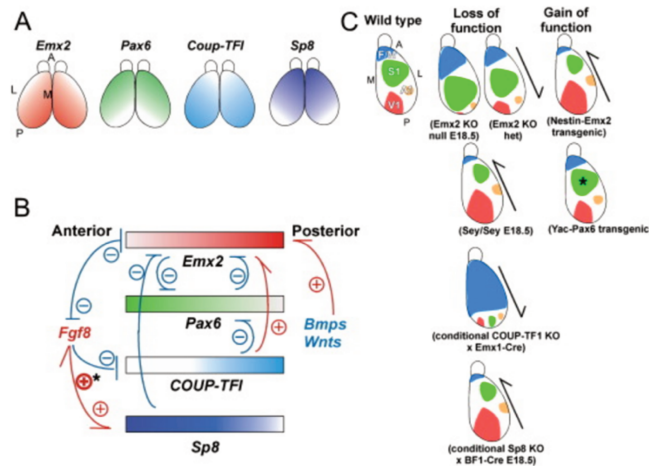


Figure 4: Summary of Intrinsic Genetic Mechanisms of Area Patterning and Mutant Phenotypes. A) Graded colours represent the graded expression of HPs in the brain. B) Arrows represent the interaction between HPs along the A-P axis. C) Loss and gain of function of HPs induce a displacement of S1 (Somatosensory), V1 (Visual), Frontal/Motor (F/M), Auditory (A1) areas. Taken from O'Leary et al., 2007.

I.3 Focus on ENGRAILED Homeoprotein

I.3.a ENGRAILED: a repressive transcription factor

During my thesis, I have focused on the function of the ENGRAILED homeoprotein in dopaminergic neurons of the midbrain (mDA neurons). ENGRAILED has two paralogs: ENGRAILED1 (EN1) and ENGRAILED2 (EN2), collectively ENGRAILED. At the molecular level, ENGRAILED is mainly considered as a transcriptional repressor (Jaynes and O'Farrell, 1991). *In vivo*, the active repression by ENGRAILED is due to its association with GROUCHO or its orthologs in vertebrates, proteins from the TLE family (*Transducin like Enhancer of Split*) (Tolkunova et al., 1998). Other protein partners, such as co-factors PBX/EXD, modulate its transcriptional activity. Around 203 genes have been identified as targets of ENGRAILED by chromatin immunoprecipitation in drosophila embryos. Those genes are involved in different developmental pathways including axon guidance, antero-posterior development and muscle development (Solano et al., 2003).

I.3.b Role of *Engrailed* during development

Collectively, EN1 and EN2 regulate the formation of the boundary between the diencephalon and the mesencephalon, as well as the rostral-caudal axis of the optic tectum in the chick. During mouse development, *En1* is expressed in the anterior neuroepithelium as

soon as the first somite stage. Invalidation of *En1* results in the absence of the midbrain and homozygous mice deleted for *En1* die after birth. *En2* is expressed at later stages (five-somite) and deletion gives rise to a reduction in the size of the cerebellum (Wurst and Bally-Cuif, 2001; Wurst et al., 1994) and to an altered cerebellar foliation (Joyner et al., 1991; Millen et al., 1994). *En2* mutants are, however, viable. This suggested, that *En1* and *En2* play distinct roles with *En1* being more important in the midbrain. However, replacement of *En1* with *En2* rescued the defects observed. This demonstrated that EN1 and EN2 are biochemically equivalent and suggested that it is rather the site, time and duration of *En1/2* expression that is important (Hanks et al., 1995).

Interestingly, association of *En2* with neurodevelopmental disorders such as autism spectrum disorders (ASD) has been demonstrated (Genestine et al., 2015). For ASD, studies rely not only on genetic association studies (Petit et al., 1995; Wang et al., 2008; Yang et al., 2008) but also on cerebellar morphology changes. For instance, mirroring a reported neuroanatomical feature of autistic brains, *En2* mutants display a significant decrease in the number of Purkinje, granule deep nucleus, and inferior olive cells (Gharani et al., 2004).

I.3.c Expression of ENGRAILED in the adult midbrain

Originally studied for their role during development, homeoproteins remain however expressed in the adult where they are endowed with crucial roles for neuron physiology and maintenance.

In the adult brain, *Engrailed* remains expressed in the Substantia Nigra pars compacta (SNpc) and Ventral Tegmental Area (VTA) but also in the Inferior Colliculus (IC), Cerebellum (Cb) and the Superior Olive (SO) as depicted in Figure 5. More precisely, *En1* is more expressed in the SNpc and the VTA while *En2* is more expressed in the Cb.

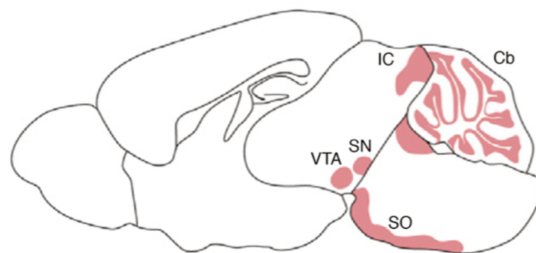


Figure 5: Expression (pink) of *Engrailed* in the adult mice brain. VTA: Ventral Tegmental area, IC: Inferior Colliculi, Cb: Cerebellum, SN; Substantia Nigra, SO: Superior Olive. Taken from Prochiantz et Di Nardo 2015.

At a cellular level in mDA neurons of the SNpc, EN1/2 is detected in the nucleus, as would be expected for a transcription factor. However, *En1* mRNA is also present in proximal dendrites and translated locally via an mTOR-dependent signalling pathway. Intriguingly, translation is activated upon depolarization suggesting a potential role of EN1 in local and activity-dependent signalling (Di Nardo et al., 2007).

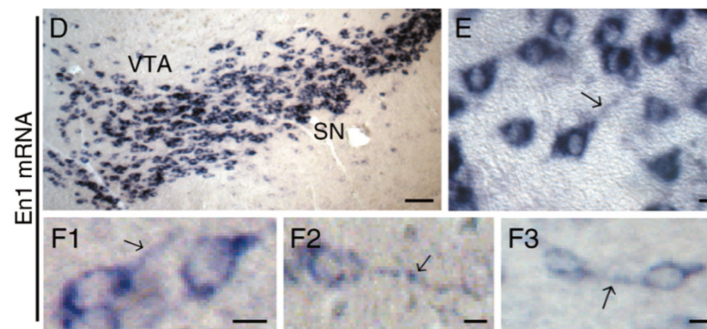


Figure 6: Detection of *En1* mRNA in dendrites (arrows) of mDA neurons in the SNpc. Taken from Di Nardo et al., 2007.

In terms of function, the cerebellum participates in the regulation of motor behaviours and coordination. Recent studies suggest its potential implication in higher cognitive functions (Riva and Giorgi, 2000). The mDA neurons of the SNpc and the VTA also participate in voluntary movement as they provide dopamine, key neurotransmitter for movement. However, they are also implicated in mood and rewarding pathways (Graybiel et al., 1994). In terms of connectivity, mDA neurons of the SNpc project to the dorsal striatum via the nigrostriatal pathway (Björklund and Dunnett, 2007). In contrast, mDA neurons of the VTA project to the ventral striatum (*nucleus accumbens*), limbic systems, ventral hippocampus and prefrontal cortex via the mesolimbic and mesocortical pathways, as illustrated in Figure 7 for some of the latter structures (Bentivoglio and Morelli, 2005).

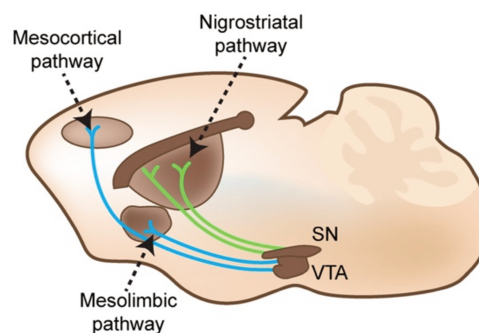


Figure 7: The mesocortical, nigrostriatal, mesolimbic pathways of the mDA neurons of the SN and VTA. Taken from Money and Stanwood, 2013.

Dysfunctions in the mDA circuitry have been implicated in numerous neuropsychiatric disorders such as schizophrenia or addiction and degeneration of mDA neurons in the SNpc is an important feature of Parkinson disease (PD) (Brisch et al., 2014; Luo and Huang, 2016; Simpson et al., 2014; Tagliaferro and Burke, 2016; Volkow et al., 2007).

I.3.d mDA neurons and Parkinson disease

Parkinson disease (PD) is the second most common neurodegenerative disease and affects around 2-3% of the population over 65 years of age (Olanow and Tatton, 1999). Although some genetic factors have been identified, such as point mutations in the gene coding for α -SYNUCLEIN and duplications/triplications of the *α -synuclein* gene (Polymeropoulos et al., 1997; Stefanis, 2012), most cases are sporadic. The major risk factor is aging, but several environmental factors have been positively correlated with the disease including exposure to pesticides (Hatcher et al., 2008; Sandy et al., 1996). Along with movement disruption, patients exhibit cognitive impairment, autonomic dysfunction, sleep disturbances, depression and hyposmia (For review (Poewe et al., 2017)).

At molecular and cellular levels, PD is characterised by the loss of mDA neurons in the SNpc. As already mentioned, mDA neurons produce dopamine, an essential neurotransmitter for harmonious movements (Marsden, 1983). Another major hallmark of the disease is the presence of intracellular inclusions containing the α -SYNUCLEIN protein (Bennett et al., 1999). The exact causes of mDA degeneration are not fully understood but several pathways are implicated including α -SYNUCLEIN proteostasis, mitochondrial function, oxidative stress, calcium homeostasis, axonal transport and neuroinflammation (Bennett et al., 1999; Braak et al., 2003; Dauer and Przedborski, 2003; Dias et al., 2013).

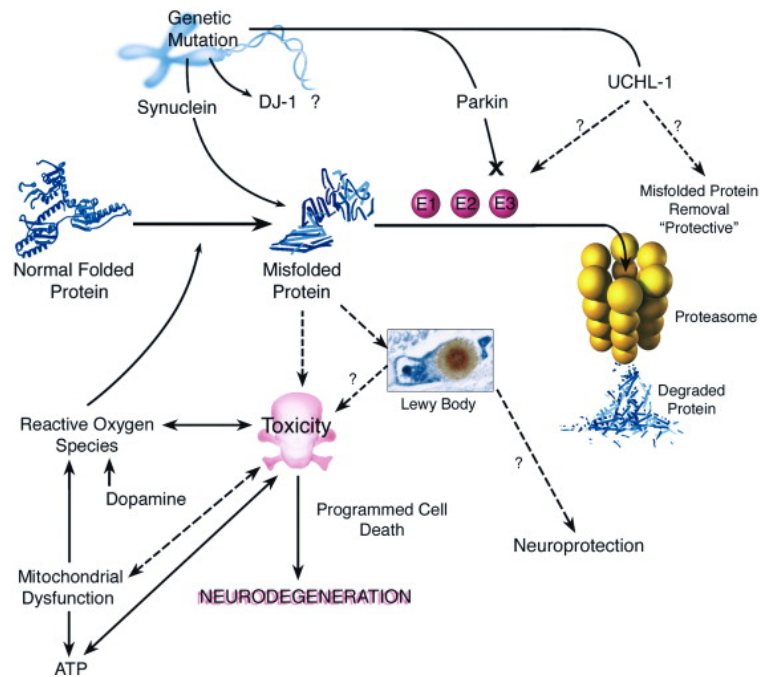


Figure 8: The main identified mechanism of neuronal degeneration in Parkinson Disease including protein misfolding, alteration of protein degradation, production of reactive oxygen specie and mitochondrial dysfunction. Taken from Dauer and Prsedborski, 2003.

I.3.e ENGRAILED protects mDA neurons in Parkinson Disease models

Coming back to ENGRAILED, some studies have reported that genetic variability within the *En1/2* genes is a susceptibility factor for sporadic PD (Haubenberger et al., 2011; Rissling et al., 2009). Even more interestingly, the group of Horst Simon (Simon et al., 2001) provided evidence that EN1/2 regulate the expression of *α-synuclein*, a major culprit in PD.

Engrailed has been demonstrated to be crucial for the maintenance of mDA neurons (Albéri et al., 2004; Simon et al., 2001; Sonnier et al., 2007). Mice disposing of only one allele of *En1*, have comparable numbers of mDA neurons at birth but exhibit a progressive and specific mDA neuron loss between 8 weeks and 24 weeks. As in PD, the loss of mDA neurons in the SNpc is more pronounced than in the VTA (38% versus 23%) (Sonnier et al., 2007). Correlating with mDA neuron death in the SNpc, there is a significant 37% decrease in dopamine in the striatum, as assessed by high performance liquid chromatography (HPLC).

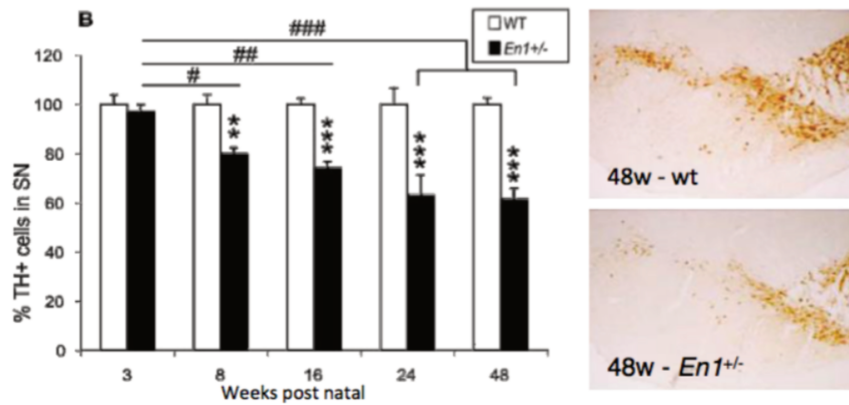


Figure 9: *En1*^{+/-} mice exhibit a loss of dopaminergic neurons in the Substantia Nigra. Left panel : % of TH cells in the SN over weeks. Right panel : Image of TH staining in wt and *En1*^{+/-} mice at 48w. Taken from Sonnier et al., 2007.

Engrailed1^{+/-} mice display motor symptoms that mimic some characteristics of the human disease. Indeed, they present abnormal spontaneous motor activity in the open-field test and in the motor coordination rotarod test, they tend to fall more often than wildtype (WT) siblings. In terms of non-motor symptoms, they exhibit impaired social interactions and depressive like behaviours. This is summarized in the following table.

MOTOR SYMPTOMS	NON-MOTOR SYMPTOMS
Abnormal spontaneous motor activity	Anhedonia and Adipsia
Deficit in motor coordination	Impaired social interaction
Sensitization to amphetamine	Depressive like behaviour

Figure 10: *En1*^{+/-} mice exhibit motor and non-motor symptoms characteristic of Parkinson Disease. Results extracted from Sonnier et al., 2007.

The occurrence of (i) the selective loss of mDA neurons in the SNpc with (ii) the motor and non-motor symptoms, mirrors key aspects of PD indicating that these mice might be a good model for the human disease. Several studies from other laboratories came in support of this idea, including those from the group of Patrick Brundin demonstrating that the autophagic protein degradation pathway is altered in *En1*^{+/-} mice (Nordströma et al., 2015). The same study reports fragmentation of mDA axons, supporting retrograde degeneration of mDA neurons as in PD (Tagliaferro and Burke, 2016). Furthermore, neuroinflammation in the SNpc of *En1*^{+/-} mice was found (Ghosh et al., 2016). A very recent study (Chatterjee et al., 2019) puts forward that *En1*^{+/-} mice display enhanced aggregation of pathological α -SYNUCLEIN following intrastriatal injection of pre-formed α -SYNUCLEIN fibrils, suggesting that this mouse line might provide a highly relevant model to test experimental therapeutic strategies.

Indeed, in the meantime a study has been using *En1*^{+/-} mice in pre-clinical testing of a potential PD drug (Ghosh et al., 2016).

An exciting finding in therapeutic context is that EN2 infusion reverses the behavioural phenotype observed in the *En1*^{+/-} mouse and protects mDA neurons from death (Sonnier 2017). The fact that the administration of EN2 reverts the effect of *En1* loss, also adds up to the idea that both EN1 and EN2 are biochemically equivalent as discussed above (Hanks et al., 1995; Sonnier et al., 2007). Indeed, the latter use of EN1/2 as a therapeutic protein is based on its ability to translocate across membranes and on its long-lasting activity. The protective abilities of ENGRAILED have been continuously studied in the laboratory. They imply different levels of action, including local protein translation, transcription and epigenetic modifications.

Regarding translational regulation, ENGRAILED upregulates the expression of NDUFS3 and NDUFS1, two key regulators of the mitochondrial respiratory chain complex I, thus inducing an increase in ATP synthesis. ENGRAILED does so through direct regulation of translation via its specific binding to EIF4e (Alvarez-Fischer et al., 2011).

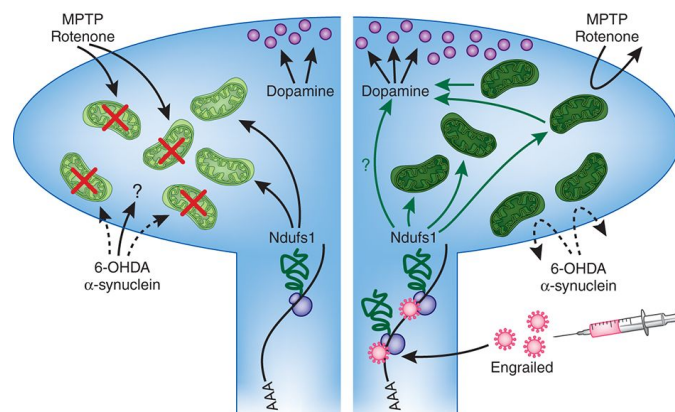


Figure 11: Left: MPTP and rotenone induce a degeneration of dopamine by binding to mitochondrial complex I. Right: Engrailed injection protects mDA neurons by binding to the mRNA machinery and increasing the translation of *Ndufs1*. Taken from Sanders and Greenameyre, 2011.

Finally, ENGRAILED promotes the expression of anti-apoptotic factors upon acute oxidative stress in a transcription dependant manner (Rekaik et al., 2015). The protective effect of ENGRAILED on heterochromatin maintenance will be presented in Chapter II.

I.4. Homeoproteins can transfer between cells through unconventional pathways

I.4.a Discovery and mechanism

A very striking feature of homeoproteins is that they possess a non-conventional mechanism for cell to cell translocation. As many ground-breaking observations, this novel signalling mechanism was discovered by chance. Indeed, while Alain Joliot and Alain Prochiantz were studying the effect of a HD on neuronal morphology, a negative control yielded positive results. As a mean to internalize the HD, cells in culture were scraped to disrupt their cell membrane. The negative control consisted of “unscraped cells”. Surprised to see an effect of the HD on neuronal morphology even with “unscraped cells”, Joliot and Prochiantz tagged the HD with FITC and observed its intracellular and intra-nuclear accumulation (Joliot et al., 1991). This was followed by the demonstration that full-length HPs are secreted and internalized thanks to two secretion and internalization domains embedded within the HD (Figure 12), thus highly conserved. This is greatly interesting as it suggests that around 300 or so homeoproteins may use this direct inter-cellular signalling pathway to exert part of their biological functions (Di Nardo et al., 2018). So far, this pathway has been validated for 13 HPs out of 13 tested, including ENGRAILED, PAX6, VAX1, HOXD1 and OTX2 (Di Nardo et al 2018). This signalling mode is a reminder of well described direct cell to cell transfer of transcription factors in plants through plasmodesmata (Bolduc et al., 2008; Ruiz-Medrano et al., 2004; Winter et al., 2007).

The exact mode of transfer is still under investigation. It appears, however, that internalisation and secretion do not rely on the same processes nor on the same sequences (Figure 12).

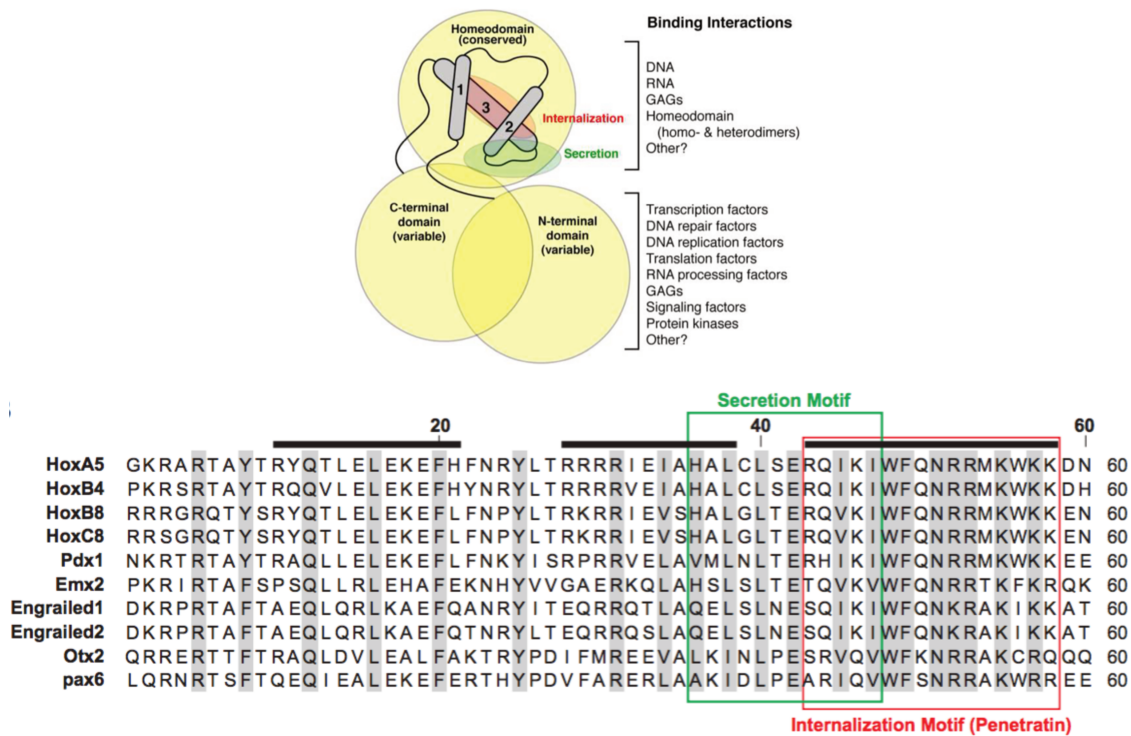


Figure 12: Top) Homeoproteins domains and associated functions. Taken from Prochiantz et Di Nardo 2015.

Bottom) Alignment of HDs for 10 HP verified for intercellular transport. The helices are indicated by bold dark lines. Of note, internalization and secretion sequences contain hydrophobic and basic residues characteristic of nuclear import and export sequences.

The internalisation sequence has been named penetratin. Internalisation occurs at 4°C as well as at 37°C, suggesting an energy-independent capture mechanism (Derossi et al., 1994). Internalisation is dependent on a two-step membrane disruption event thanks to the third alpha-helix comprised in the HD (Dupont et al., 2007). However, the alpha-helical structure of the helix is not necessary since the insertion of prolines does not disturb internalisation (Derossi et al., 1996). The tryptophan in position 48 is of main importance for internalisation. Seemingly, penetratin can cross pure lipid membranes without forming pores (Thorén et al., 2000). This is in agreement with the very low toxicity of penetratin observed in cell studies (Derossi et al., 1998).

The sequence required for secretion spans from the end of the second helix to the middle of the third helix. Secretion has been mainly studied for EN2. EN2 is found associated with lipid-rich caveolae-like vesicles, suggesting that these vesicles could participate in EN2 secretion (Joliot et al., 1997).

Besides its physiological importance in biology, this signalling mechanism has also opened the field of peptide transduction, a category of peptides used to target hydrophilic compounds into the cell interior, following cargo-peptide coupling (Prochiantz, 2011). As an example, we have taken advantage of the natural internalisation of homeoproteins *in vivo* by injecting or infusing the ENGRAILED protein locally and directly into the brain (See paragraph on the protective activities of ENGRAILED).

I.4.b The difficulty to distinguish cell autonomous from non-cell autonomous functions

Since HPs translocate between cells, it is important to distinguish (i) autonomous functions from (ii) non-cell autonomous functions. However, as the secretion and internalisation sequences are within the HD it makes it impossible to mutate those sequences without affecting both cell autonomous and non-cell autonomous functions. To address this issue, mini-genes encoding single chain antibodies (scFvs) have been developed to specifically impede HP non-cell autonomous functions. Indeed, following expression, scFvs, thanks to a secretion signal, are secreted into the extra-cellular matrix (ECM) where they trap the HPs extracellularly. Most of the time, and as verified for those used in the laboratory, scFvs are inactive intracellularly due to glutathione which reduces the disulphide bonds necessary for antigen recognition. This strategy has been used and published for PAX6, ENGRAILED and OTX2 in order to study the importance of non-cell autonomous transfer in specific biological functions (Lesaffre 2007; Wizenmann 2009; Layalle 2011; Di Lullo 2011; Bernard 2016, Kaddour 2019).

The results conducted so far on non-cell autonomous functions have been summarized in Figure 15.

I.4.c Non-cell autonomous functions of PAX6 and OTX2

Regarding OTX2, recent work in the team has demonstrated that OTX2 is produced and secreted by the choroid plexus and then internalised in parvalbumine (PV) positive interneurons in the visual cortex. Accumulation of OTX2 induces the maturation of PV interneurons that in turn regulate the opening and closure of the critical period for the acquisition of binocular vision.

Expressing the anti-OTX2 scFv and blocking OTX2 transfer in the adult mouse reopens plasticity and restores binocular vision in an experimental model of *amblyopia*, a developmental disorder in which one eye does not achieve normal visual acuity (Bernard et al., 2016).

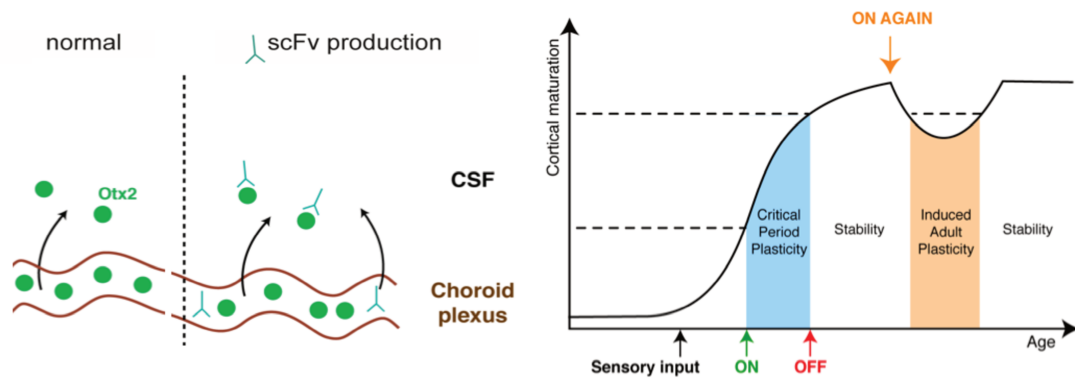


Figure 13: A two-threshold model for Otx2 in critical period timing. In normal situation, Otx2 is produced by the Choroid plexus and secreted in the CSF, Otx2 then accumulates in PV cells. When a certain threshold is reached the critical period opens (ON) and then closes at a second threshold (OFF). Blocking the accumulation of Otx2 with the scFv strategy, induces a visual plasticity in the adult (On again).

The effects of blocking extra-cellular PAX6 in the zebrafish eye has also been studied (Lesaffre et al., 2007). Induction of scFv-AntiPAX6 and analysis of the eye morphology 30 hours post-fertilisation demonstrated a decrease in eye size, either symmetrical (as in Figure 14 B) or asymmetrical (Figure 14 C) compared to normal eyes (Figure 14 A). In extreme cases, one eye can be completely absent (Figure 14 D). Total eye loss as in Figure 14F corresponds to the cyclopean phenotype and might be an injection-induced artefact.

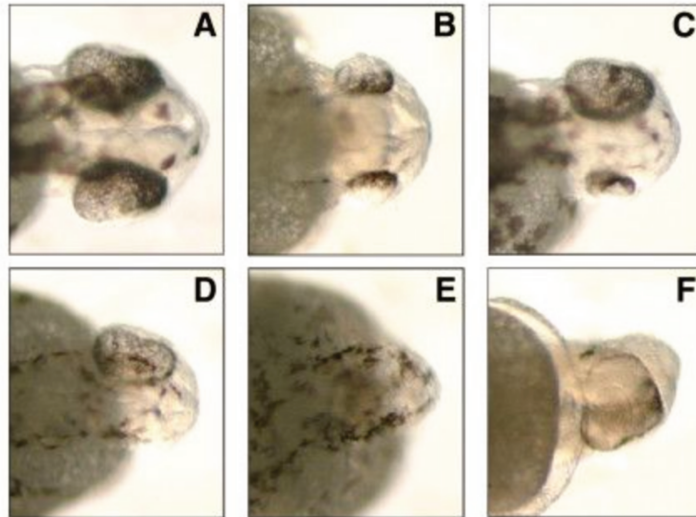


Figure 14: Eye phenotypes induced by secreted anti-Pax6 single-chain antibody. (a-f) Eye phenotypes observed at 30 hours post-fertilization after injection of secreted single-chain anti-Pax6 (spaP6) mRNA into one cell embryos. (a) Normal, (b) small eyes, (c) dissymmetric eyes, (d) single eye, (e) no eye, (f) cyclops. Taken from Lesaffre et al, 2007.

Neutralizing PAX6 extracellular activity also demonstrated that non-cell autonomous PAX6 regulates oligodendrocyte precursor cell (OPC) migration in the chick embryonic neural tube (Lullo et al., 2011) and cajal-retzius cell migration in the developing neocortex (Kaddour et al., 2019). In the context of this thesis, these effects on migration are interesting, as they suggest that HPs may act on cytoskeleton reorganizing proteins to modify migration.

<i>HP</i>	Function	Model	Pathway	Publication
<i>Engrailed</i>	Guidance of retinal growth cones	Retinal axons of <i>Xenopus</i>	Potentiates Ephrin signalling	(Brunet et al., 2005)
	Retinotectal patterning	Retinal axons of chick		(Wizenmann et al., 2009) (Stettler et al., 2012)
	Formation of the anterior cross vein	<i>Drosophila</i>	Interacts with Decapentaplegic	(Layalle et al., 2011)
	Promotes motor neuron survival	Spinal cord of mice	?	(In prep. Leboeuf M, Vargas S, et al. 2019)
<i>Otx2</i>	Regulates the opening and closure of the critical periods of plasticity in the visual system	Layer IV of the visual cortex of mice		(Bernard et al., 2016)
<i>Pax6</i>	Migration of cajal-retzius cells	Mouse		(Kaddour et al., 2018)
	Promotes cell migration of oligodendrocyte precursor cells	Chick embryonic neural tube	Not investigated	(Lullo et al., 2011)
	Eye anlagen	Zebrafish	Not investigated	(Lesaffre et al., 2007)

Figure 15: Studies of non-cell autonomous functions of Homeoproteins.

I.4.d Non-cell autonomous functions of ENGRAILED

Non-cell autonomous ENGRAILED has been demonstrated as crucial for guidance of retinal growth cones (Brunet et al., 2005) and retino-tectal patterning (Wizenmann et al., 2009b).

The couple formed by EphrinA ligands and their receptors were long thought to be key for retino-tectal patterning. However, in total absence of EphrinAs, degenerated retino-tectal maps still form suggesting the existence of alternative and complementary pathways (Cang et al., 2008). In line with this, studies demonstrated that an external gradient of EN2 withholds signalling cues for retino-tectal mapping (Brunet et al 2005; Wizenmann et al, 2009). Indeed, axons of retinal ganglion cell (RGC) cultured in gradients of EN2 display different behaviours according to whether they are from nasal or temporal origin (Brunet et al, 2005). As depicted in Figure 16, nasal axons are attracted by EN2 (the gradient of EN2 is in blue), whereas temporal axons are repelled.

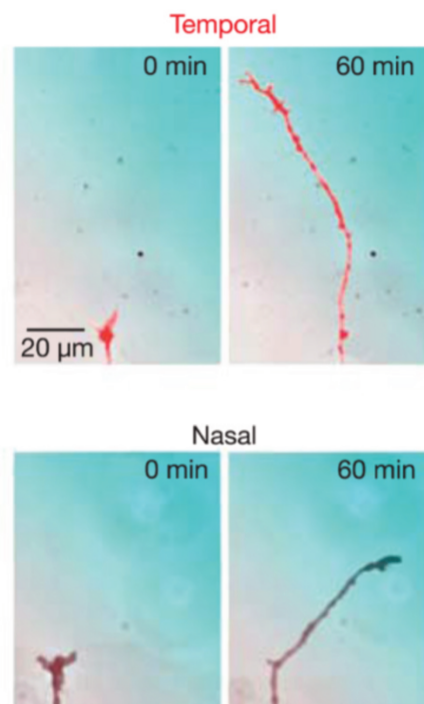


Figure 16: In the top panel the temporal axons are repelled by EN2 (blue gradient) while in the bottom panel, nasal axons are attracted. Taken from Brunet et al, 2005.

This is due to non-cell autonomous signalling as it is demonstrated, with an internalization deficient EN2, that internalization is necessary for axon guidance.

By using transcription and translation inhibitors (anisomycin, rapamycin, actinomycin) as well as tritiated leucine, the same authors show that EN2 signals not by transcriptional means but by inducing protein translation. This is also supported by elevated phosphorylation levels of EIF4E in the presence of EN2.

Non-cell autonomous function of ENGRAILED was further validated *in vivo* by the scFv approach (Wizenmann et al., 2009). Indeed, antero-posterior tectal membranes of *Xenopus* display a gradient of extracellular ENGRAILED and blocking the extracellular ENGRAILED with an scFv approach induces an abnormal growth of temporal axons in the chick and in *Xenopus* (Wizenmann et al 2009). Interestingly, EN1/2 activity is synergistic with EphrinA5 signalling (Wizenmann et al 2009). As demonstrated in the *in vitro* turning assay (Brunet et al, 2005), this non-cell autonomous ENGRAILED/EphrinA5 synergistic signalling relies on a translational regulation by ENGRAILED.

The analysis of this pathway was further dissected demonstrating that internalised non-cell autonomous ENGRAILED acts on the local translation of NDUFS3 (Stettler et al., 2012). NDUFS3 is part of the complex I of the mitochondria and this stimulates ATP synthesis. ATP is then exported and hydrolysed into adenosine in the ECM. Adenosine signals back on the growth cone via membrane receptors that in turn impact on EphrinA5 signalling. This is engaging as it appends to the fact that adult HPs carry regulatory roles independently of their initially studied transcriptional functions. It further nurtures the idea that HPs can act as sensitizers or co-signalling partners of renowned signalling molecules. The fact that non-cell autonomous ENGRAILED has the capacity to act as a co-signalling molecule was also demonstrated in the case of Decapentaplegic (*Drosophila* TGF- β ortholog) in the *Drosophila* wing disk (Layalle et al., 2011). Of note, NDUFS3 is an already identified target described in studies on mDA neuron protection by cell autonomous ENGRAILED.

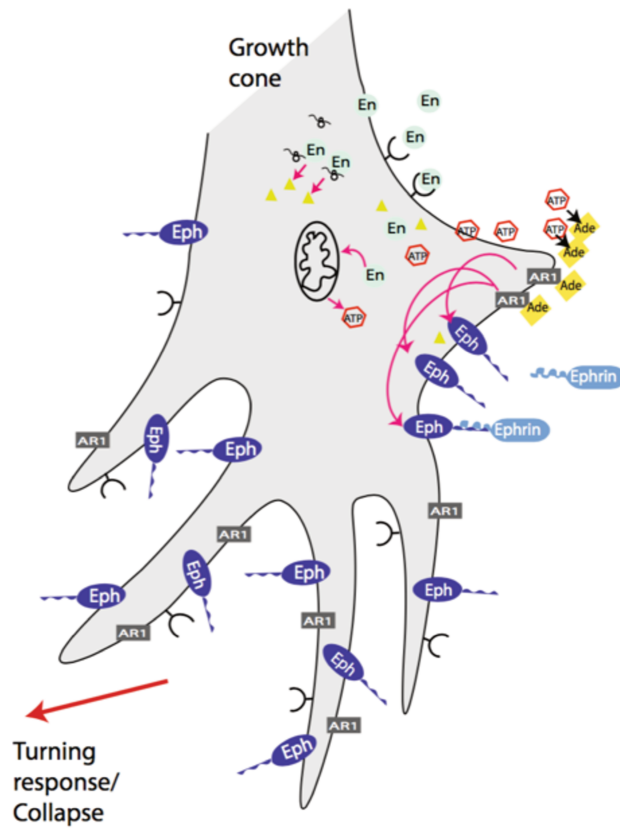


Figure 17: En signalling at the growth cone. En is internalized by the growth cone. Within the growth cone it stimulates the translation of *Ndufs3*, a complex I mitochondrial protein. This activates ATP synthesis, which is externalized into the extracellular matrix and hydrolysed to adenosine. Adenosine activates the AIR receptor, which acts synergistically with *EphrinA5* signalling perhaps via adenylate cyclase to cause growth cone collapse and arrest. Taken from Wizenmann et al., 2015

Working Hypothesis of Chapter I:

The importance of non-cell autonomous ENGRAILED for the physiology and protective activity of mDA neurons has been understudied. As mentioned above, (Di Nardo et al., 2007) demonstrate that EN1 is present in the dendrites of mDA neurons. This pool of EN1 could transfer to adjacent cells and exert local physiological functions in dendrites far from the nucleus. This refers to non-cell autonomous functions and could be independent of its transcriptional activity. Indeed, association of HPs with the translation factor EIF4E has been demonstrated (Nédélec et al., 2004). Since the mTOR pathway is implicated in dendritic growth, maintenance and synaptic plasticity, one could not preclude that local EN1/2 might directly impact dendritic morphology or maintenance.

This is supported with a recent study where authors added recombinant EN1 and EN2 on hippocampal cell cultures and demonstrated that this increased the complexity of the dendritic trees of glutamatergic neurons (Soltani et al., 2017). Furthermore, the impact of non-cell autonomous HPs on remodelling the cytoskeleton has been demonstrated in axon guidance (Brunet et al., 2005) as well as in cell migration (Lesaffre et al., 2007). EN1/2 also impacts on the expression of cell adhesion molecules which shape neuronal morphology (Siegler and Jia, 1999).

We therefore tested whether non-cell autonomous ENGRAILED impacts mDA neuron morphology and survival *in vivo* and *in vitro*, and if so, by which pathway. In analogy with other studies from the laboratory described above, I used an scFv antibody directed against ENGRAILED. This strategy will allow us to specifically interfere with non-cell autonomous functions while leaving cell autonomous functions intact, as the antibody is produced by adjacent astrocytes as depicted in Figure 18.

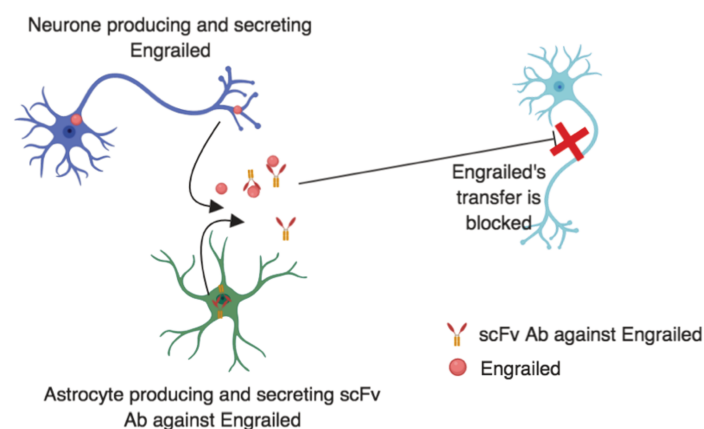


Figure 18: The neurone produces Engrailed that is trapped in the intercellular space by the scFv secreted by the Astrocyte.

Chapter II: From Engrailed protective abilities to transposable elements

II.1 ENGRAILED protects mDA neurons against oxidative stress through the reduction of DNA strand breaks and heterochromatin maintenance

II.1.a. Oxidative stress, genomic instability and epigenetic alteration in Parkinson Disease and aging

Mitochondrial dysfunction and oxidative stress constitute a hallmark of PD. Oxidative stress arises from an unbalance between the production of reactive oxygen species (ROS) and the inefficient clearing of ROS by anti-oxidant enzymes. ROS can be produced as a consequence of ATP synthesis. Therefore, neurons with very high energy demands are more prone to oxidative stress. Furthermore, the dopamine synthesis pathway also produces ROS (Delcambre et al., 2016). Mesencephalic DA neurons are thus likely to have high ROS production. This can be aggravated by the fact that detoxification of ROS by antioxidants enzymes is probably impaired in PD patients (Ambani et al., 1975; Kish et al., 1985). The idea of oxidative stress as a driver in PD has also been underscored by the recent identification of deletion and point mutations in the *DJ-1* gene in familial forms of PD (Bonifati et al., 2003). Indeed, DJ-1 is part of the anti-oxidative stress response and *DJ-1* loss of function triggers oxidative stress (Lavara-Culebras and Paricio, 2007; Taira et al., 2004).

ROS can be damaging to the cell in multiple ways. With regard to PD, ROS can induce protein oxidation that inhibits protein degradation and leads to subsequent protein aggregation such as α -SYNUCLEIN aggregates (Giasson et al., 2000). ROS can also induce DNA damage. DNA damage might potentially be more harmful to neurons. Indeed, as post-mitotic cells, neurons cannot use homologous recombination for DNA repair and are confined to the error prone non-homologous end joining DNA repair pathway (Fishel et al., 2007). Furthermore, DNA damage repair becomes less effective with aging in neurons (Lu et al., 2004; Vyjayanti and Rao, 2006). Accordingly, accumulation of DNA strand breaks in the brain of PD patients compared to controls has been reported in several studies (Hegde et al., 2006). This DNA damage hypothesis is further supported by quantifications of the levels of 8-hydroxyguanosine, a marker of oxidative-stress induced DNA damage, that are increased in the SNpc of PD

patients (Alam et al., 1997). In the long run, this accumulation of DNA damage in the mitochondria and the nucleus can trigger cell death (Madabhushi et al., 2014).

Furthermore, DNA damage can inhibit rRNA synthesis leading to nucleolar disruption and elevated P53 levels inducing apoptosis (Rubbi and Milner, 2003). In line with this, NUCLEOLIN, a protein that regulates the architecture of the nucleolus, has differential levels of expression in PD patients, compared to healthy controls (Rieker et al., 2011). Staining for NUCLEOLIN is also altered in the *En1*^{+/-} mouse (Rekaik et al., 2015).

Aside from DNA damage and nucleolar stress, it is noteworthy to point out that alterations of epigenetic marks have been reported in the context of PD. For instance, MeCP2, a transcriptional repressor involved in chromatin remodelling, is less expressed in SNpc mDA neurons of animals with altered nigrostriatal pathways (Gantz et al., 2011). Another example is provided by the hypomethylation of the *α-synuclein* intron-1 in the brain and blood of patients with PD (Ai et al., 2014; Edwards et al., 2010). For reviews on epigenetic changes associated to PD, refer to (Feng et al., 2015; Klein and Benarroch, 2014).

In the field of aging (as a reminder the main risk factor for PD is aging), heterochromatin loss is well documented and suspected to play an active role in the process. The initial hypothesis of heterochromatin loss as a driver of aging was first put forward by Villeponteau in 1997 (Villeponteau, 1997). The central idea is that heterochromatin loss induces aberrant gene expression leading to cell dysfunction. Since then, numerous studies have come to underpin heterochromatin loss during aging or in aging disease models such as Progeria (Burgess et al., 2012; Fasolino et al., 2017; Larson et al., 2012; Pegoraro et al., 2009; Scaffidi and Misteli, 2006; Tsurumi and Li, 2012).

II.1.b ENGRAILED guarantees proper heterochromatin maintenance and reduces DSBs

As presented in Chapter I, loss of one *En1* allele in mice induces degeneration of mDA neurons and injection of EN1/2 protects mDA neurons in multiple PD models (A30P α -synuclein, MPTP, 6-OHDA) (Alvarez-Fischer et al., 2011).

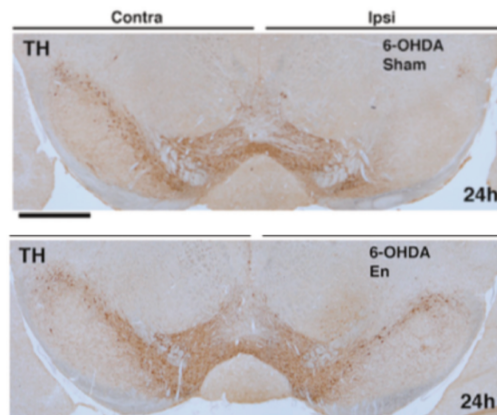


Figure 19: Injection of Engrailed protects mDA neurons (TH⁺) from degeneration in 6-OHDA model. TH staining in the midbrain in 6-OHDA +/- En. Taken from Rekaik et al., 2015.

Additional mechanisms by which EN1/2 exerts its protective functions have been analyzed (Rekaik et al., 2015). Indeed, upon oxidative stress, there is:

- (i) loss of heterochromatin maintenance through alteration of epigenetic marks inducing expression of aberrant genes
- (ii) increased DNA double strand breaks (DSBs).

Injection of EN1/2 rescues the loss of heterochromatin and reduces the number of DSBs, thus protecting mDA neurons from degeneration. In Figure 20, one can appreciate: the formation of DSBs stained by γ -H2AX, altered H3K27me3 epigenetic marks induced by 6OHDA injections and reversal by ENGRAILED between 24 h and 7 days.

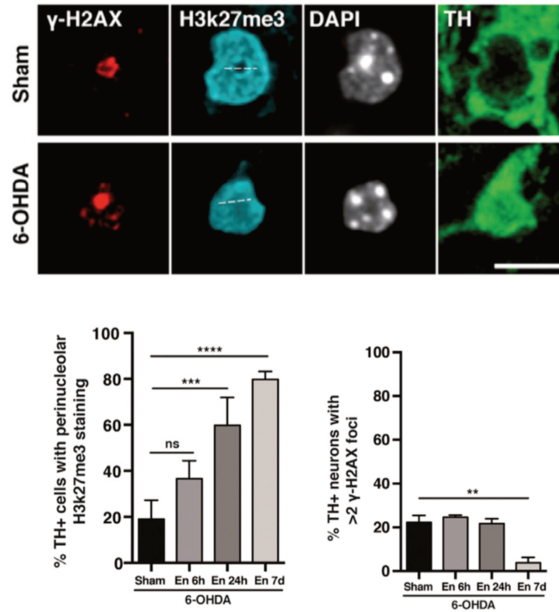


Figure 20: 6-OHDA injection induces DSBs (stained by γ -H2AX-red) and altered H3K27me3 staining (cyan) - Top Panel - That are reversed following Engrailed injection - Bottom Panel- Taken from Rekaik et al., 2015.

Of particular interest, in *En1*^{+/-} mice, we observed an increased expression of the LINE-1 (L1) family of transposable elements. This is noteworthy as L1 can induce DSBs, a hallmark of acute oxidative stress and *En1*^{+/-} models.

II.2 Transposable elements: purely “parasitic” elements alive in our genome?

II.2.a. Discovery and classification of transposable elements (TEs)

Discovered by Barbara McClintock in maize while studying chromosome breakage, transposons are elements that move (or “jump”) within the genome (McClintock, 1950). McClintock came to the conclusion that mobile DNA elements led to the somatic mosaicism and phenotypic diversity observed in the maize kernel. Her discovery received little consideration at the time and was accepted by the scientific community more than 20 years later with the understanding of the DNA code. She was awarded the Nobel Prize in 1983.



Transposable elements (TEs) represent nearly half of our genome but were long thought to be “junk” DNA. In the last decades, the discovery of novel regulatory roles (presented in II.4) and of their involvement in diseases (presented in II.3) have led a regain of scientific interest for TEs (Biéumont, 2010).

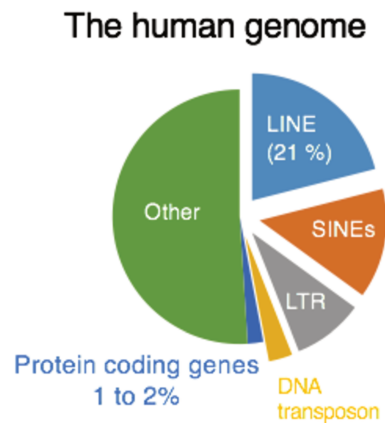


Figure 21 : The composition of the Human Genome. L1 elements represent around 21% of the genome.

Transposable elements are classified in different subfamilies:

- 1) **Class I: retrotransposons** need an RNA intermediate and mobilize in a “copy and paste” manner (Boeke et al., 1985)
- 2) **Class II: DNA transposons** directly mobilize as DNA sequence in a “cut and paste” manner (Kleckner, 1990)

Retrotransposons are further subdivided:

- 1) As **autonomous**: they encode the protein machinery sufficient to support mobilization (LINE-1 or ERVs elements for example)
- 2) As **non-autonomous**: their mobilization relies on protein coded by other elements (for instance SINEs co-opt the LINE machinery).

In this thesis work, I will focus on LINE-1 elements (L1) as they constitute the most prominent family of TEs that are still active and capable of transposition in an autonomous manner in humans.



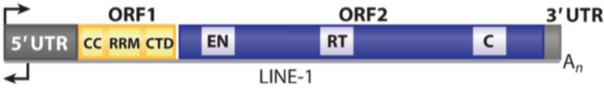
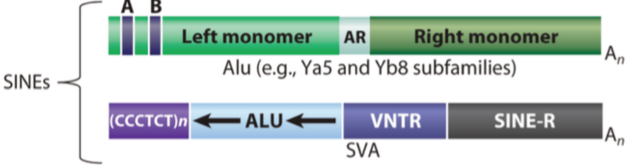

Type of mobile element	Example structure	HGR percentage	Active?
DNA transposons			
Transposons	 Mariner	~3%	No
Retrotransposons			
Autonomous retrotransposons			
LTR retrotransposons	 HERV-K	~8%	Uncertain (none known)
Non-LTR retrotransposons	 LINE-1	~21%	Yes
Nonautonomous retrotransposons			
SINEs		~10% ~2,700 copies	Yes
Processed pseudogenes		<1% ~11,000 copies	

Figure 22: The classes of transposable elements families, according to their type, structure, percentage within the human genome reference sequence (HGR) and whether each class is transposition competent (=active) or not. Taken from Beck et al., 2001

II.2.b. The structure of L1 elements and Life Cycle

L1 are ~ 6kb long, contain a 5' untranslated region (UTR), encode 2 proteins ORF1p and ORF2p (Figure 23) and terminate with a 3' UTR punctuated by a poly(A) tail (Scott et al., 1987) (Dombroski et al., 1991).

ORF1p	40kDa	RNA recognition motif for association with RNAs
ORF2p	150kDa	Endonuclease for DNA nicking Reverse transcriptase

Figure 23 : Structure of L1 elements

It has recently been discovered that L1 elements also encode an ORF0 that may assist L1 in mobility (Denli et al., 2015). The translation mechanism of ORF2p is much debated. It is thought to be translated by an unconventional termination-reinitiation mechanism. It is to be noted that the ratio ORF2p /ORF1p is of about 1/200 (Alisch et al., 2006).

L1 is transcribed in the nucleus and the mRNA is exported to the cytoplasm where it is translated and associates with ORF1p and ORF2p (Hohjoh and Singer, 1996). This forms a ribonucleoprotein (RNP) that translocates back into the nucleus where the endonuclease activity of ORF2p induces a DNA break (Feng et al., 1996). The RNA serves as a template for reverse transcription into cDNA allowing for the reinsertion of a novel L1 DNA copy. This process is called Target Primed Reversed Transcription (TPRT) and is still under active investigation (Cost et al., 2002). For detail of the life cycle see Figure 24

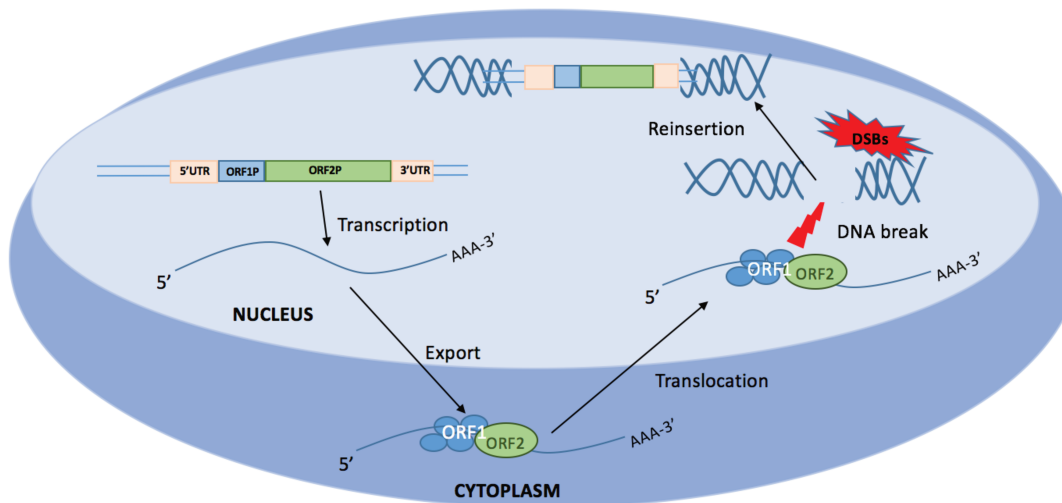


Figure 24 : Life cycle of L1 elements in the cell. L1 are transcribed in the nucleus then exported and translated in the cytoplasm. The L1 protein associates with the L1 mRNA and translocates back in the nucleus where it can induce DNA breaks and reinsert itself in the genome by target primed reverse transcription.

Most L1 elements are truncated and in the human genome only ~ 80-100 L1 copies are “full-length” (fL1) and potentially able to transpose. Some of these fL1 copies (around 10) are the most active and considered as “hot” elements (Brouha et al., 2003). Due to incomplete retrotranscription most L1 are 5' truncated and are thus unable to mobilise (Lander et al, 2001). This does not mean that they have no function. Among these functions they provide DNA binding sites, favour the formation of DNA loops and be transcribed as non-coding RNAs if inserted in frame with a transcription starting site.

II. 3 Dynamics of L1 elements in the genome

II.3.a L1: a potential genomic threat

L1 elements can negatively impact the genome in multiple ways:

- (i) Direct insertion in a coding DNA sequence inducing a functional mutation: As such several diseases have been associated with a **mutagenic L1 insertion**, amongst which we can cite haemophilia (Kazazian et al., 1988) or some cancers (Deininger and Batzer, 1999)
- (ii) Disturbance of the heterochromatin/genomic environment of nearby genes impacting **gene expression**: Rheostat hypothesis for reduced speed of transcription (Han and Boeke, 2005), alteration of the methylation environment (Le et al., 2015), or insertion of the L1-promoter inducing altered gene expression
- (iii) **DNA nicks** due to the endonuclease activity of ORF2p (without the need of subsequent transposition) inducing genomic instability (Gasior et al., 2006)

II.3.b The Genome's defence tactics

Due to the potential genomic threat, cells have developed an active line of defence to repress TE activity. They mainly take the following forms:

- (i) Chromatin repressive marks limiting TE expression through DNA methylation or histone modification. They can be deposited by recognition and binding of repressive proteins such as the Krüppel associated box containing zinc finger proteins (KRAB-ZFPs)
- (ii) TE-mRNA cleavage by the Piwi system (Tóth et al., 2016) or microprocessors such as Drosha (Heras et al., 2013)

Heterochromatin maintenance blocking L1 activity has been described as mediated by either DNA methylation (MeCP2 mediated repression, CpG methylation) or histone modification (H3K9me3, H3K27me3). This allows for DNA compaction in the vicinity of L1 elements, thus limiting transcription (Le et al., 2015; Muotri et al., 2010). Transposable elements are for example repressed by the association of KRAB-ZFPs with their co-factor KAP1. KAP1 then serves as a recruiter for heterochromatin-inducing proteins including DNA

methyltransferases, histone deacetylases and methyltransferases. Very interestingly, the repressive process of TE elements mediated by KAP1 differs between early embryonic and adult somatic tissues (Ecco et al., 2017; Friedli and Trono, 2015; Iyengar and Farnham, 2011; Quenneville et al., 2012). Indeed, in early embryonic stages or in ES cells, recruitment of KRAB-KAP1 to specific loci induces a DNA methylation while at later stages, in differentiated tissues, it rather induces histone-based reversible modifications (Quenneville et al., 2012). Furthermore, at adult stages KRAB-ZFPs present specific patterns of expression, suggesting a tissue specific repression of endogenous retroviral elements. However, in regards to L1 elements, KAP-1 deleted mice exhibit only a modest up-regulation suggesting a regulation via alternative pathways (Matsui et al., 2010; Rowe et al., 2010).

The Piwi repressive system is very well characterised in the germline and is an illustrative example of bimodal repression of TEs. Indeed, Piwi acts at two levels: at the chromatin level to silence TE transcription by deposition of repressive histone marks (Sienski et al., 2012) and DNA methylation (Kuramochi-Miyagawa et al., 2008) but also by degradation of TE-mRNA. To degrade TE-elements, PIWI proteins rely on TE transcripts templates (Figure 25). Indeed, piRNAs, mostly anti-sense to TE mRNA sequence, guide PIWI proteins for TE degradation. The piRNAs originate from remnants TE copies (Aravin et al., 2007) or directly from RNA transcripts of active TE copies. This implies that piRNA formation and L1 repression through piRNAs require minimal L1 transcription. One could compare this mechanism to an adaptive immune response: there is a memory of former TE invasion within the clusters generating piRNAs. For review of the germinal cells repressive system of L1 elements see (Yang and Wang, 2016).

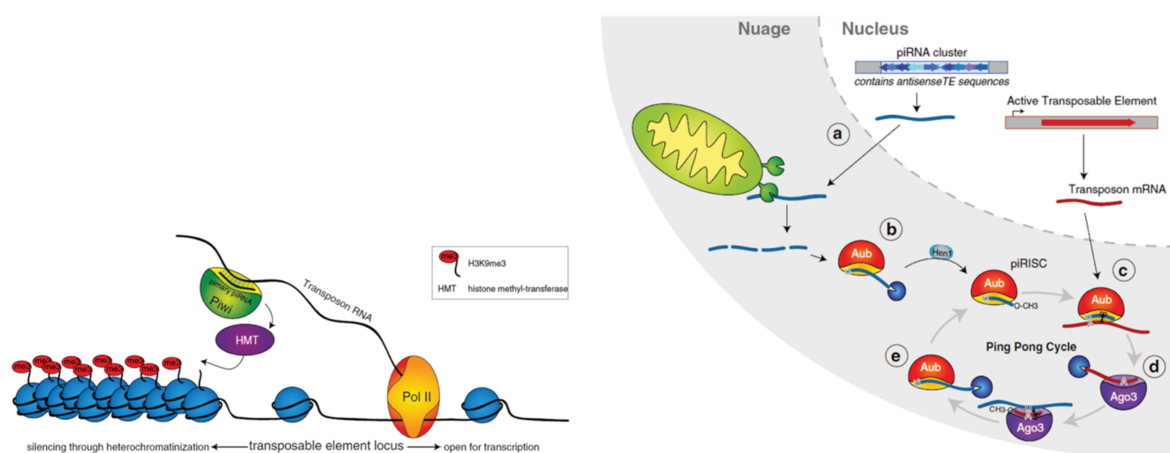


Figure 25: Piwi repress TE elements through heterochromatinization by deposition of H3Kme3 marks (left panel) and piRNA interference (right panel) via Aubergine (Aub) and Ago proteins. Taken from Yang and Wang, 2016.

Some piRNAs have been detected in somatic brain cells (Lee et al., 2011; Yan et al., 2011) as well as expression of 2 PIWI proteins, AGO and AUB (Perrat et al., 2013). Two independent studies suggest the importance of piRNAs in synaptic transmission. Indeed, (Lee et al., 2011) demonstrate that anti-sense suppression of piRNAs in cultured hippocampal neurons reduced the size of the dendritic spines. In terms of long-term synaptic facilitation, piRNA/Piwi could harbour a regulatory role by methylating CREB2, a critical plasticity related gene, in *Aplysia* (Rajasethupathy et al., 2012).

However, whether the Piwi system is active in somatic brain cells such as mDA neurons, in order to repress L1 elements, is not known.

II. 3 L1 elements in the CNS or age related diseases

L1 elements have been associated with many diseases. For example, L1 expression or transposition seems altered in different pathological conditions such as schizophrenia (Bundo et al., 2014; Doyle et al., 2017), Rett Syndrome and Ataxia telangiectasia.

Rett Syndrome is particular interesting as it is due to mutations in MeCP2 (Amir et al., 1999), a known repressor of L1 elements (Muotri et al., 2010). Rett syndrome is an X-linked disease that mostly affects girls. It is characterised by normal development until 6-18 months followed by the appearance of autistic symptoms, loss of speech, hand-wringing, anxiety, and eventually motor deterioration (Chahrour and Zoghbi, 2007). Post-mortem brain tissue from Rett Syndrome patient brains shows more L1 DNA copies compared with age-matched control patients (Jacob-Hirsch et al., 2018). This implies that neurons of Rett Syndrome patients may undergo more retrotransposition. However, the impact of L1 activity on the pathology is unknown. Indeed, L1 overexpression and retrotransposition could simply be by-products of the MeCP2 loss of function.

The case of Ataxia telangiectasia (A-T) is also worth attention as it caused by a defect in ATM, a sensor of DNA damage. ATM activates the DNA-damage checkpoint involving p53, and induces DNA repair (Tichý et al., 2010). In A-T patients, there is a higher DNA copy number of L1 elements (Coufal et al., 2011). The question of whether ATM is an inhibitor of L1 retrotransposition or whether L1 takes advantage of unrepaired breaks to integrate more frequently is unresolved.

In the scope of neurodegenerative disorders, an increased expression of L1 has been reported in Alzheimer disease (AD) and Amyotrophic Lateral Sclerosis (ALS) (Guo et al., 2018; Liu et al., 2019). ALS is characterised by the degeneration of motor neurons leading to muscle weakness and shares common clinical features with Fronto-Temporal Dementia (FTLD) (Zarei et al., 2015). At the cellular level both diseases exhibit TDP-43 deposits (Scotter et al., 2015). In a similar manner than in PD, DNA damage and chromatin decompaction are observed. By ATAC-Seq, a method to map open chromatin regions, it was found that loss of nuclear TDP-43 is associated with chromatin decondensation around L1s and increased L1 DNA content is reported (Liu et al., 2019). This increase in L1 expression could participate in the neurodegenerative process by the formation of DNA breaks and the accumulation of R loops, both being linked to the activity of repetitive genomic elements. R-loops are three-stranded nucleic acid structure due to the formation of a DNA:RNA hybrid during transcription or replication (Thomas et al., 1976).

Furthermore, expression of L1 elements has also been linked to aging. Indeed, SIRT6 represses L1 expression via KAP1 (Van Meter et al., 2014). SIRT6 is a member of the sirtuin family and exhibits ADP-ribosyl transferase and histone deacetylase activities. SIRT6 has been considered as an anti-aging protein: mice overexpressing SIRT6 have an extended lifespan, are cancer resistance and show improved metabolic function (Kanfi et al., 2010, 2012). Conversely, *Sirt6* knockout mice exhibit premature aging, shortened lifespan and genomic instability (Oberdoerffer et al., 2008). The authors observe that in the course of aging, SIRT6 is depleted from L1 loci, thus inducing an elevated expression of L1 elements that could represent a threat to genomic stability and be mutagenic. The L1 repression by SIRT6 is mediated via KAP1, a repressor of transposons very well characterized by the laboratory of Didier Trono (cf. II.3.b) The results are represented in Figure 26.

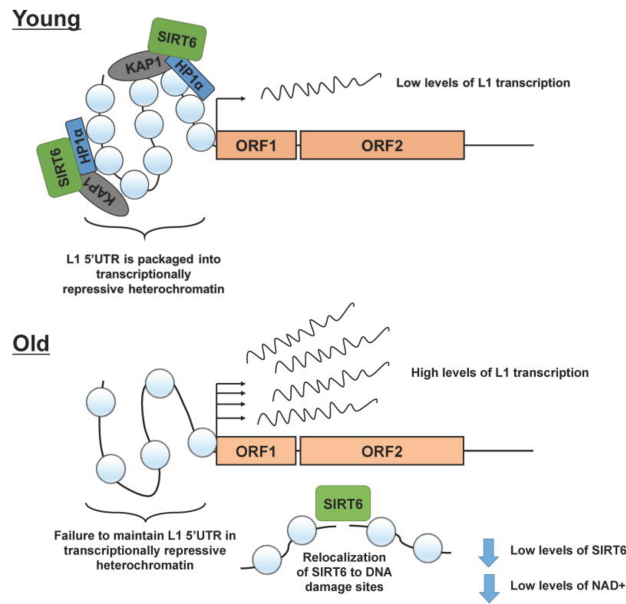
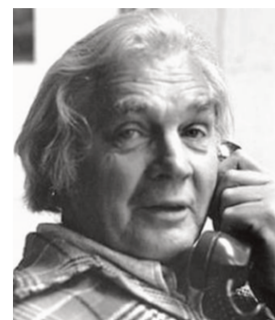
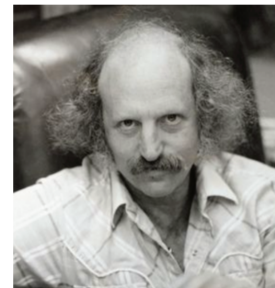


Figure 26: Model for SIRT6-mediated age-related activation of L1 expression. In young mice, Kap1 and SIRT6 compact the L1-5'UTR thus repressing the expression of L1. In old mice, depletion of SIRT6 induces a failure to compact the L1-5'UTR and induces high levels of L1 expression. Taken from Van Meter et al., 2014

II. 4 L1 elements: regulatory roles and evolutionary co-option?

When Barbara McClintock initially discovered TEs, as a pioneer, she had postulated regulatory roles for them. However, in light of the potential genomic threat and association with diseases, the view of TEs as mainly negative and harmful was prominent for many years. This was however decried as early as the 1970s by Roy J. Britten (top picture) and Eric Davidson (bottom picture) who pushed forward the regulatory hypothesis for TEs advanced by McClintock (Britten and Davidson, 1971).

They indeed hypothesized that TEs could spread regulatory elements within the genome to drive the evolution of regulatory networks. At the age of 91, 1 year before his death, Roy J. Britten published his last paper in which he proposed that many TE insertions create potentially effective genomic changes and that the selection of some of them are responsible for human lineage evolution (Britten, 2010).



The work of Britten and Davidson has gained much support in recent years. Indeed, discovery of “domestication” or “exaptation” of TEs as well as attribution of regulatory roles has made the scientific community reconsider the dominant view that L1 elements are purely “parasitic”.

The most famous example of domestication is probably the RAG enzymes allowing for V(D)J recombination creating diversity in immune repertoires (Huang et al., 2016). Indeed, RAG enzymes originate from a DNA transposon and allow for cut and paste recombination of the V, D and J segments. This process is key in the adaptive immune response of jaw vertebrates (Flajnik and Kasahara, 2010). In the prokaryote world, the parallel can be made with the CRISPR-Cas system. It consists of an endonuclease activity coupled to a guide RNA. The guide RNAs are generated by clusters that record the previous exposure of the cell to parasitic elements. It targets and digests the nucleic acids of the invader thus providing a basis for adaptive immunity (Barrangou et al., 2007). It has been demonstrated that Cas1 originates from a transposon named *Casposons* (Krupovic et al., 2014).

Furthermore, some TEs are a source of non-coding regulatory RNAs such as lncRNA, miRNAs, circRNAs (Kelley and Rinn, 2012; Liang and Wilusz, 2014; Roberts et al., 2014). Studies have shown the implication of those lncRNAs deriving from HERVH retrovirus for human stem cell pluripotency (Lu et al., 2014). Regarding L1 elements, the knockdown of L1 by antisense oligonucleotides induces a transition of embryonic stem cells (ESC) to a 2-cell (2C) state (Percharde et al., 2018). This is mediated by the recruitment of NUCLEOLIN and KAP1 by the L1 RNA repressing the 2-C transcriptional program in ESCs.

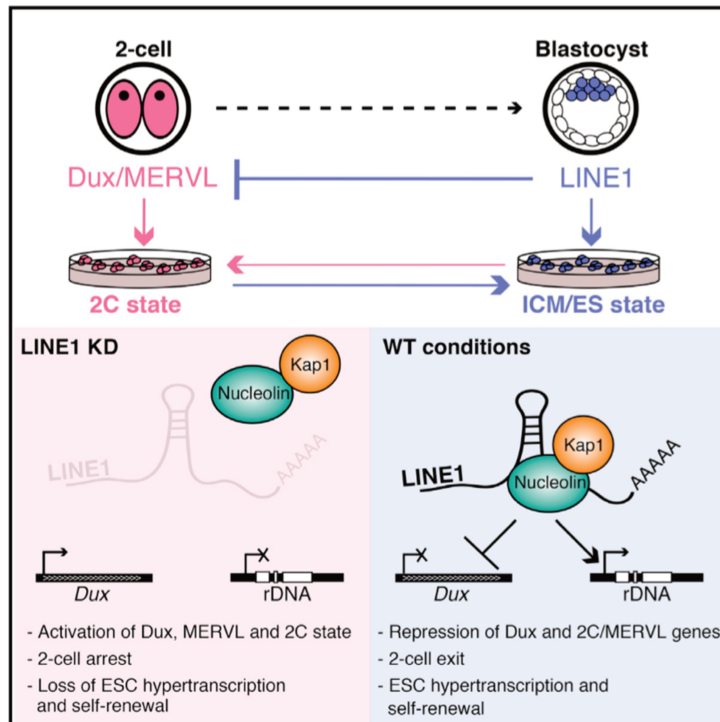


Figure 27: Graphical abstract from Percharde et al. (2018) depicting the importance of L1 elements in ESC identity and developmental progress. In the LINE1 KD model, there is activation of Dux, MERV1 and loss of ESC self-renewal while in WT conditions LINE-1 elements recruit Nucleolin and Kap1 that repress Dux and 2-cell genes allowing 2-cell exit and proper development as well as ESC self-renewal.

In the early embryo, L1 elements could also be implicated in X chromosome inactivation. X inactivation is the process by which nearly one whole X chromosome is repressed for dosage compensation in females XX. X inactivation is maintained in somatic cells. The *Xist* gene, situated at the centre of the X chromosome, is key in initiating the silencing of the chromosome which is then propagated along the chromosome. However, introducing the *Xist* in an autosomal chromosome is less efficient, suggesting the existence of repression “boosters” along the inactivated X chromosome (For review (Chow and Heard, 2009)). In the 1990s, Mary Lyon postulated that transposable elements participate in X inactivation. The Lyon Hypothesis received later support from further studies (Bailey et al., 2000 (Lyon, 2000)). Indeed, authors demonstrate that L1 elements are 2-fold enriched on the X chromosome compared to autosomes and that their density is higher in the initiation centre of inactivation. However, one cannot firmly conclude that this is causative. Indeed, L1 elements could have accumulated in the favourable X inactivated chromosome and undergone less negative selection. The authors suggest that if L1 elements were to be indeed drivers of the X inactivation, then this would be through an *XIST* RNA protein complex interacting with clusters of L1 elements to mediate the repackaging.

At the beginning of the 21st century, the global scientific view was that L1 retrotransposition was limited to germinal cells or to early development and rare in somatic cells. The team of Fred Gage however made the observation that L1 retrotransposition could occur in neural progenitors, proposing that it participates to the somatic mosaicism of the brain and affects neuronal plasticity and behaviour (Muotri et al., 2005; Coufal et al., 2009). This reopened the question of the physiological significance of L1 elements within somatic brain cells.

Working Hypothesis Chapter II:

When we started the project, most studies on L1 elements in neurodegeneration remained correlative, and, the physiological and pathological importance of L1 and retrotransposons within the brain very largely unexplored. Our goal was to investigate the potential implication of L1 elements in the degeneration of dopaminergic neurons in the context of oxidative stress and PD model.

This interest was based on results obtained in the laboratory including:

- (i) The overexpression of L1 elements in a mouse model of PD
- (ii) The occurrence of DNA damage and heterochromatin loss, two features of L1 activation (Li et al., 2013a), in our models of PD and oxidative stress

We thus pursued to study whether L1 elements could participate in the mDA degeneration observed and whether the protective activity of ENGRAILED was partly mediated by L1 regulation.

Based on the observation of a basal expression of L1 elements in mDA neurons from specific hotspots located in introns of long genes, we then questioned a potential physiological role of L1 elements in adult neurons.

RESULTS

Non-cell autonomous ENGRAILED regulates dendritic growth and maintenance

Summary and objectives:

In order to study the function of non-cell autonomous ENGRAILED, I blocked the transfer of ENGRAILED by a single chain antibody approach secreted in the extracellular milieu. I performed those experiments *in vivo* and *in vitro* demonstrating that ENGRAILED is necessary for the maintenance of dendrites and the survival of mDA neurons.

I have however not yet been able to elucidate the mechanisms through which ENGRAILED exerts these functions, and the project will be pursued. The results described below are in the form of a manuscript in progress that we intend to complete before uploading it as a preprint on the bioRxiv site.

Non-cell autonomous ENGRAILED regulates dendritic growth and maintenance

Introduction

During development, the homeoprotein (HP) transcription factors ENGRAILED -1 (EN1) and ENGRAILED -2 (EN2) participate in the brain compartmentalization (Davidson et al., 1988) and in the differentiation of progenitor neurons (Condrón et al., 1994). In the adult brain, ENGRAILED (EN1 and EN2) remains expressed in several brain regions, including in the mesencephalic dopaminergic (mDA) neurons of the *Substantia Nigra pars compacta* (SNpc) and Ventral Tegmental Area (VTA).

Parkinson disease (PD), the second most common neurodegenerative disease, is characterized by a progressive loss of mDA neurons in the SNpc and the development of motor and non-motor pathologies (Olanow and Tatton, 1999). Recent studies have shown that EN1 is a survival transcription factor for adult mDA neurons (Sonnier et al., 2007; Nordströma et al., 2014; Chatterjee et al., 2019). Similarly, to several HPs, EN1 and EN2 transfer between cells thanks to secretion and internalization sequences present in the DNA-binding homeodomain. Due to this internalization sequence, EN1 or EN2 injected in the midbrain are internalized by SNpc mDA neurons and protect them from degeneration in several mouse and non-human primate PD models (Alvarez-Fischer et al., 2011; Blaudin de Thé et al., 2018a; Rekaik et al., 2015; Thomasson et al., 2019).

This begs for a distinction between cell autonomous and direct non-cell autonomous ENGRAILED functions. The latter functions require that ENGRAILED be secreted and internalized either by the same cell that secreted it or by abutting ones. To this date the only physiological non-cell autonomous signalling function of ENGRAILED is in retinal ganglion cell (RGC) axon guidance or maintenance (Brunet et al., 2005; Wizenmann et al., 2009; Yoon et al., 2012). Strikingly, once internalized, the proteins act through the regulation of local translation and signals in interaction with the Ephrin and Adenosine signalling pathways (Brunet et al., 2005; Wizenmann et al., 2009; Stettler et al., 2012). Interestingly, in mouse PD pharmacological models, the protective activity involves the translation of mitochondrial Complex I, NDUFS1 and NDUFS3 proteins (Alvarez-Fisher et al., 2011).

In the present study, we have investigated the possibility that EN1 might signal back to the mDA neurons that produce it. Indeed, EN1 and its mRNA are present in neuronal terminals *in vivo*, thus close to possible secretion sites (Di Nardo et al., 2007). We report that the expression of a single chain antibody recognizing EN1 and EN2, thus neutralizing extracellular ENGRAILED (eEN) *in vivo*, reduces mDA neurons survival and the extent of axonal and dendritic arbours. *In vitro* loss of eEN confirms the effect on the neuropile.

Results

Non-cell autonomous ENGRAILED regulates dendrite maintenance and survival of mDA neurons *in vivo* and dendritic growth in midbrain primary culture *in vitro*

1. *In vivo* effect of non-cell autonomous Engrailed on mesencephalic dopaminergic neuron survival and dendritic arbour

In order to block the transfer of secreted ENGRAILED, we used a single chain antibody (scFv) tool (validated in **supplementary Fig. 1**) delivered by an AAV8-GFAP-scFv-GFP/mCherry virus. Due to the GFAP (Glial Fibrillary Acidic Protein) promoter, the single-chain antibody is secreted by the adjacent astrocytes and cannot interact with cell-autonomous ENGRAILED in the neurons. As negative control a single cysteine to serine point mutation (AAV8-GFAP-scFvMUT-GFP/mCherry) rendering the single chain antibody unable to recognize Engrailed was used, in parallel with non-infected conditions. The production of active and mutated scFvs can be followed thanks to a 3×Myc-tag in C-terminal position of the antibodies.

In vivo, we performed stereotaxic injection of the AAV8-GFAP-scFv and control viruses in the SNpc of adult wild-type mice for a duration of either 3 months or 3 weeks and analysed dendrite extent and the number of mDA neurons expressing the Tyrosine Hydroxylase (TH) enzyme. Indeed, in mDA neurons, EN1/2 and EN1 was previously reported to be expressed in the dendrites, together with its mRNA (Di Nardo et al., 2007). The two time points yielded similar results, with a **20%** reduction in the size of the mDA dendritic arbour in the *Substantia reticulata* and **23%** loss of mDA neurons as early as 3 weeks after infection with the active virus (**Fig 1. a and b**). This suggests that, in adult mice, not only does ENGRAILED act on dendritic maintenance but also on mDA neuron survival. In agreement with these results, TH staining in the *Striatum*, a nucleus of the forebrain receiving axonal inputs from the mDA neurons of the SNpc, was significantly reduced by **6%** (**Fig 1.c**).

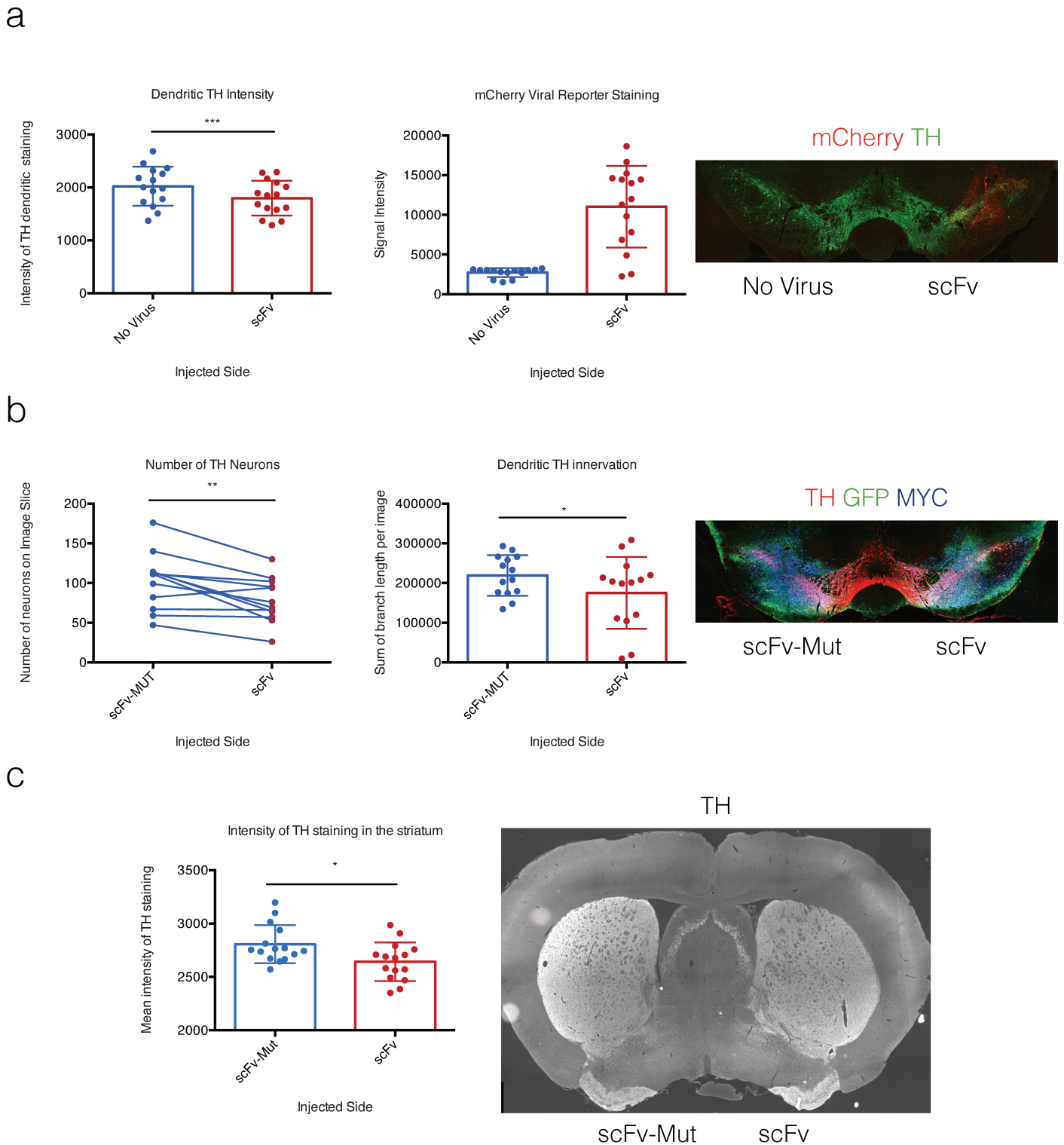


Figure 1 : Extracellular Engrailed regulates TH survival and dendritic arborisation in vivo

a) Quantification of TH-positive dendrites and mCherry expression in ventral midbrain 3 months after AAV8-GFAP-scFv-mCherry unilateral injection, number of mice $n = 5$; number of Slices $n = 3$ per mice. TH staining values passed D'Agostino and Pearson omnibus normality test. Tested for difference using Paired t-test assuming gaussian distribution number of pairs = 15. p value = 0.0005 ***. Pairing efficient Correlation = 0,8511, p value < 0.0001 ****

b) Quantification of TH-positive dendrites and of the number of TH neurons in AAV8-GFAP-scFvMUT-GFP injected side (scFv-Mut) and AAV8-GFAP-scFv-GFP (scFv) injected side and associated midbrain images. Number of mice $n = 4$; number of Slices $n = 3$ per mice. Number of TH counted on scFv-MUT and scFv sides : 1231 and 938. Passed D'Agostino and Pearson omnibus normality test. Paired t-test assuming gaussian distribution number of pairs = 12. p value = 0,0029 ** Effective pairing p -value = 0,0013 ** For dendritic innervation: Passed D'Agostino and Pearson omnibus normality test. Paired t-test assuming gaussian distribution number of pairs = 14. p value = 0,0151 * Effective pairing p -value = 0,0004 ***. This experiment has been reproduced twice with similar results.

c) Quantification and image showing a reduction of TH innervation in the *striatum*. Number of mice $n = 3$; number of slices $n = 5$ per mice. Passed D'Agostino and Pearson omnibus normality test. Unpaired t-test assuming equal SD p -value = 0,0180 *.

2. Blocking Engrailed transfer *in vitro* in midbrain primary neurons reduces dendritic length

To assess the effect of the transfer of ENGRAILED from cell to cell *in vitro* we developed a co-culture model constituted of a bottom layer of secondary cultured midbrain astrocytes plated 5 days before adding midbrain primary neurons expressing EN1 (**Fig.2.a**). The astrocytes were either not infected or infected with either AAV8-GFAPscFv or control virus, 3 days before adding the neurons dissociated from embryonic day (E14.5) mouse embryos. This co-culture was maintained for 10 days and then fixed and stained for MAP2 or TUJ1, specific neuronal markers, allowing for dendritic visualization. The GFP staining permits to visualize infected astrocytes, while the Myc-tag allows one to assess the scFv/mut-scFv production (**Fig. 2.b and c**).

As quantified and depicted in **Figure 3**, blocking ENGRAILED transfer significantly reduced by **30%** the mean dendrite length, while the mean intensity of MAP2 and TUJ1 staining in the dendrites remained unchanged. No change was observed in the negative control.

These results implicate that non-cell autonomous ENGRAILED impacts both neuronal survival as observed *in vivo* and dendritic arbour maintenance (*in vivo*) or development (*in vitro*). The latter effect on dendrite growth possibly implies the dynamic of the cytoskeleton.

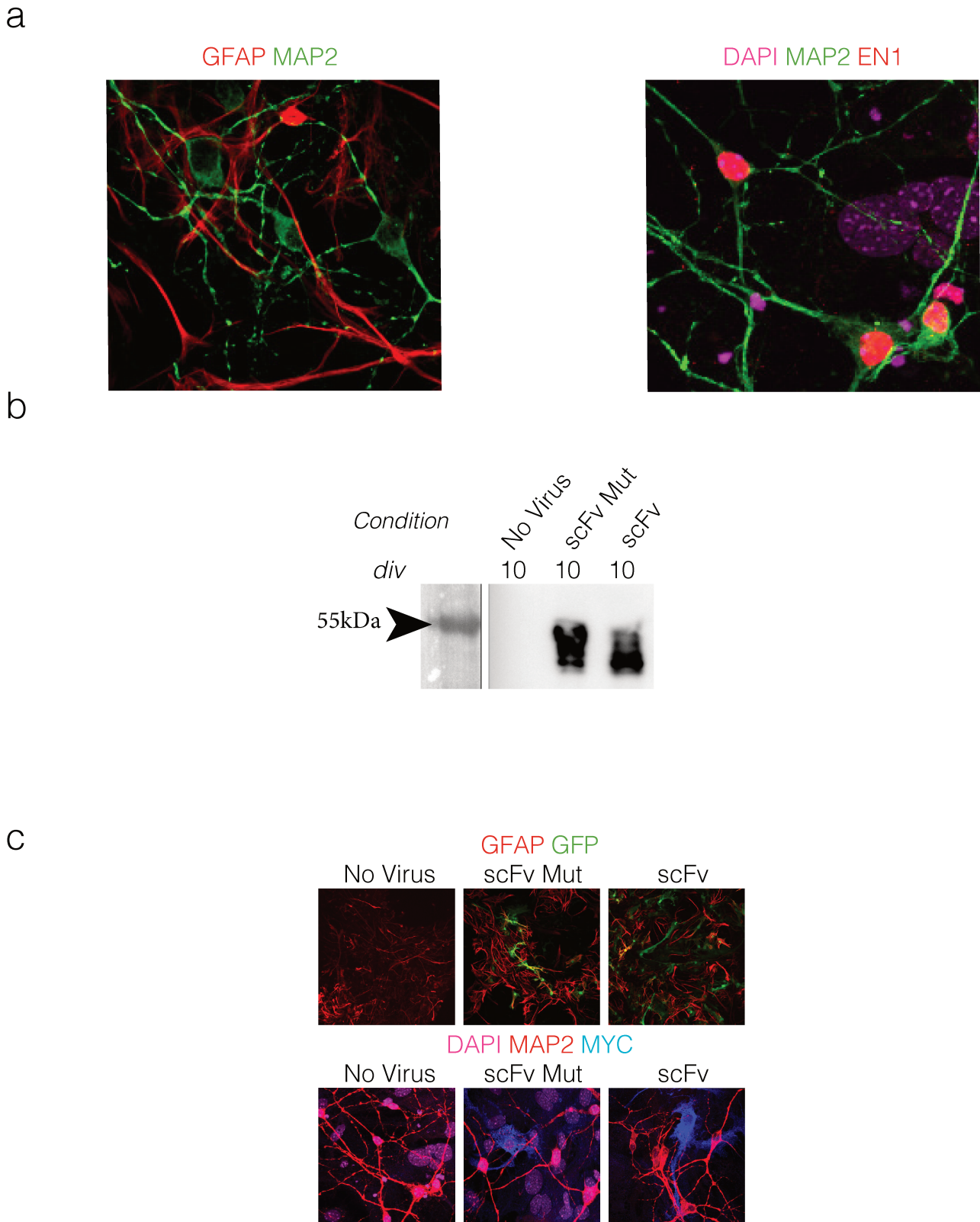


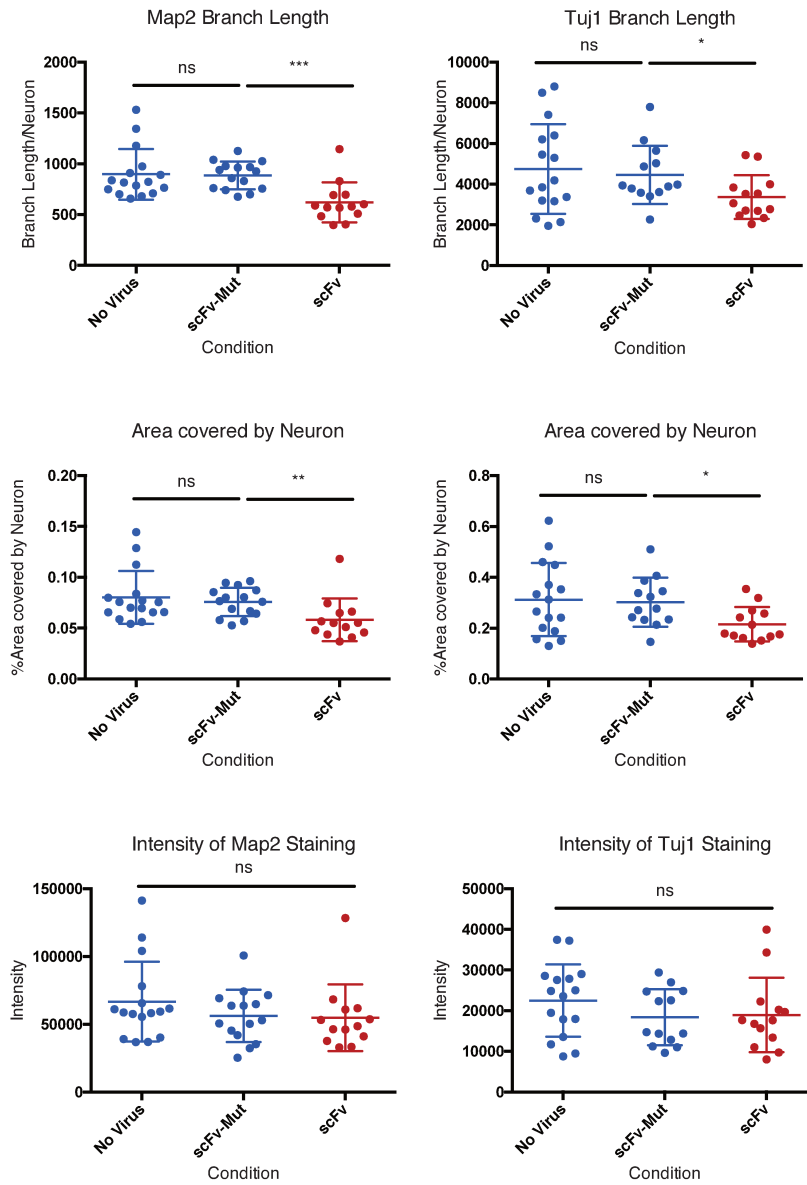
Figure 2 : Co-culture model and production of the scFv in vivo and in vitro

a) Staining against GFAP (red) and MAP2 (green). MAP2-positive neurons (green) are EN1-positive (red)

b) Western blot detection of scFv secretion in 10 days neuron-astrocyte co-cultures following infection by AAV8-GFAP-scFv or AAV8-GFAP-scFv-Mutated. Detection by Western blot using an anti-myc antibody.

c) Infection of astrocytes by the AAV8-GFAP-scFv or AAV8-GFAP-scFv-Mutated showed by GFP reporter and production of the scFv stained by anti-myc (blue).

a



b

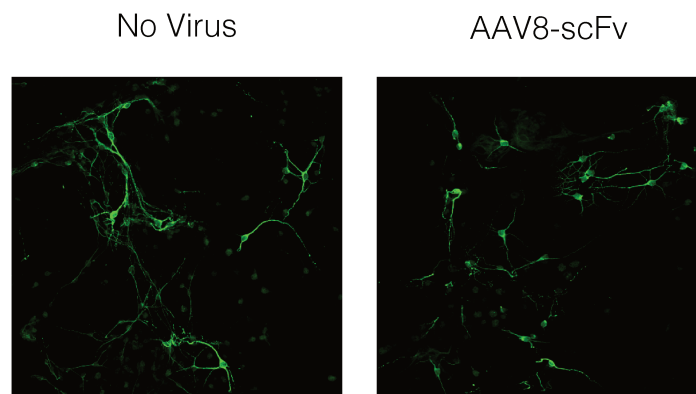


Figure 3: Blocking extracellular *Engrailed* reduces neuropile growth in vitro

a) Quantifications of branch length, area covered and staining intensity for MAP2 (left) or TUJ1 (right) in CTRL (no Virus and scFv Mut) and scFv conditions; n = 393 neurons on 16 images for no virus, n = 351 neurons on 13 images for AAV8-GFAP-scFv, n = 454 neurons on 15 images for AAV8-GFAP-scFv-Mutated)

For MAP2, data did not pass normality test; differences were tested with Kruskal-Wallis / branch length: p-value = 0.004 *** / area: p-value = 0.0024 ** / intensity p-value = 0.3907 ns

For TUJ1, all data passed normality test; differences were tested with Ordinary-One Way Anova. Branch length p-value = 0.0376 * / Area p-value = 0.0259 * / Intensity p-value = 0.8628

b) MAP2 staining of neurons in either no virus or AAV8-scFv

Discussion

Although this study is still in progress, the results presented here demonstrate for the first time a non-cell autonomous autocrine activity of ENGRAILED. However, this autocrine pathway does not exclude a paracrine with EN internalization by non mDA neurons in the *pars reticulata*. The experiments do not allow us to identify the sites from which the protein is secreted and if this activity involves EN1 and EN2 or only one of the two proteins. However, the *in vivo in situ* hybridization studies (Di Nardo 2007) showing that only the EN1 mRNA is present in the dendrites suggest that EN1 is translated locally and secreted locally. This will be investigated in the future, but if it is demonstrated, one will have to identify the signals that trigger EN1 translation and secretion and to investigate whether they are activity dependent.

The survival effect of non-cell autonomous EN was not anticipated. It seems to be also at the origin of the decrease in striatal innervation by TH terminals. One could speculate that this decrease is independent of neuronal death and based on EN1 transport into the axon and local autocrine activity. However, this was not observed (unpublished results) and the neuronal death hypothesis is favoured. Indeed, the 6% decrease in innervation is smaller than the 23% neuronal death, a discrepancy that needs to be explained but might involve compensatory sprouting. An important issue will be to analyse the retrograde information, travelling from dendrites to cell bodies and allowing one to understand how events taking place the level of dendrites can impinge on neuronal survival.

Because we find (Di Nardo et al 2007) that EN1 co-localizes in the dendrites with its mRNA, it can be speculated that the internalized protein has an activity distinct from the one present originally in the dendrites. If so, it would mean that either the internalized protein is modified to exert a novel function or that EN1 is present in distinct compartments before secretion and following re-uptake. However, it could also be proposed that dendritic protein primarily result from internalization, which could be verified by evaluating the amount of distal intra-dendritic EN1 in scFv infected mice.

In previous studies (Bruner 2005, Wizenmann 2009, Settler 2012, Yoon 2017), it was shown that EN1/2 regulates local translation, in particular that of mRNAs encoding mitochondrial complex I proteins with a rapid transient effect (100 seconds) on ATP synthesis (Stetter 2012). Indeed, this can have direct or indirect effects on cytoskeleton components and dynamic. I have

not yet have had the time to investigate this pathway. However, RT-PCR experiments on mRNA extracted from neurons in culture for 10div in presence of the scFv suggest that the effect of eEN is not at a transcriptional level for many cytoskeleton or signalling proteins including *TrkB*, *EphA5*, *Cdc42*, *RhoA*, *Rac1*, *Rock1/2*, *Pak1*, *Arp2/3*, *Actin*, *Tubulin* and *Cofilin1/2* (Figure 4).

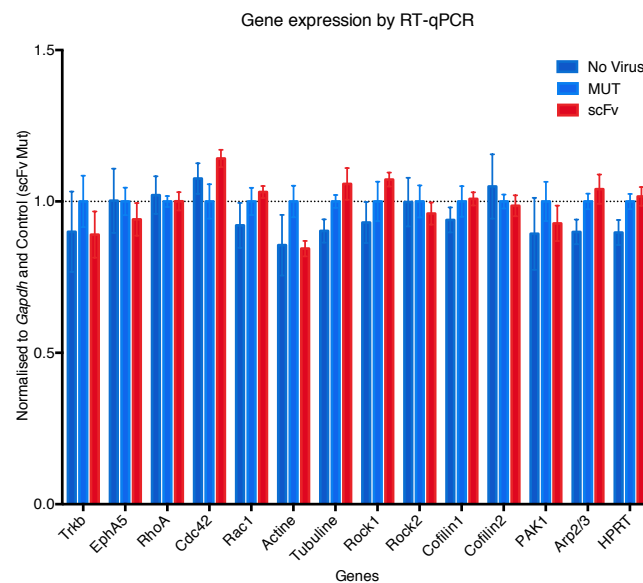


Figure 4: Analysis of Gene Expression implicated in dendritic growth after blockin extracellular Engrailed

The next step will be to analyse which mRNAs are translated in cultures of purified midbrain neurons that express EN1/2 upon EN1 internalization. To that end, we shall use a BAC-TRAP virus (Heiman et al., 2008) that will be expressed in these cells and sequence the mRNAs pulled-down with the polysomes. If the results are of interest to understand the dendrite growth and survival phenotypes, the same BAC-TRAP approach will be used *in vivo*.

Materials and Methods

Animals

Mice were treated as defined by the guidelines for the care and use of laboratory animals (US National Institute of Health) and the European Directive 2010/63/UE. All experimental procedures were validated by the ethical committee (CEA 59) of the French Ministry for Research and Education. Swiss OF1 wt (Janvier) were maintained under a 12 h day/night cycle with ad libitum access to food and water. A maximum of six mice were housed in one cage, and cotton material was provided for mice to build a nest. Experimental groups consisted of three to eight adult male mice. No randomization or blinding was used.

In Vivo stereotaxic injections

For injections, mice were placed in a stereotaxic instrument, and a burr hole was drilled into the skull 3.3 mm caudal and 1 mm lateral to the Bregma. The needle was lowered 3,8 mm from the surface of the skull, and AAV8-GFAP-scFv-GFP/mCherry or AAV8-GFAP-scFvMut-GFP (Vector Biolabs 2 μ l, 10¹³ GC/ μ l) injections were performed over 15 min at day 0.

Co-Culture system

Midbrain primary astrocytes were dissected from P 1 and cultured in DMEM F12 (Life Technologies), 10% FBS (Gibco), High Glucose, PeniStrepto, HEPES. When cells reached confluence, they were detached by trypsination and replated on poly-ornithine/laminin coated wells. Cells were infected where indicated by AAV8-GFAP-scFv-GFP/mCherry or AAV8-GFAP-scFvMut-GFP (Vector Biolabs 2 μ l, 10¹³ GC/ μ l) added into the media. Midbrain primary neurons were dissected from E 14.5 embryos and cultured in Neurobasal medium (Life Technologies) supplemented with glutamine (500 IM, Sigma), glutamic acid (3.3 mg/l Sigma) aspartic acid (3.7 mg/l, Sigma), anti-anti (Gibco), and B27 (Gibco). After 10 days, cells were fixed in 4% PFA (Life Technologies) for 20 min.

Western Blot

For protein separation gels were NuPAGE™ 4-12% Bis-Tris Protein Gels, 1.0 mm, 15-well ThermoFischer Scientific NP0323BOX. The samples migrated in 1X MES or MOPS solution at 200V for 1h. Transfer was performed at 400mA for 1h on PVDF membranes. Membranes were blocked in 5% Milk-TBST 1h, then incubated overnight at 4degrees with primary antibodies in 2.5% Milk-TBST, rinsed 30 min in TBST and incubated 1h at room temperature

with a secondary HRP antibody in 2.5% Milk-TBST. Followed 30min of TBST washes the membranes were revealed with ImageQuant LAS-400 (GE Healthcare). Myc rabbit antibody (Sigma) and Anti-Rabbit HRP were used at a concentration of 1:1000.

Immunostaining

Immunostainings were done as described earlier (Alvarez-Fischer et al, 2011). The following primary antibodies were used: anti-TH chicken (Abcam, ab76442), anti-MAP2 chicken (Abcam), anti-TUJ1 Rabbit (Life Technologies), anti-MYC Rabbit (Sigma), anti-GFAP chicken or mouse (Abcam), anti-GFP chicken (Life Technologies), anti-EN1/2 rabbit (in house), anti-RHOA mouse. All primary antibodies were used at a dilution of 1/500. Secondary antibodies were as follows: 488 anti-chicken, 647 anti-chicken, 488 anti-mouse, 546 anti-mouse, 647 anti-rabbit Alexa Fluor (Life Technologies). Secondary antibodies were used at a dilution of 1/1000. Immuno-cytochemically labelled cell cultures were imaged by confocal microscopy (CSU Yokogawa Spinning Disk W1), brain sections were imaged by confocal microscopy (CSU Yokogawa Spinning Disk W1) as well as by Wide field (Axiozoom Zeiss).

TH cell counting

TH cell counting in conditions comparing ipsi- (treated) and contralateral (control) sides were done as follows: For every brain, a minimum of four serial sections were stained, and the number of TH cells was counted in the SNpc of both ipsi- and contralateral sides. Total mice and number of TH cells were then tested for difference in a paired manner (Ipsi against corresponding Contra side).

Image quantifications

For mean dendritic length of branches, Fiji scripts as well as data treatment in R were written and used in order to compute the total sum of dendritic length. These are supplied in supplementary data (**Sup. 2**) and rely on thresholding, edge detections combined with skeleton analysis plugin. They were elaborated based on publications (Narro et al., 2007) and with guidance by Philippe Maily from the CIRB Orion Platform. Sholl analysis were considered but impossible as cell cultures could not allow isolation of unique neurons. Total length of dendrites was summed and divided by number of neurons providing the mean dendritic length.

RT- qPCR

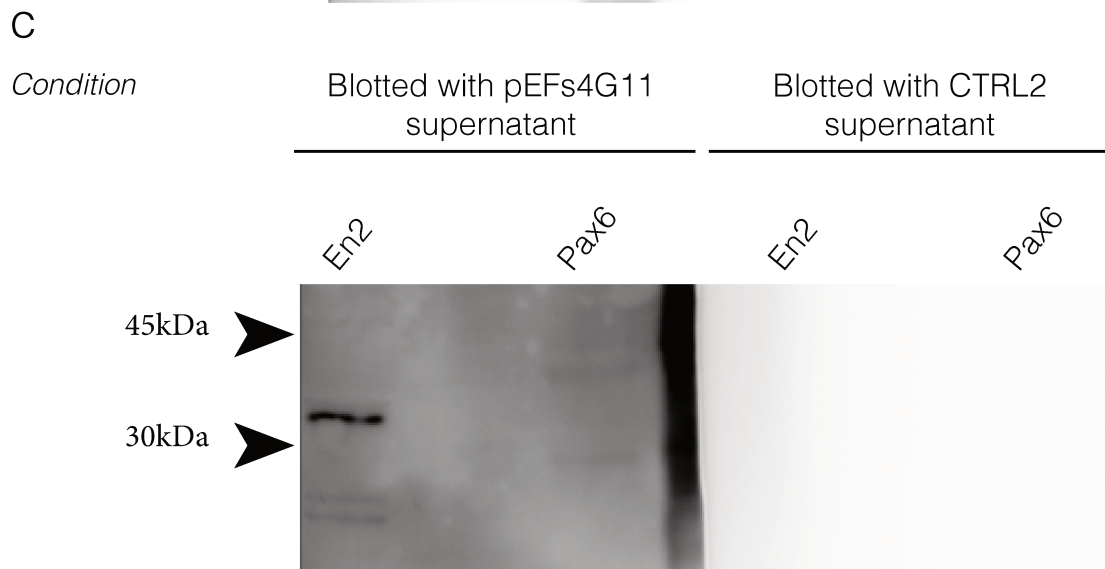
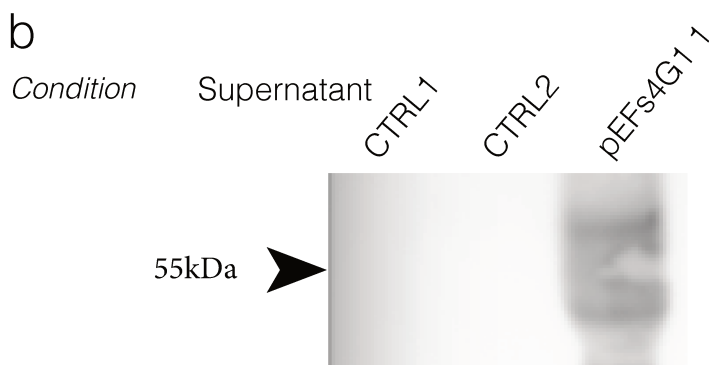
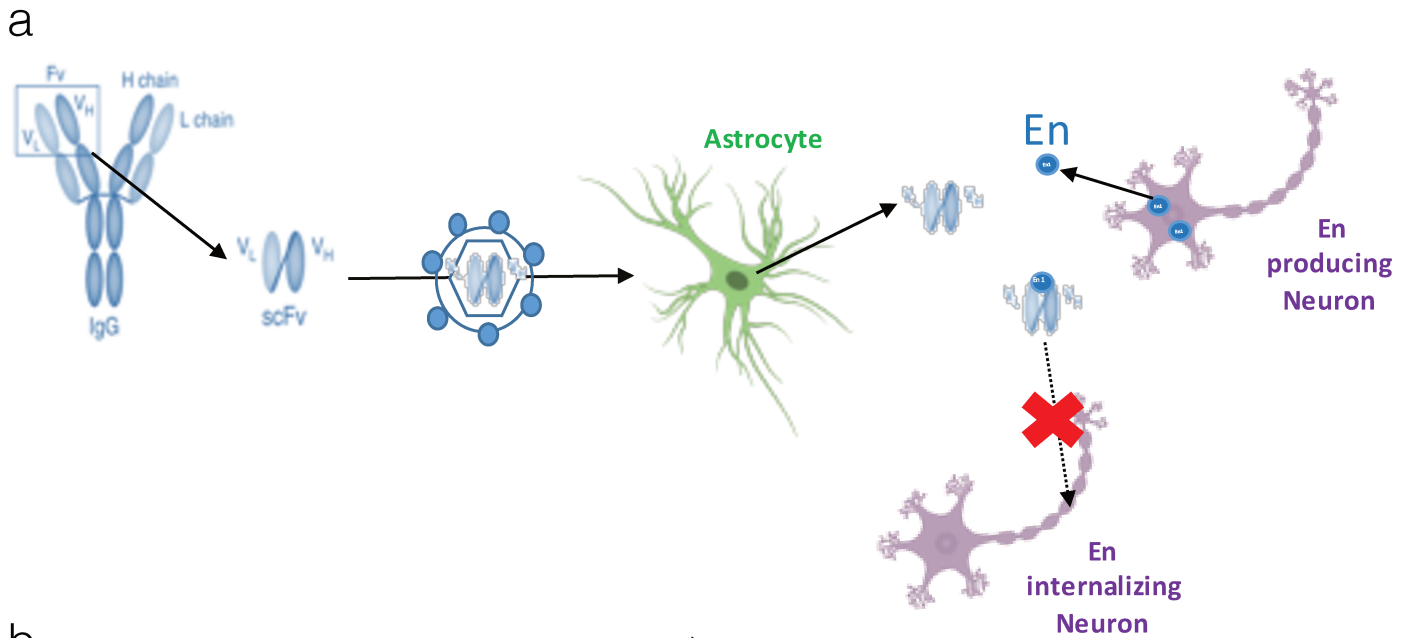
Total RNA from cultures was extracted with the mRNeasy Mini Kit (Qiagen) with DNA removal using Quiazol. RNA was processed with the QuantiTect Reverse Transcription Kit (Qiagen). cDNA was diluted 1:50 with RNase-free water for quantitative PCR samples, which were analyzed in duplicates with a LightCycler 480 II (Roche) and SYBR Green I Master mix. After T_m profile validation, gene expression was determined by the $2^{-\Delta\Delta C_t}$ method with *Hprt* or *Gapdh* as control genes.

GENE	Oligos	GENE2	Oligos3
PAK1/2-F	GCTTTGTCCCAACTGCTGAG	Ephrine A5 F	CTCTGGACGTGCCTTCTCTTGT
PAK1/2-R	AGCAGCTACTGGCGGTG	Ephrine A5 R	AATCTCTCCACCCGTTCTTT
Cofilin1-F	AGACAAGGACTGCCGCTATG	RhoA F	GGTACATGGAGTGTTAGCAAAA
Cofilin1-R	GCTTGATTCTGTCTCAGCTTCT	RhoA R	GTTACAAGGCTTCACAAGATG
Cofilin2-F	CCTCCTTCTCTCGTCCAGT	Cdc42 F	CTAGTTTAGCAAACGTGTCCCC
Cofilin2-R	ACTGTAACCCAGATGCCATAGT	Cdc42 R	CCTTCATGAGTTCATCACAGA
Rock1-F	ATCAGTGGGCTTGGGAAACG	Rac1 F	AAGCTGAAGGAGAAGAAGCTGA
Rock1-R	AAACTTTCCTGCAAGCTTTTATCC	Rac1 R	CAAACACTGTCTTGAGTCCTCG
Rock2-F	GAGTCTGCTGGATGGCTTAAA	GAPDH F	TGACGTGCCGCCTGGAGAAAC
Rock2-R	TTCACCAAAAAGCACCTCTTCCA	GAPDH R	CCGGCATCGAAGGTGGAAGAG
Arp2-F	CTCCGTCCTACCCTCGATTG	HPRT F	AGCAGGTGTTCTAGTCCTGTGG
Arp2-R	AAGGACGCCATCAAAATCTGC	HPRT R	ACGCAGCAACTGACATTTCTAA
TrkB-F	ACGTTTGTCACTCGACCCTC		
TrkB-R	CTCAGGGCTTGCGCGT		

[Supplementary material](#)

Supplemental 1: Validation of the scFv Tool

Supplemental 2: Fiji Scripts for area covered, intensity and dendrite quantifications



Supplemental 1 : Design of scFvEn virus a) The plasmid coding for the single chain antibody tagged by 6xMyc tested *in vitro* is cloned into a viral vector under GFAP promoter in order to be produced by astrocytes. By doing so, we prevent any cell-autonomous effect of the antibody. The single chain is secreted and traps En1/2 in the extra-cellular compartment. b) HEK cells are either not transfected (CTRL1), transfected with eGFP plasmid (CTRL2) or with scFv plasmid (pEFs4G11). As shown by Anti-Myc WB the scFvEn is secreted in the supernatant. c) The scFvEn is specific for En1/2 as the pEFs4G11 supernatant recognizes En2 and not Pax6.

```

#@ File (label = "Output directory for Skeleton Image", style = "directory") output
#@ File (label = "Output directory for Branch information", style = "directory") output2
#@ File (label = "Input directory", style = "directory") input

```

```
processFile(input, output, output2);
```

```

function processFile(input, output, output2) {
    image = getFileList(input);
    image = Array.sort(image);

    setBatchMode(true);

    for (i = 275 ;i<image.length; i++) {
        if (endsWith(image[i], "561.TIF") && indexOf(image[i], "thumb") <= -1) {
            open(image[i]);
            run("Z Project...", "projection=[Max Intensity]");
            run("Median...", "radius=3");
            run("Tubeness", "sigma=1.00 use");
            setThreshold(9, 900);
            setOption("BlackBackground", false);
            run("Convert to Mask");
            rename("Threshold"+image[i]);
            save(output2 + "Threshold"+image[i]);

            open(image[i]);
            run("Z Project...", "projection=[Max Intensity]");
            run("Median...", "radius=3");
            run("Tubeness", "sigma=1.00 use");
            setMinAndMax(9, 65535);
            setAutoThreshold("Default dark no-reset");
            run("Find Edges");
            rename("Edges "+image[i]);
            imageCalculator("AND create", "Threshold"+image[i],"Edges "+image[i]);
            selectWindow("Result of Threshold"+image[i]);
            save(output2 + "Somme"+image[i]);
            selectWindow("Threshold"+image[i]);
            run("8-bit");
            run("Skeletonize (2D/3D)");
            run("Analyze Skeleton (2D/3D)", "prune=none show");
            saveAs(".tiff", output + "/Skeleton Image " +image[i]+".tiff");
            selectWindow("Branch information");
            saveAs("Results", output2 + "/Branch information " +image[i]+".csv");
            close("Results");
            close("Branch information");
        }
    }
}

```

```

#@ File (label = "Output directory for Zone d'innervation", style = "directory") output
#@ File (label = "Output directory for Intensite du signal", style = "directory") output2
#@ File (label = "Output directory for Images Zone d'innervation", style = "directory") output3
#@ File (label = "Input directory", style = "directory") input

```

```
processFile(input, output, output2);
```

```

function processFile(input, output, output2) {
    image = getFileList(input);
    image = Array.sort(image);

    for (i = 0 ;i<image.length; i++) {
        if (endsWith(image[i], "642.TIF")) {
            open(image[i]);
            run("Z Project...", "projection=[Max Intensity]");
            run("Median...", "radius=3");
            run("Tubeness", "sigma=1.00 use");
            setAutoThreshold("Huang dark no-reset");

```

```

setOption("BlackBackground", false);
run("Convert to Mask");
run("Set Measurements...", "area area_fraction limit redirect=None decimal=3");
run("Measure");
saveAs("Results", output+"/Zone d'innervation "+image[i]+".csv");
close("Results");

run("Analyze Particles...", "size=10-Infinity circularity=0.0-1.00 show=Outlines display clear summarize add");

selectWindow("tubeness of MAX_"+image[i]);

rename("Analyse particles " + image[i]);
saveAs(".tiff", output3 + "/Analyse particles " +image[i]+".tiff");
close("Results");
close("Summary");
selectWindow(image[i]);
run("Z Project...", "projection=[Max Intensity]");
run("Set Measurements...", "mean area_fraction limit redirect=None");
selectWindow("MAX_"+image[i]);
roiManager("Show None");
roiManager("Show All");
roiManager("Measure");
saveAs("Results", output2+"/Intensite du signal "+image[i]+".csv");
run("Close All");
close("Results");
}}

```

ENGRAILED homeoprotein blocks degeneration in adult dopaminergic neurons through LINE-1 repression

Summary and objectives:

The aim of this project was to decorticate the link between ENGRAILED and L1 elements in the degeneration of midbrain dopaminergic (mDA) neurons. Indeed, *En1*^{+/-} mice depict a progressive loss of mDA neurons accompanied by DNA strand breaks and genomic instability. As *En1*^{+/-} mice also exhibit an increase in the expression of L1 elements, we questioned whether L1 elements could play a role in mDA neurodegeneration.

We carried out loss of function (LOF) of L1 elements by three different means: a siRNA approach, a PIWI gain of function (GOF) as well as the inhibition of reverse transcriptases by the drug stavudine. We successfully rescued the mDA neurons from death and reduced the number of DNA breaks in acute oxidative stress models as well as in the *En1*^{+/-} mice.

We further demonstrate that ENGRAILED is an endogenous repressor of L1 elements by direct binding to the L1 promoter.

Engrailed homeoprotein blocks degeneration in adult dopaminergic neurons through LINE-1 repression

François-Xavier Blaudin de Thé[†], Hocine Rekaik[†], Eugenie Peze-Heidsieck[†], Olivia Massiani-Beaudoin, Rajiv L Joshi, Julia Fuchs^{*}  & Alain Prochiantz 

Abstract

LINE-1 mobile genetic elements have shaped the mammalian genome during evolution. A minority of them have escaped fossilization which, when activated, can threaten genome integrity. We report that LINE-1 are expressed in substantia nigra ventral midbrain dopaminergic neurons, a class of neurons that degenerate in Parkinson's disease. In *Engrailed-1* heterozygotes, these neurons show a progressive degeneration that starts at 6 weeks of age, coinciding with an increase in LINE-1 expression. Similarly, DNA damage and cell death, induced by an acute oxidative stress applied to embryonic midbrain neurons in culture or to adult midbrain dopaminergic neurons *in vivo*, are accompanied by enhanced LINE-1 expression. Reduction of LINE-1 activity through (i) direct transcriptional repression by *Engrailed*, (ii) a siRNA directed against LINE-1, (iii) the nucleoside analogue reverse transcriptase inhibitor stavudine, and (iv) viral *Piwi1* expression, protects against oxidative stress *in vitro* and *in vivo*. We thus propose that LINE-1 overexpression triggers oxidative stress-induced DNA strand breaks and that an *Engrailed* adult function is to protect mesencephalic dopaminergic neurons through the repression of LINE-1 expression.

Keywords dopaminergic neurons; *Engrailed* adult functions; L1 retrotransposons; neurodegeneration; oxidative stress

Subject Categories Chromatin, Epigenetics, Genomics & Functional Genomics; Neuroscience

DOI 10.15252/embj.201797374 | Received 17 May 2017 | Revised 7 May 2018 | Accepted 28 May 2018 | Published online 25 June 2018

The EMBO Journal (2018) 37: e97374

Introduction

More than half of the mammalian genome derives from active or fossilized transposable elements (Lander *et al*, 2001; de Koning *et al*, 2011). Among them, Long Interspersed Elements (LINEs) are

the most abundant representing $\approx 21\%$ of the human genome (Lander *et al*, 2001). LINE-1 (L1), a subfamily of the non-LTR LINE retrotransposons, are the only active mobile elements in the human genome “jumping” from one genomic position to another by retrotransposition (reviewed in Beck *et al*, 2011). Of more than 500,000 copies in the human genome, most are truncated, rearranged, or otherwise mutated leaving approximately 100 full-length L1 elements in the human (Brouha *et al*, 2003) and 3,000 in the mouse (Goodier *et al*, 2001). Full-length L1 elements are comprised of a 6–8 kB sequence containing a promoter in the 5'UTR, two open reading frames (ORFs), and a 3'UTR with a poly(A) tail. ORF1 encodes an RNA-binding protein with strong *cis* preference, and ORF2 encodes an endonuclease, which creates a DNA strand break (DSB), and a reverse transcriptase (Beck *et al*, 2011). The full-length L1 sequence provides thus all the necessary machinery for mobilization and expansion in the genome.

Until recently, full-length L1 were thought to be primarily expressed in germ cells in conditions alleviating the strong repressive activities of Piwi proteins of the Argonaut family (Siomi *et al*, 2011). These conditions correspond to an endangering stress, and the resulting L1-induced mutations in germ cells have been described as the last line of defense of organisms in highly unfavorable environmental conditions (Siomi *et al*, 2011). This view has changed with the finding that mobile elements are also active in somatic tissues, particularly in the brain (Erwin *et al*, 2014). L1 activity has been demonstrated in dividing neural stem cells (Muotri *et al*, 2005), but a few reports provide data supporting the existence of L1 activity and retrotransposition in non-dividing cells (Kubo *et al*, 2006) and in post-mitotic neurons (Evrony *et al*, 2012; Macia *et al*, 2017). As in the germline, L1 become activated primarily upon stress, during aging (Li *et al*, 2013) and in age-related diseases (Li *et al*, 2012).

Mesencephalic dopaminergic (mDA) neurons from the substantia nigra pars compacta (SNpc) become dysfunctional during aging with a decrease in SNpc volume in non-human primates (Collier *et al*, 2007) and in humans (Alho *et al*, 2015). This dysfunction can be accelerated and associated with mDA neuron death in response

to specific mutations or environmental stressors, such as exposure to neurotoxins, giving rise to Parkinson's disease (PD; Kalia & Lang, 2015). Various mouse models of PD exist based on toxin administration or on mutations in genes that cause familial PD. A recent murine model, with a progressive degeneration of mDA neurons along with motor and non-motor phenotypes, consists in the deletion of one allele of *Engrailed-1* (*En1*; Sonnier et al, 2007; Nordström et al, 2015). Engrailed-1 (*En1*) is a homeoprotein transcription factor specifically expressed in adult mDA neurons together with its paralogue Engrailed-2 (*En2*). In the absence of one *En1* allele (*En1*-het mouse), mDA neurons die faster and, after 1 year, their number in the SNpc is reduced to 62% of that observed in wild-type (wt) siblings. Dopaminergic cell death is less pronounced in the ventral tegmental area (VTA), as also observed in PD (Sonnier et al, 2007).

En1 and *En2* (collectively Engrailed or *En1/2*) are biochemically equivalent in the midbrain (Hanks et al, 1995) and, similarly to most homeoproteins, are secreted and internalized by live cells (Joliot & Prochiantz, 2004). The latter property has allowed us to use *En1* and *En2* as therapeutic proteins in the *En1*-het mice and in three other mouse models of PD: 1-methyl-4-phenyl-1,2,3,6-tetrahydropyridine (MPTP) or 6-hydroxydopamine (6-OHDA) intoxication and the injection of cell-permeable mutated (A30P) α -synuclein (Sonnier et al, 2007; Alvarez-Fischer et al, 2011). More recently, we have shown that mDA neurons from *En1*-het mice show signs of, and are more sensitive to, oxidative stress. In particular, they present numerous DSBs, a strong alteration of several epigenetic marks and an abnormal expression of genes primarily in the chromatin remodeling and DNA damage response (DDR) pathways (Rekaik et al, 2015). Accordingly, following the local injection of 6-OHDA, a drug that induces oxidative stress and that mDA neurons capture specifically, wt mDA neurons exhibit similar changes in their epigenetic marks and enter cell death. Subsequent Engrailed injection into the SNpc blocks cell death and restores all examined epigenetic marks in the surviving neurons (Rekaik et al, 2015).

The latter experiments suggest that Engrailed is important to protect mDA neurons against oxidative stress associated with normal or pathological aging and demonstrate that part of this protection is associated with heterochromatin maintenance. Following the idea that the expression of L1 and other mobile elements increases with heterochromatin loss (Wang & Elgin, 2011), with age (Van Meter et al, 2014), in some neurodegenerative diseases (Li et al, 2012; Tan et al, 2012), and in conditions of oxidative stress (Giorgi et al, 2011), we undertook to explore a possible relationship between L1 expression and Engrailed protective activity. The results demonstrate that Engrailed represses the expression of L1 mobile elements in neurons within its expression territory, in particular by adult mDA neurons, and that this repression protects these neurons against oxidative stress negative effects.

Results

L1 families are expressed in adult mDA neurons

Analysis of next-generation RNA sequencing (RNA-Seq) data of RNA extracted from laser microdissected SNpc from 6-week-old wt

Swiss OF1 mice (Rekaik et al, 2015; GEO accession number: GSE72321) showed that the three main active L1 families (A, Tf, and Gf) are expressed, with a number of reads for the Tf and A subfamilies in the same order than that found for tyrosine hydroxylase (*Th*), a strongly expressed marker of mDA neurons (Fig 1A). This was confirmed on SNpc tissue punches by RT-qPCR, using primers in the 5'UTR of L1 Tf/Gf or L1 A (Fig 1A).

Thanks to its poly(A) tail (Doucet et al, 2015), L1 mRNA was purified from adult mouse ventral midbrain tissue on oligo-dT columns to ensure the presence of the 3'UTR, digested with DNase and reverse-transcribed with oligo-dT primers. PCR was achieved with forward and reverse primers in the 5'UTR and 3' region of Orf2, respectively (Fig 1B). L1 amplicons of the Tf/Gf and A families are detectable at the expected sizes (Fig 1B), and enzyme digestion patterns were as expected (data not shown). Amplicon identity was confirmed by Sanger sequencing in three regions, the 5'UTR, Orf1, and Orf2. The sequenced amplicons obtained with the L1 Tf/Gf-specific 5'UTR forward primer were pairwise aligned (EMBOSS Water) to a consensus sequence of the L1 subfamily L1 Tf (L1spa; GenBank AF016099.1; Fig EV1) and those obtained with a primer in the L1 A 5'UTR to a consensus L1 A sequence, respectively (L1 A; GenBank AY053455.1; data not shown).

Expression of full-length L1 in the adult ventral midbrain is further demonstrated by L1 mRNA translation into protein, as shown in Fig 1C where L1 Orf1p was identified by Western blot. Further, L1 expression in post-mitotic mDA neurons was verified, and Fig 1D–F illustrate by immunohistochemistry and *in situ* hybridization the co-localization of TH and Orf1p (Fig 1D and F) and L1 Tf RNA (Fig 1E).

L1 expression in the ventral midbrain is not exclusive to mDA neurons as other neuronal subtypes, identified in Fig 1D by NeuN staining, also express Orf1p. However, Orf1p staining intensity is significantly higher in TH⁺ neurons compared to adjacent neurons as quantified in Fig 1D. Figure 1F shows, by double immunohistochemistry, that Orf1p is present in all TH-positive mDA neurons in the SNpc. The specificity of the staining was verified by the neutralizing effect of the polypeptide used to raise the anti-Orf1p antibody (Fig 1C and F).

Figure 1G further shows that brain L1 expression is not limited to the ventral midbrain but is present in other brain regions. Expression is generally higher in neural tissues than in heart or kidney and more abundant in testis. We also compared the expression of Piwi genes in the same tissues (Fig 1H). Piwil1, 2, and 4 are expressed at extremely low levels compared to the expression in the testis (logarithmic scale). The comparison between testis and brain for L1 and Piwi expression suggests that other repressive mechanisms than Piwi proteins might be operative in the brain to restrain L1 activity.

This series of experiments demonstrates that L1 RNA is expressed in different brain regions and that full-length L1 RNA and the Orf1 protein are expressed in post-mitotic ventral midbrain neurons and, most particularly, in mDA SNpc neurons.

Kinetic analysis of oxidative stress-induced L1 expression and DNA damage *in vitro* and *in vivo*

Midbrain DA neurons are particularly sensitive to oxidative stress due to sustained intrinsic activity and dopaminergic metabolism,

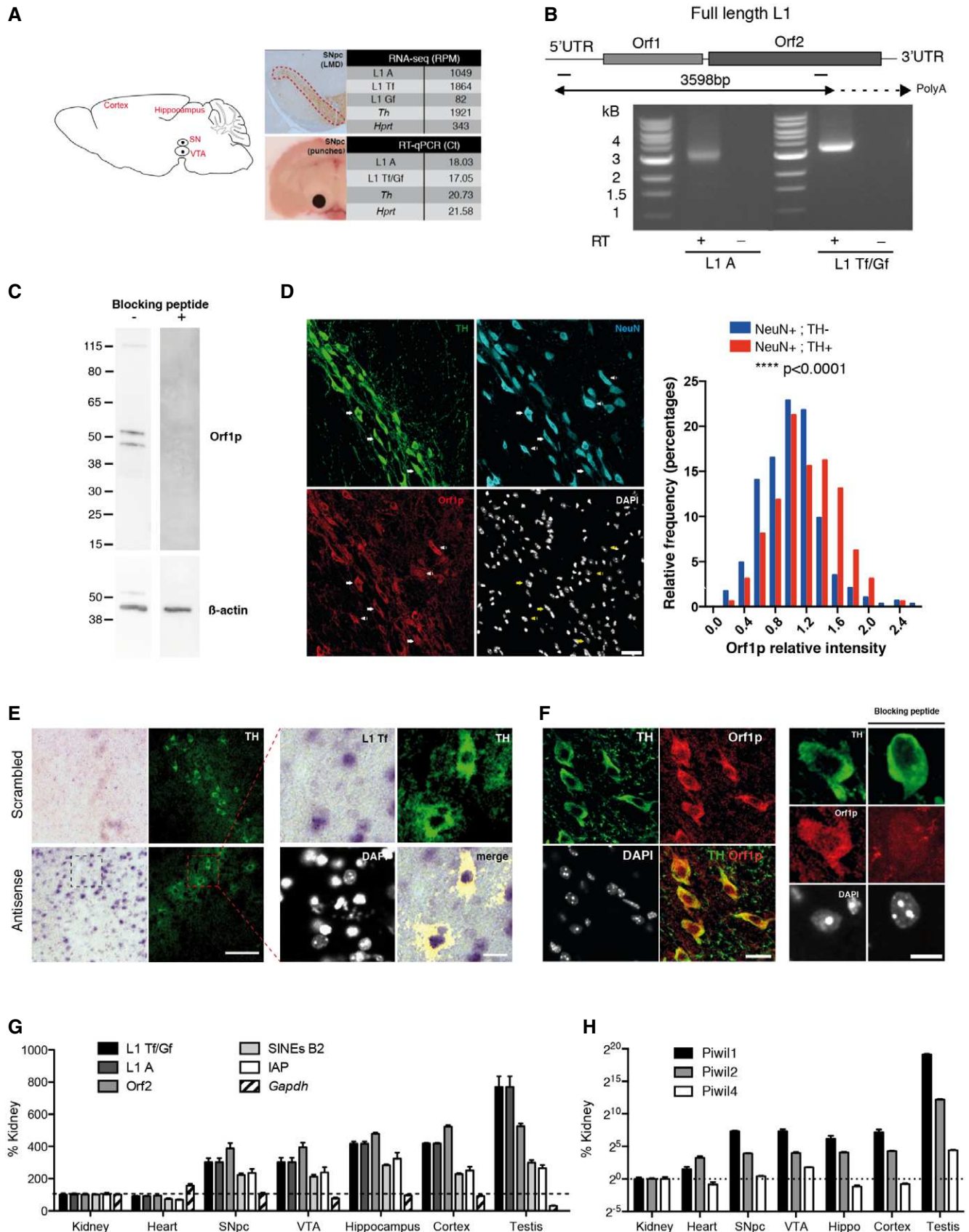


Figure 1.

Figure 1. Full-length L1 elements are expressed in the adult mouse ventral midbrain and in TH⁺ neurons of the SNpc.

- A RNA from the three main L1 families (A, Tf, and Gf), *Hprt*, and *Th* was measured in RNA-Seq data on laser microdissected SNpc [GEO accession number GSE72321 (Rekaik *et al*, 2015)] and by RT-qPCR in SNpc tissue punches. RPM, reads per million; Ct, qPCR cycle threshold.
- B Poly(A)⁺ RNA was purified from manually microdissected ventral midbrain, digested with DNase I, and reverse-transcribed with oligo(dT) primers. The sequence between the 5'UTR and Orf2 was amplified by PCR (the position of the primers is indicated by two bars) and sequenced. The experiment was also done using the RT buffer but not the enzyme (RT⁻) to control for genomic DNA contamination. Local alignments of the L1 Tf/Gf amplicons to a L1 Tf consensus sequence are shown in Fig EV1.
- C Orf1p from ventral midbrain was measured using Western blot analysis (first lane). The same experiment was made but this time blocking the antibody with the Orf1p peptide before incubation (second lane).
- D Midbrain slices were analyzed by immunofluorescence against Orf1p in TH⁺, NeuN⁺, or TH⁻ NeuN⁺ neurons, and Orf1p fluorescence intensity distribution was measured (right). Scale bar represents 30 μ m. **** $P < 0.0001$; $n = 284$ NeuN⁺/TH⁻ neurons, and $n = 160$ NeuN⁺/TH⁺ neurons were quantified from three mice (three sections per mouse); two-sample Kolmogorov-Smirnov test.
- E Midbrain slices were analyzed by *in situ* hybridization with L1 Tf 5'UTR oligonucleotide antisense probes in TH⁺ neurons of the SNpc (labeled by immunofluorescence). Scrambled probes were used as a negative control (left). The right panels show an enlargement of the region delineated by a square. Scale bars represent 100 and 20 μ m (left and right panels, respectively).
- F Midbrain slices were analyzed by immunofluorescence against Orf1p in TH⁺ neurons. The same experiment was made blocking the antibody with the Orf1p peptide. Scale bars represent 20 and 10 μ m (left and right panels, respectively).
- G RNA from neuronal and non-neuronal tissues was analyzed for L1 expression by RT-qPCR with primers located in the 5'UTR for subfamily detection (L1 Tf/Gf, L1 A) and in Orf2. Cycle thresholds from tissues obtained from three mice were normalized to values obtained from kidney tissues using the ddCt method relative to the expression of *Gapdh*; error bars represent SEM.
- H RNA from neuronal and non-neuronal tissues was analyzed for Piwi family expression by RT-qPCR. Cycle thresholds from tissues obtained from three mice were normalized to values obtained from kidney tissues using the ddCt method relative to *Gapdh*; error bars represent SEM.

itself a generator of oxidant molecular species (Chen *et al*, 2008). Following reports highlighting an induction of L1 elements upon stress in different systems (Rockwood *et al*, 2004; Giorgi *et al*, 2011), we tested whether oxidative stress modifies L1 expression in midbrain neurons in culture and in adult mDA neurons *in vivo*.

Embryonic day 14.5 (E14.5) ventral midbrain mouse neurons, which at this stage all express Engrailed but of which mDA neurons represent a small percentage, were cultured for 7 days. H₂O₂ was then added to the culture for 1 h, thus inducing an oxidative stress to all neurons. The analysis was limited to 1 h of H₂O₂ exposure because DNA damage is still repairable under these conditions. We followed L1 transcription by fluorescence *in situ* hybridization (FISH) at different time points and observed that L1 transcription, as measured by the number of L1 foci and foci intensity, is significantly increased already after 15 min of stress and stays so for at least 1 h (Fig 2A). The increase in L1 transcription thus reflects the recruitment of new L1 expression foci as well as an increase in expression at L1 foci. A simultaneous analysis of DNA break formation by γ -H2AX staining and quantification reveals that DSBs are detectable posterior to the increase in L1 transcription.

A strong oxidative stress was then inflicted *in vivo* to mDA neurons specifically, by injecting 6-OHDA at the level of the SNpc, and immunostaining for Orf1p was performed. Figure 2B illustrates and quantifies the increase in L1 expression observed 3 h after stress and also establishes that this increase does not take place in TH-negative neurons that do not capture 6-OHDA due to the absence of a DA uptake mechanism.

To have a better idea of the kinetics, we followed DNA guanine oxidation, DSB formation (γ -H2AX staining) in TH-positive cells, and the increase in L1 Tf/Gf transcripts in SNpc tissue punches 15 min, 1 h, and 3 h after injection of 6-OHDA. Figure 2C demonstrates that guanine oxidation in TH-positive cells is significantly increased 1 h post-stress and remains stable thereafter, while DNA breaks appear only between 1 and 3 h specifically on the injected side. In comparison, the same Figure (right panel) shows that an

increase in L1 Tf/Gf expression, already observable 15 min post-stress, is pursued for 1 h and followed by a slight expression decrease during the following hours (Fig 2C), but still significantly higher at 6 h compared to the non-injected side (Fig EV2A).

Data on the activation of other stress pathways in the same punch biopsies can be found in Fig EV2B. *TH* expression was not modified confirming that no dopaminergic cell death takes place during this time frame (Rekaik *et al*, 2015).

L1 transcription is part of the H₂O₂-induced DNA strand break pathway

Following the nuclear import of the L1 ribonucleoprotein complex, the *Orf2*-encoded endonuclease generates one or several nicks in the DNA, and L1 RNA reverse transcription is initiated at the newly generated 3'OH terminus by target-site primed reverse transcription (Beck *et al*, 2011). The kinetics demonstrating that DSB formation is detectable posterior to the oxidative stress-induced L1 transcriptional increase led us to envisage that part of these breaks may be a consequence of L1 overexpression.

The classical repressor pathway of L1 involves the Argonaut proteins of the Piwi family that bind piRNAs and block LINE transcription (Kuramochi-Miyagawa *et al*, 2008). As shown in Fig 1H, Piwi family members are expressed at low levels in the adult brain, including in the SNpc. The most highly expressed Piwi is Piwil1 (mouse Miwi), which was thus used as a tool to inhibit L1 expression. To verify a protective effect of Piwil1, midbrain neurons were infected with an AAV2 expressing Piwil1 and exposed to H₂O₂. As a negative control, neurons were infected with the same viral vector expressing GFP and also exposed to H₂O₂. As illustrated (left) and quantified (right) in Fig 3A, the strong H₂O₂-induced L1 transcription (FISH analysis) and DSB formation observed in the control condition (AAV2-GFP) are antagonized by Piwil1 expression (AAV2-Piwil1).

To further ascertain the ability of Piwil1 to protect midbrain neurons against oxidative stress, the protein was expressed by transfection together with GFP. This allowed us to count in the same

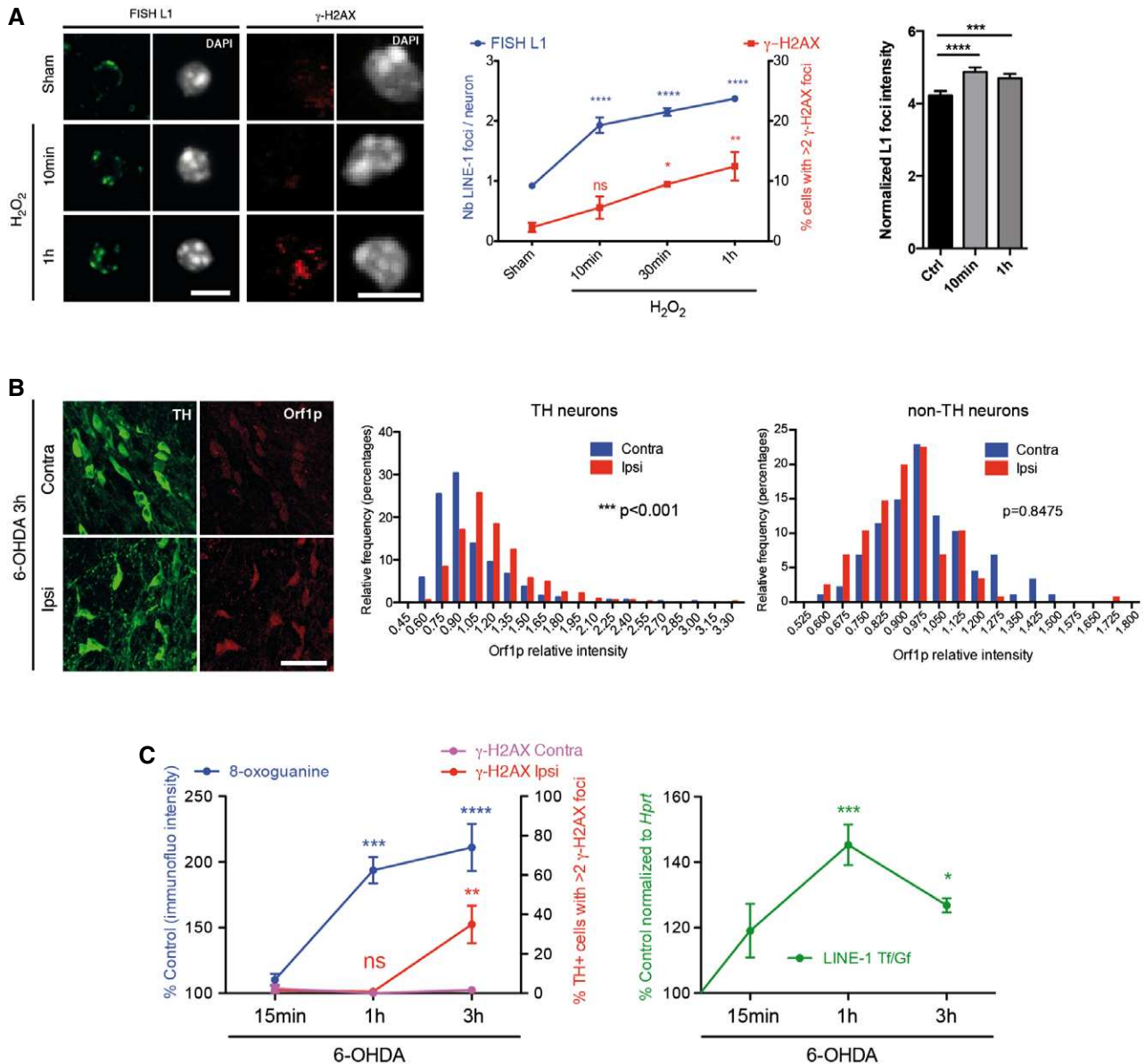


Figure 2. Kinetics of L1 activation and DNA strand breaks induced by oxidative stress *in vitro* and *in vivo*.

A Midbrain primary neurons were treated with H_2O_2 , active L1 transcription sites were analyzed by fluorescence *in situ* hybridization (FISH), and DNA damage was revealed by γ -H2AX immunofluorescence (left) and quantified (middle) at different time points. Scale bars represent 5 μ m. * P < 0.05; ** P < 0.01; **** P < 0.0001; n = 4 wells per condition; 150 neurons were counted per condition; one-way ANOVA with Dunnett's multiple comparison test; error bars represent SEM. L1 FISH foci fluorescence intensity was quantified at the same time points (right). **** P < 0.001; **** P < 0.0001; n = 208 foci per condition from three different wells; Kruskal–Wallis test with Dunn's multiple comparisons test; error bars represent SEM.

B Midbrain sections were stained for Orf1p, 3 h after 6-OHDA injection and analyzed by confocal microscopy (left), and Orf1p fluorescence intensity distribution was measured in TH (middle) and non-TH (right) neurons. Scale bar represents 50 μ m; **** P < 0.001; For Orf1p quantification, 370 (ipsilateral; injected) and 326 (contralateral; non-injected) TH neurons and 100 (ipsi) and 120 (contra) non-TH neurons were analyzed from three mice (three sections per mouse); two-sample Kolmogorov–Smirnov test.

C Midbrain sections were stained at several time points after 6-OHDA injection and analyzed by confocal microscopy for 8-oxoguanine (left panel left axis) and γ -H2AX (left panel right axis). L1 transcription was measured by RT–qPCR at the same time points in SNpc punches (right panel Ctrl at 100%). * P < 0.05; ** P < 0.01; *** P < 0.001; **** P < 0.0001; n = 4 for γ H2AX, n = 6 mice per condition for 8-oxoguanine, n = 5 mice per condition for RT–qPCR; the statistical testing was performed as compared to 15 min time point (left) or to control condition (right) using one-way ANOVA with Bonferroni's multiple comparison test; error bars represent SEM.

dishes the number of γ -H2AX foci in cells expressing or not Piwil1 (based on GFP expression). As illustrated and quantified in Fig 3B, the decrease in the number of γ -H2AX foci is only seen in transfected cells.

This series of experiments brings strong evidence in favor of an important implication of L1 expression in the formation of DNA breaks and shows that overexpression of Piwil1 represses H_2O_2 -induced L1 transcription and DNA damage.

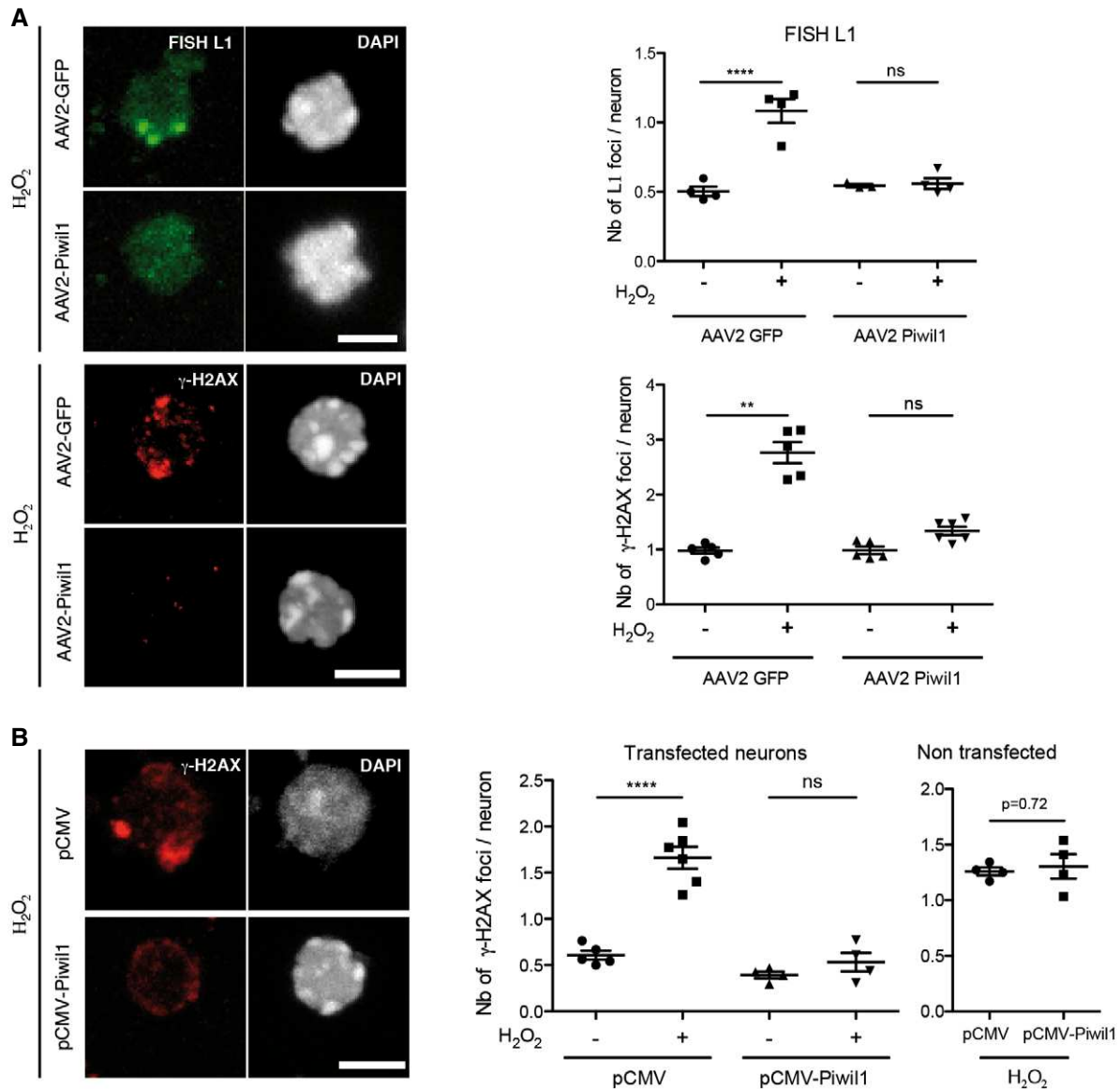


Figure 3. Piwil1 overexpression protects *in vitro* against oxidative stress-induced DNA damage.

A Midbrain primary neurons were infected with an AAV2-Piwil1 or AAV2-GFP for 1 week. Neurons were then treated with H₂O₂ for 1 h, L1 transcription was analyzed by FISH (top panel), and DNA damage was examined by γ-H2AX immunofluorescence (bottom panel). Quantifications are shown on the right. Scale bars represent 5 μm. ***P* < 0.01; *****P* < 0.0001; *n* = 3–4 for FISH and *n* = 5–6 for γ-H2AX wells per condition, 300–400 neurons were quantified per condition; one-way ANOVA with Tukey's multiple comparisons test for FISH quantification and Kruskal–Wallis test with Dunn's multiple comparisons test for γ-H2AX; error bars represent SEM.

B Midbrain primary neurons were transfected with pCMV-GFP and pCMV-Piwil1 or pCMV-GFP and a void pCMV plasmid for 48 h, after which neurons were treated with H₂O₂ for 1 h. DNA damage was then analyzed by γ-H2AX immunofluorescence in either transfected (GFP⁺) or untransfected (GFP⁻) neurons (left) and quantified (right). Scale bar represents 5 μm. *****P* < 0.0001; *n* = 4–6 wells per condition, 200 neurons were quantified per condition; ANOVA with Tukey's multiple comparisons test was used for transfected neurons and Student's *t*-test for untransfected neurons; error bars represent SEM.

L1 expression and activity lead to DNA damage and neuronal death

To directly evaluate whether L1 activation induces DNA damage, embryonic midbrain neurons were transfected with a mouse codon-optimized L1 expression vector containing the endogenous L1 5'UTR promoter downstream of a CMV promoter (Newkirk *et al*, 2017). As illustrated and quantified in Fig 4A, the average number

of DNA breaks identified by γ-H2AX staining was increased by the expression of L1 but not by that of the same L1 expression vector carrying a double mutation abolishing Orf2p reverse transcriptase and endonuclease activities as in (Xie *et al*, 2011).

L1 activity requires the transcription and translation of its bicistronic mRNA followed by reverse transcription. To inhibit reverse transcription, we used stavudine (2',3'-dideohydro-2',3'-dideoxythymidine, d4T), a nucleoside analogue and strong L1 reverse

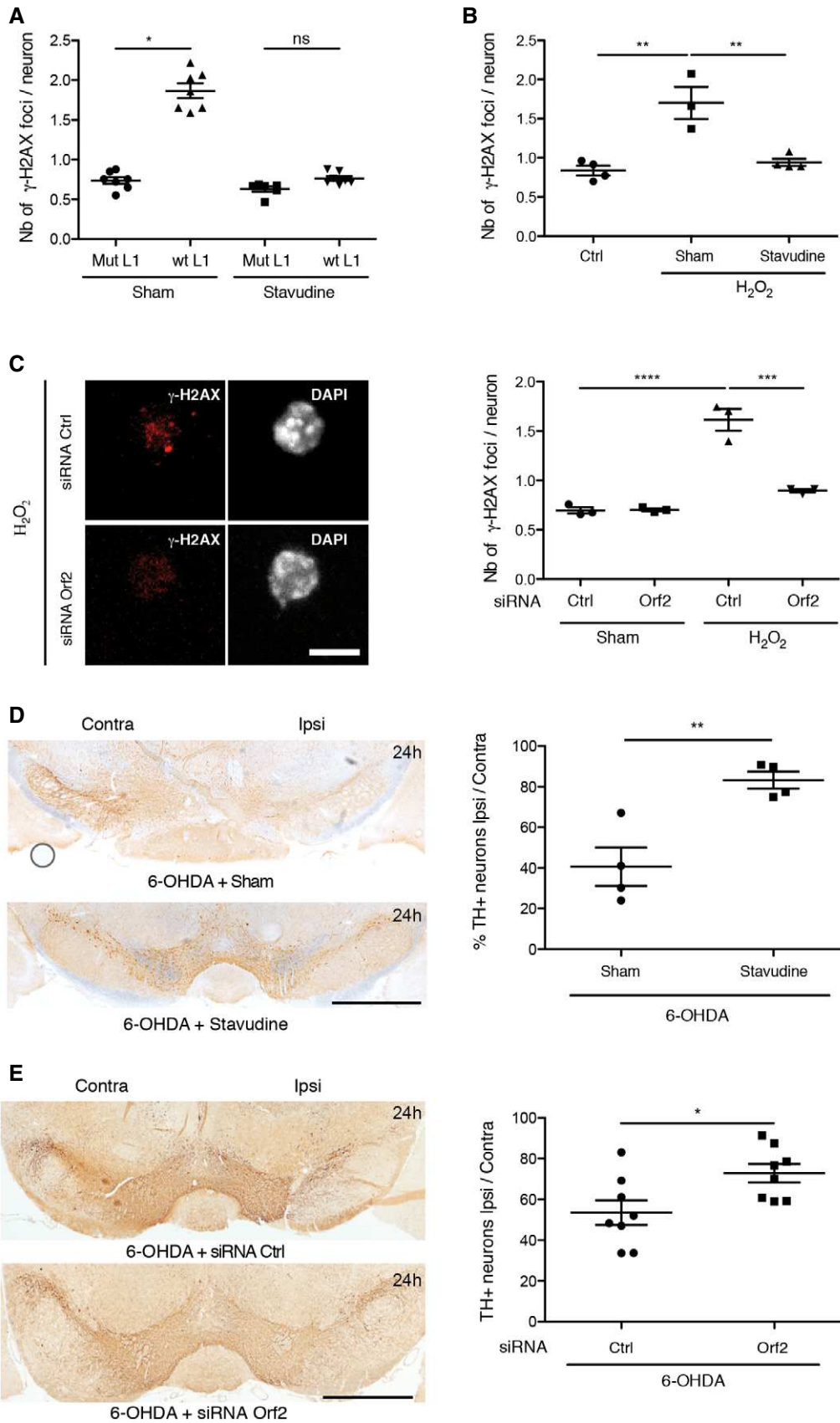


Figure 4.

Figure 4. Stavudine and siRNA against Orf2 protect *in vivo* against oxidative stress-induced DNA damage and cell death.

- A Midbrain primary neurons were treated overnight with stavudine or sham and then transfected with a wt or a retrotransposition-incompetent (mutated) L1 plasmid for 48 h; DNA damage was measured by γ -H2AX immunofluorescence. $*P < 0.05$; $n = 6$ wells per condition, 400 neurons quantified per condition; Kruskal–Wallis test with Dunn's multiple comparisons test; error bars represent SEM.
- B Midbrain primary neurons were treated with stavudine or sham overnight and then with H₂O₂ and stavudine or sham for 1 h; DNA damage was measured by γ -H2AX immunofluorescence. $**P < 0.01$; $n = 3$ –4 wells per condition, this experiment was done three times and a representative experiment is displayed, 300 neurons were quantified per condition; one-way ANOVA with Tukey's multiple comparisons test; error bars represent SEM.
- C Midbrain primary neurons were transfected with an anti Orf2 siRNA or a control siRNA for 4 days and treated with H₂O₂ during 1 h; DNA damage was analyzed by γ -H2AX immunofluorescence (left) and quantified (right). Scale bar represents 5 μ m. $***P < 0.001$; $****P < 0.0001$; $n = 3$ wells per condition, 150 neurons quantified per condition; ANOVA with Tukey's multiple comparisons test; error bars represent SEM.
- D Midbrain sections were stained for TH, 24 h after 6-OHDA sham or 6-OHDA stavudine injections in the SNpc, and the number of TH⁺ neurons was quantified by unbiased stereological counting on both ipsilateral (injected) and contralateral (uninjected) sides. Scale bar represents 1 mm; $**P < 0.01$; $n = 4$ mice per group; Student's *t*-test; error bars represent SEM. The experiment was done twice. The results of an independent experiment are shown in Fig EV4.
- E Orf2 or control siRNA was coupled to the cell-penetrating peptide Penetratin and infused for 3 days in the SNpc of wt mice. Mice were then injected with 6-OHDA and sacrificed 24 h later, and the number of TH⁺ neurons was counted. Scale bar represents 1 mm. $*P < 0.05$; $n = 8$ mice per group, Student's *t*-test; error bars represent SEM. The experiment was done twice. The results of an independent experiment are shown in Fig EV4.

transcriptase inhibitor as shown previously (Jones *et al*, 2008) and confirmed here by the gradual decrease in L1 retrotransposition in response to increasing doses of stavudine (Fig EV3A, left panel). We next quantified the inhibitory activity of stavudine on DNA break formation induced either by L1 overexpression (Fig 4A) or H₂O₂ addition (Fig 4B). A similar inhibition of DNA break formation induced by H₂O₂ was obtained by transfecting embryonic midbrain neurons with a siRNA directed against Orf2p but not with a control siRNA (Fig 4C).

A protective effect of stavudine was also obtained *in vivo* in the 6-OHDA experimental paradigm. Indeed, the results of Fig 4D demonstrate that the injection of stavudine, 30 min before and at the same time as 6-OHDA, protects against mDA neuron death measured 24 h later (replicate experiment shown in Fig EV3C). In a similar experiment, the anti-Orf2p siRNA linked to the cell-permeable peptide Penetratin was infused for 3 days at the level of the SNpc before an acute 6-OHDA injection. Figure 4E demonstrates the protective effect of the anti-Orf2p siRNA, and Fig EV3B confirms, using the Orf1p antibody, the efficiency of this strategy to block the expression of the bicistronic L1 mRNA *in vivo* (64% inhibition of Orf1p expression). A second, independent, experiment demonstrating the *in vivo* efficacy of the anti-Orf2p siRNA is shown in Fig EV3D.

Engrailed is a direct repressor of L1 expression

Adult mDA neurons from *En1*-het mice present an enhanced rate of progressive cell death starting at 6 weeks of age (Sonnier *et al*, 2007). At this time, all neurons are still present but abnormal nuclear phenotypes are observed, including DNA damage and the loss of heterochromatin marks (Rekaik *et al*, 2015). In a previous study, we reported that En2 internalization strongly protects midbrain neurons in culture and mDA neurons *in vivo* against H₂O₂- and 6-OHDA-induced stress, respectively (Rekaik *et al*, 2015). In view of the data presented above, we decided to investigate whether protection by Engrailed could, in part, be due to L1 repression by this transcription factor. The *in vitro* experiments of Fig 5A support this idea. Indeed, the DNA breaks provoked by L1 overexpression are not formed if the cells have been treated with recombinant En2 (Fig 5A), and L1 transcription (FISH analysis) induced by H₂O₂ treatment is also strongly repressed by En2 (Fig 5B).

In the *in vivo* paradigm, Fig 5C demonstrates the repressive effect of En2 injected in the SNpc on L1 Tf/Gf and L1 A transcription 6 h after an acute oxidative stress in the SNpc. Repression takes place in the presence of cycloheximide (CHX), a potent inhibitor of translation. It is thus in favor of a direct effect of internalized En2 as no intermediate protein synthesis is required. The only alternative to a

Figure 5. Engrailed protects against L1-induced DNA damage and is a direct transcriptional repressor of L1.

- A Plasmids overexpressing mouse L1 (wt or mutated) were transfected in midbrain primary neurons and subsequently treated with recombinant En2 or sham. DNA damage was measured by γ -H2AX immunofluorescence 48 h later. $***P < 0.001$; $n = 6$ wells per condition; 200 neurons were quantified per condition; Kruskal–Wallis test with Dunn's multiple comparisons test; error bars represent SEM.
- B Midbrain primary neurons were treated overnight with sham or En2 (100 ng/ml; 3 nM) and then with H₂O₂ for 1 h. Active L1 transcription sites were analyzed by FISH. Scale bar represents 5 μ m; $****P < 0.0001$; $n = 4$ wells per condition, 200 neurons quantified per condition; ANOVA with Tukey's multiple comparisons test; error bars represent SEM.
- C Mice were injected in the SNpc with 6-OHDA and 30 min later with 2 μ l En2 protein (150 ng/ μ l) in the presence of the protein synthesis inhibitor CHX; L1 transcription was measured by RT–qPCR. $**P < 0.01$; $n = 5$ mice per group; Student's *t*-test; error bars represent SEM.
- D Mice were injected in the SNpc with En2 protein, and L1 transcription was measured by RT–qPCR. $*P < 0.05$; $n = 3$ wells per condition, three experiments were done (*in vitro*), $n = 3$ mice (*in vivo*); Student's *t*-test; error bars represent SEM.
- E Electrophoretic mobility shift assay (EMSA) was done using recombinant En2, a biotinylated oligonucleotide of the region encompassing a *in silico* predicted Engrailed-binding site in the L1 5'UTR and NP6, a competing oligonucleotide with six Engrailed-binding sites. The experiment was done three times. An extract from the consensus L1 Tf 5'UTR sequence (GenBank: AF016099.1) indicates in red and underlined the two predicted binding sites for Engrailed (left scheme). Both binding sites were tested in EMSA experiments and bind Engrailed protein, and the results shown (right) were obtained for binding site 2. The sequence in red indicates the L1 5'UTR oligonucleotide used for the gel shift.
- F Chromatin from adult cerebellum expressing En2 was incubated with the anti-Engrailed antibodies 4G11, 86/8 or the respective IgG. DNA was extracted and L1 Tf/Gf and A promoter regions and a putative binding site in the *Otx2* gene were amplified by qPCR. The *Tdp1* gene was included as a genomic region where Engrailed does not bind (negative binding site). Engrailed binding to the L1 Tf/Gf promoter is eightfold (4G11) and fivefold (86/8) enriched relative to *Tdp1*. Results are represented as % input. $n = 2$ technical replicates, error bars represent SEM.

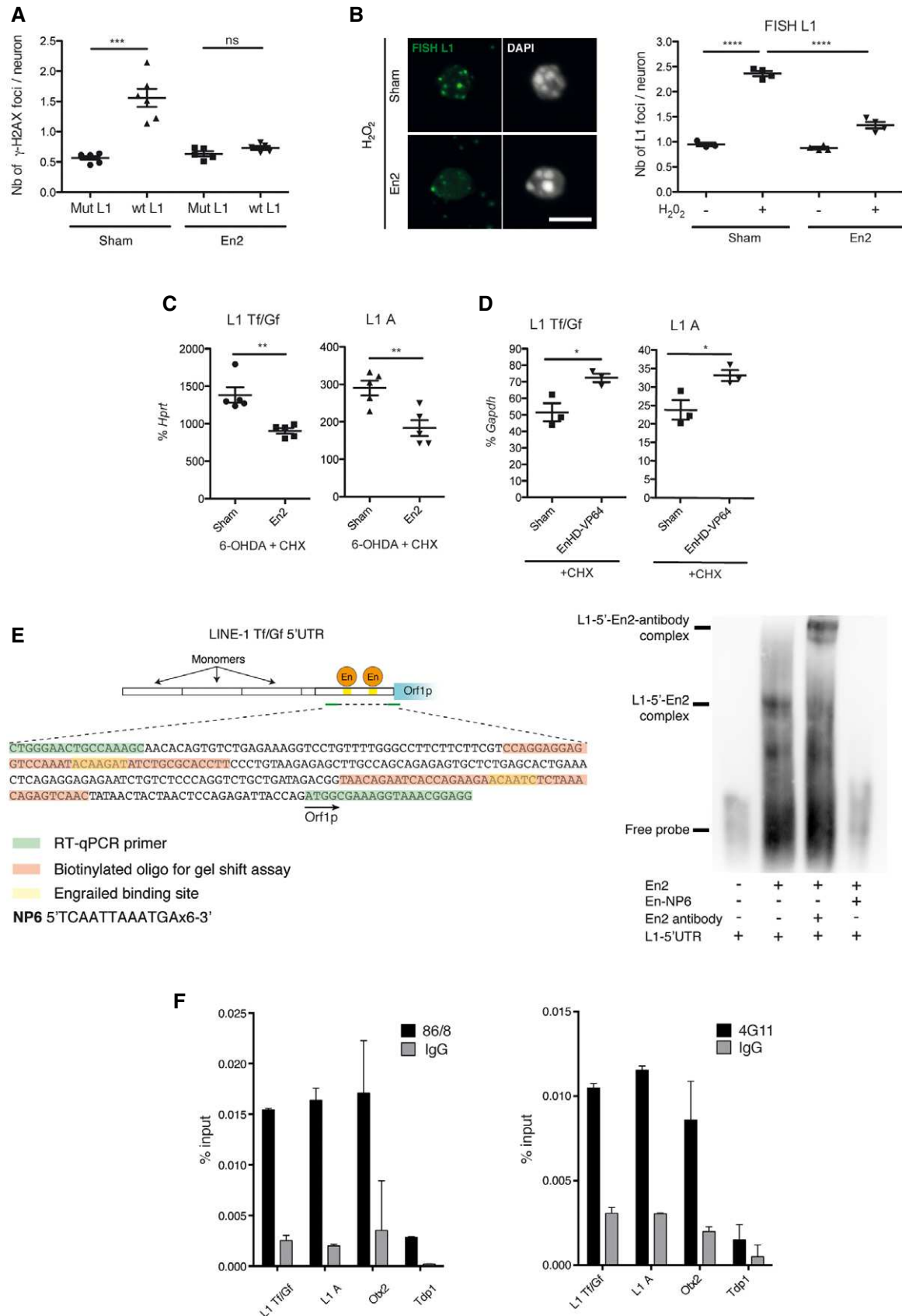


Figure 5.

direct transcriptional effect of En2 is an En2-induced structural chromatin change or RNA intermediate.

Engrailed is primarily a transcriptional repressor. To further verify a direct regulation of L1 transcription, an activator form of Engrailed (EnHD-VP64) constructed by fusing its homeodomain to a tetramerized Herpes virus activator domain (Rekaik *et al*, 2015) was added to midbrain neurons in culture or injected in the SNpc, in the presence of CHX. Figure 5D demonstrates that EnHD-VP64 activates L1 transcription *in vivo* (and Fig EV5C *in vitro*), thus behaving as an anti-Engrailed, and further supporting a direct transcriptional regulation of L1 expression by Engrailed. Accordingly, it has been previously reported that EnHD-VP64 infused in the SNpc activates the formation of DSBs and induces mDA neuron death (Rekaik *et al*, 2015).

Three putative Engrailed-binding sites in the 5'UTR of the consensus L1 Tf (GenBank: AF016099.1) were identified by *in silico* analysis, allowing for the design of primers spanning two of the predicted binding sites (Fig 5E). We used these putative Engrailed-binding domains present in the L1 5'UTR to design a gel shift experiment. Both domains were bound by the Engrailed recombinant protein. Figure 5E illustrates En2 binding to domain II (shift and supershift with an anti-Engrailed antibody) and its specific displacement by NP6 (a competing multimerized Engrailed-binding site (Desplan *et al*, 1988)). In the adult mouse brain, mDA neurons expressing Engrailed in the SNpc are sparse (< 14,000). In contrast, granules cells in the cerebellum, also expressing Engrailed, constitute the most abundant brain neuronal population (about 10 million neurons). Chromatin immunoprecipitation (ChIP) was performed with two distinct Engrailed antibodies on 20 manually microdissected ventral midbrains and four cerebella. H3K9me3, a repressive mark on full-length L1 promoters (Bulut-Karslioglu *et al*, 2014; Pezic *et al*, 2014), was used as a positive control. Compared to a negative binding site (*Tdp1*) and to an IgG, ChIP with an H3K9me3 antibody gave a 55-fold and sixfold enrichment of the L1 promoter in cerebellar and midbrain tissues, respectively (Fig EV5A).

In the same conditions, a monoclonal (4G11) and polyclonal (86/8; Di Nardo *et al*, 2007) Engrailed antibody immunoprecipitated the L1 Tf/Gf and A promoter regions encompassing the Engrailed-binding sites starting from cerebellar chromatin with a eightfold (4G11) and fivefold (86/8) enrichment relative to the negative binding site *Tdp1* and to an IgG (Fig 5F). This demonstrates that Engrailed binds the L1 promoter region *in vivo*. Midbrain chromatin did not allow us to immunoprecipitate the same region, presumably due to the lower number of Engrailed expressing cells in this tissue. We thus turned to nuclei isolated from primary midbrain neurons incubated with 10 nM En2 (the concentration used in the protection essays), with poly(dI-dC) or NP6, and the chromatin was immunoprecipitated with the anti-Engrailed polyclonal antibody. Figure EV5B shows that the antibody specifically pulls down DNA fragments of the 5'UTR of L1 Tf/Gf and L1 A families containing the putative En1/2-binding site and that this immunoprecipitation is entirely eliminated by NP6 but not by dI:dC, in full agreement with the gel shift experiment, thus demonstrating specificity.

Finally, we followed the repression of retrotransposition by Engrailed by inducing its expression in HEK cells transfected with the wt and mutated L1 reporter plasmids described above (Fig EV3A, right panel). In this model, L1 activity is monitored by

GFP expression. This experiment illustrates that only the wt L1 plasmid is retrotranspositionally active but that this activity is reduced upon the induction of En2 by doxycycline.

All in all, this series of experiments establishes that Engrailed is a repressor of L1 expression in the adult midbrain and in primary midbrain neuron cultures and that part of the protective Engrailed activity against oxidative stress-induced DNA breaks is through direct L1 repression by this transcription factor.

Piwil1 expression decreases mDA neuron cell death in *En1*-het mice

The repression of L1 by Engrailed made it plausible that the progressive mDA neuron loss observed in *En1*-het mice, and starting at 6 weeks of age, involves a partial de-repression of L1 transcription. This led us to analyze L1 expression in these mice. RNA-Seq data (GEO GSE72321) from laser microdissected SNpc (Rekaik *et al*, 2015) were mapped onto a consensus L1 Tf sequence (L1spa; GenBank AF016099.1). Figure 6A demonstrates an increase in the number of L1 reads in *En1*-het mice in 6-week-old *En1*-het mice compared to wt siblings, including in the 5'UTR region which should be enriched for non-truncated full-length L1 elements (Fig 6A, expanded view in the right panel). Expression at 6 weeks in both genotypes was verified by RT-qPCR on laser-captured SNpc, VTA, and cortex, showing a specific up-regulation of L1 Tf/Gf RNA and L1 A (Fig 6B) in the SNpc. Orf1p increase in *En1*-het mice was confirmed by immunohistochemistry as shown and quantified in Fig 6C.

The results described so far demonstrate that an important adult function of Engrailed is to repress L1 expression, thus protecting mDA neurons against oxidative stress. If so, it could be anticipated that the overexpression of Piwil1, a *bona fide* L1 repressor, would have an Engrailed-like activity on accelerated mDA cell death in *En1*-het mice. To verify this point, an AAV8 encoding Piwil1, or mCherry as a control, was injected in the ventral midbrain of *En1*-het or wt mice at 5 weeks of age, and the animals were analyzed at 9 weeks. Figure 7A illustrates the expression of exogenous Piwil1 in infected midbrain neurons, including mDA neurons, and Fig 7B quantifies, by RT-qPCR and Western blot, Piwil1 expression levels after infection with either Piwil1 or mCherry expressing viruses in wt animals. To validate the use of Piwil1 as a tool to decrease Orf1p expression, Orf1p staining intensity was quantified in neurons expressing TH. Figure 7C shows the significant decrease in ORF1p upon Piwil1 overexpression in mDA neurons. As reported before (Sonnier *et al*, 2007), the number of mDA neurons at 9 weeks is reduced by more than 20% in *En1*-het mice compared to wt siblings, both groups being injected with an AAV8-mCherry (Fig 7D). In the same experiment, injection of *En1*-het mice with an AAV8 Piwil1 rescues a significant number of mDA neurons, confirming that part of mDA cell death observed in *En1*-het mice is triggered by L1 de-repression in Engrailed hypomorphs.

Discussion

Homeoprotein transcription factors are expressed throughout life, and their sites of expression vary considerably between developmental and adult stages (Prochiantz & Di Nardo, 2015). Adult

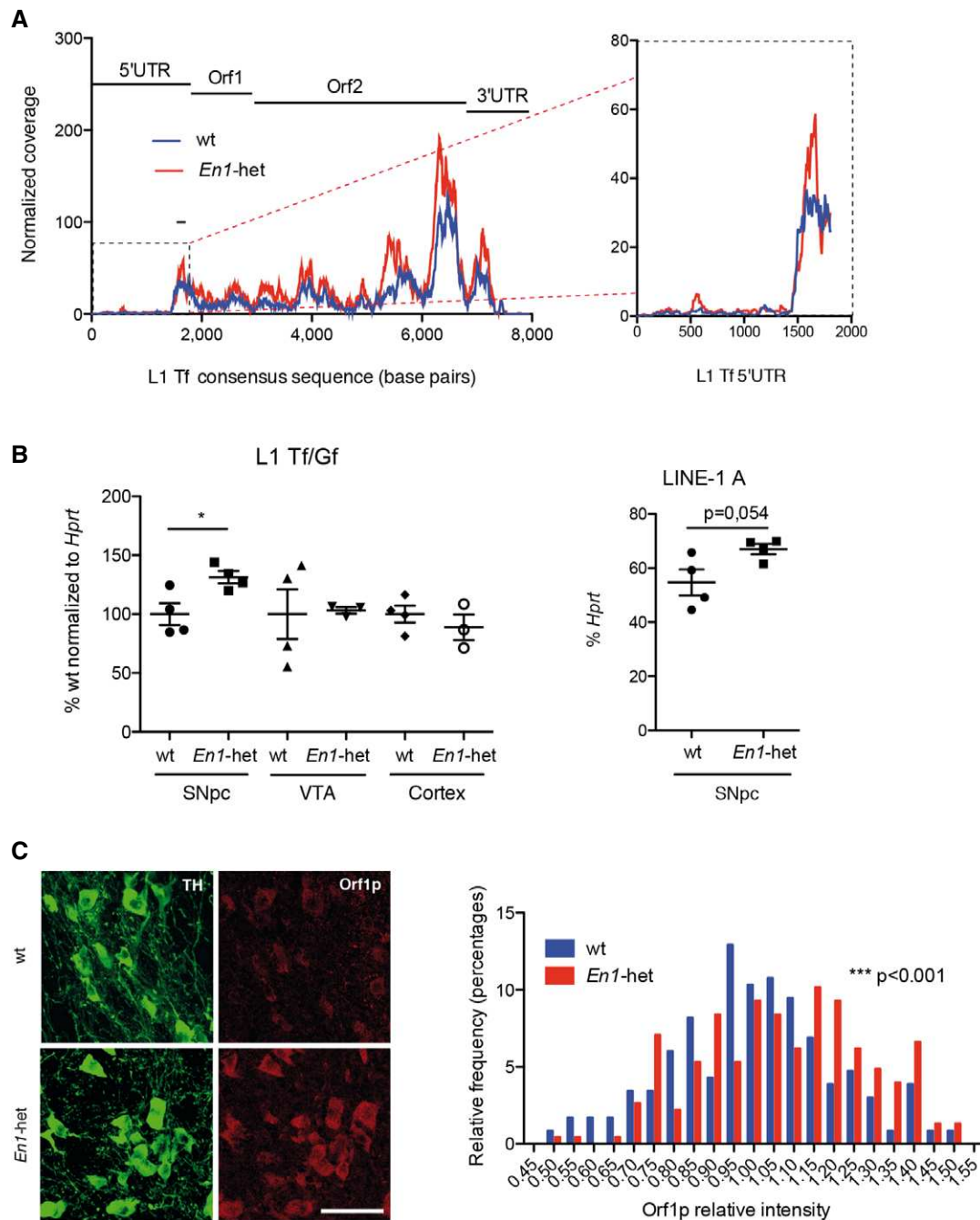


Figure 6. LINEs are implicated in *En1-het* neurodegeneration.

A RNA-Seq data of laser microdissected SNpc from *En1-het* and wt mice (GEO accession number GSE72321) were mapped against a consensus L1 Tf sequence. The area underneath the curve for wt was 140,745, compared to 219,725 for *En1-het*. The black line on the graph corresponds to the sequence amplified by RT-qPCR (L1 Tf). Enlarged view of the 5'UTR region is shown on the right.

B RNA from laser-dissected SNpc, VTA, and entorhinal cortex of 6-week-old *En1-het* mice and their wt littermates was analyzed by RT-qPCR. * $P < 0.05$; $n = 4$ mice per group; Student's *t*-test; error bars represent SEM.

C Midbrain sections of 8-week-old wt and *En1-het* mice were stained for Orf1p and analyzed by confocal microscopy (left), and Orf1p fluorescence intensities were quantified (right). Scale bar represents 50 μ m; *** $P < 0.001$; 231 (wt) and 227 (*En1-het*) neurons were quantified in three different mice; Kolmogorov–Smirnov test.

functions are poorly understood, and previous studies from our laboratory have demonstrated that Engrailed and Otx2 are involved in the regulation of neuronal survival and cerebral cortex plasticity

in the adult (Sonnier *et al*, 2007; Alvarez-Fischer *et al*, 2011; Torero-Ibad *et al*, 2011; Beurdeley *et al*, 2012; Spatzza *et al*, 2013; Bernard *et al*, 2014, 2016; Rekaik *et al*, 2015). A case of particular

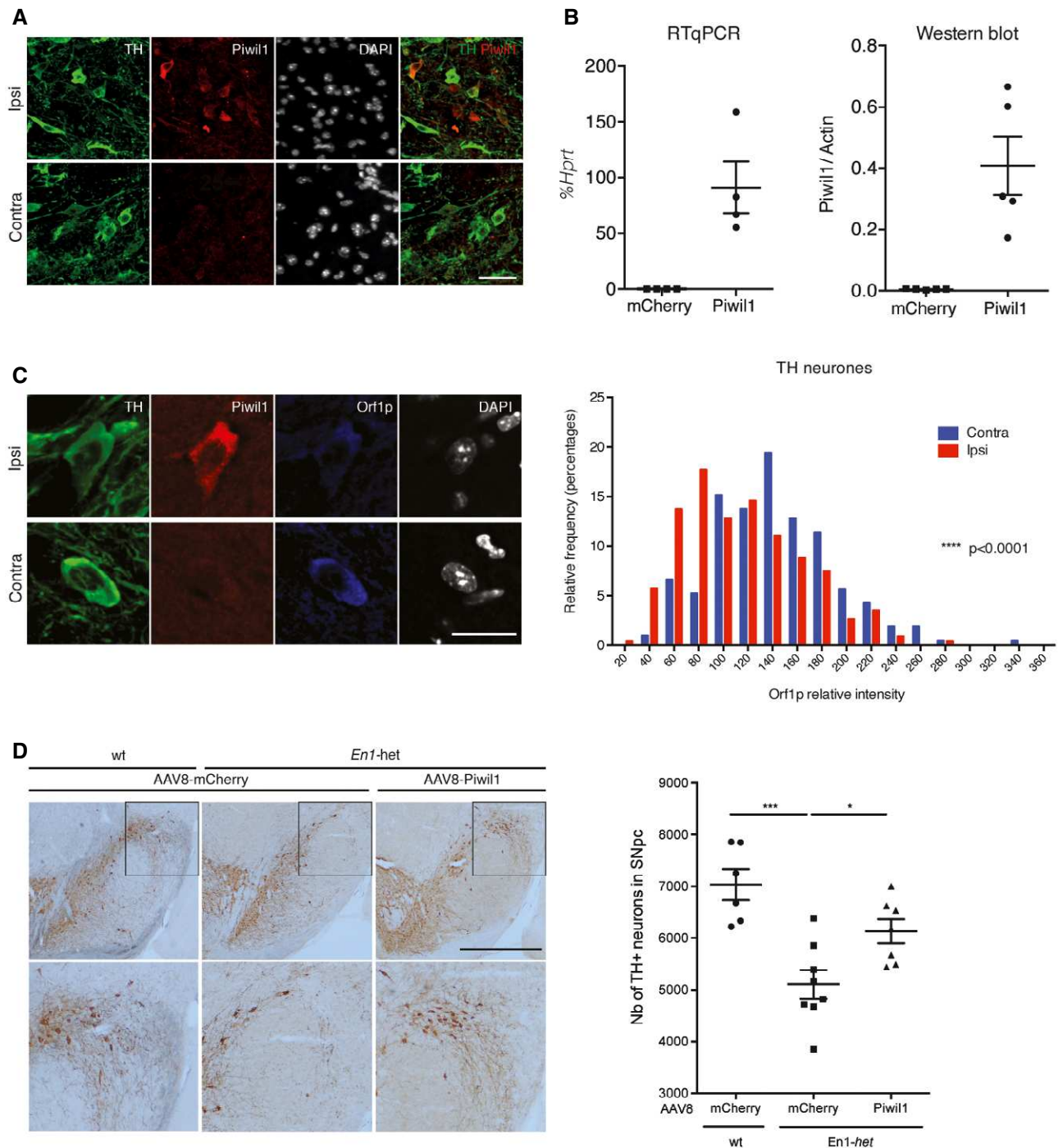


Figure 7. Piwil1 overexpression in *En1*-het mice rescues mDA neurons.

- A** Five-week-old *En1*-het mice were injected with AAV8-Piwil1. Four weeks later, midbrain sections were stained for TH and Piwil1 to verify Piwil1 expression (see upper panel for injected side compared to lower panel non-injected, contralateral side). Scale bar represents 40 μ m.
- B** Eight-week-old wt mice were injected with AAV8-Piwil1 or AAV8-mCherry control. Three weeks later, mice were sacrificed, the SNpc region manually dissected and RNA or proteins extracted. Piwil1 RNA was quantified by RT-qPCR relative to *Hprt* and Piwil1 protein by Western blot relative to β -actin. $n = 4$ mice (RT-qPCR) and $n = 5$ mice (WB); error bars represent SEM.
- C** Eight-week-old wt mice were unilaterally injected with either AAV8-Piwil1 or AAV8-mCherry as above. Three weeks later, Orf1p fluorescence was measured in TH⁺ neurons from on the contralateral side (Contra) or on the ipsilateral, injected side (Ipsi) as illustrated, **** $P < 0.0001$; 211 (Contra) and 226 (Ipsi) neurons were quantified from three different wt mice (three sections per mouse); Kolmogorov-Smirnov test. Scale bar represents 20 μ m.
- D** Five-week-old *En1*-het mice were injected with AAV8-Piwil1 or AAV8-mCherry, and wt littermates were injected with AAV8-mCherry. Four weeks later, midbrain sections were stained for TH, and the number of TH⁺ neurons on the injected side was measured by unbiased stereological counting. Scale bar represents 1 mm; * $P < 0.05$; *** $P < 0.001$; $n = 6-8$ mice per group, ANOVA with Tukey's multiple comparisons test; error bars represent SEM.

interest is provided by mDA neurons which are protected against oxidative stress by Engrailed (Rekaik *et al*, 2015). The present study was aimed at better deciphering some of the mechanisms involved in the latter protection. The RNA-Seq experiments comparing *En1*-het and wild-type SNpc suggested that L1 mobile elements may have a role in mDA cell death and, most importantly, in Engrailed protective activity.

A first hint is the observation that the three main L1 families are expressed in post-mitotic nerve cells of the central nervous system, including mDA neurons of the ventral mesencephalon. Expression is full-length and, in the latter neurons, L1 baseline expression is increased upon oxidative stress leading to the formation of DNA breaks and, in some cases, to cell death. Conversely, different anti-L1 strategies protect adult mDA neurons against oxidative stress. These strategies include Orf2p-siRNA, overexpression of the anti-L1 protein Piwil1 and stavudine, a pharmacological inhibitor of the reverse transcriptase encoded by the L1-Orf2. Using the *En1*-het mouse genetic model where mDA neurons from the SNpc degenerate progressively starting at 6 weeks of age, we find that L1 expression is increased in mutant animals compared to wt siblings. The direct repressive activity of Engrailed on L1 transcription and experiments demonstrating that L1 overexpression impinges on mDA neuron physiology and survival leads us to propose that the protective activity of Engrailed reported in earlier studies involves its ability to repress L1 transcription.

L1 expression in the nervous system has been reported before (Thomas *et al*, 2012). A striking finding is their activity during development and in adult neural stem cells, providing a basis for neuronal genetic mosaicism (Singer *et al*, 2010). The significance of this mosaicism is not yet understood, but given the Darwinian somatic selection exerted on neuronal progenitor cells, it is possible that the survivors may have a selective advantage. What is reported here is a basal L1 expression in post-mitotic mammalian neurons. Indeed, not all the L1 RNA species sequenced or amplified by RT-qPCR are necessarily full-length or present in neuronal cells, but it is clear that nerve cells do express full-length L1 RNAs and also Orf1p, as demonstrated by Western blot, *in situ* hybridization and immunohistochemistry. It is of note that mDA neurons in the ventral midbrain, co-stained with the TH and the Orf1p antibodies, show a higher intensity of Orf1p expression compared to adjacent non-dopaminergic neurons.

L1 expression must be regulated as uncontrolled expression is a threat to genome integrity. The Piwi Argonaut family plays in this context an important role in the germline (Malone & Hannon, 2009; Malone *et al*, 2009; Pezic *et al*, 2014). We find Piwi protein family members to be expressed in different brain regions at a higher level compared to non-neuronal tissue but, as expected, at a much lower level than in testis. The most expressed Piwi is Piwil1 and, as shown in prostate epithelial cells, Piwil1 downregulation increases L1 Orf2 expression thus inducing DSBs (Lin *et al*, 2009). For these reasons, we used its overexpression as a tool to inhibit L1 activity in this study and to demonstrate that mDA cell death in the *En1*-het mutant is in part due to L1 overexpression. However, this is an artificial mean, just as is the infusion of a cell-permeable anti-Orf2p siRNA, and this does not mean that Piwi proteins are active in mDA neurons, even if it might be an interesting hypothesis to explore.

In fact, we demonstrate that L1 expression can be physiologically inhibited by Engrailed and artificially by Piwil1. Central to the

demonstration is that any strategy used to decrease L1 expression (Piwil1, anti-Orf2p siRNA, Engrailed) or activity (stavudine) prevents oxidative stress-induced mDA cell death. Indeed, our Engrailed gain and loss of function experiments incite us to favor a central role of Engrailed through its direct binding to L1 promoters, a mechanism different from what has been described for Piwi proteins. In the case of the anti-Orf2p siRNA, the lack of sensitive antibodies and the 1/250 ratio between Orf2p and Orf1p (Taylor *et al*, 2013) due to the low re-initiation of Orf2p synthesis (Han *et al*, 2004; Alisch, 2006) did not allow us to follow Orf2p downregulation. However, the same bicistronic mRNA encodes both Orf1p and Orf2p, and we could verify that, as a result, Orf1p expression is strongly downregulated by the siRNA.

Other situations and factors in other cellular contexts have been shown to exert a regulation on L1 activity. A first level of regulation is through the modification of chromatin domains. Many genetic L1 sequences are compacted in heterochromatin regions, and their expression is thus repressed. Accordingly, it is well established that L1 expression is regulated by all events that can, inside and outside of the nervous system, modify the extent of heterochromatin (Van Meter *et al*, 2014; Skene *et al*, 2010). Among the factors that can modify chromatin organization are aging and oxidative stress (Oberdoerffer & Sinclair, 2007; De Cecco *et al*, 2013; López-Otín *et al*, 2013). Accordingly, it was shown in the fly and in the mouse that aging is associated with an enhanced expression of mobile elements that can contribute to the formation of DNA breaks and genome instability (St Laurent *et al*, 2010; Maxwell *et al*, 2011; Chow & Herrup, 2015).

An interesting recent example is provided by a cocaine-induced change in heterochromatic H3K9me3 and the ensuing unsilencing of repetitive elements in the nucleus accumbens (Maze *et al*, 2011). The same correlation was reported at the level of the hippocampus (Hunter *et al*, 2012). The present study adds to the concept by showing that oxidative stress increases L1 expression *in vivo* and *in vitro* and that a siRNA designed against Orf2p blocks the formation of DSBs and cell death induced by the stress.

Some factors can act on L1 gene expression, both by modifying chromatin structure and by direct transcriptional regulation. Direct regulation was shown for p53 and SIRT6, two proteins involved in the regulation of aging (Van Meter *et al*, 2014; Wylie *et al*, 2016) and it must be noted that L1 repression by SIRT6 fails with age and stress (Van Meter *et al*, 2014). The present study identifies the homeoprotein Engrailed as a repressor of L1 transcription. Indeed, we have shown earlier that Engrailed protects mDA neurons against age-related progressive oxidative stress, as well as against an acute stress provoked by the local injection of 6-OHDA at the level of the SNpc (Rekaik *et al*, 2015). In the latter study, it was shown that Engrailed restores several heterochromatin marks, including H3K9me3, H3K27me3, and the nucleolar marker Nucleolin. It can thus be proposed that protection by Engrailed involves the repression of L1 expression in part through heterochromatin maintenance (Rekaik *et al*, 2015) and in part through transcriptional repression as demonstrated in this study. Indeed chromatin changes and repression are not mutually exclusive as the binding of Engrailed to the 5'UTR of L1 might induce heterochromatin nucleation, similarly to Pax3 and Pax6 homeoproteins that regulate chromatin states through their binding to intergenic major satellite repeats (Bulut-Karslioglu *et al*, 2012).

Engrailed protects mDA neurons in three pharmacological models of PD by a mechanism involving the regulation of the translation of mitochondrial complex I mRNAs (Alvarez-Fischer *et al*, 2011). More recently, the same transcription factor was shown to save the same neurons, following an acute oxidative stress, through its ability to restore a healthy epigenetic state (Rekaik *et al*, 2015). The present study now demonstrates that Engrailed controls mDA cell physiology and survival through the regulation of L1 transcription, thus adding an additional facet to its protective and curative activities in the mouse.

Protection mediated by L1 repression made it plausible to block 6-OHDA-induced cell death with L1 inhibitors. Indeed, this was shown with the siRNA designed against Orf2p, with the anti-L1 protein Piwil1, but also with stavudine, a reverse transcriptase inhibitor. Having verified its repressive activity on L1 retrotransposition, we show that stavudine blocks DSBs and degeneration induced by oxidative stress. We can only speculate on how stavudine works, but we could show that, at least *in vitro* and under conditions of oxidative stress, the drug decreases the amount of chromatin-bound L1 RNA (Fig EV4), supporting the hypothesis that, blocking reverse transcription after the first nick in the DNA has been made, allows better access of repair enzymes at the chromatin level. Another possibility is that full-length L1 elements actually retrotranspose and that breaks and death are a consequence of this activity. In that case, the action of stavudine would be clearly by preventing retrotransposition through the inhibition of the reverse transcription initiated by the Orf2p-encoded reverse transcriptase. It is of interest, in this context, that Engrailed induction and stavudine addition both block retrotransposition in the reporter cell line expressing L1. Retrotransposition in post-mitotic cells is considered unlikely because of the integrity of the nuclear membrane in the absence of mitosis, thus the impossibility for the ribonucleoparticle composed of the L1 mRNA, Orf2p, and Orf1p to gain access to the nucleus. However, one cannot preclude that Orf2p could be individually transported to the nucleus thanks to its nuclear localization signal (Goodier, 2004) and thus introduce a nick in the DNA and reverse transcribe nuclear resident L1 transcripts. This hypothesis will be explored in a future study.

Given that, as demonstrated here, anti-L1 activity is sufficient to partially prevent oxidative stress-induced neuronal cell death, it is conceivable that L1-mediated genetic instability via the generation of DSBs is a general driver of cell death in age-related diseases and neurodegeneration. In a preceding report, we demonstrated that mDA neurons from *En1*-het mice are more sensitive than their wt siblings to age-associated oxidative stress, leading to a progressive death of this specific cell type (Rekaik *et al*, 2015). The demonstration that *in vivo* Piwil1 overexpression partially protects against mDA neuron death in *En1*-het mice not only lends weight to the idea that *En1* activity is through the control of L1 expression, but also suggests that age-associated oxidative stress and neurodegeneration involves L1 expression. This is indeed possible as we observe L1 expression in non-dopaminergic ventral midbrain neurons and the presence of L1 mRNA in all tested brain regions. Thus, repressors other than Engrailed might operate to control L1 expression in different regions of the central nervous system.

The analysis of L1 expression in different structures demonstrates a basal, thus physiological, level of expression in all regions examined. It can thus be proposed that L1 expression becomes toxic only after a given threshold has been reached due to an endogenous (e.g.,

oxidative) or environmental (e.g., toxic agent) stress. Homeoproteins are expressed throughout the adult brain, and *Otx2* has a protective effect at the level of the eye (Torero-Ibad *et al*, 2011; Bernard *et al*, 2014) and of the SNpc (Rekaik *et al*, 2015). It is thus tempting to speculate that other transcription factors of this family could repress the expression of mobile elements in the adult and thus behave like anti-aging proteins in normal and pathological situations.

Materials and Methods

Animals

Mice were treated as defined by the guidelines for the care and use of laboratory animals (US National Institute of Health) and the European Directive 2010/63/UE. All experimental procedures were validated by the ethical committee (CEA 59) of the French Ministry for Research and Education. Swiss OF1 wt (Janvier) and *En1*-het mice (Hanks *et al*, 1995) were maintained under a 12 h day/night cycle with *ad libitum* access to food and water. A maximum of six mice were housed in one cage, and cotton material was provided for mice to build a nest. Experimental groups consisted of three to eight male mice at the indicated ages. Sample size calculations were based on previous experiments. No randomization or blinding was used.

Tissue dissection

Where indicated, the SNpc of wt and *En1*-het mice was isolated by laser capture microdissection (LMD7000, Leica) as in Rekaik *et al* (2015). Samples from four animals per group were analyzed. For punch biopsies of the SNpc, brains were put into a brain slicer, covered with Tissue Tek O.C.T. (Sakura Finetek), and frozen on dry ice. A 2 mm slice encompassing the SNpc was excised (−2 to −4 mm/−2.5 to −4.5 caudal from the Bregma) and placed on a cold cover slide with the caudal side facing up. The stereotaxic arm holding the tissue punch was zeroed on the aqueduct, and two biopsies of the SNpc were taken at −/+1.3 (M/L) and −2 (A/P).

In vivo treatments

For injections, mice were placed in a stereotaxic instrument, and a burr hole was drilled into the skull 3.3 mm caudal and 1 mm lateral to the bregma. The needle was lowered 4 mm from the surface of the skull, and 6-OHDA (2 μl; 0.5 μg/μl Sigma) injections were performed over 4 min. For Engrailed rescue experiments, a solution (2 μl) of bacterial recombinant *En2* (300 ng; 4.5 μM) and colominic acid (3 μg; Alvarez-Fischer *et al*, 2011; Rekaik *et al*, 2015) or vehicle (NaCl 0.9%) and colominic acid was injected 30 min after 6-OHDA injection using the same coordinates. When indicated, CHX (0.1 μg/μl, Sigma) was added. Stavudine (d4T, 10 μM, Sigma) was injected 30 min before and at the same time as 6-OHDA. For Piwil1 overexpression, we used an AAV8-Piwil1 or an AAV8-mCherry virus (Vector Biolabs) injected using the same coordinates. SNpc tissues for RT-qPCR and Western blot analysis were obtained from punch biopsies. For siRNA experiments, osmotic mini-pumps (Alzet) with 100 μl of a solution containing cell-permeable peptide Penetratin-coupled siRNA (5 μM) and colominic acid (1.5 μg/μl) in 0.9% NaCl were

implanted for 3 days at -3.8 mm (dorso/ventral). Mice were then anesthetized and perfused for TH immunostaining.

Cell culture

Midbrain primary neurons were dissected from E 14.5 embryos and cultured in Neurobasal medium (Life Technologies) supplemented with glutamine (500 μ M, Sigma), glutamic acid (3.3 mg/l Sigma) aspartic acid (3.7 mg/l, Sigma), anti-anti (Gibco), and B27 (Gibco). Cells were treated with H_2O_2 (100 μ M) for 1 h or as indicated and either RNA was extracted or cells were fixed for immunocytochemistry. Transfections were done by preincubating plasmids (0.75 μ g per transfection) with 8 μ l lipofectamine 2000 (Life Technologies) for 20 min at RT in Opti-MEM medium (Life Technologies). The mix was then added to the cells for 48 h at 37°C. The plasmids used to express mouse wt L1 (pWA-125) and mutated (pWA-126) contain a codon-optimized L1 with its endogenous 5'UTR, an upstream CMV promoter and a retrotransposition-dependent GFP expression cassette (Xie *et al*, 2011). pCMV-Piwil1 was purchased from Origene (MR222484); pCMV, a void plasmid, was used as a negative control. A pEGFP plasmid was co-transfected in all cases. The AAV2 virus (6×10^6 TU/well of a 24-well plate) expressing Piwil1 under the control of the synapsin promoter was purchased from Vector Biolabs. Seven days after transduction, cells were treated for 1 h with H_2O_2 and fixed. Where indicated, midbrain primary neurons were treated with stavudine (10 μ M) for 16 h, treated with H_2O_2 in the presence of stavudine for 1 h, and fixed. Cells were treated where indicated by adding recombinant En2 diluted in culture medium to the culture wells at a concentration of 500 ng/ml (15 nM).

Chromatin immunoprecipitation

Nuclei from midbrain primary neurons were incubated in a cytoplasm lysis buffer (10 mM HEPES, 40 mM KCl, 1 mM $CaCl_2$, 0.5% NP-40) for 10 min on ice and washed twice (same buffer without NP-40) by centrifugation for 10 min at 800 g, at 4°C. Nuclei were then treated 20 min at 37°C with En2 (500 ng/ml), sham (0.9% NaCl), and poly (dI-dC) (Sigma, 50 ng/ μ l) or NP6 (0.4 pmol/ μ l). NP6 oligonucleotide is composed of six times the En binding sequence TCAATTAATGA. Nuclei were then fixed in 1% formaldehyde (Sigma) in PBS. The Magna ChIP kit (Millipore) was used for chromatin purification. Immunoprecipitations were performed with 1 μ g of anti-En antibody (86/8, in-house rabbit polyclonal) or 1 μ g of rabbit IgG (Millipore) overnight at 4°C on a rotating wheel. Immunoprecipitated DNA was analyzed by qPCR with the same primers used for RT-qPCR.

ChIP on tissue was done using the ChIP-IT High Sensitivity Kit (Active Motif) with 10 μ g antibody per ChIP, 4–10 μ g chromatin per H3K9me3-ChIP, and 10–30 μ g chromatin per Engrailed-ChIP. Antibodies used were as follows: H3K9me3 (Active Motif; Clone MABI 0319, mouse monoclonal), 4G11 (DSHB, mouse monoclonal), and 86/8 (anti-En1/2, in-house, rabbit polyclonal).

RNA-Seq data

RPM values from the RNA-Seq experiment reported previously (Rekaik *et al*, 2015) are deposited at GEO under the accession number GSE72321. RNA-Seq data alignment against a consensus L1 Tf sequence was performed using R software. Individual wt and

En1-het reads were aligned using pairwise alignment function and plotted on a normalized coverage graph.

RT-qPCR

Total RNA from laser microdissected tissue was extracted using the AllPrep DNA/RNA Micro Kit (Qiagen) followed by DNase I digestion using the RNeasy MinElute Cleanup protocol for on-column DNase I treatment, followed by RT-qPCR. Total RNA from SNpc biopsies was extracted using the RNeasy Lipid Tissue kit (Qiagen) followed by DNase I (Thermo) digestion. For *in vitro* RNA analysis, RNA was extracted using the RNeasy kit (Qiagen). RNA (200 ng) was reverse-transcribed using the QuantiTect Reverse Transcription kit (Qiagen). RT-qPCR was performed using SYBR Green (Roche Applied Science) on the LightCycler 480 (Roche Applied Science). The primers used for RT-qPCR are indicated in Appendix Table S1. Primer efficiencies were tested using 10-fold dilution series of cDNA spanning at least three orders of magnitude. Data were analyzed using the ddCt method and values normalized to hypoxanthine-guanine phosphoribosyltransferase (*Hprt*) and/or glyceraldehyde-3-phosphate dehydrogenase (*Gapdh*). Chromatin-bound RNA was extracted from isolated nuclei from midbrain neurons culture, and RT-qPCR was performed as above.

RT-PCR and sequencing

RNA from adult ventral midbrain tissue was extracted using the AllPrep DNA/RNA/Protein Extraction Kit (Qiagen). RNA (1 μ g) was incubated with DNase I (Thermo) for 30 min at 37°C and inactivated by EDTA for 10 min at 65°C. RNA was then passed on poly (A)+ columns (Qiagen) to purify poly(A)+ RNA and reverse-transcribed using Superscript II (Invitrogen) and oligo(dT) primer. PCR was then performed using the Phusion Taq polymerase (NEB) and GC-buffer using the primers indicated in Appendix Table S1. PCR conditions were as follows: 98°C 30 s, then 40 cycles of 98°C 10 s, 63°C 30 s, 72°C for 2.4 min, followed by a final extension at 72°C for 10 min. The L1 A amplicons were verified by enzymatic digestion (BamHI, NcoI, PstI). PCR products were excised, purified, and analyzed by Sanger sequencing (MWG-Biotech).

Immunostaining

Immunostainings were done as described earlier (Alvarez-Fischer *et al*, 2011). The following primary antibodies used: mouse anti- γ -H2AX, 1:200 (Millipore, clone JBW301), chicken anti-TH, 1:500 (Abcam, ab76442), guinea pig Orf1p (09), 1:200 (in-house), rabbit MIWI (=Piwil1), 1:300 (Cell Signaling, 6915) and NeuN (Millipore, MAB377), 1:300. Secondary antibodies were as follows: 488 anti-chicken, 647 anti-chicken, 488 anti-mouse, and 546 anti-mouse Alexa Fluor (Life Technologies). Labeled sections were imaged by confocal microscopy (SP5, Leica). Visible TH immunohistochemistry was done as described earlier (Rekaik *et al*, 2015). Images were taken on a Nikon Eclipse 90i microscope.

Cell counting and stereology

Serial sections (30 μ m) of mouse ventral midbrains encompassing the SNpc were cut on a freezing microtome, and TH immunostaining

(Immunostar, monoclonal mouse; 1:1,000) was done as described above. Unbiased stereological TH cell counting was done after Piwil1/mCherry overexpression in *En1*-het mice and wt littermates [*En1*-het + AAV8-EF1a-mCherry ($n = 8$) or AAV8-EF1a-mPiwil1 ($n = 7$) and wt littermates with AAV8-EF1a-mCherry ($n = 6$)]. Eight to 10 sections per animal were analyzed (every third section of serial sections encompassing the entire SNpc). Counting was done blinded. Parameters used (Stereo Investigator Software (Micro Bright Field) on a Nikon E800 microscope) were as follows: The counting frame area was $8,100 \mu\text{m}^2$, and the sampling grid area was $20,445 \mu\text{m}^2$. The mean of total markers counted was 353 ± 63 . The mean number of sampling sites was 174 ± 29 . The disector height was $22 \mu\text{m}$, and guard zone distance was $1.5 \mu\text{m}$. The mean coefficient of error (Gundersen $m = 1$) was 0.06 ± 0.01 . Standard deviation errors (\pm) are reported.

TH cell counting in conditions comparing ipsi- (treated) and contralateral (non-treated) sides were done as follows: For every brain, a minimum of four serial sections were stained, and the number of TH cells was counted in the SNpc of both ipsi- and contralateral sides. An ipsi/contra ratio was calculated for each section, and the resulting mean of four sections was used to quantify the difference between the TH cell number of the ipsi- and contralateral side of the same animal.

Orf1p antibody production

Orf1p polyclonal antibodies (rabbit and guinea pig) were produced using the speed 28-day protocol (Eurogentec) after injection of the recombinant full-length Orf1 protein (Eurogenix). The final bleeds were then subjected to a protein-A purification step. The rabbit antibody was used for the detection of the Orf1p protein in Western blots, and the guinea pig was used in immunostainings.

Western blots

Western blots were performed as described earlier (Rekaik *et al*, 2015). Orf1p rabbit antibody (in-house) and Piwil1 (Miw1, sc-398534, Cell Signaling) were used at a concentration of 1:500, and mCherry (Clontech no. 632543) was used at 1:1,000. Blots were quantified using ImageJ with actin (actin-HRP, 1:20,000, Sigma clone AC-15) as a reference. To determine specificity of the ORF1p antibody, the antibody was blocked with the Orf1p peptide (two molecules of peptide per molecule of antibody) for 3 h on a rotating wheel at room temperature and diluted for Western blot or immunofluorescence experiments.

Image quantification

Quantifications of immunofluorescence were performed using a $63\times$ (*in vivo*) or $40\times$ (*in vitro*) magnification and 1- or $5\text{-}\mu\text{m}$ -thick successive focal planes, for γ -H2AX and L1 FISH or Orf1p staining, respectively.

We define L1 FISH and γ -H2AX foci as individual fluorescent objects in the nucleus with an intensity that allows us to distinguish them from the background. The foci size cutoff was $0.3 \mu\text{m}$. For L1 FISH experiments and depending on immunostaining conditions, the intensity ratio between the foci and the background was higher than 1.5. For the quantification of the number of foci (L1 FISH and

γ -H2AX), individual foci were counted within each neuron. For intensity quantification of L1 FISH foci, we measured the maximal value of intensity within an individual focus after background subtraction.

Orf1p staining in wt, *En1*-het, and 6-OHDA or AAV8-Piwil1-injected mice was quantified by measuring fluorescence intensity in TH⁺ or TH⁻ cells after background subtraction. Values were plotted in a relative frequency distribution histogram.

For each experiment, image acquisition was performed during a single session with the same parameter set-up of the confocal microscope to allow for comparison between experimental conditions. Images were analyzed by the same experimenter using ImageJ software with the same semi-automated workflow for all experimental conditions.

In situ hybridization

Mice were anesthetized, perfused with PBS in RNase-free conditions, and frozen in isopentane (embedded in TissueTek O.C.T). Brain slices ($20 \mu\text{m}$) were fixed in 4% PFA in PBS for 10 min at RT and then permeabilized twice for 10 min in RIPA buffer (150 mM NaCl, 1% NP-40, 0.5% Na deoxycholate, 0.1% SDS, 1 mM EDTA, 50 mM Tris-HCl pH 8). Brain sections were fixed again for 5 min, demasked for 10 min with TEA buffer (Triethanolamine 100 mM, 0.8% acetic acid pH 8) containing 0.25% acetic anhydride, permeabilized for 30 min in PBS with 1% Triton X-100, and blocked for 1 h in hybridization buffer (50% formamide, $5\times$ SSC, $5\times$ Denhardt (1% Ficoll, 1% SSC, 1% Tween-20), 500 $\mu\text{g}/\text{ml}$ Salmon sperm DNA, 250 $\mu\text{g}/\text{ml}$ yeast tRNA). Slides were incubated overnight with a total 10 nM mix of six digoxigenin (DIG)-labeled oligonucleotide probes in hybridization buffer at 37°C (DIG Oligonucleotide 3'-End Labeling Kit, 2nd generation, Roche). Probes sequences are indicated in Appendix Table S1. Sections were rinsed with FAM/SSC (50% formamide, $2\times$ SSC, 0.1% Tween-20) twice 30 min at 37°C , then twice in $0.2\times$ SSC at 42°C , blocked in B1 buffer (100 mM maleic acid pH 7.5, 150 mM NaCl) with 10% fetal bovine serum (FBS) for 1 h, and incubated overnight at 4°C in B1 buffer with an anti-DIG antibody coupled to alkaline phosphatase (Roche, 1:2,000). After three washes in B1 buffer and one wash in B3 buffer (100 mM Tris-HCl pH 9, 50 mM MgCl_2 , 100 mM NaCl, 0.1% Tween-20), slides were stained using the NBT/BCIP kit (Vector lab), rinsed with PBS, and immunostained for TH. *In situ* hybridization in primary neurons was done using an adaptation of the same protocol. The same buffers were used, but probes were detected with an anti-DIG antibody coupled to horseradish peroxidase (Roche, 1:1,000). RNA staining was revealed using the TSA-cyanine 3 system (Perkin Elmer) according to the manufacturer's protocol.

In silico analysis

En1/2-binding sites in the consensus L1Tf 5'UTR sequence (GenBank: AF016099.1) were analyzed *in silico* using Allgen-Promo 3.0 with a 15% maximum matrix dissimilarity rate. Binding sites for En1 were found at position 1,877–1,883->CTTTGT, 2,965–2,971->ACAAGA, and 3,091–3,097->ACAATC.

Electrophoretic mobility shift assay

Biotinylated oligonucleotide probes (100 μM) were annealed in a 1:1 molar ratio in boiling water for 5 min and slowly cooled

down to room temperature. Biotin-labeled double-stranded L1 5'UTR DNA fragments (200 fmol) containing the predicted En2 binding site were incubated with 400 nM recombinant En2 protein (chicken) with the Light Shift Chemiluminescent EMSA kit (Thermo Scientific) in the presence of 1 µg poly(dI-dC), 5 mM MgCl₂, 2.5% glycerol, and 1 µg BSA in a final volume of 20 µl. After incubation for 20 min on ice, DNA-protein complexes were analyzed by gel electrophoresis on 6% polyacrylamide gels in 0.5× TBE buffer and transferred to a positively charged nylon membrane (Roche). Transferred DNA was cross-linked by UV-light at 120 mJ/cm² for 1 min and detected by chemiluminescence. For competition experiments, a 200-fold molar excess of double-stranded unlabeled NP6 was added. The sequences of oligonucleotide probes are indicated in Appendix Table S1. Supershift experiments were done by preincubating 0.4 µg 4D9 antibody (mouse monoclonal, Abcam Ab12454) with 2 µM recombinant En2 for 30 min at RT, followed by the addition of the biotin-labeled L1 probe and 30-min incubation on ice.

Retrotransposition assay

L1 retrotransposition reporter plasmids allow one to follow and quantify retrotransposition events through the quantification of a reporter gene. The reporter gene (in this case GFP) becomes functional only after the reverse transcription of L1 RNA, splicing by the cellular machinery and subsequent integration of the transcript into genomic DNA. HEK293 cells were treated with stavudine or sham 16 h prior to transfection with 8 µg plasmids, either pWA125 (mouse codon-optimized L1 containing the endogenous 5'UTR) or pWA126 (as pWA125, but double-mutated, retrotransposition-incompetent L1; Newkirk et al, 2017). At day 1 post-transfection (p.t.), cells were split and at day 2 p.t. puromycin (0.7 µg/ml; Sigma) was added to eliminate non-transfected cells. Stavudine was added every time cells were split or the medium changed in the concentration indicated in Fig EV3A. At day 9 p.t., the percentage of GFP-positive cells was measured using fluorescence-activated cell sorting (FACS).

To test the activity of Engrailed on the retrotransposition of L1, HEK293 cells (control or doxycycline-inducible for En2 expression; a generous gift from A. Joliot) were cultured and treated with doxycycline or sham for 24 h and transfected with either pWA125 or pWA126 as above.

Statistics

Unless otherwise stated, the graphs represent the mean of replicates. An experimental replicate consisted, if not otherwise indicated, of a single animal or a single culture well. Error bars and values of *n* are as stated in the figure legends. Results were considered as statistically significant for *P*-value < 0.05; in some cases, the exact *P*-value is given. Parametric tests for normal distribution (D'Agostino–Pearson omnibus normality test) and equality of variances (Brown–Forsythe test) were performed prior to the statistical test. The appropriate parametric or non-parametric statistical tests were used as indicated in the figure legends. All statistical analyses were done with the software Prism.

Expanded View for this article is available online.

Acknowledgements

The study was supported by ERC Advanced Grant HOMEOSIGN no. 339379, ANR-11-BLAN-069467, BrainEver, Région Ile de France, Fondation Bettencourt Schueller, and GRL program No. 2009-00424. None of the authors has a financial interest in this study. We thank Wenfeng An and Jef D. Boeke for providing the wt and mutated L1 plasmids, Alain Joliot for the En2 recombinant protein and the doxycycline-inducible HEK293 cells for En2 expression induction, Michel Volovitch for the help in producing Orf1p and Sandy Martin for the initial aliquot of anti-Orf1p antibody used to initiate the study. We thank Thomas Tcheudjio for helping with stereological cell counting and the CIRB imaging and animal facilities for their helpful contributions. We thank Yves Dupraz for the manufacturing of a customized mouse brain slicer.

Author contributions

AP conceived the project with JF and RLJ. AP, JF, and F-XBT wrote the manuscript with the help of RLJ and HR. F-XBT, HR, JF, EP-H, and OM-B conducted all experiments.

Conflict of interest

The authors declare that they have no conflict of interest.

References

- Alho ATL, Suemoto CK, Polichiso L, Tampellini E, Oliveira KC, Molina M, Santos GAB, Nascimento C, Leite REP, Ferreti-Rebustini REL, Silva AV, Nitri R, Pasqualucci CA, Jacob-Filho W, Heinsen H, Grinberg LT (2015) Three-dimensional and stereological characterization of the human substantia nigra during aging. *Brain Struct Funct* 221: 3393–3403
- Alich RS (2006) Unconventional translation of mammalian LINE-1 retrotransposons. *Genes Dev* 20: 210–224
- Alvarez-Fischer D, Fuchs J, Castagner F, Stettler O, Massiani-Beaudoin O, Moya KL, Bouillot C, Oertel WH, Lombès A, Faigle W, Joshi RL, Hartmann A, Prochiantz A (2011) Engrailed protects mouse midbrain dopaminergic neurons against mitochondrial complex I insults. *Nat Neurosci* 14: 1260–1266
- Beck CR, Garcia-Perez JL, Badge RM, Moran JV (2011) LINE-1 elements in structural variation and disease. *Annu Rev Genomics Hum Genet* 12: 187–215
- Bernard C, Kim H-T, Torero-Ibad R, Lee EJ, Simonutti M, Picard S, Acampora D, Simeone A, Di Nardo AA, Prochiantz A, Moya KL, Kim JW (2014) Graded Otx2 activities demonstrate dose-sensitive eye and retina phenotypes. *Hum Mol Genet* 23: 1742–1753
- Bernard C, Vincent C, Testa D, Bertini E, Ribot J, Di Nardo AA, Volovitch M, Prochiantz A (2016) A mouse model for conditional secretion of specific single-chain antibodies provides genetic evidence for regulation of cortical plasticity by a non-cell autonomous homeoprotein transcription factor. *PLoS Genet* 12: e1006035
- Beurdeley M, Spatzza J, Lee HHC, Sugiyama S, Bernard C, Di Nardo AA, Hensch TK, Prochiantz A (2012) Otx2 binding to perineuronal nets persistently regulates plasticity in the mature visual cortex. *J Neurosci* 32: 9429–9437
- Brouha B, Schustak J, Badge RM, Lutz-Prigge S, Farley AH, Moran JV, Kazazian HH (2003) Hot L1s account for the bulk of retrotransposition in the human population. *Proc Natl Acad Sci USA* 100: 5280–5285

- Bulut-Karslioglu A, Perra V, Scaranaro M, de la Rosa-Velazquez IA, van de Nobelen S, Shukeir N, Popow J, Gerle B, Opravil S, Pagani M, Meidhof S, Brabletz T, Manke T, Lachner M, Jenuwein T (2012) A transcription factor-based mechanism for mouse heterochromatin formation. *Nat Struct Mol Biol* 19: 1023–1030
- Bulut-Karslioglu A, De La Rosa-Velázquez IA, Ramirez F, Barenboim M, Onishi-Seebacher M, Arand J, Galán C, Winter GE, Engist B, Gerle B, O'Sullivan RJ, Martens JHA, Walter J, Manke T, Lachner M, Jenuwein T (2014) Suv39h-dependent H3K9me3 marks intact retrotransposons and silences LINE elements in mouse embryonic stem cells. *Mol Cell* 55: 277–290
- Chen L, Ding Y, Cagniard B, Van Laar AD, Mortimer A, Chi W, Hastings TG, Kang UJ, Zhuang X (2008) Unregulated cytosolic dopamine causes neurodegeneration associated with oxidative stress in mice. *J Neurosci* 28: 425–433
- Chow H-M, Herrup K (2015) Genomic integrity and the ageing brain. *Nat Rev Neurosci* 16: 672–684
- Collier TJ, Lipton J, Daley BF, Palfi S, Chu Y, Sortwell C, Bakay RAE, Sladek JR, Kordower JH (2007) Aging-related changes in the nigrostriatal dopamine system and the response to MPTP in nonhuman primates: diminished compensatory mechanisms as a prelude to parkinsonism. *Neurobiol Dis* 26: 56–65
- De Cecco M, Criscione SW, Peterson AL, Neretti N, Sedivy JM, Kreiling JA (2013) Transposable elements become active and mobile in the genomes of aging mammalian somatic tissues. *Aging (Albany NY)* 5: 867–883
- Desplan C, Theis J, O'Farrell PH (1988) The sequence specificity of homeodomain-DNA interaction. *Cell* 54: 1081–1090
- Di Nardo AA, Nédélec S, Trembleau A, Volovitch M, Prochiantz A, Montesinos ML (2007) Dendritic localization and activity-dependent translation of Engrailed1 transcription factor. *Mol Cell Neurosci* 35: 230–236
- Doucet AJ, Wilusz JE, Miyoshi T, Liu Y, Moran JV (2015) Poly(A) tract is required for LINE-1 retrotransposition. *Mol Cell* 60: 728–741
- Erwin JA, Marchetto MC, Gage FH (2014) Mobile DNA elements in the generation of diversity and complexity in the brain. *Nat Rev Neurosci* 15: 497–506
- Evrony GD, Cai X, Lee E, Hills LB, Elhosary PC, Lehmann HS, Parker JJ, Atabay KD, Gilmore EC, Poduri A, Park PJ, Walsh CA (2012) Single-neuron sequencing analysis of L1 retrotransposition and somatic mutation in the human brain. *Cell* 151: 483–496
- Giorgi G, Marcantonio P, Del Re B (2011) LINE-1 retrotransposition in human neuroblastoma cells is affected by oxidative stress. *Cell Tissue Res* 346: 383–391
- Goodier JL, Ostertag EM, Du K, Kazazian HH (2001) A novel active L1 retrotransposon subfamily in the mouse. *Genome Res* 11: 1677–1685
- Goodier JL (2004) A potential role for the nucleolus in L1 retrotransposition. *Hum Mol Genet* 13: 1041–1048
- Han JS, Szak ST, Boeke JD (2004) Transcriptional disruption by the L1 retrotransposon and implications for mammalian transcriptomes. *Nature* 429: 268–274
- Hanks M, Wurst W, Anson-Cartwright L, Auerbach AB, Joyner AL (1995) Rescue of the En-1 mutant phenotype by replacement of En-1 with En-2. *Science* 269: 679–682
- Hunter RG, Murakami G, Dewell S, Seligsohn M, Baker MER, Datson NA, McEwen BS, Pfaff DW (2012) Acute stress and hippocampal histone H3 lysine 9 trimethylation, a retrotransposon silencing response. *Proc Natl Acad Sci USA* 109: 17657–17662
- Joliot A, Prochiantz A (2004) Transduction peptides: from technology to physiology. *Nat Cell Biol* 6: 189–196
- Jones RB, Garrison KE, Wong JC, Duan EH, Nixon DF, Ostrowski MA (2008) Nucleoside analogue reverse transcriptase inhibitors differentially inhibit human LINE-1 retrotransposition. *PLoS One* 3: e1547
- Kalia LV, Lang AE (2015) Parkinson's disease. *Lancet* 386: 896–912
- de Koning APJ, Gu W, Castoe TA, Batzer MA, Pollock DD (2011) Repetitive elements may comprise over two-thirds of the human genome. *PLoS Genet* 7: e1002384
- Kubo S, Seleme MDC, Soifer HS, Perez JLG, Moran JV, Kazazian HH, Kasahara N (2006) L1 retrotransposition in nondividing and primary human somatic cells. *Proc Natl Acad Sci USA* 103: 8036–8041
- Kuramochi-Miyagawa S, Watanabe T, Gotoh K, Totoki Y, Toyoda A, Ikawa M, Asada N, Kojima K, Yamaguchi Y, Ijiri TW, Hata K, Li E, Matsuda Y, Kimura T, Okabe M, Sasaki Y, Sasaki H, Nakano T (2008) DNA methylation of retrotransposon genes is regulated by Piwi family members MILI and MIWI2 in murine fetal testes. *Genes Dev* 22: 908–917
- Lander ES, Linton LM, Birren B, Nusbaum C, Zody MC, Baldwin J, Devon K, Dewar K, Doyle M, FitzHugh W, Funke R, Gage D, Harris K, Heaford A, Howland J, Kann L, Lehoczky J, LeVine R, McEwan P, McKernan K et al (2001) Initial sequencing and analysis of the human genome. *Nature* 409: 860–921
- Li W, Jin Y, Prazak L, Hammell M, Dubnau J (2012) Transposable elements in TDP-43-mediated neurodegenerative disorders. *PLoS One* 7: e44099
- Li W, Prazak L, Chatterjee N, Grüninger S, Krug L, Theodorou D, Dubnau J (2013) Activation of transposable elements during aging and neuronal decline in *Drosophila*. *Nat Neurosci* 16: 529–531
- Lin C, Yang L, Tanasa B, Hutt K, Ju B-G, Ohgi K, Zhang J, Rose DW, Fu X-D, Glass CK, Rosenfeld MG (2009) Nuclear receptor-induced chromosomal proximity and DNA breaks underlie specific translocations in cancer. *Cell* 139: 1069–1083
- López-Otín C, Blasco MA, Partridge L, Serrano M, Kroemer G (2013) The hallmarks of aging. *Cell* 153: 1194–1217
- Macía A, Widmann TJ, Heras SR, Ayllon V, Sanchez L, Benkaddour-Boumzaouad M, Muñoz-Lopez M, Rubio A, Amador-Cubero S, Blanco-Jimenez E, Garcia-Castro J, Menendez P, Ng P, Muotri AR, Goodier JL, Garcia-Perez JL (2017) Engineered LINE-1 retrotransposition in nondividing human neurons. *Genome Res* 27: 335–348
- Malone CD, Brenneke J, Dus M, Stark A, McCombie WR, Sachidanandam R, Hannon GJ (2009) Specialized piRNA pathways act in germline and somatic tissues of the *Drosophila* ovary. *Cell* 137: 522–535
- Malone CD, Hannon GJ (2009) Small RNAs as guardians of the genome. *Cell* 136: 656–668
- Maxwell PH, Burhans WC, Curcio MJ (2011) Retrotransposition is associated with genome instability during chronological aging. *Proc Natl Acad Sci USA* 108: 20376–20381
- Maze I, Feng J, Wilkinson MB, Sun H, Shen L, Nestler EJ (2011) Cocaine dynamically regulates heterochromatin and repetitive element unsilencing in nucleus accumbens. *Proc Natl Acad Sci USA* 108: 3035–3040
- Muotri AR, Chu VT, Marchetto MCN, Deng W, Moran JV, Gage FH (2005) Somatic mosaicism in neuronal precursor cells mediated by L1 retrotransposition. *Nature* 435: 903–910
- Newkirk SJ, Lee S, Grandi FC, Gaysinskaya V, Rosser JM, Vanden Berg N, Hogarth CA, Marchetto MCN, Muotri AR, Griswold MD, Ye P, Bortvin A, Gage FH, Boeke JD, An W (2017) Intact piRNA pathway prevents L1 mobilization in male meiosis. *Proc Natl Acad Sci USA* 114: E5635–E5644
- Nordström U, Beauvais G, Ghosh A, Pulikkaparambil Sasidharan BC, Lundblad M, Fuchs J, Joshi RL, Lipton JW, Roholt A, Medicetty S, Feinstein TN, Steiner JA, Escobar Galvis ML, Prochiantz A, Brundin P (2015) Progressive

- nigrostriatal terminal dysfunction and degeneration in the engrailed1 heterozygous mouse model of Parkinson's disease. *Neurobiol Dis* 73: 70–82
- Oberdoerffer P, Sinclair DA (2007) The role of nuclear architecture in genomic instability and ageing. *Nat Rev Mol Cell Biol* 8: 692–702
- Pezic D, Manakov SA, Sachidanandam R, Aravin AA (2014) piRNA pathway targets active LINE1 elements to establish the repressive H3K9me3 mark in germ cells. *Genes Dev* 28: 1410–1428
- Prochiantz A, Di Nardo AA (2015) Homeoprotein signaling in the developing and adult nervous system. *Neuron* 85: 911–925
- Rekaik H, Blaudin de Thé F-X, Fuchs J, Massiani-Beaudoin O, Prochiantz A, Joshi RL (2015) Engrailed homeoprotein protects mesencephalic dopaminergic neurons from oxidative stress. *Cell Rep* 13: 242–250
- Rockwood LD, Felix K, Janz S (2004) Elevated presence of retrotransposons at sites of DNA double strand break repair in mouse models of metabolic oxidative stress and MYC-induced lymphoma. *Mutat Res* 548: 117–125
- Singer T, McConnell MJ, Marchetto MCN, Coufal NG, Gage FH (2010) LINE-1 retrotransposons: mediators of somatic variation in neuronal genomes? *Trends Neurosci* 33: 345–354
- Siomi MC, Sato K, Pezic D, Aravin AA (2011) PIWI-interacting small RNAs: the vanguard of genome defence. *Nat Rev Mol Cell Biol* 12: 246–258
- Skene PJ, Illingworth RS, Webb S, Kerr ARW, James KD, Turner DJ, Andrews R, Bird AP (2010) Neuronal MeCP2 is expressed at near histone-octamer levels and globally alters the chromatin state. *Mol Cell* 37: 457–468
- Sonnier L, Le Pen G, Hartmann A, Bizot J-C, Trovero F, Krebs M-O, Prochiantz A (2007) Progressive loss of dopaminergic neurons in the ventral midbrain of adult mice heterozygote for Engrailed1. *J Neurosci* 27: 1063–1071
- Spatazza J, Lee HHC, Di Nardo AA, Tibaldi L, Joliot A, Hensch TK, Prochiantz A (2013) Choroid-plexus-derived Otx2 homeoprotein constrains adult cortical plasticity. *Cell Rep* 3: 1815–1823
- St Laurent G, Hammell N, Mccaffrey TA (2010) A LINE-1 component to human aging: do LINE elements exact a longevity cost for evolutionary advantage? *Mech Ageing Dev* 131: 299–305
- Tan H, Qurashi A, Poidevin M, Nelson DL, Li H, Jin P (2012) Retrotransposon activation contributes to fragile X premutation rCGG-mediated neurodegeneration. *Hum Mol Genet* 21: 57–65
- Taylor MS, LaCava J, Mita P, Molloy KR, Huang CRL, Li D, Adney EM, Jiang H, Burns KH, Chait BT, Rout MP, Boeke JD, Dai L (2013) Affinity proteomics reveals human host factors implicated in discrete stages of LINE-1 retrotransposition. *Cell* 155: 1034–1048
- Thomas CA, Paquola ACM, Muotri AR (2012) LINE-1 retrotransposition in the nervous system. *Annu Rev Cell Dev Biol* 28: 555–573
- Torero-Ibad R, Rhee J, Mrejen S, Forster V, Picaud S, Prochiantz A, Moya KL (2011) Otx2 promotes the survival of damaged adult retinal ganglion cells and protects against excitotoxic loss of visual acuity *in vivo*. *J Neurosci* 31: 5495–5503
- Van Meter M, Kashyap M, Rezazadeh S, Geneva AJ, Morello TD, Seluanov A, Gorbunova V (2014) SIRT6 represses LINE1 retrotransposons by ribosylating KAP1 but this repression fails with stress and age. *Nat Commun* 5: 5011
- Wang SH, Elgin SCR (2011) *Drosophila* Piwi functions downstream of piRNA production mediating a chromatin-based transposon silencing mechanism in female germ line. *Proc Natl Acad Sci USA* 108: 21164–21169
- Wylie A, Jones AE, D'Brot A, Lu W-J, Kurtz P, Moran JV, Rakheja D, Chen KS, Hammer RE, Comerford SA, Amatruda JF, Abrams JM (2016) p53 genes function to restrain mobile elements. *Genes Dev* 30: 64–77
- Xie Y, Rosser JM, Thompson TL, Boeke JD, An W (2011) Characterization of L1 retrotransposition with high-throughput dual-luciferase assays. *Nucleic Acids Res* 39: e16

Exploring the physiological significance of L1 expression

Summary and objectives:

Based on the observation that L1 elements (RNA and the ORF1P/2P proteins) are expressed at basal level in midbrain dopaminergic (mDA) neurons, we are currently investigating whether L1 elements could participate to neuronal cell physiology.

By bioinformatic analysis of the distribution of full-length L1 in the mouse reference genome and of RNA-seq data from laser captured SNpc, we observed an enrichment in their frequency in introns of long genes and in their expression from these introns of neuronal long genes harbouring important synaptic functions. We observed that some of these genes identified show altered levels of expression following L1 loss of function. Finally, we questioned the L1-RNP “interactome” in the neuron to address the mechanism by which L1 elements could interfere with gene expression.

Our results are preliminary but constitute leads in understanding the potential physiological role of L1 elements in mDA neurons. In the last part of this section, I will present the methodology we plan to pursue in order to ascertain these results.

Exploring the physiological significance of L1 expression

Introduction

When, in her pioneering work, Barbara McClintock initially discovered transposable elements (TEs), she had postulated that they may carry regulatory roles. For many years, however, scientists disregarded this hypothesis and viewed TEs as selfish parasitic and harmful elements which cells needed to tightly repress. Indeed, TEs were considered potentially useful only in case of a stressful environment as providers of genetic novelty and variability allowing for genomic adaptation. In line with this idea, TE expression and activity have been described in many pathologies such as cancer, schizophrenia or neurodegenerative disorders (Anwar et al., 2017; Blaudin de Thé et al., 2018a; Bundo et al., 2014; Doyle et al., 2017; Simon et al., 2019a)

However, this view of TEs as purely negative, or as adaptive at most, is now challenged with the notion of “domestication” or “exaptation” of TE elements and the acceptance that their transcripts may serve as regulatory long non coding RNA (lncRNA) (Percharde et al., 2018). Even in the brain, retrotransposition in adult neural stem cells has been proposed to give rise to neuronal somatic mosaicism allowing some Darwinian somatic selection in the adult (Muotri et al., 2005). TE elements could influence gene expression in multiple ways ranging from:

- (i) adding promoter regions, attracting transcription factors, influencing DNA compaction and inducing the formation of topologically associated domains (TADs)
- (ii) generating transcripts variants by alternative splicing of the L1 intronic sequence
- (iii) inducing premature polyadenylation
- (iv) releasing regulatory RNAs
- (v) inserting cytosine methylation sites and histone recognition sequences (epigenetic regulators)

In the following study, we focused on the L1 family of TEs. Sequences of this family represent around 21% of the genome. However, most L1 sequences are truncated and unable to mobilise but approximately 100 of them in the human (3000 in the mouse) are full-length and potentially active. When they mobilize, they do it autonomously as their bicistronic transcript encodes the enzymatic apparatus necessary for reverse transcription and insertion into the genome. While analysing the effect of L1 elements in the pathology of midbrain dopaminergic (mDA) neurons,

our team has made the observation that L1 elements are expressed at basal levels in healthy wild-type neurons. This has led us to question whether these L1 elements could participate in normal cell function. In order to address this question, we have mapped the localisation of full-length L1 (fL1) elements throughout the reference mouse (mm9) genome and observed that they are enriched in neuronal long genes (>100kb). In order to test the importance of L1 elements in neuronal physiology we blocked L1 activity by multiple approaches *in vivo* and *in vitro* and assessed the levels of expression of selected long genes encompassing an intronic L1 sequence. Our results show that blocking L1 greatly impacts expression levels for genes of decisive importance in neuronal communication and function. We hypothesize that L1 elements facilitate the transcription of long genes, by inducing DNA breaks in a topoisomerase-like manner. Mechanistically, we propose that L1 activity exerts the latter activity by interacting with multiple cellular factors, including topoisomerase 1 (TOP1), but also host RNA-binding proteins implicated in the expression of long genes such as SFPQ, TDP-43 and FUS.

Results

fIL1 are enriched in Long Genes

Analysing the mouse (mm9) reference genome, we find that 651 of the 2887 total fIL1 elements annotated in the L1Basev2 database are located in gene introns. Most of these “hosting genes” are exceptionally long genes (>100kB) (**Fig 1.a**). Comparing this frequency with random distribution, it appears that the presence of fIL1s in introns of long genes is higher than by pure chance and thus independently of gene length (**Fig 1.b**). Full-length L1 do not insert randomly, but the basis of their insertion preferences is still not completely understood. However, no evidence points, so far, toward a preferential insertion of fIL1s in intronic regions. Thus, the preferential presence of fIL1s in introns of long genes, specifically, could suggest that fIL1 have been retained during evolution in long introns through positive or neutral selection. It is known that, of the approximately 3000 fIL1 annotated in the mouse genome, only a subset is expressed from so-called “hotspots” in a tissue-specific manner (Philippe et al. 2016; Deininger et al., 2016). We have re-analyzed our previously generated RNA-seq data from laser-capture microdissected wildtype mouse substantia nigra pars compacta tissue (SNpc, n=2, each n comprised of four pooled SNpcs) to specifically identify genomic regions from which L1 elements are expressed (“L1 hotspot” analysis, RepEnrich). Concordantly, in the SNpc, we find evidence of expression of only a small subset of fIL1. Interestingly, these fIL1 expression hotspots are preferentially located in long genes and we observe a positive correlation between the expression level of fIL1 and that of fIL1 containing host genes (**Fig 1.c and d**).

a

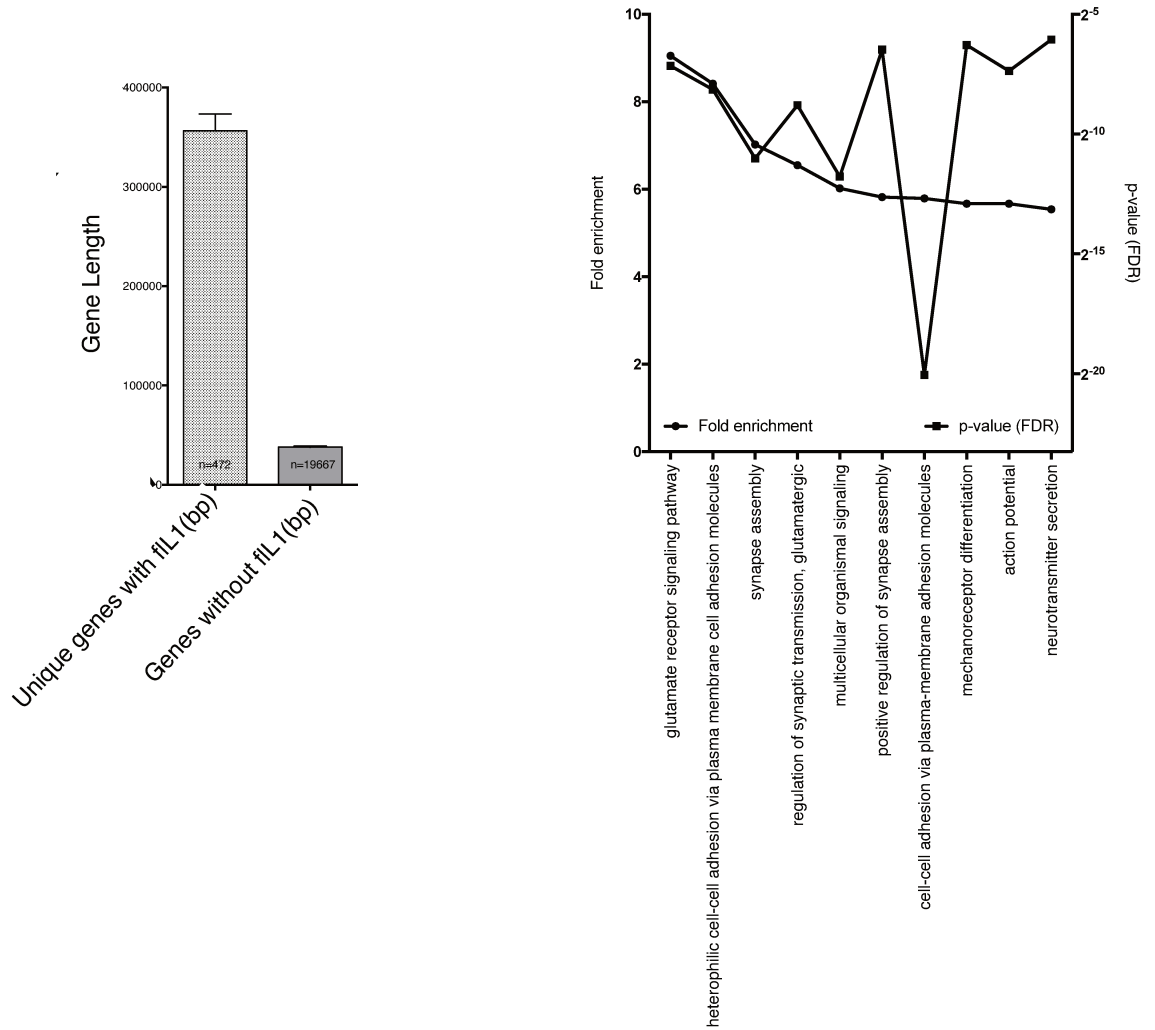


Figure 1: Analysis of genes containing intronic fil1

a) Size of genes containing fil1 or without fil1 using all annotated genes in the *Mus musculus* (house mouse) genome assembly MGSCv37 (mm9) from Genome Reference Consortium [GCA_000001635.1 GCF_000001635.18] (n=20318). All fil1-hosting genes (n=472) were analyzed in GO. Depicted are the top10 categories of 95 significantly enriched and 2 significantly depleted GO categories in GO biological process (right Y-axis: FDR p-value and left Y-axis: Fold-enrichment). Genes containing an intronic fil1 are enriched in neuronal-related GO terms.

b

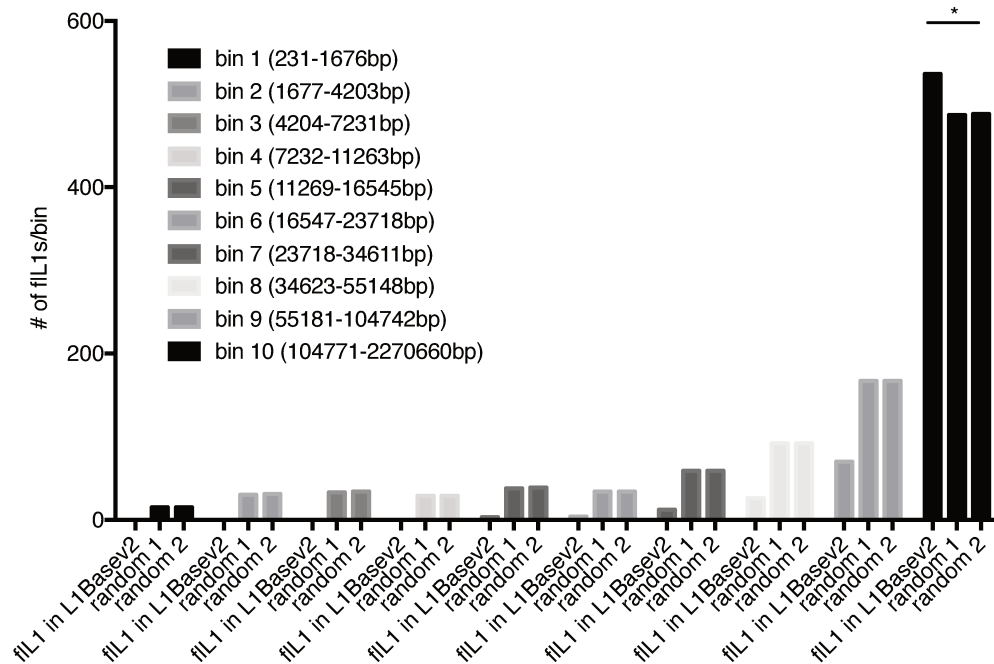


Figure 1: Analysis of genes containing intronic fil1

b) Analysis of the frequency of intronic fil1s in the mouse genome. All annotated genes in the *Mus musculus* (house mouse) genome assembly were divided into ten equally sized bins (2014 genes/bin) depending on their gene length. All gene intervals within a bin were then joined with the sequence intervals of mouse fil1s as annotated in L1Basev2 (2780 regions) adjusted through crossing with the RepeatMasker annotation using Galaxy. The presence of fil1s per bin were counted and the number of hits was divided by the length of the respective bin in base pair (bp). Two random datasets with equal interval spaces as in the fil1 annotation were generated and randomly distributed across mouse chromosomes (Kruskal-Wallis non-parametric ANOVA followed by Dunn's multiple comparison test, $\alpha < 0.05$, * $p < 0.05$).

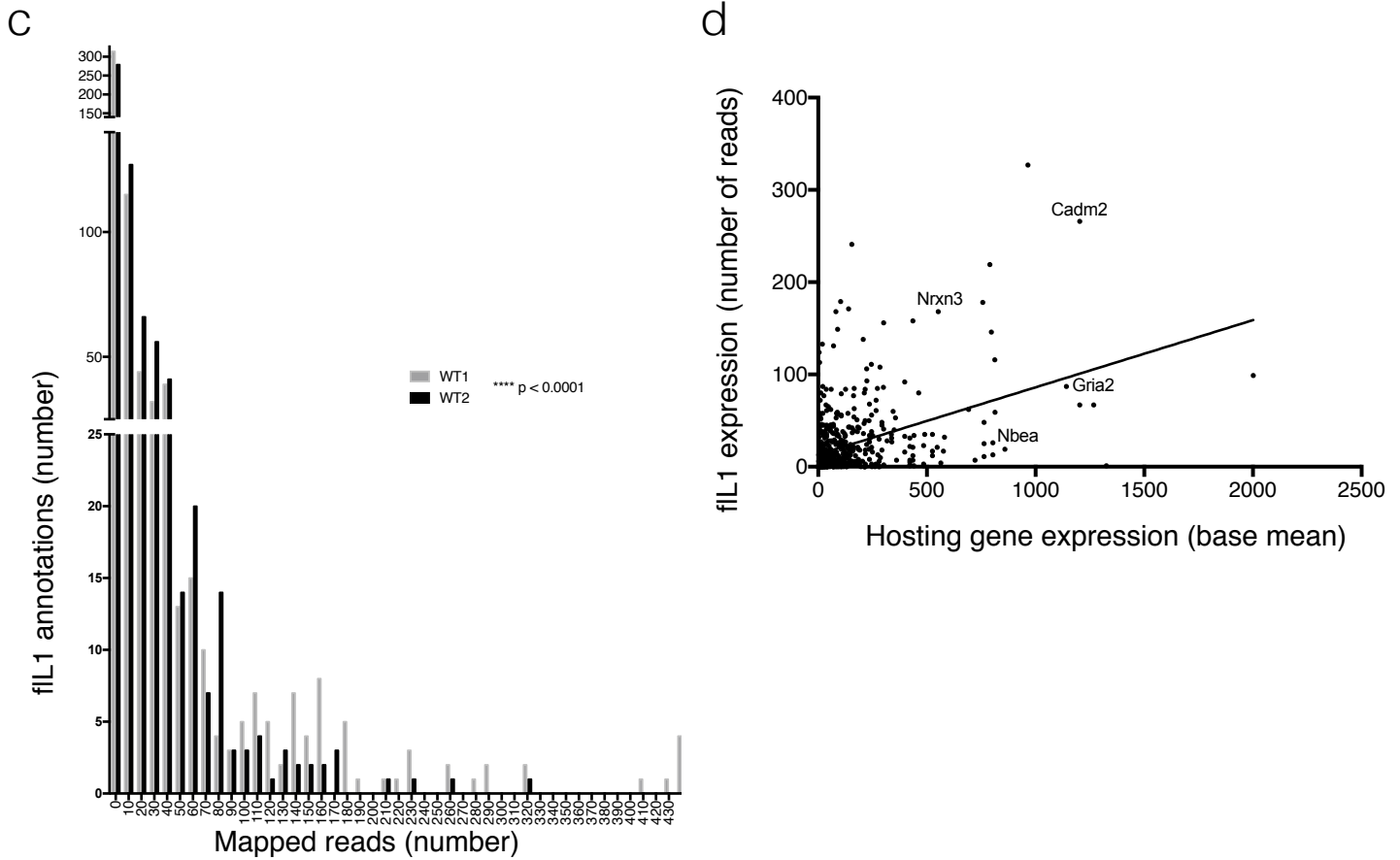


Figure 1: RNA-seq analysis of intronic *fil1* and hosting gene expression in laser-captured SNpc from two independent pools (n=4) of Swiss wildtype mice. c) “Hotspot” analysis of *fil1* reveals differences and similarities in the frequency of hotspots in the mouse SNpc. RepEnrich was used to estimate expression levels of *fil1*s annotated in L1Basev2 in RNA-seq data from mouse wildtype laser-captured SNpc (n=2 independent RNA-seq experiments, WT1 and WT2, pooled SNpcs (n=4 each)). The number of *fil1*s per bin of mapped read numbers from each pool of wildtype SNpcs was plotted in a frequency distribution (bin size=651, Kolmogorov-Smirnov test, p<0.0001). d) *FIL1*s expression correlates with the expression of hosting genes. The number of reads per *fil1* was correlated with the base mean expression of their hosting genes by linear regression analysis (p<0.0001, goodness of fit r²=0.17, Y = 0.07282*X + 13,23).

Down regulation of L1 expression impacts gene expression and respective protein levels

To test whether L1 elements could impact the expression of the long genes containing fL1 in their intronic sequences, we down regulated L1 activity by three different means *in vivo* and *in vitro*:

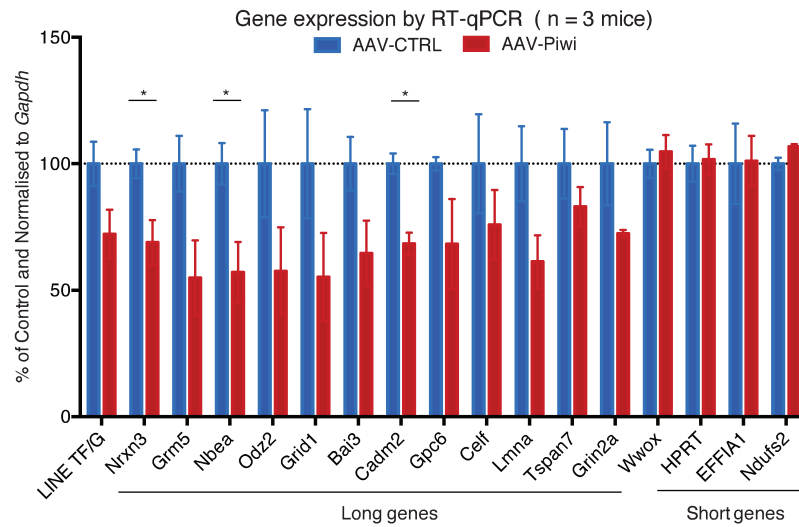
- (i) using the drug stavudine, an inhibitor of reverse transcriptase
- (ii) introducing a siRNA directed against L1-ORF2 and ORF1 sequence coupled to penetratin as well as
- (iii) inducing a gain of function of PIWI by AAV delivery, a known repressor of L1 elements in germ cells.

In vivo we performed stereotaxic injections just above the SNpc of wild type Swiss mice of either the AAV-PIWI for 5 weeks or infusion of the siRNA for 72h. *In vitro*, the stavudine treatment of 10div midbrain primary neurons was 48h. To test the efficacy of all three techniques we assessed levels of L1 elements, either by ORF1p immunohistochemistry to validate the decrease of L1 protein levels or by qPCRs to quantify RNA levels (**Sup 1 page 103**). In all three conditions, qRT-PCR were performed to assess the levels of expression of long genes containing fL1 as well as of short genes for control. The results show that the expression of long genes correlates with the expression of L1 elements: when L1 elements are repressed, the levels of expression of long genes are decreased (**Fig 2.**). On the other hand, the four short genes tested did not show altered levels of expression.

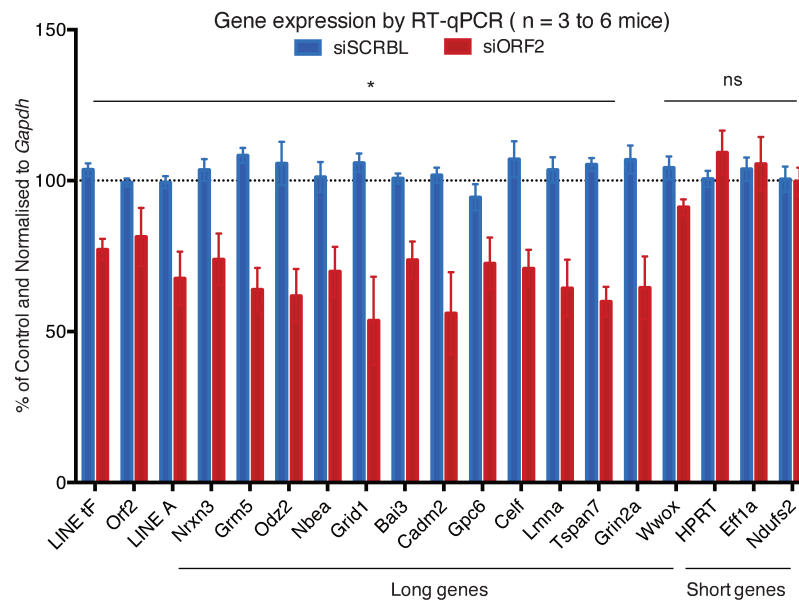
To further evaluate this effect at the protein level, we carried out immunohistochemistry staining for two candidates, NRXN3 and GRID2, in TH neurons and quantified the intensity of the staining in the control condition (siSCRBL) versus the siORF2 infused side. Quantifications demonstrate that proteins levels are decreased in the siORF2 condition. This effect is stronger for NRXN3 than for GRID2 (**Fig 3.**).

We find that the decrease in long gene expression after treatment with stavudine is mirroring the previously described effects of the topoisomerase 2 (TOP2) inhibitor etoposide (our own data not shown here and (Madabhushi et al., 2015)) and of the topoisomerase 1 (TOP1) inhibitor topotecan (our own data **Fig 2.c** and (King et al., 2013a)) on long gene expression. This suggests that L1 might facilitate long gene expression in a “topoisomerase-like” manner. We thus wondered whether L1 elements interact with TOP1 and other proteins implicated in DNA transcription.

a



b



c

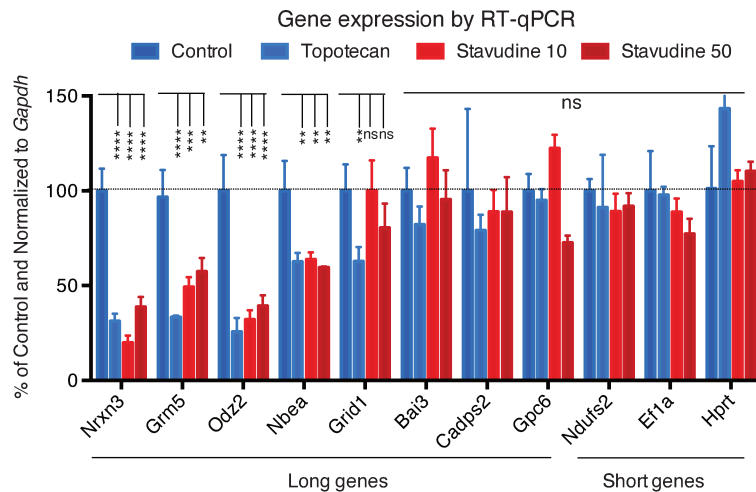
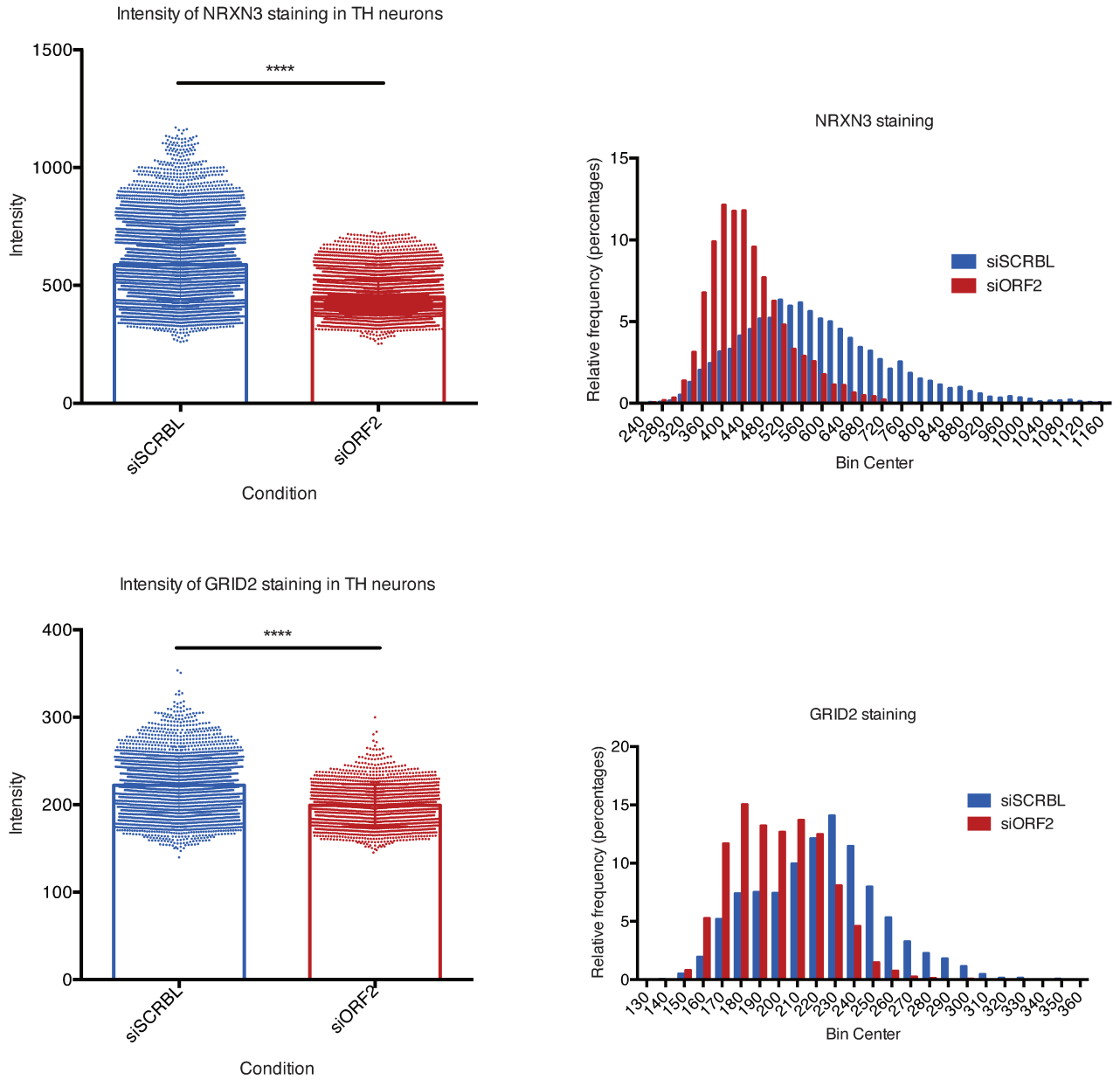


Figure 2: RT-qPCR analysis of long and short genes in vivo and in vitro expression following a L1-element LOF

- a) Injections of AAV8-Piwi versus AAV-CTRL n = 3 mice (Swiss, WT) per condition. Unpaired t-test.
- b) In vivo infusion of siSCRBL (CTRL) versus siORF2 n = 3 to 6 mice (Swiss, WT) per condition. Unpaired t-test
- c) Midbrain Primary Neurons treated with Stavudine or Topotecan 48h, 3 wells per condition Unpaired t-test.

a



b

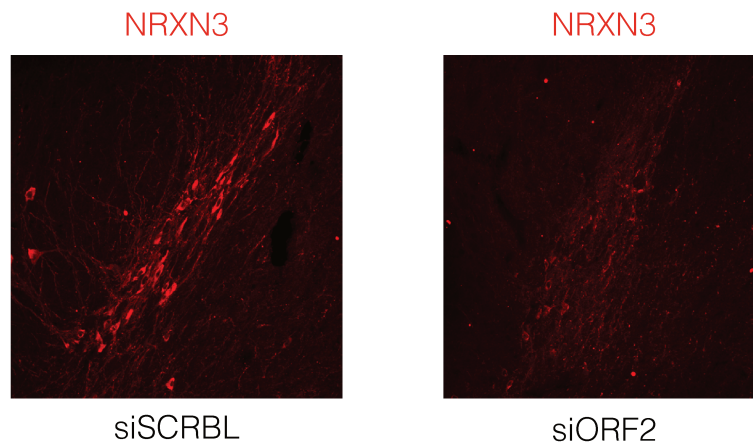


Figure 3: Expression of NRXN3 and GRID2 diminishes following siORF2 infusion in vivo
 a) Quantifications of NRXN3 and GRID2 staining in TH neurons following infusion of siSCRBL (CTRL) and siORF2. Number of mice = 3 (Swiss, WT). Number of slices = 3/mice; number of images = 9 per mice. Detection of particles using particle analysis by ImageJ after thresholding in the TH canal (mask) and measure of mean intensity per particle in NRXN3 and GRID2 canals.
 b) Immunohistochemistry against NRXN3 and GRID2 in siORF2 and siSCRBL conditions

Mapping the L1 protein interactome in neurons

In order to understand the pathway by which L1 elements might impact gene expression we decided to pursue a mass spectrometry (MS) approach in collaboration with the proteomic platform at the Institut Curie to search for interactors of the coding protein ORF1p of L1 elements. To do so, we performed a pull-down on magnetic beads coupled with anti-ORF1p or IgG rabbit (negative control) antibodies, starting from the pooled SNpc of 8 wild-type mice. This has allowed us to identify around 200 potential interactors and to conduct a GO slim ontology analysis (see Material and Method section). Very interestingly, the top three hits included ribonucleoprotein complex assembly, translation and mRNA processing, suggesting that ORF1p could interfere in association with RNA binding proteins to regulate gene expression (**Fig. 4 a**). These interactions, although very encouraging, must obviously be confirmed by other approaches, including co-immunoprecipitation. It is however comforting to realise that other teams have published ORF1p MS data that are in accordance with our own data. For example, out of the 9 proteins identified by Taylor and colleagues as interactors of ORF1p in HEK cells (Taylor et al., 2018), we find 6 proteins which are either identical or of the same family (**Fig. 4 b**). Furthermore, the demonstration by the same group that ORF2p interacts with TOP1 incited us to validate the interaction of TOP1 with ORF1p as illustrated in the co-immunoprecipitation and western blot of **Figure 4.c**.

It is of note for further studies in the field of neurodegeneration that our MS analysis revealed the presence neurodegeneration-relevant proteins including FUS and TDP43 (Amyotrophic Lateral Sclerosis), TAU (Alzheimer disease) and DJ-1 (PD). Several studies carried out in *in vitro* cell models have observed a colocalisation of ORF1p with FUS or TDP-43 (Goodier et al., 2007a; Pereira et al., 2018). Interestingly, the loss of TDP43 and FUS preferentially affects the splicing of transcripts with long (> 100 kb) first introns (Lagier-Tourenne et al., 2012). Again, direct co-immunoprecipitations will have to confirm these data.

a

GO Term	Enrichment	P-value
Ribonucleoprotein complex assembly	4,458	2,04E-10
Translation	3,891	9,45E-13
mRNA processing	3,356	2,60E-10
Generation of precursor metabolites and energy	3,315	1,92E-08
Protein-containing complex assembly	2,97	1,17E-25
Cytoskeleton organization	2,802	8,78E-17
Cell-cell signaling	2,563	3,98E-10
Cellular component assembly	2,54	3,28E-28
Cell morphogenesis	2,254	6,77E-07
Vesicle-mediated transport	2,238	1,83E-11
Transport	1,836	2,07E-17
Cellular nitrogen compound metabolic process	1,632	3,28E-09



b

Taylor et al., 2018 co-IP			Own MS		
Gene Symbol	Uniprot Symbol	Protein	Gene Symbol	Uniprot Symbol	Protein
YARS2	Q9Y2Z4	Tyrosine-tRNA ligase, mitochondrial	YARS2	Q8BYL4	Tyrosine-tRNA ligase, mitochondrial
ERAL1	O75616	GTPase Era, mitochondrial	ERAL1	Q9CZU4	GTPase Era, mitochondrial
PABPC4L	P0CB38	Polyadenylate-binding protein 4-like	PABPC1	P29341	Polyadenylate-binding protein 1-like
HIST1H2BO	P23527	Histone H2B type 1-O	HIST1	P10922	Histone H1.0
CORO1B	Q9BR76	Coronin-1B	CORO1A and CORO2B	Q8BH44/ Q89053	Coronin-1A and Coronin-2B
DDX6	P26196	Probable ATP-dependent RNA helicase DDX6	DDX3 and DDX17	Q62167/Q501J6	Probable ATP-dependent RNA helicase DDX3/17
TROVE2	P10155	60 kDa SS-A/Ro ribonucleoprotein			Not found
LARP7	Q4G0J3	La-related protein 7			Not found
MEPCE	Q7L2J0	7SK snRNA methylphosphate capping enzyme			Not found

c

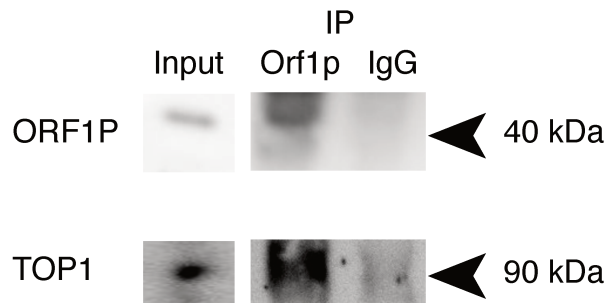


Figure 4: Characterisation of the L1 interactome in the SNpc of wild-type mice

a) GO Analysis of the ORF1p co-IP after MS with enrichment and p-value (GO terms with p-value under 10E-6 were excluded), GO method is described in Material and Method. Word Cloud of GO terms is ranked in function of enrichment values.
 b) Table comparing the ORF1P interactors described in Taylor et al.,2018 in HEK cells and our own MS results.
 c) Western blot against ORF1P and TOP1 after pull down of ORF1P antibody and IgG (control).

SFPQ, an RNA-binding protein implicated in long gene transcription, potentially interacts with ORF1p

Apart from the putative direct or indirect ORF1p interactors mentioned above SFPQ, a splicing factor and RNA-binding protein attracted our attention. Indeed, it has recently been shown that the SFPQ loss-of-function in mice leads to neurodegeneration due to a specific perturbation of long-gene transcription, a process termed “long-gene transcriptopathy” (Takeuchi et al., 2018). This supports the view that long genes enriched in neuronal functions undergo a specific transcriptional and co-transcriptional regulation and that disturbing this process leads to neurodegeneration (Gabel et al., 2015; King et al., 2013b; Zylka et al., 2015). Furthermore, SFPQ has been implicated in ALS disease (Luisier et al., 2018) and display a nucleocytoplasmic redistribution in brain neurons of patients with Alzheimer or Pick disease (Ke et al., 2012). Interestingly, one early feature of Alzheimer disease is the up-regulation of long genes in hippocampal cells (Barbash and Sakmar, 2017).

We recapitulated nuclear to cytoplasmic displacement of SFPQ in the SNpc after acute oxidative 6-OHDA stress *in vivo*. Nuclear depletion starts as early as 1h (**Fig. 5 a**) until total cytoplasmic redistribution at 24h (**Fig. 5 b**). This is specific for TH neurons that selectively uptake the 6-OHDA. This nuclear depletion of SFPQ also observed in AD and Pick might be a shared feature of several neurodegenerative diseases. Furthermore, as oxidative stress induces an increase in L1 element expression (Rekaik 2015, de Thé, 2017), we cannot exclude that SFPQ is redistributed via L1 gene products. Supporting this hypothesis, the loss of function of L1 elements following the siORF2 infusion in the SNpc of wild-type mice is characterized by a complete extinction of the SFPQ signal (**Fig. 5 c**), compared to the control condition (siSCBRL).

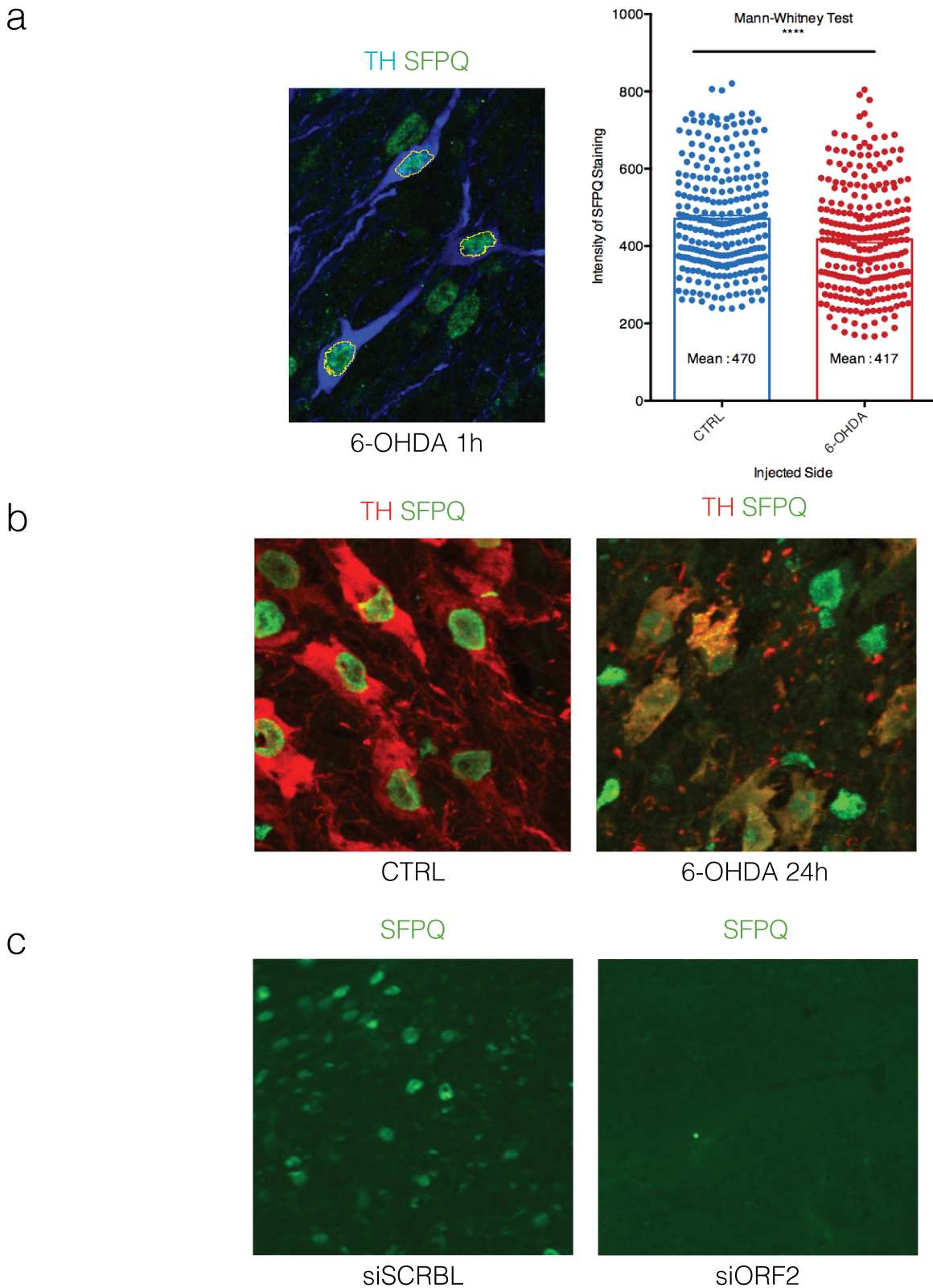


Figure 5: SFPQ protein levels vary in oxidative stress and LOF of LINE-1 conditions
 a) TH (blue) and SFPQ (green) staining after injection of 6-OHDA in the SNpc of Swiss WT mice. Quantification of SFPQ nuclear staining in TH neurons in 6-OHDA injected and non-injected side (CTRL) after 1h. Number of mice $n = 4$; number of slides per mice $n = 3$; total number of neurons counted in CTRL and 6-OHDA conditions $n = 260$ and 263 . The data did not pass Normality test, Mann-Whitney test p -value < 0.0001 ****. b) TH (red) and SFPQ (green) staining 24h after 6-OHDA injection. c) SFPQ (green) staining in LINE-1 LOF by siORF2 infusion and in CTRL condition (siSCRBL infusion)

Plan of action to ascertain current preliminary results

Our results, although of potential interest, are still preliminary and need to be completed by the following experiments:

- The group of Clemens Scherzer at Harvard Medical School has recently generated a unique single-cell post-mortem RNA-seq dataset of human dopaminergic neurons from 93 individuals with ages ranging from 38 to 99 years, available through the database of Genotypes and Phenotypes (dbGaP). We will analyse the repetitive element expression repertoire in these neurons and characterize age- and gender-associated changes in fL1 and host gene expression. More specifically, we will focus on the characterization of genomic hotspots from which fL1s are expressed.
- To specifically target L1 RNA, we will use antisense oligonucleotides (ASOs) which have been shown, in a different system, to efficiently downregulate nuclear L1-RNA expression (Percharde et al., 2018). Among the different ASOs available, we will use LNA-GapmeRs which specifically and efficiently target nuclear RNAs and degrade them via a RNaseH-dependent mechanism.
- We will analyse the effects of L1 LOF in a genome-wide manner using ATAC-seq and long-read RNA-sequencing. ATAC-seq is a method to assess genome-wide chromatin accessibility. It utilizes a hyperactive Tn5 transposase to insert sequencing adapters into open chromatin regions. Reads obtained through high-throughput sequencing thus indicate regions of increased chromatin accessibility. This will allow us to study if L1 expression can impact chromatin organization and accessibility to specific genes. Long-read sequencing will provide information on the regulation of gene expression in an unbiased way and tell us whether L1 elements specifically modify the transcription of long genes.
- Finally, we further need to characterize the mechanism by which L1 elements regulate gene expression.

The overall study will be discussed in the discussion Part III of the thesis.

Materials and Methods

Animals

Mice were treated following the guidelines for the care and use of laboratory animals (US National Institute of Health) and European Directive 2010/63/UE. All experimental procedures were validated by the ethical committee (CEA 59) of the French Ministry for Research and Education. Swiss OF1 wt (Janvier) were maintained under a 12 h day/night cycle with ad libitum access to food and water. A maximum of six mice were housed per cage, and cotton material was provided for nest building. Experimental groups consisted of three to eight adult male mice. No randomization or blinding was used.

***In vivo* stereotaxic injections**

For injections, mice were placed in a stereotaxic instrument, and a trepanation hole was drilled into the skull 3.3 mm caudal and 1 mm lateral to the Bregma. The needle was lowered 3.8 mm from the skull surface, and AAV8-Eif1a-PiwiMyc or - AAV8-Eif1a-GFP or mCherry (Vector Biolabs 2 μ l, 10¹² GC/ μ l) or siORF2/siSCRBL (QUIAGEN) injections were performed over 15 min at day 0.

Cell primary Cultures

Midbrain primary neurons were dissected from E 14.5 embryos and cultured in Neurobasal medium (Life Technologies) supplemented with glutamine (500 μ M, Sigma), glutamic acid (3.3 mg/l Sigma) aspartic acid (3.7 mg/l, Sigma), anti-anti (Gibco), and B27 (Gibco) in cell-culture dishes coated with poly-ornithine and laminin. Cells were treated where indicated by adding stavudine to the culture medium at indicated concentrations. For RNA extraction, cells were washed with PBS 1X and 500 μ l of Quiazol (Invitrogen) were added per well.

Western Blot

Protein extracts were run on NuPAGE™ 4-12% Bis-Tris gels (ThermoFischer Scientific NP0323BOX). The samples migrated in 1X MES or MOPS solution at 200V for 1h. Transfer was performed at 400mA for 1h on PVDF membranes. Membranes were blocked in 5% Milk-TBST 1h, incubated overnight at 4 °C with primary antibodies in 2.5% milk-TBST, rinsed 30 min in TBST, incubated 1h at room temperature with secondary HRP antibodies in 2.5% milk-TBST. Following a 30min TBST wash the membranes were revealed with ImageQuant LAS-400 (GE Healthcare).

Immunostaining

Immunostaining was achieved as described (Alvarez-Fischer et al, 2011). The following primary antibodies were used: anti TH chicken (Abcam, ab76442), anti Nrnx3 Sheep, anti Grid2 Rabbit, anti Orf1p Guinea Pig (In house). All primary antibodies were used at a dilution of 1/500. Secondary antibodies were as follows: 488 anti- chicken, 647 anti-guinea pig, 488 anti-mouse, 546 anti-chicken, 647 anti rabbit Alexa Fluor (Life Technologies). Secondary antibodies were used at a dilution of 1/1000. Labelled immunohistochemistry of brain sections were imaged by confocal microscopy (CSU Yokogawa Spinning Disk W1) and by Wide field (Axiozoom Zeiss).

RT- qPCR

Cultured cell total RNA was extracted with the mRNeasy Mini Kit (Qiagen) with DNA removal using Quiazol and processed with the QuantiTect Reverse Transcription Kit (Qiagen). cDNA was diluted 1:50 with RNase-free water for quantitative PCR samples, which were analyzed in duplicates with a LightCycler 480 II (Roche) and SYBR Green I Master mix. After T_m profile validation, gene expression was determined by the 2^{-ΔΔCt} method with *Hprt* or *Gapdh* as control genes.

Co-Immunoprecipitation and subsequent MS

Proteins from dissected SNpc were extracted in Tris-HCl pH 7.5 10mM, 150mM NaCl, 0.5%NP-40 with protease inhibitors (Pierce Thermo Scientific) and incubated for 2 hours at 4°C with 50μl of Orf1p/IgG Magnetic Beads prepared according to the Dynabeads Coupling Kit (LifeTech). After 5 washes with TrisHCl 10mM, 150Mm NaCl with protease inhibitors, magnetic beads were washed thrice with 100 μL of 25 mM NH₄HCO₃ and on-beads digestion was performed with 0.6 μg of trypsin/LysC (Promega) for 1 hour in 100 μL 25 mM NH₄HCO₃. Sample were desalted on homemade C18 StageTips for desalting, peptides eluted using 40/60 MeCN/H₂O + 0.1% formic acid and vacuum concentrated to dryness.

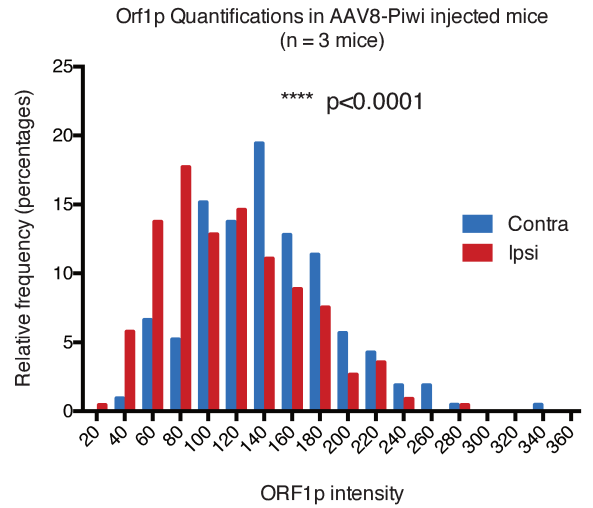
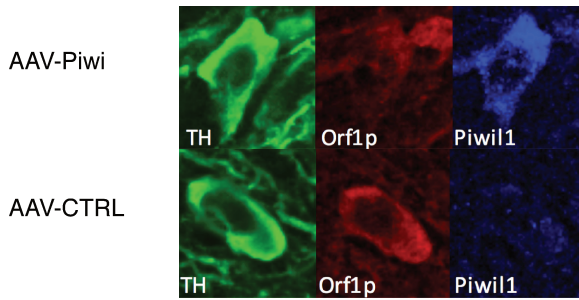
Online chromatography was performed with an RSLCnano system (Ultimate 3000, Thermo Scientific) coupled online to a Q Exactive HF-X with a Nanospay Flex ion source (Thermo Scientific). Peptides were first trapped on a C18 column (75 μm inner diameter × 2 cm; nanoViper Acclaim PepMapTM 100, Thermo Scientific) with buffer A (2/98 MeCN/H₂O in 0.1% formic acid) at a flow rate of 2.5 μL/min over 4 min. Separation was then performed on a 50 cm x 75 μm C18 column (nanoViper Acclaim PepMapTM RSLC, 2 μm, 100Å, Thermo

Scientific) regulated to a temperature of 50°C with a linear gradient of 2% to 30% buffer B (100% MeCN in 0.1% formic acid) at a flow rate of 300 nL/min over 91 min. MS full scans were performed in the ultrahigh-field Orbitrap mass analyzer in ranges m/z 375–1500 with a resolution of 120 000 at m/z 200. The top 20 intense ions were subjected to Orbitrap for further fragmentation via high energy collision dissociation (HCD) activation and a resolution of 15 000 with the intensity threshold kept at 1.3×10^5 . We selected ions with charge state from 2+ to 6+ for screening. Normalized collision energy (NCE) was set at 27 and the dynamic exclusion of 40s. For identification, the data were searched against the *Mus musculus* (UP000000589_10090 012019) database using Sequest HF through proteome discoverer (version 2.2). Enzyme specificity was set to trypsin and a maximum of two-missed cleavage sites were allowed. Oxidized and loss of methionine and N-terminal acetylation were set as variable modifications. Maximum allowed mass deviation was set to 10 ppm for monoisotopic precursor ions and 0.02 Da for MS/MS peaks. The resulting files were further processed using myProMS (Poulet et al, 2007) v3.6 (work in progress). FDR calculation used Percolator and was set to 1% at the peptide level for the whole study. GO enrichment analysis was performed as in Kowal et al. (PNAS, 2016)

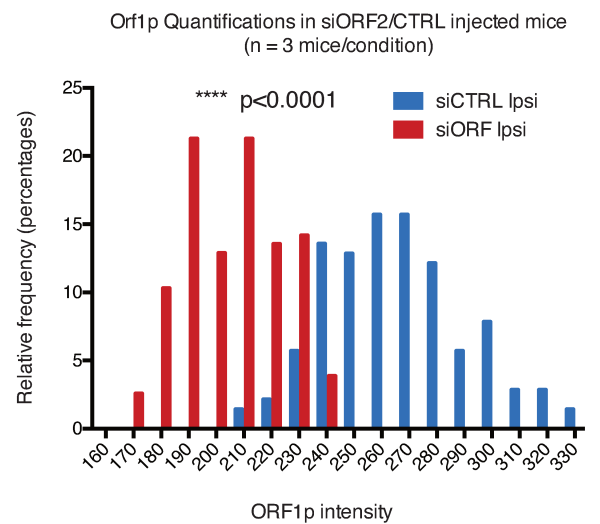
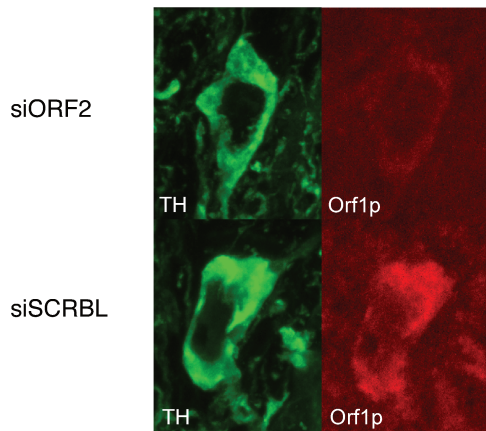
[Supplementary material](#)

Supplemental 1: Validation of the L1-LOF Tool

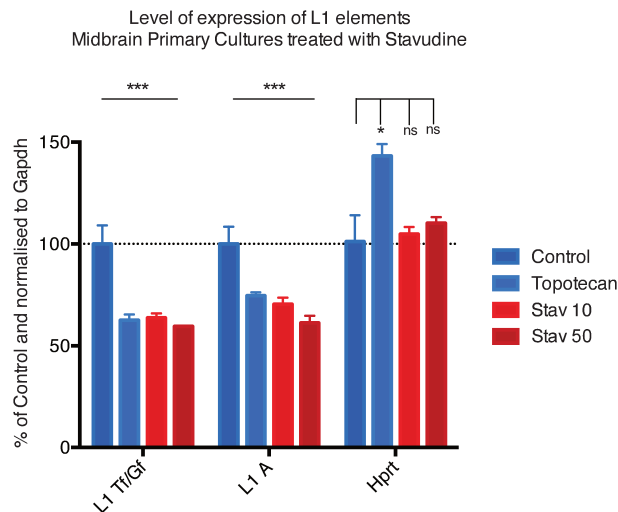
a



b



c



Supplementary 1 : Validation of anti-L1 elements tools a) Immunohistochemistry and Quantifications of Orf1p in TH neurons in AAV8-Piwi injections (N = 3 mice and 212 TH neurons on Ipsi side versus 226 neurons on Contra side) b) Immunohistochemistry and Quantifications of Orf1p in TH neurons in siORF2 Ipsi infusions and siCTRL Ipsi infusions (N = 3 mice / condition and 140 TH neurons for siORF2 versus 155 TH neurons for siCTRL) c) qPCR for LineA/Tf for in vitro treatment of midbrain primary neurons with Stavudine

DISCUSSION

Part I: ENGRAILED, a multi-faceted protein, more than just a transcription factor during development

Since ENGRAILED is a potential therapeutic protein for PD, better understanding its mode of action and deciphering its cell-autonomous versus non-cell autonomous functions in mDA neurons is important. In this study, we demonstrate that non-cell autonomous ENGRAILED plays a role in mDA neuron dendritic maintenance and survival *in vivo* and in dendritic maintenance of midbrain primary neurons expressing ENGRAILED *in vitro*. In a first approach aimed at understanding the regulation of dendrite stability, I have started to decipher the effect of ENGRAILED on small GTP binding proteins of the Rho-Rac-CDC42 family.

What are the direct targets of ENGRAILED following internalisation?

Previous studies conducted in the lab demonstrated that ENGRAILED, in addition to its transcriptional activity also regulates mRNA translation through an interaction with the translation initiation factor EIF4E and that this is part of the mechanism involved in growth cone collapse and synapse maintenance (Brunet et al., 2005; Wizenmann et al., 2009a; Nedelec 2011; Stettler 2012; Yoon 2012). Among the translational targets are mitochondrial proteins, including NDUFS1, NDUFS3, and LAMINB2. LAMINB2 is known as a protein from the intermediate filament family present in the nuclear lamina of the inner nuclear membrane (Prokocimer et al., 2009). Accordingly, lamin mutations alter the heterochromatin and induce laminopathies, rare diseases provoking rapid aging (Worman, 2012). This made the observation of LAMINB2 in the axon very surprising and suggested novel functions associated with translation-regulated mitochondrial activity and axon integrity (Yoon et al., 2012).

Before coming back to the point of mitochondrial activity, I will just indicate that I envisage to identify all ENGRAILED translational targets through an unbiased approach. To that end I will perform Translating Ribosome Affinity Purification (TRAP) experiments in gain of function paradigms. Indeed, the TRAP technique permits the purification and sequencing of mRNAs “under translation” thanks to EGFP tagged ribosomes pulled down by EGFP magnetic beads. This will be done first in EN-expressing midbrain neurons in culture and then *in vivo* using a TH or DAT promoter allowing for specific expression in mDA neurons.

Does Non-cell autonomous ENGRAILED regulate dendritic maintenance via physiological eustress?

Coming back to mitochondrial activity, it can be recalled that not only does ENGRAILED regulate the translation of complex I mitochondrial proteins (Alvarez-Fischer 2011), but also induces oligomycin-sensitive mitochondrial ATP synthesis within 100 seconds following its addition to the culture medium (Stettler et al., 2012). In the same report, Stettler and colleagues show that the ATP is secreted, degraded into adenosine and induces axonal growth cone collapse through an activation of adenosine Receptor 1. It is possible that a similar, but opposite, mechanism may contribute to dendritic elongation *in vitro*. This might also be the case *in vivo*, although the loss of dendrites could be secondary to mDA cell death or to a disruption of synaptic contact not related to dendrite growth or retraction. Finally, it must not be forgotten that ATP can have an intracellular activity by providing the energy necessary to the dynamic modification of the cytoskeleton, in particular through GTP recycling necessary for small GTP-binding protein activity (Heasman and Ridley, 2008).

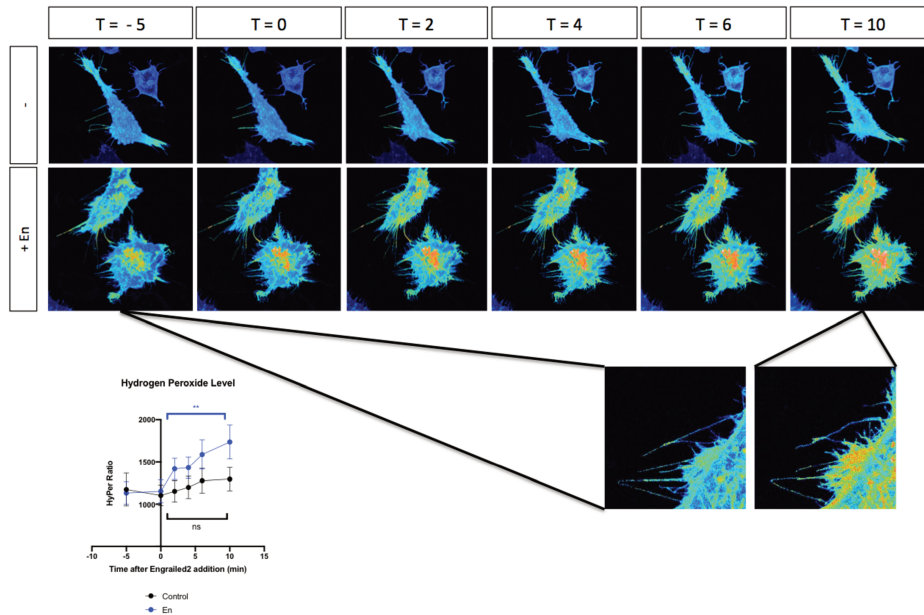
It cannot be forgotten that ATP synthesis is paralleled with reactive oxygen species (ROS) synthesis, a class of highly reactive molecules and by-products of oxygen reduction. The main sources of endogenous ROS in the cell are the respiratory chain of the mitochondria and the NADPH oxidases (NOX), a transmembrane enzyme complex (Halliwell, 1992). An improper balance between ROS production and detoxification by the antioxidant enzymes of the cell (superoxide dismutase-SOD, catalase, vitamins) has been hypothesized as one of the major culprit in neurodegenerative diseases (Ames et al., 1993; Sorce and Krause, 2009; ZHOU et al., 2008). Indeed, in PD, changes in antioxidant molecules and mitochondrial dysfunction of complex I have been reported (Dias et al., 2013).

However, in the last decade a growing body of literature has come to support the need of distinguishing (i) an overproduction of ROS inducing cell death: **distress** and (ii) a physiological levels of ROS participating in cell signalling: **eustress**. Indeed, at low levels, ROS have been shown to participate not only in development and regeneration but also in cell survival through the activation of the MAPK or NFkB pathways. In the adult central nervous system (CNS), the physiological importance of ROS produced by NOX enzymes is now under active investigation and several NOX enzymes are expressed in astrocytes as well as in neurons (for review (Sorce and Krause, 2009)). To illustrate the diversity of ROS activities, I will just mention their participation in the differentiation of neural progenitors (Le Belle et al., 2011),

the control of neurite outgrowth in *Aplysia* (Munnamalai et al., 2014) and the modulation of dopamine release (Sidló et al., 2008).

In this context, I want to thank Irene Amblard, Edmond Dupont, Alain Joliot and Sophie Vríz to have allowed me to use their unpublished results to illustrate the link between ENGRAILED, local morphological changes and ROS production. They demonstrated that the internalisation of ENGRAILED by HeLa cells induces the formation of filopodia and that this induction is mediated by an increase in ROS levels. This is demonstrated by the fact that an artificial increase in H₂O₂ is sufficient to generate filopodia formation and, conversely, that blocking the H₂O₂ increase with catalase abolishes this effect (see Figure). Indeed, this needs to be replicated in neural cells, but it strongly suggests that local morphological changes can be triggered by physiological interactions between ENGRAILED and ROS.

a



b

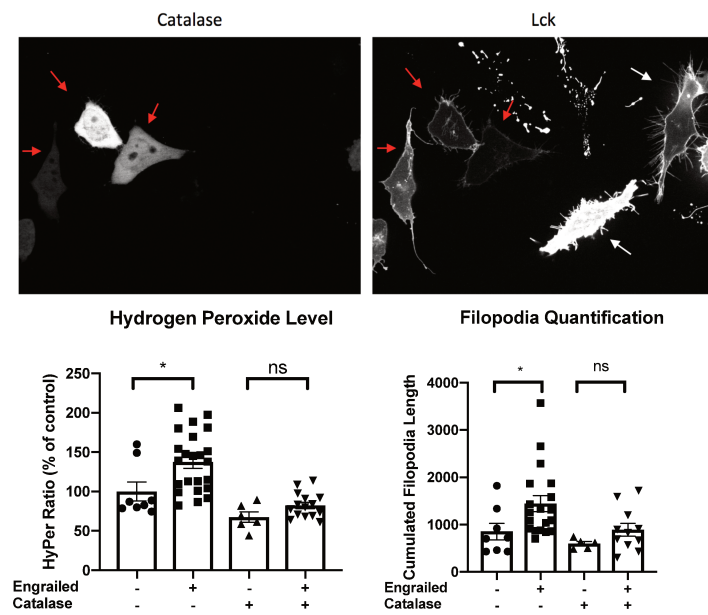


Figure 28: Engrailed internalisation increases H₂O₂ levels sufficient to induce filopodia. a) Quantifications of H₂O₂ levels upon EN2 treatment. b) Quantifications of H₂O₂ levels and filopodia formation in cells expressing catalase. From Amblard et al., in prep

ENGRAILED as a potential therapeutic protein for Parkinson disease

As depicted in Figure 29, ENGRAILED regulates many cellular pathways promoting neuronal survival. This allows ENGRAILED to multi-modally address dysregulations occurring in neurodegenerative or aging processes. In the following lines, I will highlight some of these dysregulations and how ENGRAILED could represent a therapeutic answer to the disorders that the dysregulations create.

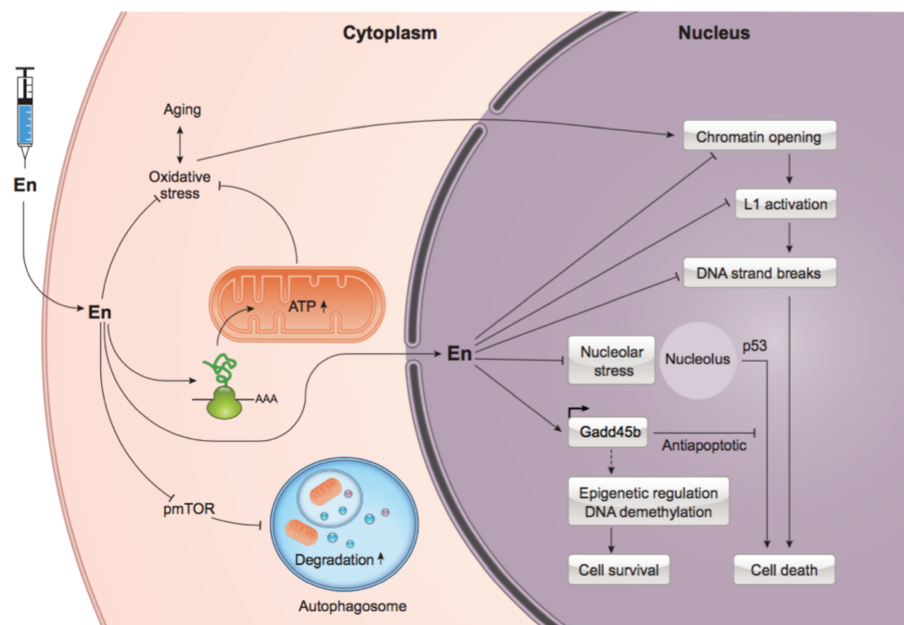


Figure 29: Engrailed multi-modal protective activity in mDA neurons. Taken from Di Nardo et al., 2018.

Oxidative stress: In addition to protecting against mutated α -synuclein, ENGRAILED is protective in several models of oxidative stress including MPTP, H_2O_2 , 6-OHDA and rotenone (Alvarez-Fisher et al 2011). Furthermore, as mentioned above, the oxidative status of the cell could impact the signalling capacity of ENGRAILED and reduce its non-cell autonomous trophic activities.

Mitochondrial dysfunctions: A decreased activity in the mitochondrial complex I with aging has been reported (Green et al., 2011). In this context, it is interesting that part of the immediate ENGRAILED pro-surviving activity is through its ability to regulate complex I protein translation (Alvarez-Fischer et al., 2011).

Epigenetic marks: As already mentioned, *Engrailed* hypomorphism and oxidative stress disrupt several epigenetic marks including H3K9me3, H3K27me3. An acute injection of ENGRAILED in the SNpc, not only saves the neurons against 6-OHDA but also restores all epigenetic marks (Rekaik et al., 2015).

Genome instability: *Engrailed* hypomorphism and oxidative stress induce the expression of mobile elements, in particular of the L1 family (Rekaik et al., 2015; Blaudin de Thé et al., 2018). This overexpression is responsible for the accumulation of breaks and a possible origin of genome instabilities. ENGRAILED protective activity is in part through its action on heterochromatin maintenance and its direct repressive activity at the level of L1 promoters (Blaudin de Thé et al., 2018).

Loss of proteostasis: many neurodegenerative diseases have for feature the aberrant accumulation of proteins. Should it be α -SYNUCLEIN for PD, HUNTINGTIN for Huntington Disease or TAU for Alzheimer Disease, this suggests inefficient protein degradation. By impacting the mTOR pathway ENGRAILED could reactivate autophagy. Furthermore, EN1/2 regulates expression of *α -synuclein* (Simon et al., 2001).

Neuroinflammation: *En1*^{+/-} mice depict elevated levels of IBA1 (Ghosh et al., 2016). IBA1 is a marker of activated microglia and a feature of many neurodegenerative disorders (Forno et al., 1992). The exact participation of activated astrocytes to the neurodegenerative process remains unclear. However, one hypothesis would be that sustained exposure of neurons to pro-inflammatory mediators induce cell death (Heneka et al., 2014).

Axonal fragmentation: our non-cell autonomous study shows that ENGRAILED maintains axons and this is also supported by another study (Nordström et al., 2015).

Our own published work on the role of cell autonomous ENGRAILED in mDA neuron survival and protection (Blaudin de Thé et al, 2018) as well as our preliminary data on the non-cell autonomous trophic activity of this transcription factor lend weight to the idea that it could be used as a potential therapeutic agent. Spontaneously, one thinks of expressing ENGRAILED through gene therapy. However, the approach favoured by the group is to use directly the protein and to avoid a viral intermediate.

The reason why this choice was made is that, through its epigenetic activity, the effects of ENGRAILED as a protein are long lasting, up to at least 16 weeks in the rodent (unpublished) or the non-human primate taking locomotion as a read-out (Thomasson et al 2019). Even though the delivery of ENGRAILED could be done through the blood-brain-barrier (Bera et al., 2016), the strategy developed by BrainEver, a biotechnology company founded to develop therapeutic homeoproteins, is a direct stereological injection allowing one to specifically target the mDA neurons from the SNpc. The first clinical trial in humans is scheduled for 2020.

Non-cell autonomous ENGRAILED signalling: questions on regulation and specificity

As detailed above, ENGRAILED is a multi-modal protein activating various pathways. For this reason, one can anticipate that its signalling activity presents some degree of regulation and specificity.

Working on EN2, Joliot and his colleagues have demonstrated that EN2 secretion is regulated *in vivo* by its phosphorylation on identified serine residues by Casein Kinase 2 (CK2) (Maizel et al., 2002). Phosphorylation of this serine-rich domains blocks both secretion and nuclear addressing, raising the possibility that the protein needs to go through the nucleus to gain access to a secretion pathway. This hypothesis is supported by the fact the $\Delta 1$ secretion sequence is also a nuclear export sequence conserved in most HPs (Joliot et al., 1998). If so, one must consider that all regulatory mechanisms for nuclear import and export may participate in the regulation of secretion. Corroborating the interest of this phosphorylation domain is the finding, in the same study, that EN2 is phosphorylated *in vivo* and can be co-immunoprecipitated with CK2 (Maizel et al., 2002). In addition, these studies raise the intriguing possibility that HP nuclear and signalling activities are closely associated.

Another important issue is how the secreted proteins can find their targets cells. As demonstrated earlier (Dupont et al., 2007; Joliot et al., 1997), EN2 associates with caveolae-like vesicles and travels from the baso-lateral to apical side of the cell, thus from the dendrites to the axon. This transport is interesting because it means that the protein might gain access to the presynaptic compartment and be secreted at the synapse level. If so, target cell specificity might be in part dictated by the neuronal network. This possibility is supported by experiments in which OTX2 injected in the eye is transported by the retinal ganglion cell axons, and at least two trans-synaptic passages later terminates in the parvalbumine GABAergic neurons (PV-cells) in layer IV of the visual cortex, their natural targets (Sugiyama et al., 2008).

This does not preclude the existence of specific binding sites present at the surface of the receiving cells. The most developed example is that of OTX2 secreted by the choroid plexus and specifically recognized, thanks to a specific glycosaminoglycan (GAG)-binding domain, a complex GAG sequence at the surface of the PV-cells (Beurdeley et al., 2012; Miyata et al., 2012). Interestingly, when EN1 was infused in the cortex, in contrast with OTX2, it did not gain access specifically to PV-cells (Sugiyama et al., 2008). It would be very interesting to characterize whether ENGRAILED, thanks to a domain very similar to the one identified in OTX2, recognizes another GAG sequence at the surface of its own target cells. In fact, the domain identified in OTX2 is present, with some variations, in most HPs (Prochiantz and Di Nardo., 2015) and one can speculate the existence of a “sugar code” allowing HPs to recognize their physiological cellular targets.

To conclude, this takes me naturally to the part of my work devoted to the non-cell autonomous activity of ENGRAILED in the SN, probably in its reticulata part. If we are correct, EN1 is secreted by the dendrites (Di Nardo et al., 2007) and recaptured by its environment, for one part the mDA cells themselves through an autocrine mechanism, but also possibly by other cell types present in the environment, including the GABAergic neurons in the SN *pars reticulata*. One can thus envisage that the different cell types that locally capture EN1 express distinct or identical binding sites that still needs to be identified.

Part II: Overactive L1 elements: drivers of neurological disorders?

While studying the cell autonomous function of ENGRAILED, our team made the observation that *En1*^{+/-} mice present an increased expression of L1 elements. This led to interrogate the importance of L1 elements in mDA degeneration. As the results of this study have been discussed in the main paper of this document (Blaudin de Thé et al., 2018), I will try to add novel elements to the discussion, hopefully without too many redundancies. Very briefly, we showed that L1 elements are overexpressed in a mouse model of PD and are a driver of neuronal degeneration by promoting DNA breaks, a form of genomic instability. Blocking L1 activity by 3 different means (siRNA, stavudine, AAV-PIWI like 1) protects the neurons from death. Finally, ENGRAILED blocks L1 expression by directly binding to their promoters.

L1 elements in the brain: false positives or real physiological phenomenon

The legitimacy of studying L1 elements in the brain is often questioned as illustrated by a 2012 report suggesting that retrotransposition in somatic brain cells occurs much less often than initially thought, almost a non-event (Evrony et al., 2012). This is at odds with the demonstration of the insertion of L1 elements in the hippocampus, cerebellum cortex and caudate nucleus of the human and rodent brain (Baillie et al., 2011; Coufal et al., 2009; Upton et al., 2015). According to these studies, the rates of retrotransposition range from 80 to less than 0.04 events per somatic neuronal cell (Coufal et al., 2009; Evrony et al., 2016). This controversy raises the issue of the significance of L1 retrotransposition studies in somatic brain cells and of its possible role in shaping neuronal diversity, possibly through Darwinian somatic selection (Muotri et al., 2005, 2007).

Due to the repetitive nature of TEs, studying the rate of L1 retrotransposition is particularly strenuous and requires specific analysis tools. Three main tools have allowed for the study of the retrotransposition of L1. The first consists of an engineered L1 transfection with an EGFP reporter to detect retrotransposition. This was used as first evidence in cultured cells and rodent models to demonstrate that neuronal progenitor cells could accommodate retrotransposition at high frequency (Muotri et al., 2005). The second, which replicated previous studies, consists of a TaqMan quantitative PCR-based L1 copy number variation

assay in order to estimate the enrichment of L1 copies (Coufal et al., 2009). Finally, the emergence of whole-genome sequencing coupled with PCR validation and Sanger sequencing allowed for more precise analyses of L1 insertion. The diversity of tools and models (single-cell vs bulk) used as well as the bioinformatics tools to deconvolute the data could explain the discrepancies reported in the rates of retrotransposition across studies.

However, the brain contains approximately 86 billions of neurons (Azevedo et al., 2009) suggesting, as pointed out by many, that even low rates of retrotransposition at a cellular level multiplied by the total number of neurons could greatly affect the neural network. Furthermore, retrotransposition rates do not take into account functional and biological relevance of TE expression, for example by providing a repertoire of non-coding RNAs, or introducing breaks in the genome through the endonuclease activity of ORF2p. In this sense, transcription, without subsequent retrotransposition, of mobile element sequences could have regulatory functions. Unless one believes that 45% of the genome is composed of junk DNA without physiological interest, this supports the necessity to study the importance of L1 in physiological and pathological processes. My work and that of my colleagues in the laboratory has primarily focused on the latter aspects (consequences of L1 expression and L1-RNP association), independently of retrotransposition *strictu senso*. However, I will also discuss some studies on retrotransposition, even though one must keep in mind that doubts exist concerning the extent of retrotransposition in neural tissues.

L1 expression: drivers of local inflammation

Supporting our own work on the role of L1 expression in mDA neuron physiopathology (Blaudin de Thé et al., 2018), recent publications underscore the idea that L1 over-expression or retrotransposition is a driver of aging (De Cecco et al., 2013; Li et al., 2013; Simon et al., 2019; Wood et al., 2016; Maxwell et al., 2011), of neurodevelopmental disorders such as autism or schizophrenia (Shpyleva et al., 2018, Doyle et al., 2017) or of neurodegenerative diseases (Guo et al., 2018; Krug et al., 2017; Savage et al., 2019;). Whereas our study concentrates on how L1-induced DNA breaks can drive neurodegeneration, a recent report puts forward L1-driven neuroinflammation (Thomas et al., 2017). This could be a complementary path by which L1 elements are harmful to neurons.

An interesting illustration of a role of L1 elements in inflammation is the auto-immune disease called Aicardi Goutieres Syndrome (AGS). AGS is a genetic encephalopathy, that can

be misdiagnosed as an *in utero* viral infection due to common clinical features (Rice et al., 2007). At the molecular level, one of the main feature of AGS is the activation of the Interferon immunity pathways (Goutière et al., 1998). A set of seven genes has been linked to AGS: *Trex1*, three types of *RNaseH*, *Smad1*, *Adar1* and *Ifih1* (Crow et al., 2006, 2015). Very interestingly, many of these genes are associated with L1 elements. For instance, TREX1, ADAR1 and SMAD1 repress the expression of L1 elements (Orecchini et al., 2017; Zhao et al., 2013). Recently RNASEH has been implicated in the life cycle of L1 elements (Benitez-Guijarro et al., 2018) and association of L1 elements with RNASEH has been observed (Goodier et al., 2007b). We also found this association in our co-immunoprecipitation studies (unpublished).

The idea of L1 elements driving inflammation resulting in neuronal loss has been studied in the context of TREX1 deficiency (Thomas et al., 2017). Indeed, L1 expression due to TREX1 deficiency, drives an inflammatory response in astrocytes by activating the interferon (IFN) immune response in a similar manner than in AGS. The IFN is secreted in the extracellular environment and drives neuronal degeneration while seemingly leaving astrocytes unaffected. TREX1 is an exonuclease that depletes cytosolic aberrant ssDNA while RNASEH resolves and degrades DNA-RNA hybrids. Deficiency in TREX1 and RNASEH induces the accumulation of L1 ssDNA, and this accumulation triggers the inflammatory response. However, the origin of the cytosolic ssDNA issued from L1 elements raises questions. The authors suggest two potential sources (1) since L1 mRNA as well as the L1-RNP are present in the cytosol they could produce ssDNA through a mechanism independent of chromosomal DNA template (2) as by-product of the TPRT cycle in the nucleus, a fraction of the ssDNA is cleaved and exits the nucleus towards the cytosol where it accumulates.

In the context of inflammation in other biological processes, L1 elements are overexpressed in SIRT-6 deficient mice compared to control mice (Simon et al., 2019). The overexpression of L1 elements drives inflammation and blocking L1 retrotransposition, through reverse transcriptase inhibitors (analogue to stavudine), significantly improved the health and lifespan of the SIRT-6 deficient mice. The significance of L1 elements in age-associated inflammation is also supported by another recent analysis demonstrating that L1 derepression with aging induces the expression of IFN in senescent cells (De Cecco et al., 2019).

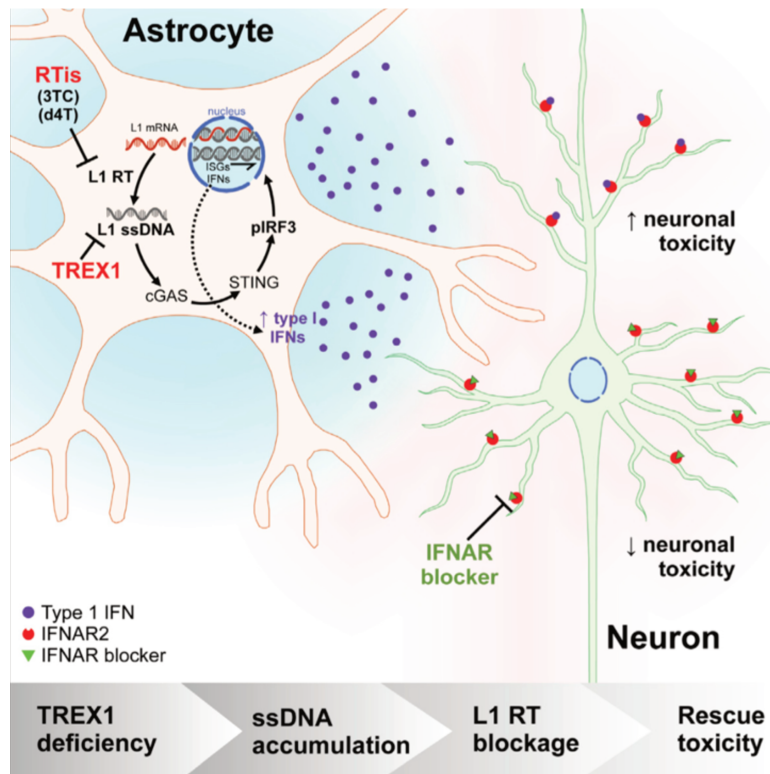


Figure 30: TREX1 deficiency induces L1 ssDNA accumulation in astrocytes and thus IFN1 production. IFN1 is released in the extracellular milieu and recaptured by adjacent neurons inducing neuronal toxicity. Blocking L1 ssDNA accumulation by RT inhibitors and IFN1 capture by IFNAR blocker rescues the neurons. Taken from Thomas et al., 2017

Inflammation mediated by L1 elements in astrocytes raises interest for neurodegenerative diseases as a growing body of literature now involves astrocytes in pathological processes (Amor et al., 2010; Fellner et al., 2013; Forno et al., 1992; Koedel et al., 2007; Lotz et al., 2005; Okun et al., 2009). In the context of neurodegenerative disorders, the drivers of inflammation have been hypothesized to be the misfolded proteins that aggregate, such as α -SYNUCLEIN in PD. The chronic activation of microglia secreting pro-inflammatory cytokines drives subsequent neuronal death (Fellner et al., 2013; Nagatsu and Sawada, 2005). Furthermore, activated microglia show retracted processes that may impact their participation at the level of synapses (Paolicelli et al., 2011; Schafer et al., 2012). In this sense, the idea that L1 elements induces an inflammatory response is particularly relevant for neurodegenerative diseases and adds up to their interest in the studies of brain pathologies.

Reverse transcriptase inhibitors as potential medication?

The fact that anti-L1 strategies rescued neurons from degeneration brings forward the idea of using anti-L1 strategies in therapeutic protocols. Indeed, we provide evidence that L1 over activity induces genomic instability, or at least harmful DNA strand breaks, which is a feature of PD. Blocking L1 activity by three different means reduced the formation of the breaks and rescued the neurons from degeneration (Blaudin de Thé et al., 2018).

In our study, we used the reverse transcriptase inhibitor named stavudine. Reverse transcriptase inhibitors limit L1 retrotransposition by blocking the L1 ORF2p reverse transcriptase activity (De Clercq, 2013). Reverse transcriptase inhibitors are divided in three different families according to whether they are nucleoside (like stavudine), nucleotide or non-nucleoside analogues. Since they inhibit retroviral progression, reverse transcriptase inhibitors constitute the main therapeutic approach against HIV (Cory et al., 2015; Martin et al., 2010). In a study comparing different nucleoside analogues, stavudine proved to be highly efficient to block L1 retrotransposition assessed by GFP reporter (Martin et al., 2010). However, in our study, we showed that using stavudine also reduced the number of breaks induced by ORF2P (Blaudin de Thé et al., 2018). This constitutes a non-canonical role for reverse transcriptase inhibitors against L1-elements. The exact mode of action is not elucidated, yet we showed that chromatin bound L1-RNA was reduced upon stavudine treatment. We hypothesize that stavudine reduces DNA damage, either by giving access to the DNA repair machinery by unhooking the L1-RNP from the chromatin, or by preventing the second break occurring at the last steps of TPRT to reinsert the L1. However, this is only speculative and other modes of action cannot be precluded.

As already discussed, L1-induced inflammation, also a feature of the disease, was antagonized by reverse transcriptase inhibitors with positive effects on neuronal survival (De Cecco et al., 2019; Thomas et al., 2017). Furthermore, whole genome analysis of 20 brain samples and 80 non-brain samples and characterization of retrotransposition events demonstrated that retrotransposition is higher in patients affected by neurodevelopmental disorders such as Rett syndrome, ataxia-telangiectasia and autism (Jacob-Hirsch et al., 2018). The correlative nature of the study does not allow one to formally conclude that retrotransposition is a driver of the disorders. However, in light of the genomic threat imposed by retrotransposition, its participation in the pathology cannot be bluntly precluded. In support

of this hypothesis, a recent study shows that using reverse transcriptase inhibitors can prevent somatic APP recombination and modify AD progression (Lee et al., 2019). The authors postulate that HIV patients, subjected to reverse transcriptase inhibitors as part of their treatment, exhibit lower occurrence of neurodegenerative disease such as AD. It would indeed be interesting to analyse whether this also true in the context of PD.

All in all, several studies point towards a potential use of reverse transcriptase inhibitors as potential therapeutic agents and our own group has deposited a patent protecting the use of reverse transcriptase inhibitors in the treatment of neurodegenerative diseases (FR n° 14 60535, 31/10/ 2014 / International PCT/IB2015/ 058404, 30/10/2015). The hope is that anti reverse transcriptase drugs, already approved for HIV treatments, could also be of use in neurodegenerative diseases.

Part III: Physiological roles of L1

What are the different levels of regulation by TE elements?

We made the observation that L1 elements are expressed at basal levels in the brain, raising the issue of whether this expression could be of physiological relevance. Physiological relevance of transposable elements is gaining ground in the scientific community. However, most studies focused on the evolutionary emergence of regulatory sequences thanks to TEs. This is an effect in “cis” whereby TEs act as regulatory sequences by adding promoter regions, attracting transcription factors, forcing premature polyA insertion, influencing DNA compaction and bringing evolutionary novelty by genomic rearrangements (Bourque et al., 2008; Chuong et al., 2017; Kelley and Rinn, 2012; Lynch et al., 2011; Trizzino et al., 2017). Several studies have shown the tissue-specific pattern enrichment of TEs in regulatory sequences suggesting that TE can contribute to regulatory sequences in a tissue-specific way (Trizzino et al., 2018). As potential heterochromatic “nucleators”, they could also shape the genome in Hi-C/3D structure. Indeed, they potentially have the capacity to bind CTCF that are known regulators of chromatin loops and domain boundaries for topologically associated domains (TADs) establishments (Choudhary et al., 2018; Fudenberg et al., 2016; Jacques et al., 2013). Since TEs actively move (or have moved) within the genome, they are good candidates to “spread around” their sequences that are reminiscent of classical gene regulatory networks. This overturns completely the view of TEs as purely parasitic but rather supports an important co-optation of TEs with evolutionary benefits for the host (Friedli and Trono, 2015).

Our own preliminary results on the physiological role of L1 in neurons are of a different flavour as they propose a role of L1 elements in “trans” in post-mitotic neuronal cells. The capacity of TEs to act in “trans” as long non-coding RNAs has been addressed in few studies. For instance, it has been demonstrated that the L1-RNA serves as a lncRNA essential for ESCs renewal (Percharde et al., 2018) or the expression of L1 elements has been studied in neural progenitors (Muotri et al., 2005). To my knowledge, no physiological “trans” role of L1 elements had been described in adult post-mitotic neurons.

L1 elements could affect cellular processes in “trans” in multiple ways: release of regulatory RNAs and association of the RNP with host co-factors influencing mRNA splicing or gene expression. For the moment, we are privileging the latter hypothesis, yet we do not

exclude also a regulation of alternative splicing. Indeed, we have preliminary RNA-seq data (not shown in the results section) that show altered levels of transcript splice variants in genes containing L1 elements in the *En1*^{+/-} mouse model which can be seen as an indirect gain of function of L1 elements. We have started to analyse the expression of specific splice variants of candidate genes upon L1 LOF. *Nrxn3* caught our interest as there are two families of variants: alpha and beta, with different functions. The beta family is expressed from a secondary promoter located between Exon 17 and Exon 18 (Rowen et al., 2002; Tabuchi and Südhof, 2002). *Nrxn3* alterations are also implicated in neurological disorders including autism and AD (Vaags et al., 2012; Zheng et al., 2018). Interestingly, a fL1 element is located exactly in this alpha/beta switch region. Even though it is too early to raise any conclusions, we are keeping an open eye on alternative transcription initiation and splicing.

We have carried out LOF of L1 elements by three different means *in vivo* and *in vitro* and assessed by RT-qPCR gene expression of long and short genes. Long genes were selected based on their expression and function in mDA neurons and on the presence of intronic fL1. We demonstrate a positive correlation between L1 expression and long gene expression. On the other hand, the few short genes tested, more are needed, do not show altered levels of expression in L1 LOF. At the protein level, two proteins (out of two tested) participating to synaptic transmission, NRNXN3 and GRID2, showed diminished levels upon L1 LOF.

For the moment, we are focusing on:

- 1) The biological interest of using fL1 elements within long genes to facilitate transcription
- 2) The extent of long genes concerned: is it only long genes containing fL1 or all long genes? To address this question, we will perform genome wide unbiased Nanopore-Seq in LOF paradigms of L1 elements.
- 3) The potential mechanism and the L1 interactome

Physiological role of L1 elements: breaking the strand to better transcribe?

Our main hypothesis on the importance of L1 elements for transcription originates from the capacity of L1 elements to induce breaks combined with the topological constraints arising during transcription. Indeed, as the transcription machinery moves along the gene, it induces positive and negative supercoiling (Liu and Wang, 1987). In order to reduce the topological constraints, topoisomerases induce transient DNA breaks by transesterification reactions to relax the double strand (Chen et al., 2013).

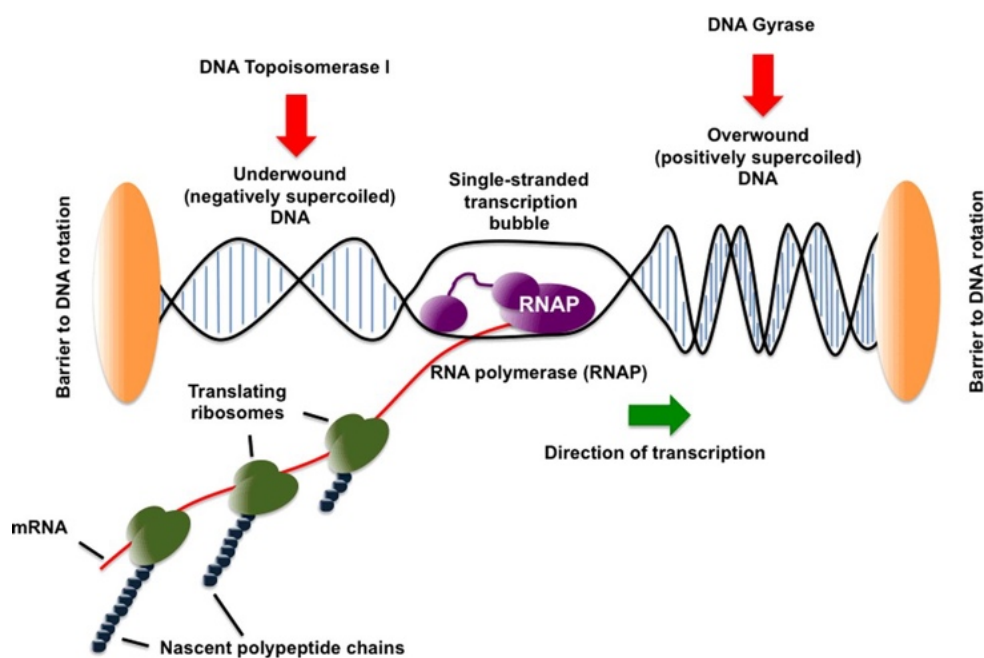


Figure 31: As the RNA polymerase moves along the DNA for transcription this induces positive supercoiling upstream and negative supercoiling downstream thus blocking RNA transcription. DNA topoisomerase and DNA gyrase help resolve the topological constraints. DNA gyrase is found in bacterial organisms, the equivalent in humans would be DNA Topoisomerase II. Taken from Dorman et al., 2016

In line with this, several studies have put forward the need to make breaks to better transcribe. For instance, active breaks in promoter regions facilitate the rapid expression of early response genes (Madabhushi et al., 2015). The results from the above paper are presented in Figure 32.

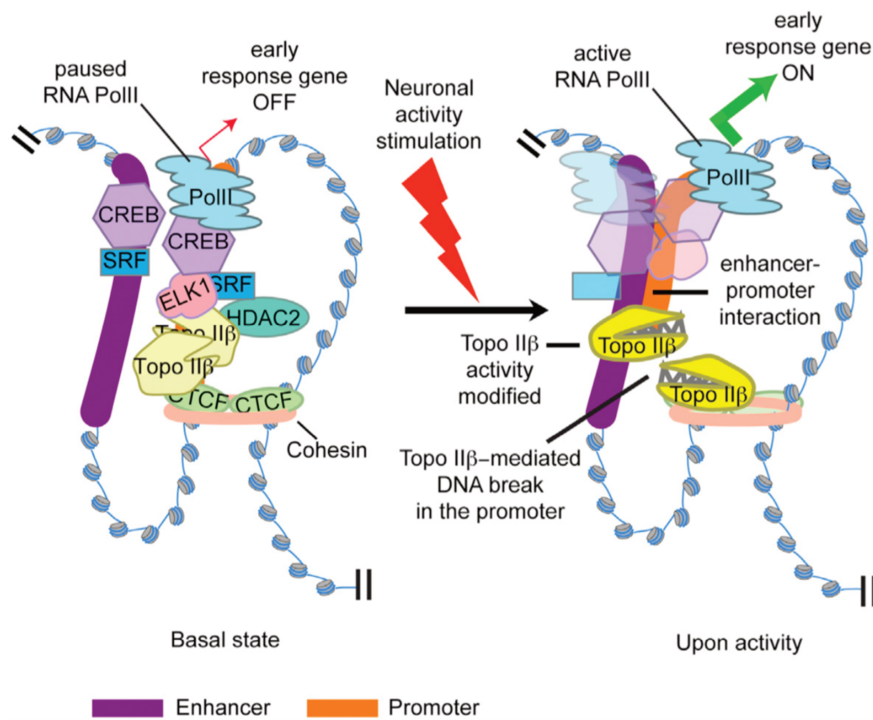


Figure 32: Neuronal activity causes the formation of DNA double strand breaks (DSBs) within the promoters of a subset of early response genes. Topoisomerase II is necessary for activity-induced DSB formation and facilitates the expression of early-response genes. Taken from Madabhushi et al, 2015

As such, the longer the gene (> 100kb), the more subject it is to topological constraints. It has been demonstrated that, in cultured cortical neurons, topoisomerase inhibition reduces the levels of long-genes implicated in synaptic function and associated with autism (King et al., 2013). Coincidentally, transcripts of long genes are enriched in neural tissues where they harbour important neuronal functions (Zylka et al., 2015). We used topotecan, an inhibitor of topoisomerases, in our *in vitro* embryonic midbrain cell cultures, and could recapitulate the finding that long genes are particularly sensitive to topoisomerases inhibitors. Along with the inhibition of topoisomerases, topotecan also reduced L1 expression (a one time finding to be confirmed).

We would like to propose that the endonuclease activity of the L1-RNP helps the transcription machinery to access or elongate highly constrained long genes in a similar manner to, or in association with, topoisomerases. Indeed, TOP1 has been described as partner of the L1-RNP in study by (Taylor et al., 2018) in HEK cells. TOP1 also appeared in our preliminary MS analysis and we further validated the association of ORF1p with TOP1 by co-immunoprecipitation on Western blots.

How do L1 elements regulate specific genes?

We hypothesize that ORF1p is at the centre of a protein complex composed of several RNA binding proteins. Collectively, these proteins regulate long gene expression important for neuron-specific synaptic function. As already mentioned, SFPQ is in our scope of interest since SFPQ has been linked to degeneration and “long-gene transcriptopathies” (Takeuchi et al., 2018). In this study by Takeuchi and colleagues, it is demonstrated that SFPQ is required to recruit kinases that phosphorylate RNA polymerase II (PolII) on serine 2. Loss of SFPQ in knockdown mice resulted in a decreased density of PolII on gene bodies and impaired elongation of long genes.

Intriguingly, nuclear loss of SFPQ is a hallmark of AD (Luisier et al., 2018) and in conditions of acute oxidative stress, we observed a nuclear loss of SFPQ and its redistribution to the cytoplasm. Furthermore, our co-immunoprecipitation data show that Engrailed (which inhibits L1 transcription) and SFPQ interact together (data unpublished).

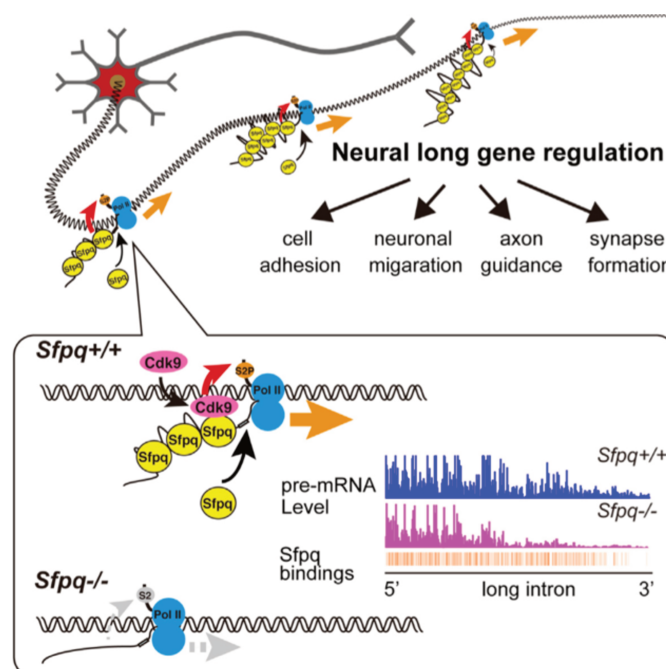


Figure 33: SFPQ knockdown mice demonstrate neuronal loss and misregulation of long gene expression. Co-transcriptional SFPQ binds pre-mRNAs and facilitates long-gene transcription by mediating CDK9 recruitment to the elongation complex and Pol II-CTD activation. Taken from Takeuchi et al, 2018.

We also identified FUS and TDP-43 in our MS of the ORF1p interactome. These proteins raised our interest as they are at the centre of ALS/FTLD disease and regulate multiple steps of mRNA processing (Lagier-Tourenne et al., 2012; Rogelj et al., 2012; Scotter et al., 2015). In line with our long gene hypothesis, FUS and TDP-43 bind long genes (Cortese et al., 2014) and their disruption induces altered long gene expression (Polymenidou et al., 2012). As presented in the introduction, increased L1 expression has been reported in both diseases and TDP-43 has recently been showed to be a repressor of TE elements (Liu et al., 2019).

How did fL1 elements get enriched in long genes?

Given the potential threat to genome integrity associated with fL1 overexpression, we speculate that basal fL1 expression presents an evolutionary-acquired benefit for the host. However, neurons being post-mitotic cells, how and when in germ cells the enrichment of fL1 in introns of long-genes occurred is an interesting question. The distribution of L1 elements within the genome can be shaped by two concomitant mechanisms: **Integration bias** coupled with **Darwinian selection** and this will be discussed below.

Just this month, two independent studies focused on the integration preferences of L1 elements (Flasch et al., 2019; Sultana et al., 2019). They respectively used HeLa cells or 5 human cell lines transfected with engineered L1 constructs containing a reporter cassette. This reporter cassette discriminates endogenous and *de novo* integration of L1. By ATLAS-seq/PacBio and mapping to the reference genome, the studies characterised the landscape of *de novo* L1 insertion. Interestingly, the authors failed to observe that endogenous L1 elements serve as “lightning rods” to attract *de novo* L1 elements as proposed by (Jacob-Hirsch et al., 2018). The latter proposal is that the enrichment of fL1 in introns of long genes is due to the targeting of the L1-RNP to pre-existing intronic L1 elements, possibly explaining why some introns of long genes harbour 3 to 4 fL1. In contrast, both studies are consistent with previous results implying the TTTT/AA 7-mer consensus sequence for integration preference. This preference is best explained by the biochemical properties of the L1-ORF2p endonuclease activity (Feng et al., 1996). Coincidentally, introns of long genes are enriched in A/T sequences (Amit et al., 2012) thus perhaps partly clarifying the enrichment of L1 in introns of long genes.

Genome wide screening reveals that (1) globally L1 elements are more abundant in gene-poor regions (Graham and Boissinot, 2006), while others report that (2) they can locally be enriched in neural genes (Baillie et al., 2011; Upton et al., 2015). Both observations are not mutually exclusive but underline a biased behaviour of L1 elements. This biased behaviour (should it be preference or avoidance for gene-coding regions) is in conflict with studies reporting that L1 elements integrate indiscriminately within the genome and independently of gene content (Flasch et al., 2019; Sultana et al., 2019). This brings forward Darwinian selection. Negative selection easily explains the depletion of L1 in gene-coding regions globally, due to the mutagenic effect of L1 insertions. In accordance with this, we found that short genes have less or no fIL1 elements. Indeed, short genes are more likely to have their function altered by a 6kb long insertion. Positive selection of intronic L1 elements in long-genes might be beneficial at the scale of a species fitness. If indeed, as we suggest, L1 elements participate in the regulation of genes yielding important neuronal functions, specific L1 elements could have conferred a developmental and cognitive advantage selected by evolution. Interestingly, the expansion of L1 families coincides with major evolutionary bursts, urging some scientists to speculate that they could have participated to human speciation (Cordaux and Batzer, 2009; Jangam et al., 2017).

Another possibility resides in the striking observation that neurons and sperm cells share common features including classical neurotransmitters (Meizel, 2004). With regard to *Grid2*, mRNA levels are detected in the testis (Pubmed Gene Reference) and ionotropic glutamate receptors are indeed present at the head of the sperm cells (Hu et al., 2004). If neuronal long genes present a potential role for sperm physiology and intronic L1 elements regulate their transcription, this could would explain the positive retention of intronic L1 elements at the level of the germline.

Integration preference and evolutionary selection of L1 elements provide very important insights. However, as L1 elements undergo genetic drift over time, they might evolve beyond recognition of the canonical sequence thus distorting the results of these analysis.

On neural diversity and somatic mosaicism: Darwinian selection at the cell population level?

Above, we discussed the fixation of full-length L1 in introns of long genes in the germline. However, looking at somatic retrotransposition in neural progenitors through Darwinian selection is also interesting. The hypothesis of L1 retrotransposition as a source of somatic mosaicism is advocated by a growing pool of scientists (Baillie et al., 2011; Bodea et al., 2018; Coufal et al., 2009; Muotri et al., 2005; Richardson et al., 2014; Singer et al., 2010; Upton et al., 2015). Somatic mosaicism is defined by the presence of genetically distinct cells within one homogenous population (e.g. motoneurons). The brain harbours a very high neuronal functional and phenotypic diversity, thus, somatic mosaicism could account for the emergence of distinct populations and the reshaping of neural circuitry during development, or in adult neurogenesis (without forgetting glial cells, in particular astrocytes). This, along with epigenetic and environment interplay, would partly explain the range of individual differences in behaviour observed in almost genetically identical animals as in monozygotic twins. The idea of somatic recombination as a driver of neuronal diversity is not new. This hypothesis arose with the observation that the RAG-1 enzyme, responsible for V(D)J recombination (presented in II.4) in the immune system is expressed in cortical and hippocampal NPCs during neurodevelopment (Chun et al., 1991). However, until this date, RAG-1 has not been proven active in the neural system. Considering that RAG-1 originates from domestication of transposable elements, proposing L1 elements for neuronal somatic mosaicism is alluring. First advanced by (Muotri et al., 2005), authors observed that the L1 promoter is transiently released from epigenetic repression mediated by Sox2 during neural differentiation. Furthermore, transgenic reporter mice exhibited neuronal transposition indicating L1 mobilisation during embryonic and adult neurogenesis.

Interestingly, throughout development and windows of plasticity, the brain undergoes an extensive amount of programmed cell death (PCD). According to (Blaschke et al., 1998) around 50-70% of neurons die. PCD regulates, amongst other, the pool size of progenitor populations, the removal of neurons with errors and the pruning of synaptic connections. One could imagine that PCD could also be an adequate moment and mean to remove deleterious or promote beneficial L1 insertions. Per se, one could continue the parallel with the immune system where antigen repertoires are shaped by positive and negative selection. Here, selection would take place in neuronal niches. Ironically, somatic mosaicism in NPCs creating neuronal diversity represents a seductive return to the initial observation leading to the discovery of TEs

by Barbara McClintock, based on the phenotypic variation of kernel due to somatic recombination.

L1 elements: environmental and stress sensors for adaptive response?

When Barbara McClintock discovered TEs, she proposed that they might be activated in response to changes in the environment. As discussed above, at the scale of a species, TEs can induce mutations and genomic arrangements allowing for genomic diversity followed by positive, neutral or negatively selection. However, at the scale of an individual, viewing TE elements as regulators of gene expression, the capacity of TEs to respond to environmental stimuli is also very interesting. For instance, it could confer to regulated genes the capacity to respond to stress and activate specific gene pathways while explaining inter-individual variability.

First, TEs show responsiveness to hormone or environmental stimuli. Indeed, steroid hormone-like agents can induce L1 activity. This was notably studied by (Morales et al., 2002), where the transcription from L1 promoters was followed by a chemi-luminescent assay upon addition of hormones *in vitro*. In response to stress, L1 transcription is differentially induced in different brain regions and varies between distinct mouse strains (Cappucci et al., 2018). The authors argue that the strain-dependant increase in L1 expression denotes individual susceptibility or resilience to stress and suggest that induced L1 expression could contribute to stress disorders. As the study is correlative, the question of whether L1 expression is indeed deleterious or a tentative response to create *de novo* adaptation remains unresolved. As another example, (Muotri et al., 2009) studied physical exercise, another environmental stimuli, and assessed L1 retrotransposition using the GFP reporter in mouse brains. They show that hippocampal neurones undergo an increase in L1 retrotransposition upon exercise and conclude that this may participate to neuronal plasticity. Other environmental factors like early-life experience and maternal care also influence L1 activity and individual L1 fingerprint (Bedrosian et al., 2018).

Finally, natural activity and discovery of new environments (= neuronal stimulation) induce transient breaks in the DNA of neurons which are exacerbated in AD (Suberbielle et al., 2013). This is interesting since it points, in analogy with our threshold model for L1 levels in neurons, to a threshold for physiological strand breaks necessary for neuronal function which

when passed (i.e. in PD) might contribute to neurodegeneration. Whether activity-dependent DNA breaks could be L1 mediated remains hypothetical but it would be of great interest to study the occurrence of those breaks upon L1 LOF following environmental stimulation.

As TEs yield such important regulatory roles and potential environmental sensors, one cannot exclude that, inter-individual variability in the landscape of TEs s also accounts for variability within sensitivity to diseases and to stress (Stuart et al.). To come back to PD, one can hypothesize that L1 over-activation is partly environmentally driven and that resilience to this over activation explains the inter-individual variability in the sporadic forms of the disease.

General Conclusion:

To conclude on the work developed throughout this thesis, I have studied the impact of the transfer of ENGRAILED between mDA neurons and underlined the importance of this autocrine transfer for the maintenance and survival of mDA neurons. This is an interesting example of a homeoprotein being cell autonomous and non-cell autonomously active in a neuronal population with direct implication on survival. The mechanism involved will be further studied. The fact that *En1*^{+/-} mice exhibit an increase of expression of L1 elements has urged us to study the link between ENGRAILED, L1 elements and neurodegeneration. This has lead us to propose a threshold model of L1 expression.

In this model, basal expression could be beneficial to the neurons while overexpression induces neurodegeneration. Indeed, with age and environmental pressure, repression of L1 elements is less effective leading to progressive overexpression of L1 elements. This induces increased double strand breaks, possibly inflammation, leading to neuronal cell-death and the progression of age-related neurodegenerative diseases. This suggests that anti-L1 elements strategies could represent an important therapeutic approach for diseases linked to L1 dysregulations.

However, we observe basal expression of L1 elements in neurons and we propose that it could participate to the normal cell physiology and regulate the expression of long genes that constitute a susceptibility checkpoint in neurons where they carry key neuronal functions. This model is recapitulated in the following figure.

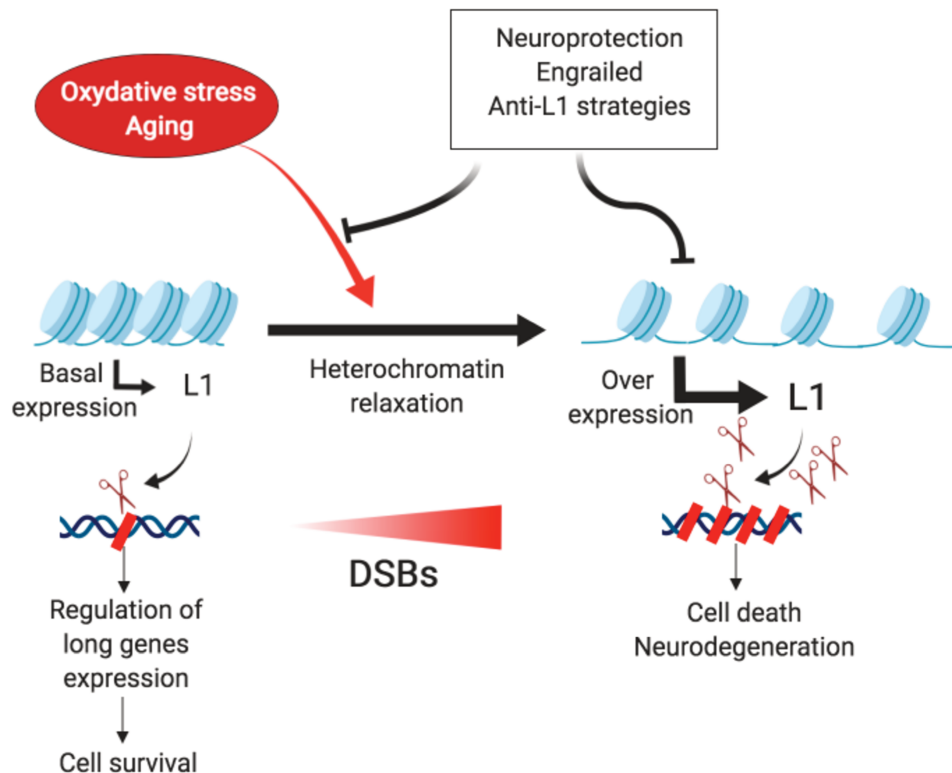


Figure 34 : Threshold model of L1 expression. Courtesy of Marguerite Jamet

This endows L1 elements with important regulatory roles in accordance with the initial view of Barbara McClintock and the growing body of literature. There is still much to investigate in this direction and the field should provide exciting insights in the coming years, should it be on environmental responsiveness of L1 elements, the potential implication in creating neuronal variability, the interaction of L1 elements with the hosting cell and the participation of TE elements to human speciation. We also demonstrated that ENGRAILED represses the expression of L1 elements by direct and indirect means. In analogy to the evolutionary race between transposons and KRAB-ZFPs, it would be interesting to study the co-evolution of HPs and L1 elements as well as investigate whether the repression of L1 or TEs is a shared feature between HPs.

References

- Ai, S., Xu, Q., Hu, Y., Song, C., Guo, J., Shen, L., Wang, C., Yu, R., Yan, X., and Tang, B. (2014). Hypomethylation of SNCA in blood of patients with sporadic Parkinson's disease. *Journal of the Neurological Sciences* 337, 123–128.
- Alam, Z.I., Jenner, A., Daniel, S.E., Lees, A.J., Cairns, N., Marsden, C.D., Jenner, P., and Halliwell, B. (1997). Oxidative DNA damage in the parkinsonian brain: an apparent selective increase in 8-hydroxyguanine levels in substantia nigra. *J. Neurochem.* 69, 1196–1203.
- Albéri, L., Sgadò, P., and Simon, H.H. (2004). Engrailed genes are cell-autonomously required to prevent apoptosis in mesencephalic dopaminergic neurons. *Development* 131, 3229–3236.
- Alisch, R.S., Garcia-Perez, J.L., Muotri, A.R., Gage, F.H., and Moran, J.V. (2006). Unconventional translation of mammalian LINE-1 retrotransposons. *Genes Dev* 20, 210–224.
- Alvarez-Fischer, D., Fuchs, J., Castagner, F., Stettler, O., Massiani-Beaudoin, O., Moya, K.L., Bouillot, C., Oertel, W.H., Lombès, A., Faigle, W., et al. (2011). Engrailed protects mouse midbrain dopaminergic neurons against mitochondrial complex I insults. *Nat. Neurosci.* 14, 1260–1266.
- Ambani, L.M., Van Woert, M.H., and Murphy, S. (1975). Brain peroxidase and catalase in Parkinson disease. *Arch. Neurol.* 32, 114–118.
- Ames, B.N., Shigenaga, M.K., and Hagen, T.M. (1993). Oxidants, antioxidants, and the degenerative diseases of aging. *Proc. Natl. Acad. Sci. U.S.A.* 90, 7915–7922.
- Amir, R.E., Van den Veyver, I.B., Wan, M., Tran, C.Q., Francke, U., and Zoghbi, H.Y. (1999). Rett syndrome is caused by mutations in X-linked MECP2, encoding methyl-CpG-binding protein 2. *Nat. Genet.* 23, 185–188.
- Amit, M., Donyo, M., Hollander, D., Goren, A., Kim, E., Gelfman, S., Lev-Maor, G., Burstein, D., Schwartz, S., Postolsky, B., et al. (2012). Differential GC content between exons and introns establishes distinct strategies of splice-site recognition. *Cell Rep* 1, 543–556.
- Amor, S., Puentes, F., Baker, D., and van der Valk, P. (2010). Inflammation in neurodegenerative diseases. *Immunology* 129, 154–169.
- Anwar, S.L., Wulaningsih, W., and Lehmann, U. (2017). Transposable Elements in Human Cancer: Causes and Consequences of Deregulation. *Int J Mol Sci* 18.
- Aravin, A.A., Hannon, G.J., and Brennecke, J. (2007). The Piwi-piRNA pathway provides an adaptive defense in the transposon arms race. *Science* 318, 761–764.
- Azevedo, F.A.C., Carvalho, L.R.B., Grinberg, L.T., Farfel, J.M., Ferretti, R.E.L., Leite, R.E.P., Jacob Filho, W., Lent, R., and Herculano-Houzel, S. (2009). Equal numbers of neuronal and nonneuronal cells make the human brain an isometrically scaled-up primate brain. *J. Comp. Neurol.* 513, 532–541.

- Bailey, J.A., Carrel, L., Chakravarti, A., and Eichler, E.E. (2000). Molecular evidence for a relationship between LINE-1 elements and X chromosome inactivation: the Lyon repeat hypothesis. *Proc. Natl. Acad. Sci. U.S.A.* *97*, 6634–6639.
- Baillie, J.K., Barnett, M.W., Upton, K.R., Gerhardt, D.J., Richmond, T.A., De Sapio, F., Brennan, P.M., Rizzu, P., Smith, S., Fell, M., et al. (2011). Somatic retrotransposition alters the genetic landscape of the human brain. *Nature* *479*, 534–537.
- Barbash, S., and Sakmar, T.P. (2017). Length-dependent gene misexpression is associated with Alzheimer’s disease progression. *Sci Rep* *7*.
- Barrangou, R., Fremaux, C., Deveau, H., Richards, M., Boyaval, P., Moineau, S., Romero, D.A., and Horvath, P. (2007). CRISPR provides acquired resistance against viruses in prokaryotes. *Science* *315*, 1709–1712.
- Bedrosian, T.A., Quayle, C., Novaresi, N., and Gage, F.H. (2018). Early life experience drives structural variation of neural genomes in mice. *Science* *359*, 1395–1399.
- Benitez-Guijarro, M., Lopez-Ruiz, C., Tarnauskaitė, Ž., Murina, O., Mian Mohammad, M., Williams, T.C., Fluteau, A., Sanchez, L., Vilar-Astasio, R., Garcia-Canadas, M., et al. (2018). RNase H2, mutated in Aicardi-Goutières syndrome, promotes LINE-1 retrotransposition. *EMBO J.* *37*.
- Bennett, M.C., Bishop, J.F., Leng, Y., Chock, P.B., Chase, T.N., and Mouradian, M.M. (1999). Degradation of alpha-synuclein by proteasome. *J. Biol. Chem.* *274*, 33855–33858.
- Bentivoglio, M., and Morelli, M. (2005). Chapter I The organization and circuits of mesencephalic dopaminergic neurons and the distribution of dopamine receptors in the brain. In *Handbook of Chemical Neuroanatomy*, S.B. Dunnett, M. Bentivoglio, A. Björklund, and T. Hökfelt, eds. (Elsevier), pp. 1–107.
- Bera, S., Kar, R.K., Mondal, S., Pahan, K., and Bhunia, A. (2016). Structural Elucidation of Cell-Penetrating Penetratin Peptide in Model Membranes at Atomic Level: Probing Hydrophobic Interactions in the Blood-Brain-Barrier. *Biochemistry* *55*, 4982–4996.
- Bernard, C., Vincent, C., Testa, D., Bertini, E., Ribot, J., Di Nardo, A.A., Volovitch, M., and Prochiantz, A. (2016). A Mouse Model for Conditional Secretion of Specific Single-Chain Antibodies Provides Genetic Evidence for Regulation of Cortical Plasticity by a Non-cell Autonomous Homeoprotein Transcription Factor. *PLoS Genet* *12*.
- Beurdeley, M., Spatazza, J., Lee, H.H.C., Sugiyama, S., Bernard, C., Di Nardo, A.A., Hensch, T.K., and Prochiantz, A. (2012). Otx2 binding to perineuronal nets persistently regulates plasticity in the mature visual cortex. *J Neurosci* *32*, 9429–9437.
- Biémont, C. (2010). A Brief History of the Status of Transposable Elements: From Junk DNA to Major Players in Evolution. *Genetics* *186*, 1085–1093.
- Billeter, M., Qian, Y., Otting, G., Müller, M., Gehring, W.J., and Wüthrich, K. (1990). Determination of the three-dimensional structure of the Antennapedia homeodomain from *Drosophila* in solution by 1H nuclear magnetic resonance spectroscopy. *J. Mol. Biol.* *214*, 183–197.

- Bishop, K.M., Goudreau, G., and O'Leary, D.D. (2000). Regulation of area identity in the mammalian neocortex by *Emx2* and *Pax6*. *Science* 288, 344–349.
- Björklund, A., and Dunnett, S.B. (2007). Dopamine neuron systems in the brain: an update. *Trends in Neurosciences* 30, 194–202.
- Blaschke, A.J., Weiner, J.A., and Chun, J. (1998). Programmed cell death is a universal feature of embryonic and postnatal neuroproliferative regions throughout the central nervous system. *Journal of Comparative Neurology* 396, 39–50.
- Blaudin de Thé, F.-X., Rekaik, H., Peze-Heidsieck, E., Massiani-Beaudoin, O., Joshi, R.L., Fuchs, J., and Prochiantz, A. (2018a). Engrailed homeoprotein blocks degeneration in adult dopaminergic neurons through LINE-1 repression. *EMBO J.* 37.
- Blaudin de Thé, F.-X., Rekaik, H., Peze-Heidsieck, E., Massiani-Beaudoin, O., Joshi, R.L., Fuchs, J., and Prochiantz, A. (2018b). Engrailed homeoprotein blocks degeneration in adult dopaminergic neurons through LINE-1 repression. *EMBO J.* 37.
- Bodea, G.O., McKelvey, E.G.Z., and Faulkner, G.J. (2018). Retrotransposon-induced mosaicism in the neural genome. *Open Biol* 8.
- Boeke, J.D., Garfinkel, D.J., Styles, C.A., and Fink, G.R. (1985). Ty elements transpose through an RNA intermediate. *Cell* 40, 491–500.
- Bolduc, N., Hake, S., and Jackson, D. (2008). Dual functions of the KNOTTED1 homeodomain: sequence-specific DNA binding and regulation of cell-to-cell transport. *Sci Signal* 1, pe28.
- Bonifati, V., Rizzu, P., van Baren, M.J., Schaap, O., Breedveld, G.J., Krieger, E., Dekker, M.C.J., Squitieri, F., Ibanez, P., Jooisse, M., et al. (2003). Mutations in the DJ-1 gene associated with autosomal recessive early-onset parkinsonism. *Science* 299, 256–259.
- Bourque, G., Leong, B., Vega, V.B., Chen, X., Lee, Y.L., Srinivasan, K.G., Chew, J.-L., Ruan, Y., Wei, C.-L., Ng, H.H., et al. (2008). Evolution of the mammalian transcription factor binding repertoire via transposable elements. *Genome Res.* 18, 1752–1762.
- Braak, H., Del Tredici, K., Rüb, U., de Vos, R.A.I., Jansen Steur, E.N.H., and Braak, E. (2003). Staging of brain pathology related to sporadic Parkinson's disease. *Neurobiol. Aging* 24, 197–211.
- Brisch, R., Saniotis, A., Wolf, R., Biela, H., Bernstein, H.-G., Steiner, J., Bogerts, B., Braun, K., Jankowski, Z., Kumaratilake, J., et al. (2014). The Role of Dopamine in Schizophrenia from a Neurobiological and Evolutionary Perspective: Old Fashioned, but Still in Vogue. *Front Psychiatry* 5.
- Britten, R.J. (2010). Transposable element insertions have strongly affected human evolution. *PNAS* 107, 19945–19948.
- Britten, R.J., and Davidson, E.H. (1971). Repetitive and non-repetitive DNA sequences and a speculation on the origins of evolutionary novelty. *Q Rev Biol* 46, 111–138.

- Brouha, B., Schustak, J., Badge, R.M., Lutz-Prigge, S., Farley, A.H., Moran, J.V., and Kazazian, H.H. (2003). Hot L1s account for the bulk of retrotransposition in the human population. *Proc. Natl. Acad. Sci. U.S.A.* *100*, 5280–5285.
- Brunet, I., Weinl, C., Piper, M., Trembleau, A., Volovitch, M., Harris, W., Prochiantz, A., and Holt, C. (2005). The transcription factor Engrailed-2 guides retinal axons. *Nature* *438*, 94–98.
- Bundo, M., Toyoshima, M., Okada, Y., Akamatsu, W., Ueda, J., Nemoto-Miyauchi, T., Sunaga, F., Toritsuka, M., Ikawa, D., Kakita, A., et al. (2014). Increased l1 retrotransposition in the neuronal genome in schizophrenia. *Neuron* *81*, 306–313.
- Burgess, R.C., Misteli, T., and Oberdoerffer, P. (2012). DNA damage, chromatin, and transcription: the trinity of aging. *Curr. Opin. Cell Biol.* *24*, 724–730.
- Cang, J., Wang, L., Stryker, M.P., and Feldheim, D.A. (2008). Roles of ephrin-As and Structured Activity in the Development of Functional Maps in the Superior Colliculus. *J Neurosci* *28*, 11015–11023.
- Cappucci, U., Torromino, G., Casale, A.M., Camon, J., Capitano, F., Berloco, M., Mele, A., Pimpinelli, S., Rinaldi, A., and Piacentini, L. (2018). Stress-induced strain and brain region-specific activation of LINE-1 transposons in adult mice. *Stress* *21*, 575–579.
- Chahrour, M., and Zoghbi, H.Y. (2007). The story of Rett syndrome: from clinic to neurobiology. *Neuron* *56*, 422–437.
- Chatterjee, D., Sanchez, D.S., Quansah, E., Rey, N.L., George, S., Becker, K., Madaj, Z., Steiner, J.A., Ma, J., Galvis, M.L.E., et al. (2019). Loss of one Engrailed1 allele enhances induced α -synucleinopathy. *BioRxiv* 530915.
- Chen, S.H., Chan, N.-L., and Hsieh, T. (2013). New Mechanistic and Functional Insights into DNA Topoisomerases. *Annual Review of Biochemistry* *82*, 139–170.
- Choudhary, M.N., Friedman, R.Z., Wang, J.T., Jang, H.S., Zhuo, X., and Wang, T. (2018). Co-opted transposons help perpetuate conserved higher-order chromosomal structures. *BioRxiv* 485342.
- Chow, J., and Heard, E. (2009). X inactivation and the complexities of silencing a sex chromosome. *Current Opinion in Cell Biology* *21*, 359–366.
- Chun, J.J., Schatz, D.G., Oettinger, M.A., Jaenisch, R., and Baltimore, D. (1991). The recombination activating gene-1 (RAG-1) transcript is present in the murine central nervous system. *Cell* *64*, 189–200.
- Chuong, E.B., Elde, N.C., and Feschotte, C. (2017). Regulatory activities of transposable elements: from conflicts to benefits. *Nat. Rev. Genet.* *18*, 71–86.
- Condron, B.G., Patel, N.H., and Zinn, K. (1994). engrailed controls glial/neuronal cell fate decisions at the midline of the central nervous system. *Neuron* *13*, 541–554.
- Cordaux, R., and Batzer, M.A. (2009). The impact of retrotransposons on human genome evolution. *Nat Rev Genet* *10*, 691–703.

- Cortese, A., Plagnol, V., Brady, S., Simone, R., Lashley, T., Acevedo-Arozena, A., de Silva, R., Greensmith, L., Holton, J., Hanna, M.G., et al. (2014). Widespread RNA metabolism impairment in sporadic inclusion body myositis TDP43-proteinopathy. *Neurobiol Aging* 35, 1491–1498.
- Cory, T.J., Midde, N.M., Rao, P., and Kumar, S. (2015). Investigational reverse transcriptase inhibitors for the treatment of HIV. *Expert Opin Investig Drugs* 24, 1219–1228.
- Cost, G.J., Feng, Q., Jacquier, A., and Boeke, J.D. (2002). Human L1 element target-primed reverse transcription in vitro. *EMBO J* 21, 5899–5910.
- Coufal, N.G., Garcia-Perez, J.L., Peng, G.E., Yeo, G.W., Mu, Y., Lovci, M.T., Morell, M., O’Shea, K.S., Moran, J.V., and Gage, F.H. (2009). L1 retrotransposition in human neural progenitor cells. *Nature* 460, 1127–1131.
- Coufal, N.G., Garcia-Perez, J.L., Peng, G.E., Marchetto, M.C.N., Muotri, A.R., Mu, Y., Carson, C.T., Macia, A., Moran, J.V., and Gage, F.H. (2011). Ataxia telangiectasia mutated (ATM) modulates long interspersed element-1 (L1) retrotransposition in human neural stem cells. *Proc. Natl. Acad. Sci. U.S.A.* 108, 20382–20387.
- Crow, Y.J., Hayward, B.E., Parmar, R., Robins, P., Leitch, A., Ali, M., Black, D.N., van Bokhoven, H., Brunner, H.G., Hamel, B.C., et al. (2006). Mutations in the gene encoding the 3’-5’ DNA exonuclease TREX1 cause Aicardi-Goutières syndrome at the AGS1 locus. *Nat. Genet.* 38, 917–920.
- Crow, Y.J., Chase, D.S., Lowenstein Schmidt, J., Szykiewicz, M., Forte, G.M.A., Gornall, H.L., Oojageer, A., Anderson, B., Pizzino, A., Helman, G., et al. (2015). Characterization of human disease phenotypes associated with mutations in TREX1, RNASEH2A, RNASEH2B, RNASEH2C, SAMHD1, ADAR, and IFIH1. *Am. J. Med. Genet. A* 167A, 296–312.
- Dauer, W., and Przedborski, S. (2003). Parkinson’s disease: mechanisms and models. *Neuron* 39, 889–909.
- Davidson, D., Graham, E., Sime, C., and Hill, R. (1988). A gene with sequence similarity to *Drosophila engrailed* is expressed during the development of the neural tube and vertebrae in the mouse. *Development* 104, 305–316.
- De Cecco, M., Criscione, S.W., Peterson, A.L., Neretti, N., Sedivy, J.M., and Kreiling, J.A. (2013). Transposable elements become active and mobile in the genomes of aging mammalian somatic tissues. *Aging (Albany NY)* 5, 867–883.
- De Cecco, M., Ito, T., Petrashen, A.P., Elias, A.E., Skvir, N.J., Criscione, S.W., Caligiana, A., Broccoli, G., Adney, E.M., Boeke, J.D., et al. (2019). L1 drives IFN in senescent cells and promotes age-associated inflammation. *Nature* 566, 73–78.
- De Clercq, E. (2013). The nucleoside reverse transcriptase inhibitors, nonnucleoside reverse transcriptase inhibitors, and protease inhibitors in the treatment of HIV infections (AIDS). *Adv. Pharmacol.* 67, 317–358.
- Deininger, P.L., and Batzer, M.A. (1999). Alu repeats and human disease. *Mol. Genet. Metab.* 67, 183–193.

- Delcambre, S., Nonnenmacher, Y., and Hiller, K. (2016). Dopamine Metabolism and Reactive Oxygen Species Production. In *Mitochondrial Mechanisms of Degeneration and Repair in Parkinson's Disease*, L.M. Buhlman, ed. (Cham: Springer International Publishing), pp. 25–47.
- Denli, A.M., Narvaiza, I., Kerman, B.E., Pena, M., Benner, C., Marchetto, M.C.N., Diedrich, J.K., Aslanian, A., Ma, J., Moresco, J.J., et al. (2015). Primate-specific ORF0 contributes to retrotransposon-mediated diversity. *Cell* *163*, 583–593.
- Derelle, R., Lopez, P., Le Guyader, H., and Manuel, M. (2007). Homeodomain proteins belong to the ancestral molecular toolkit of eukaryotes. *Evol. Dev.* *9*, 212–219.
- Derossi, D., Joliot, A.H., Chassaing, G., and Prochiantz, A. (1994). The third helix of the Antennapedia homeodomain translocates through biological membranes. *J. Biol. Chem.* *269*, 10444–10450.
- Derossi, D., Calvet, S., Trembleau, A., Brunissen, A., Chassaing, G., and Prochiantz, A. (1996). Cell internalization of the third helix of the Antennapedia homeodomain is receptor-independent. *J. Biol. Chem.* *271*, 18188–18193.
- Derossi, D., Chassaing, G., and Prochiantz, A. (1998). Trojan peptides: the penetratin system for intracellular delivery. *Trends in Cell Biology* *8*, 84–87.
- Di Bonito, M., Narita, Y., Avallone, B., Sequino, L., Mancuso, M., Andolfi, G., Franzè, A.M., Puellas, L., Rijli, F.M., and Studer, M. (2013). Assembly of the auditory circuitry by a Hox genetic network in the mouse brainstem. *PLoS Genet.* *9*, e1003249.
- Di Nardo, A.A., Nedelec, S., Trembleau, A., Volovitch, M., Prochiantz, A., and Montesinos, M.L. (2007). Dendritic localization and activity-dependent translation of Engrailed1 transcription factor. *Mol. Cell. Neurosci.* *35*, 230–236.
- Dias, V., Junn, E., and Mouradian, M.M. (2013). The Role of Oxidative Stress in Parkinson's Disease. *J Parkinsons Dis* *3*, 461–491.
- Dombroski, B.A., Mathias, S.L., Nanthakumar, E., Scott, A.F., and Kazazian, H.H. (1991). Isolation of an active human transposable element. *Science* *254*, 1805–1808.
- Doyle, G.A., Crist, R.C., Karatas, E.T., Hammond, M.J., Ewing, A.D., Ferraro, T.N., Hahn, C.-G., and Berrettini, W.H. (2017). Analysis of LINE-1 Elements in DNA from Postmortem Brains of Individuals with Schizophrenia. *Neuropsychopharmacology* *42*, 2602–2611.
- Dupont, E., Prochiantz, A., and Joliot, A. (2007). Identification of a Signal Peptide for Unconventional Secretion. *J. Biol. Chem.* *282*, 8994–9000.
- Ecco, G., Imbeault, M., and Trono, D. (2017). KRAB zinc finger proteins. *Development* *144*, 2719–2729.
- Edwards, T.L., Scott, W.K., Almonte, C., Burt, A., Powell, E.H., Beecham, G.W., Wang, L., Züchner, S., Konidari, I., Wang, G., et al. (2010). Genome-wide association study confirms SNPs in SNCA and the MAPT region as common risk factors for Parkinson disease. *Ann. Hum. Genet.* *74*, 97–109.

- Evrony, G.D., Cai, X., Lee, E., Hills, L.B., Elhosary, P.C., Lehmann, H.S., Parker, J.J., Atabay, K.D., Gilmore, E.C., Poduri, A., et al. (2012). Single-Neuron Sequencing Analysis of L1 Retrotransposition and Somatic Mutation in the Human Brain. *Cell* 151, 483–496.
- Evrony, G.D., Lee, E., Park, P.J., and Walsh, C.A. (2016). Resolving rates of mutation in the brain using single-neuron genomics. *ELife* 5, e12966.
- Fasolino, M., Liu, S., Wang, Y., and Zhou, Z. (2017). Distinct cellular and molecular environments support aging-related DNA methylation changes in the substantia nigra. *Epigenomics* 9, 21–31.
- Fellner, L., Irschick, R., Schanda, K., Reindl, M., Klimaschewski, L., Poewe, W., Wenning, G.K., and Stefanova, N. (2013). Toll-like receptor 4 is required for α -synuclein dependent activation of microglia and astroglia. *Glia* 61, 349–360.
- Feng, Q., Moran, J.V., Kazazian, H.H., and Boeke, J.D. (1996). Human L1 retrotransposon encodes a conserved endonuclease required for retrotransposition. *Cell* 87, 905–916.
- Feng, Y., Jankovic, J., and Wu, Y.-C. (2015). Epigenetic mechanisms in Parkinson's disease. *Journal of the Neurological Sciences* 349, 3–9.
- Fishel, M.L., Vasko, M.R., and Kelley, M.R. (2007). DNA repair in neurons: so if they don't divide what's to repair? *Mutat. Res.* 614, 24–36.
- Flajnik, M.F., and Kasahara, M. (2010). Origin and evolution of the adaptive immune system: genetic events and selective pressures. *Nat. Rev. Genet.* 11, 47–59.
- Flasch, D.A., Macia, Á., Sánchez, L., Ljungman, M., Heras, S.R., García-Pérez, J.L., Wilson, T.E., and Moran, J.V. (2019). Genome-wide de novo L1 Retrotransposition Connects Endonuclease Activity with Replication. *Cell* 177, 837-851.e28.
- Forno, L.S., DeLanney, L.E., Irwin, I., Di Monte, D., and Langston, J.W. (1992). Astrocytes and Parkinson's disease. *Prog. Brain Res.* 94, 429–436.
- Friedli, M., and Trono, D. (2015). The developmental control of transposable elements and the evolution of higher species. *Annu. Rev. Cell Dev. Biol.* 31, 429–451.
- Fudenberg, G., Imakaev, M., Lu, C., Goloborodko, A., Abdennur, N., and Mirny, L.A. (2016). Formation of Chromosomal Domains by Loop Extrusion. *Cell Reports* 15, 2038–2049.
- Gabel, H.W., Kinde, B.Z., Stroud, H., Gilbert, C.S., Harmin, D.A., Kastan, N.R., Hemberg, M., Ebert, D.H., and Greenberg, M.E. (2015). Disruption of DNA methylation-dependent long gene repression in Rett syndrome. *Nature* 522, 89–93.
- Gantz, S.C., Ford, C.P., Neve, K.A., and Williams, J.T. (2011). Loss of *Mecp2* in substantia nigra dopamine neurons compromises the nigrostriatal pathway. *J. Neurosci.* 31, 12629–12637.
- Garber, R.L., Kuroiwa, A., and Gehring, W.J. (1983). Genomic and cDNA clones of the homeotic locus *Antennapedia* in *Drosophila*. *EMBO J.* 2, 2027–2036.
- Gasior, S.L., Wakeman, T.P., Xu, B., and Deininger, P.L. (2006). The Human LINE-1 Retrotransposon Creates DNA Double-strand Breaks. *J Mol Biol* 357, 1383–1393.

- Gehring, W.J. (1987). Homeo boxes in the study of development. *Science* 236, 1245–1252.
- Genestine, M., Lin, L., Durens, M., Yan, Y., Jiang, Y., Prem, S., Bailoor, K., Kelly, B., Sonsalla, P.K., Matteson, P.G., et al. (2015). Engrailed-2 (En2) deletion produces multiple neurodevelopmental defects in monoamine systems, forebrain structures and neurogenesis and behavior. *Hum Mol Genet* 24, 5805–5827.
- Gharani, N., Benayed, R., Mancuso, V., Brzustowicz, L.M., and Millonig, J.H. (2004). Association of the homeobox transcription factor, ENGRAILED 2, 3, with autism spectrum disorder. *Mol. Psychiatry* 9, 474–484.
- Ghosh, A., Tyson, T., George, S., Hildebrandt, E.N., Steiner, J.A., Madaj, Z., Schulz, E., Machiela, E., McDonald, W.G., Escobar Galvis, M.L., et al. (2016). Mitochondrial pyruvate carrier regulates autophagy, inflammation, and neurodegeneration in experimental models of Parkinson’s disease. *Sci Transl Med* 8, 368ra174.
- Giasson, B.I., Duda, J.E., Murray, I.V., Chen, Q., Souza, J.M., Hurtig, H.I., Ischiropoulos, H., Trojanowski, J.Q., and Lee, V.M. (2000). Oxidative damage linked to neurodegeneration by selective alpha-synuclein nitration in synucleinopathy lesions. *Science* 290, 985–989.
- Goodier, J.L., Zhang, L., Vetter, M.R., and Kazazian, H.H. (2007a). LINE-1 ORF1 Protein Localizes in Stress Granules with Other RNA-Binding Proteins, Including Components of RNA Interference RNA-Induced Silencing Complex. *Mol Cell Biol* 27, 6469–6483.
- Goodier, J.L., Zhang, L., Vetter, M.R., and Kazazian, H.H. (2007b). LINE-1 ORF1 Protein Localizes in Stress Granules with Other RNA-Binding Proteins, Including Components of RNA Interference RNA-Induced Silencing Complex. *Mol Cell Biol* 27, 6469–6483.
- Goutières, F., Aicardi, J., Barth, P.G., and Lebon, P. (1998). Aicardi-Goutières syndrome: An update and results of interferon- α studies. *Annals of Neurology* 44, 900–907.
- Graham, T., and Boissinot, S. (2006). The Genomic Distribution of L1 Elements: The Role of Insertion Bias and Natural Selection. *J Biomed Biotechnol* 2006.
- Graybiel, A.M., Aosaki, T., Flaherty, A.W., and Kimura, M. (1994). The basal ganglia and adaptive motor control. *Science* 265, 1826–1831.
- Guo, C., Jeong, H.-H., Hsieh, Y.-C., Klein, H.-U., Bennett, D.A., Jager, P.L.D., Liu, Z., and Shulman, J.M. (2018). Tau Activates Transposable Elements in Alzheimer’s Disease. *Cell Reports* 23, 2874–2880.
- Halliwell, B. (1992). Reactive oxygen species and the central nervous system. *J. Neurochem.* 59, 1609–1623.
- Han, J.S., and Boeke, J.D. (2005). LINE-1 retrotransposons: modulators of quantity and quality of mammalian gene expression? *Bioessays* 27, 775–784.
- Hanks, M., Wurst, W., Anson-Cartwright, L., Auerbach, A.B., and Joyner, A.L. (1995). Rescue of the En-1 mutant phenotype by replacement of En-1 with En-2. *Science* 269, 679–682.
- Hatcher, J.M., Pennell, K.D., and Miller, G.W. (2008). Parkinson’s disease and pesticides: a toxicological perspective. *Trends Pharmacol Sci* 29, 322–329.

- Haubenberger, D., Reinthaler, E., Mueller, J.C., Pirker, W., Katzenschlager, R., Froehlich, R., Bruecke, T., Daniel, G., Auff, E., and Zimprich, A. (2011). Association of transcription factor polymorphisms PITX3 and EN1 with Parkinson's disease. *Neurobiol. Aging* 32, 302–307.
- Heasman, S.J., and Ridley, A.J. (2008). Mammalian Rho GTPases: new insights into their functions from in vivo studies. *Nat. Rev. Mol. Cell Biol.* 9, 690–701.
- Hegde, M.L., Gupta, V.B., Anitha, M., Harikrishna, T., Shankar, S.K., Muthane, U., Subba Rao, K., and Jagannatha Rao, K.S. (2006). Studies on genomic DNA topology and stability in brain regions of Parkinson's disease. *Arch. Biochem. Biophys.* 449, 143–156.
- Heiman, M., Schaefer, A., Gong, S., Peterson, J.D., Day, M., Ramsey, K.E., Suárez-Fariñas, M., Schwarz, C., Stephan, D.A., Surmeier, D.J., et al. (2008). A Translational Profiling Approach for the Molecular Characterization of CNS Cell Types. *Cell* 135, 738–748.
- Heneka, M.T., Kummer, M.P., and Latz, E. (2014). Innate immune activation in neurodegenerative disease. *Nat. Rev. Immunol.* 14, 463–477.
- Heras, S.R., Macias, S., Plass, M., Fernandez, N., Cano, D., Eyra, E., Garcia-Perez, J.L., and Cáceres, J.F. (2013). The Microprocessor controls the activity of mammalian retrotransposons. *Nat. Struct. Mol. Biol.* 20, 1173–1181.
- Hohjoh, H., and Singer, M.F. (1996). Cytoplasmic ribonucleoprotein complexes containing human LINE-1 protein and RNA. *EMBO J.* 15, 630–639.
- Hu, J.H., Yang, N., Ma, Y.H., Jiang, J., Zhang, J.F., Fei, J., and Guo, L.H. (2004). Identification of glutamate receptors and transporters in mouse and human sperm. *J. Androl.* 25, 140–146.
- Huang, S., Tao, X., Yuan, S., Zhang, Y., Li, P., Beilinson, H.A., Zhang, Y., Yu, W., Pontarotti, P., Escrava, H., et al. (2016). Discovery of an Active RAG Transposon Illuminates the Origins of V(D)J Recombination. *Cell* 166, 102–114.
- Iyengar, S., and Farnham, P.J. (2011). KAP1 protein: an enigmatic master regulator of the genome. *J. Biol. Chem.* 286, 26267–26276.
- Jacob-Hirsch, J., Eyal, E., Knisbacher, B.A., Roth, J., Cesarkas, K., Dor, C., Farage-Barhom, S., Kunik, V., Simon, A.J., Gal, M., et al. (2018). Whole-genome sequencing reveals principles of brain retrotransposition in neurodevelopmental disorders. *Cell Res.* 28, 187–203.
- Jacques, P.-É., Jeyakani, J., and Bourque, G. (2013). The Majority of Primate-Specific Regulatory Sequences Are Derived from Transposable Elements. *PLOS Genetics* 9, e1003504.
- Jangam, D., Feschotte, C., and Betrán, E. (2017). Transposable element domestication as an adaptation to evolutionary conflicts. *Trends Genet* 33, 817–831.
- Jaynes, J.B., and O'Farrell, P.H. (1991). Active repression of transcription by the engrailed homeodomain protein. *EMBO J* 10, 1427–1433.
- Joliot, A., Pernelle, C., Deagostini-Bazin, H., and Prochiantz, A. (1991). Antennapedia homeobox peptide regulates neural morphogenesis. *Proc. Natl. Acad. Sci. U.S.A.* 88, 1864–1868.

- Joliot, A., Trembleau, A., Raposo, G., Calvet, S., Volovitch, M., and Prochiantz, A. (1997). Association of Engrailed homeoproteins with vesicles presenting caveolae-like properties. *Development* *124*, 1865–1875.
- Joliot, A., Maizel, A., Rosenberg, D., Trembleau, A., Dupas, S., Volovitch, M., and Prochiantz, A. (1998). Identification of a signal sequence necessary for the unconventional secretion of Engrailed homeoprotein. *Curr. Biol.* *8*, 856–863.
- Joyner, A.L., Kornberg, T., Coleman, K.G., Cox, D.R., and Martin, G.R. (1985). Expression during embryogenesis of a mouse gene with sequence homology to the *Drosophila* engrailed gene. *Cell* *43*, 29–37.
- Joyner, A.L., Herrup, K., Auerbach, B.A., Davis, C.A., and Rossant, J. (1991). Subtle cerebellar phenotype in mice homozygous for a targeted deletion of the *En-2* homeobox. *Science* *251*, 1239–1243.
- Kanfi, Y., Peshti, V., Gil, R., Naiman, S., Nahum, L., Levin, E., Kronfeld-Schor, N., and Cohen, H.Y. (2010). SIRT6 protects against pathological damage caused by diet-induced obesity. *Aging Cell* *9*, 162–173.
- Kanfi, Y., Naiman, S., Amir, G., Peshti, V., Zinman, G., Nahum, L., Bar-Joseph, Z., and Cohen, H.Y. (2012). The sirtuin SIRT6 regulates lifespan in male mice. *Nature* *483*, 218–221.
- Kazazian, H.H., Wong, C., Youssoufian, H., Scott, A.F., Phillips, D.G., and Antonarakis, S.E. (1988). Haemophilia A resulting from de novo insertion of L1 sequences represents a novel mechanism for mutation in man. *Nature* *332*, 164.
- Ke, Y.D., Ke, Y., Dramiga, J., Schütz, U., Kril, J.J., Ittner, L.M., Schröder, H., and Götz, J. (2012). Tau-mediated nuclear depletion and cytoplasmic accumulation of SFPQ in Alzheimer's and Pick's disease. *PLoS ONE* *7*, e35678.
- Kelley, D., and Rinn, J. (2012). Transposable elements reveal a stem cell-specific class of long noncoding RNAs. *Genome Biol.* *13*, R107.
- King, I.F., Yandava, C.N., Mabb, A.M., Hsiao, J.S., Huang, H.-S., Pearson, B.L., Calabrese, J.M., Starmer, J., Parker, J.S., Magnuson, T., et al. (2013a). Topoisomerases facilitate transcription of long genes linked to autism. *Nature* *501*, 58–62.
- King, I.F., Yandava, C.N., Mabb, A.M., Hsiao, J.S., Huang, H.-S., Pearson, B.L., Calabrese, J.M., Starmer, J., Parker, J.S., Magnuson, T., et al. (2013b). Topoisomerases facilitate transcription of long genes linked to autism. *Nature* *501*, 58–62.
- Kish, S.J., Morito, C., and Hornykiewicz, O. (1985). Glutathione peroxidase activity in Parkinson's disease brain. *Neurosci. Lett.* *58*, 343–346.
- Kleckner, N. (1990). Regulation of Transposition in Bacteria. *Annual Review of Cell Biology* *6*, 297–327.
- Klein, C.J., and Benarroch, E.E. (2014). Epigenetic regulation: basic concepts and relevance to neurologic disease. *Neurology* *82*, 1833–1840.

- Koedel, U., Merbt, U.M., Schmidt, C., Angele, B., Popp, B., Wagner, H., Pfister, H.-W., and Kirschning, C.J. (2007). Acute brain injury triggers MyD88-dependent, TLR2/4-independent inflammatory responses. *Am. J. Pathol.* *171*, 200–213.
- Krug, L., Chatterjee, N., Borges-Monroy, R., Hearn, S., Liao, W.-W., Morrill, K., Prazak, L., Rozhkov, N., Theodorou, D., Hammell, M., et al. (2017). Retrotransposon activation contributes to neurodegeneration in a *Drosophila* TDP-43 model of ALS. *PLoS Genet.* *13*, e1006635.
- Krupovic, M., Makarova, K.S., Forterre, P., Prangishvili, D., and Koonin, E.V. (2014). Casposons: a new superfamily of self-synthesizing DNA transposons at the origin of prokaryotic CRISPR-Cas immunity. *BMC Biol.* *12*, 36.
- Kuramochi-Miyagawa, S., Watanabe, T., Gotoh, K., Totoki, Y., Toyoda, A., Ikawa, M., Asada, N., Kojima, K., Yamaguchi, Y., Ijiri, T.W., et al. (2008). DNA methylation of retrotransposon genes is regulated by Piwi family members MILI and MIWI2 in murine fetal testes. *Genes Dev.* *22*, 908–917.
- Lagier-Tourenne, C., Polymenidou, M., Hutt, K.R., Vu, A.Q., Baughn, M., Huelga, S.C., Clutario, K.M., Ling, S.-C., Liang, T.Y., Mazur, C., et al. (2012). Divergent roles of ALS-linked proteins FUS/TLS and TDP-43 intersect in processing long pre-mRNAs. *Nat. Neurosci.* *15*, 1488–1497.
- Larson, K., Yan, S.-J., Tsurumi, A., Liu, J., Zhou, J., Gaur, K., Guo, D., Eickbush, T.H., and Li, W.X. (2012). Heterochromatin Formation Promotes Longevity and Represses Ribosomal RNA Synthesis. *PLOS Genetics* *8*, e1002473.
- Lavara-Culebras, E., and Paricio, N. (2007). *Drosophila* DJ-1 mutants are sensitive to oxidative stress and show reduced lifespan and motor deficits. *Gene* *400*, 158–165.
- Layalle, S., Volovitch, M., Mugat, B., Bonneaud, N., Parmentier, M.-L., Prochiantz, A., Joliot, A., and Maschat, F. (2011). Engrailed homeoprotein acts as a signaling molecule in the developing fly. *Development* *138*, 2315–2323.
- Le, T.N., Miyazaki, Y., Takuno, S., and Saze, H. (2015). Epigenetic regulation of intragenic transposable elements impacts gene transcription in *Arabidopsis thaliana*. *Nucleic Acids Res.* *43*, 3911–3921.
- Lee, E.J., Banerjee, S., Zhou, H., Jammalamadaka, A., Arcila, M., Manjunath, B.S., and Kosik, K.S. (2011). Identification of piRNAs in the central nervous system. *RNA* *17*, 1090–1099.
- Lee, M.-H., Siddoway, B., Kaeser, G.E., Segota, I., Rivera, R., Romanow, W.J., Liu, C.S., Park, C., Kennedy, G., Long, T., et al. (2019). Publisher Correction: Somatic APP gene recombination in Alzheimer's disease and normal neurons. *Nature* *566*, E6.
- Lesaffre, B., Joliot, A., Prochiantz, A., and Volovitch, M. (2007). Direct non-cell autonomous Pax6 activity regulates eye development in the zebrafish. *Neural Development* *2*, 2.
- Lewis, E.B. (1978). A gene complex controlling segmentation in *Drosophila*. *Nature* *276*, 565.

- Li, W., Prazak, L., Chatterjee, N., Grüninger, S., Krug, L., Theodorou, D., and Dubnau, J. (2013a). Activation of transposable elements during aging and neuronal decline in *Drosophila*. *Nat. Neurosci.* *16*, 529–531.
- Li, W., Prazak, L., Chatterjee, N., Grüninger, S., Krug, L., Theodorou, D., and Dubnau, J. (2013b). Activation of transposable elements during aging and neuronal decline in *Drosophila*. *Nat Neurosci* *16*, 529–531.
- Liang, D., and Wilusz, J.E. (2014). Short intronic repeat sequences facilitate circular RNA production. *Genes Dev.* *28*, 2233–2247.
- Liu, L.F., and Wang, J.C. (1987). Supercoiling of the DNA template during transcription. *Proc. Natl. Acad. Sci. U.S.A.* *84*, 7024–7027.
- Liu, E.Y., Russ, J., Cali, C.P., Phan, J.M., Amlie-Wolf, A., and Lee, E.B. (2019). Loss of Nuclear TDP-43 Is Associated with Decondensation of LINE Retrotransposons. *Cell Rep* *27*, 1409-1421.e6.
- Lotz, M., Ebert, S., Esselmann, H., Iliev, A.I., Prinz, M., Wiazewicz, N., Wiltfang, J., Gerber, J., and Nau, R. (2005). Amyloid beta peptide 1-40 enhances the action of Toll-like receptor-2 and -4 agonists but antagonizes Toll-like receptor-9-induced inflammation in primary mouse microglial cell cultures. *J. Neurochem.* *94*, 289–298.
- Lu, T., Pan, Y., Kao, S.-Y., Li, C., Kohane, I., Chan, J., and Yankner, B.A. (2004). Gene regulation and DNA damage in the ageing human brain. *Nature* *429*, 883–891.
- Lu, X., Sachs, F., Ramsay, L., Jacques, P.-É., Göke, J., Bourque, G., and Ng, H.-H. (2014). The retrovirus HERVH is a long noncoding RNA required for human embryonic stem cell identity. *Nat. Struct. Mol. Biol.* *21*, 423–425.
- Luisier, R., Tyzack, G.E., Hall, C.E., Mitchell, J.S., Devine, H., Taha, D.M., Malik, B., Meyer, I., Greensmith, L., Newcombe, J., et al. (2018). Intron retention and nuclear loss of SFPQ are molecular hallmarks of ALS. *Nat Commun* *9*, 2010.
- Lullo, E.D., Haton, C., Poupon, C.L., Volovitch, M., Joliot, A., Thomas, J.-L., and Prochiantz, A. (2011). Paracrine Pax6 activity regulates oligodendrocyte precursor cell migration in the chick embryonic neural tube. *Development* *138*, 4991–5001.
- Luo, S.X., and Huang, E.J. (2016). Dopaminergic Neurons and Brain Reward Pathways. *Am J Pathol* *186*, 478–488.
- Lynch, V.J., Leclerc, R.D., May, G., and Wagner, G.P. (2011). Transposon-mediated rewiring of gene regulatory networks contributed to the evolution of pregnancy in mammals. *Nature Genetics* *43*, 1154–1159.
- Lyon, M.F. (2000). LINE-1 elements and X chromosome inactivation: a function for “junk” DNA? *Proc. Natl. Acad. Sci. U.S.A.* *97*, 6248–6249.
- Madabhushi, R., Pan, L., and Tsai, L.-H. (2014). DNA damage and its links to neurodegeneration. *Neuron* *83*, 266–282.

- Madabhushi, R., Gao, F., Pfenning, A.R., Pan, L., Yamakawa, S., Seo, J., Rueda, R., Phan, T.X., Yamakawa, H., Pao, P.-C., et al. (2015). Activity-Induced DNA Breaks Govern the Expression of Neuronal Early-Response Genes. *Cell* *161*, 1592–1605.
- Maizel, A., Tassetto, M., Filhol, O., Cochet, C., Prochiantz, A., and Joliot, A. (2002). Engrailed homeoprotein secretion is a regulated process. *Development* *129*, 3545–3553.
- Marsden, C.D. (1983). Neuromelanin and Parkinson's disease. *J. Neural Transm. Suppl.* *19*, 121–141.
- Martin, J.C., Hitchcock, M.J.M., De Clercq, E., and Prusoff, W.H. (2010). Early nucleoside reverse transcriptase inhibitors for the treatment of HIV: a brief history of stavudine (D4T) and its comparison with other dideoxynucleosides. *Antiviral Res.* *85*, 34–38.
- Matsui, T., Leung, D., Miyashita, H., Maksakova, I.A., Miyachi, H., Kimura, H., Tachibana, M., Lorincz, M.C., and Shinkai, Y. (2010). Proviral silencing in embryonic stem cells requires the histone methyltransferase ESET. *Nature* *464*, 927–931.
- Maxwell, P.H., Burhans, W.C., and Curcio, M.J. (2011). Retrotransposition is associated with genome instability during chronological aging. *Proc. Natl. Acad. Sci. U.S.A.* *108*, 20376–20381.
- McClintock, B. (1950). The Origin and Behavior of Mutable Loci in Maize. *Proc Natl Acad Sci U S A* *36*, 344–355.
- McGinnis, W., Garber, R.L., Wirz, J., Kuroiwa, A., and Gehring, W.J. (1984). A homologous protein-coding sequence in *Drosophila* homeotic genes and its conservation in other metazoans. *Cell* *37*, 403–408.
- Meizel, S. (2004). The sperm, a neuron with a tail: 'neuronal' receptors in mammalian sperm. *Biological Reviews* *79*, 713–732.
- Millen, K.J., Wurst, W., Herrup, K., and Joyner, A.L. (1994). Abnormal embryonic cerebellar development and patterning of postnatal foliation in two mouse *Engrailed-2* mutants. *Development* *120*, 695–706.
- Miyata, S., Komatsu, Y., Yoshimura, Y., Taya, C., and Kitagawa, H. (2012). Persistent cortical plasticity by upregulation of chondroitin 6-sulfation. *Nat. Neurosci.* *15*, 414–422, S1-2.
- Morales, J.F., Snow, E.T., and Murnane, J.P. (2002). Environmental factors affecting transcription of the human L1 retrotransposon. I. Steroid hormone-like agents. *Mutagenesis* *17*, 193–200.
- Muotri, A.R., Chu, V.T., Marchetto, M.C.N., Deng, W., Moran, J.V., and Gage, F.H. (2005). Somatic mosaicism in neuronal precursor cells mediated by L1 retrotransposition. *Nature* *435*, 903–910.
- Muotri, A.R., Marchetto, M.C.N., Coufal, N.G., and Gage, F.H. (2007). The necessary junk: new functions for transposable elements. *Hum Mol Genet* *16*, R159–R167.
- Muotri, A.R., Zhao, C., Marchetto, M.C.N., and Gage, F.H. (2009). Environmental influence on L1 retrotransposons in the adult hippocampus. *Hippocampus* *19*, 1002–1007.

- Muotri, A.R., Marchetto, M.C.N., Coufal, N.G., Oefner, R., Yeo, G., Nakashima, K., and Gage, F.H. (2010). L1 retrotransposition in neurons is modulated by MeCP2. *Nature* 468, 443–446.
- Nagatsu, T., and Sawada, M. (2005). Inflammatory process in Parkinson's disease: role for cytokines. *Curr. Pharm. Des.* 11, 999–1016.
- Narro, M.L., Yang, F., Kraft, R., Wenk, C., Efrat, A., and Restifo, L.L. (2007). NeuronMetrics: Software for Semi-Automated Processing of Cultured-Neuron Images. *Brain Res* 1138, 57–75.
- Nédélec, S., Foucher, I., Brunet, I., Bouillot, C., Prochiantz, A., and Trembleau, A. (2004). Emx2 homeodomain transcription factor interacts with eukaryotic translation initiation factor 4E (eIF4E) in the axons of olfactory sensory neurons. *PNAS* 101, 10815–10820.
- Nordströma, U., Beauvais, G., Ghosh, A., Pulikkaparambil Sasidharan, B.C., Lundblad, M., Fuchs, J., Joshi, R.L., Lipton, J.W., Roholt, A., Medicetty, S., et al. (2015). Progressive nigrostriatal terminal dysfunction and degeneration in the engrailed1 heterozygous mouse model of Parkinson's disease. *Neurobiol. Dis.* 73, 70–82.
- Oberdoerffer, P., Michan, S., McVay, M., Mostoslavsky, R., Vann, J., Park, S.-K., Hartlerode, A., Stegmüller, J., Hafner, A., Loerch, P., et al. (2008). SIRT1 redistribution on chromatin promotes genomic stability but alters gene expression during aging. *Cell* 135, 907–918.
- Okun, E., Griffioen, K.J., Lathia, J.D., Tang, S.-C., Mattson, M.P., and Arumugam, T.V. (2009). Toll-like receptors in neurodegeneration. *Brain Res Rev* 59, 278–292.
- Olanow, C.W., and Tatton, W.G. (1999). Etiology and Pathogenesis of Parkinson's Disease. *Annual Review of Neuroscience* 22, 123–144.
- O'Leary, D.D.M., Chou, S.-J., and Sahara, S. (2007). Area Patterning of the Mammalian Cortex. *Neuron* 56, 252–269.
- Orecchini, E., Doria, M., Antonioni, A., Galardi, S., Ciafrè, S.A., Frassinelli, L., Mancone, C., Montaldo, C., Tripodi, M., and Michienzi, A. (2017). ADAR1 restricts LINE-1 retrotransposition. *Nucleic Acids Res.* 45, 155–168.
- Paolicelli, R.C., Bolasco, G., Pagani, F., Maggi, L., Scianni, M., Panzanelli, P., Giustetto, M., Ferreira, T.A., Guiducci, E., Dumas, L., et al. (2011). Synaptic pruning by microglia is necessary for normal brain development. *Science* 333, 1456–1458.
- Pegoraro, G., Kubben, N., Wickert, U., Göhler, H., Hoffmann, K., and Misteli, T. (2009). Ageing-related chromatin defects through loss of the NURD complex. *Nat. Cell Biol.* 11, 1261–1267.
- Percharde, M., Lin, C.-J., Yin, Y., Guan, J., Peixoto, G.A., Bulut-Karslioglu, A., Biechele, S., Huang, B., Shen, X., and Ramalho-Santos, M. (2018). A LINE1-Nucleolin Partnership Regulates Early Development and ESC Identity. *Cell* 174, 391-405.e19.
- Pereira, G.C., Sanchez, L., Schaughency, P.M., Rubio-Roldán, A., Choi, J.A., Planet, E., Batra, R., Turelli, P., Trono, D., Ostrow, L.W., et al. (2018). Properties of LINE-1 proteins and repeat element expression in the context of amyotrophic lateral sclerosis. *Mobile DNA* 9, 35.

- Perrat, P.N., DasGupta, S., Wang, J., Theurkauf, W., Weng, Z., Rosbash, M., and Waddell, S. (2013). Transposition-driven genomic heterogeneity in the *Drosophila* brain. *Science* *340*, 91–95.
- Petit, E., Hérault, J., Martineau, J., Perrot, A., Barthélémy, C., Hameury, L., Sauvage, D., Lelord, G., and Müh, J.P. (1995). Association study with two markers of a human homeogene in infantile autism. *J. Med. Genet.* *32*, 269–274.
- Poewe, W., Seppi, K., Tanner, C.M., Halliday, G.M., Brundin, P., Volkman, J., Schrag, A.-E., and Lang, A.E. (2017). Parkinson disease. *Nature Reviews Disease Primers* *3*, 17013.
- Polymenidou, M., Lagier-Tourenne, C., Hutt, K.R., Bennett, C.F., Cleveland, D.W., and Yeo, G.W. (2012). Misregulated RNA processing in amyotrophic lateral sclerosis. *Brain Res.* *1462*, 3–15.
- Polymeropoulos, M.H., Lavedan, C., Leroy, E., Ide, S.E., Dehejia, A., Dutra, A., Pike, B., Root, H., Rubenstein, J., Boyer, R., et al. (1997). Mutation in the alpha-synuclein gene identified in families with Parkinson's disease. *Science* *276*, 2045–2047.
- Prochiantz, A. (2011). Homeoprotein intercellular transfer, the hidden face of cell-penetrating peptides. *Methods Mol. Biol.* *683*, 249–257.
- Prochiantz, A., and Di Nardo, A.A. (2015). Homeoprotein signaling in the developing and adult nervous system. *Neuron* *85*, 911–925.
- Prochiantz, A., and Joliot, A. (2003). Can transcription factors function as cell-cell signalling molecules? *Nat. Rev. Mol. Cell Biol.* *4*, 814–819.
- Prokocimer, M., Davidovich, M., Nissim-Rafinia, M., Wiesel-Motiuk, N., Bar, D.Z., Barkan, R., Meshorer, E., and Gruenbaum, Y. (2009). Nuclear lamins: key regulators of nuclear structure and activities. *J. Cell. Mol. Med.* *13*, 1059–1085.
- Quenneville, S., Turelli, P., Bojkowska, K., Raclot, C., Offner, S., Kapopoulou, A., and Trono, D. (2012). The KRAB-ZFP/KAP1 system contributes to the early embryonic establishment of site-specific DNA methylation patterns maintained during development. *Cell Rep* *2*, 766–773.
- Rajasethupathy, P., Antonov, I., Sheridan, R., Frey, S., Sander, C., Tuschl, T., and Kandel, E.R. (2012). A role for neuronal piRNAs in the epigenetic control of memory-related synaptic plasticity. *Cell* *149*, 693–707.
- Rekaik, H., Blaudin de Thé, F.-X., Fuchs, J., Massiani-Beaudoin, O., Prochiantz, A., and Joshi, R.L. (2015). Engrailed Homeoprotein Protects Mesencephalic Dopaminergic Neurons from Oxidative Stress. *Cell Rep* *13*, 242–250.
- Rice, G., Patrick, T., Parmar, R., Taylor, C.F., Aeby, A., Aicardi, J., Artuch, R., Montalto, S.A., Bacino, C.A., Barroso, B., et al. (2007). Clinical and molecular phenotype of Aicardi-Goutieres syndrome. *Am. J. Hum. Genet.* *81*, 713–725.
- Richardson, S.R., Morell, S., and Faulkner, G.J. (2014). L1 Retrotransposons and Somatic Mosaicism in the Brain. *Annu. Rev. Genet.* *48*, 1–27.

- Rieker, C., Engblom, D., Kreiner, G., Domanskyi, A., Schober, A., Stotz, S., Neumann, M., Yuan, X., Grummt, I., Schütz, G., et al. (2011). Nucleolar disruption in dopaminergic neurons leads to oxidative damage and parkinsonism through repression of mammalian target of rapamycin signaling. *J. Neurosci.* *31*, 453–460.
- Rissling, I., Strauch, K., Höft, C., Oertel, W.H., and Möller, J.C. (2009). Haplotype analysis of the engrailed-2 gene in young-onset Parkinson's disease. *Neurodegener Dis* *6*, 102–105.
- Riva, D., and Giorgi, C. (2000). The cerebellum contributes to higher functions during development: evidence from a series of children surgically treated for posterior fossa tumours. *Brain* *123* (Pt 5), 1051–1061.
- Roberts, J.T., Cardin, S.E., and Borchert, G.M. (2014). Burgeoning evidence indicates that microRNAs were initially formed from transposable element sequences. *Mob Genet Elements* *4*, e29255.
- Rogelj, B., Easton, L.E., Bogu, G.K., Stanton, L.W., Rot, G., Curk, T., Zupan, B., Sugimoto, Y., Modic, M., Haberman, N., et al. (2012). Widespread binding of FUS along nascent RNA regulates alternative splicing in the brain. *Sci Rep* *2*, 603.
- Rowe, H.M., Jakobsson, J., Mesnard, D., Rougemont, J., Reynard, S., Aktas, T., Maillard, P.V., Layard-Liesching, H., Verp, S., Marquis, J., et al. (2010). KAP1 controls endogenous retroviruses in embryonic stem cells. *Nature* *463*, 237–240.
- Rowen, L., Young, J., Birditt, B., Kaur, A., Madan, A., Philipps, D.L., Qin, S., Minx, P., Wilson, R.K., Hood, L., et al. (2002). Analysis of the human neurexin genes: alternative splicing and the generation of protein diversity. *Genomics* *79*, 587–597.
- Rubbi, C.P., and Milner, J. (2003). Disruption of the nucleolus mediates stabilization of p53 in response to DNA damage and other stresses. *EMBO J.* *22*, 6068–6077.
- Ruiz-Medrano, R., Xoconostle-Cazares, B., and Kragler, F. (2004). The plasmodesmatal transport pathway for homeotic proteins, silencing signals and viruses. *Curr. Opin. Plant Biol.* *7*, 641–650.
- Sandy, M.S., Armstrong, M., Tanner, C.M., Daly, A.K., Di Monte, D.A., Langston, J.W., and Idle, J.R. (1996). CYP2D6 allelic frequencies in young-onset Parkinson's disease. *Neurology* *47*, 225–230.
- Savage, A.L., Schumann, G.G., Breen, G., Bubb, V.J., Al-Chalabi, A., and Quinn, J.P. (2019). Retrotransposons in the development and progression of amyotrophic lateral sclerosis. *J Neurol Neurosurg Psychiatry* *90*, 284–293.
- Scaffidi, P., and Misteli, T. (2006). Lamin A-dependent nuclear defects in human aging. *Science* *312*, 1059–1063.
- Schafer, D.P., Lehrman, E.K., Kautzman, A.G., Koyama, R., Mardinly, A.R., Yamasaki, R., Ransohoff, R.M., Greenberg, M.E., Barres, B.A., and Stevens, B. (2012). Microglia sculpt postnatal neural circuits in an activity and complement-dependent manner. *Neuron* *74*, 691–705.

- Scott, A.F., Schmeckpeper, B.J., Abdelrazik, M., Comey, C.T., O'Hara, B., Rossiter, J.P., Cooley, T., Heath, P., Smith, K.D., and Margolet, L. (1987). Origin of the human L1 elements: proposed progenitor genes deduced from a consensus DNA sequence. *Genomics* *1*, 113–125.
- Scotter, E.L., Chen, H.-J., and Shaw, C.E. (2015). TDP-43 Proteinopathy and ALS: Insights into Disease Mechanisms and Therapeutic Targets. *Neurotherapeutics* *12*, 352–363.
- Shpyleva, S., Melnyk, S., Pavliv, O., Pogribny, I., and Jill James, S. (2018). Overexpression of LINE-1 Retrotransposons in Autism Brain. *Mol. Neurobiol.* *55*, 1740–1749.
- Siegler, M.V., and Jia, X.X. (1999). Engrailed negatively regulates the expression of cell adhesion molecules connectin and neuroglian in embryonic *Drosophila* nervous system. *Neuron* *22*, 265–276.
- Sienski, G., Dönertas, D., and Brennecke, J. (2012). Transcriptional silencing of transposons by Piwi and maelstrom and its impact on chromatin state and gene expression. *Cell* *151*, 964–980.
- Simeone, A. (2000). Positioning the isthmus organizer where Otx2 and Gbx2 meet. *Trends Genet.* *16*, 237–240.
- Simon, H.H., Saueressig, H., Wurst, W., Goulding, M.D., and O'Leary, D.D.M. (2001). Fate of Midbrain Dopaminergic Neurons Controlled by the Engrailed Genes. *J. Neurosci.* *21*, 3126–3134.
- Simon, M., Van Meter, M., Ablueva, J., Ke, Z., Gonzalez, R.S., Taguchi, T., De Cecco, M., Leonova, K.I., Kogan, V., Helfand, S.L., et al. (2019a). LINE1 Derepression in Aged Wild-Type and SIRT6-Deficient Mice Drives Inflammation. *Cell Metab.* *29*, 871-885.e5.
- Simon, M., Meter, M.V., Ablueva, J., Ke, Z., Gonzalez, R.S., Taguchi, T., Cecco, M.D., Leonova, K.I., Kogan, V., Helfand, S.L., et al. (2019b). LINE1 Derepression in Aged Wild-Type and SIRT6-Deficient Mice Drives Inflammation. *Cell Metabolism* *29*, 871-885.e5.
- Simpson, E.H., Winiger, V., Biezonski, D.K., Haq, I., Kandel, E.R., and Kellendonk, C. (2014). Selective overexpression of dopamine D3 receptors in the striatum disrupts motivation but not cognition. *Biol. Psychiatry* *76*, 823–831.
- Singer, T., McConnell, M.J., Marchetto, M.C.N., Coufal, N.G., and Gage, F.H. (2010). LINE-1 retrotransposons: mediators of somatic variation in neuronal genomes? *Trends Neurosci.* *33*, 345–354.
- Solano, P.J., Mugat, B., Martin, D., Girard, F., Huibant, J.-M., Ferraz, C., Jacq, B., Demaille, J., and Maschat, F. (2003). Genome-wide identification of in vivo *Drosophila* Engrailed-binding DNA fragments and related target genes. *Development* *130*, 1243–1254.
- Soltani, A., Lebrun, S., Carpentier, G., Zunino, G., Chantepie, S., Maïza, A., Bozzi, Y., Desnos, C., Darchen, F., and Stettler, O. (2017). Increased signaling by the autism-related Engrailed-2 protein enhances dendritic branching and spine density, alters synaptic structural matching, and exaggerates protein synthesis. *PLoS One* *12*.

- Sonnier, L., Le Pen, G., Hartmann, A., Bizot, J.-C., Trovero, F., Krebs, M.-O., and Prochiantz, A. (2007). Progressive loss of dopaminergic neurons in the ventral midbrain of adult mice heterozygote for *Engrailed1*. *J. Neurosci.* *27*, 1063–1071.
- Sorce, S., and Krause, K.-H. (2009). NOX Enzymes in the Central Nervous System: From Signaling to Disease. *Antioxidants & Redox Signaling* *11*, 2481–2504.
- Stefanis, L. (2012). α -Synuclein in Parkinson's Disease. *Cold Spring Harb Perspect Med* *2*.
- Stettler, O., Joshi, R.L., Wizenmann, A., Reingruber, J., Holcman, D., Bouillot, C., Castagner, F., Prochiantz, A., and Moya, K.L. (2012). *Engrailed* homeoprotein recruits the adenosine A1 receptor to potentiate ephrin A5 function in retinal growth cones. *Development* *139*, 215–224.
- Stuart, T., Eichten, S.R., Cahn, J., Karpievitch, Y.V., Borevitz, J.O., and Lister, R. Population scale mapping of transposable element diversity reveals links to gene regulation and epigenomic variation. *ELife* *5*.
- Suberbielle, E., Sanchez, P.E., Kravitz, A.V., Wang, X., Ho, K., Eilertson, K., Devidze, N., Kreitzer, A.C., and Mucke, L. (2013). Physiologic brain activity causes DNA double-strand breaks in neurons, with exacerbation by amyloid- β . *Nat. Neurosci.* *16*, 613–621.
- Sugiyama, S., Di Nardo, A.A., Aizawa, S., Matsuo, I., Volovitch, M., Prochiantz, A., and Hensch, T.K. (2008). Experience-dependent transfer of *Otx2* homeoprotein into the visual cortex activates postnatal plasticity. *Cell* *134*, 508–520.
- Sultana, T., van Essen, D., Siol, O., Bailly-Bechet, M., Philippe, C., Zine El Aabidine, A., Pioger, L., Nigumann, P., Saccani, S., Andrau, J.-C., et al. (2019). The Landscape of L1 Retrotransposons in the Human Genome Is Shaped by Pre-insertion Sequence Biases and Post-insertion Selection. *Molecular Cell* *74*, 555-570.e7.
- Tabuchi, K., and Südhof, T.C. (2002). Structure and evolution of neurexin genes: insight into the mechanism of alternative splicing. *Genomics* *79*, 849–859.
- Tagliaferro, P., and Burke, R.E. (2016). Retrograde Axonal Degeneration in Parkinson Disease. *J Parkinsons Dis* *6*, 1–15.
- Taira, T., Saito, Y., Niki, T., Iguchi-Arigo, S.M.M., Takahashi, K., and Ariga, H. (2004). DJ-1 has a role in antioxidative stress to prevent cell death. *EMBO Rep.* *5*, 213–218.
- Takeuchi, A., Iida, K., Tsubota, T., Hosokawa, M., Denawa, M., Brown, J.B., Ninomiya, K., Ito, M., Kimura, H., Abe, T., et al. (2018). Loss of *Sfpq* Causes Long-Gene Transcriptopathy in the Brain. *Cell Rep* *23*, 1326–1341.
- Taylor, M.S., Altukhov, I., Molloy, K.R., Mita, P., Jiang, H., Adney, E.M., Wudzinska, A., Badri, S., Ischenko, D., Eng, G., et al. (2018). Dissection of affinity captured LINE-1 macromolecular complexes. *ELife* *7*, e30094.
- Thomas, C.A., Tejwani, L., Trujillo, C.A., Negraes, P.D., Herai, R.H., Mesci, P., Macia, A., Crow, Y.J., and Muotri, A.R. (2017). Modeling of TREX1-dependent autoimmune disease using human stem cells highlights L1 accumulation as a source of neuroinflammation. *Cell Stem Cell* *21*, 319-331.e8.

- Thomas, M., White, R.L., and Davis, R.W. (1976). Hybridization of RNA to double-stranded DNA: formation of R-loops. *PNAS* *73*, 2294–2298.
- Thomasson, N., Pioli, E., Friedel, C., Monseur, A., Lavour, J., Moya, K.L., Bezard, E., Bousseau, A., and Prochiantz, A. (2019). Engrailed-1 induces long-lasting behavior benefit in an experimental Parkinson primate model. *Mov. Disord.*
- Thorén, P.E.G., Persson, D., Karlsson, M., and Nordén, B. (2000). The Antennapedia peptide penetratin translocates across lipid bilayers – the first direct observation. *FEBS Letters* *482*, 265–268.
- Tichý, A., Vávrová, J., Pejchal, J., and Rezáčová, M. (2010). Ataxia-telangiectasia mutated kinase (ATM) as a central regulator of radiation-induced DNA damage response. *Acta Medica (Hradec Kralove)* *53*, 13–17.
- Tolkunova, E.N., Fujioka, M., Kobayashi, M., Deka, D., and Jaynes, J.B. (1998). Two Distinct Types of Repression Domain in Engrailed: One Interacts with the Groucho Corepressor and Is Preferentially Active on Integrated Target Genes. *Mol Cell Biol* *18*, 2804–2814.
- Tóth, K.F., Pezic, D., Stuwe, E., and Webster, A. (2016). The piRNA Pathway Guards the Germline Genome Against Transposable Elements. *Adv Exp Med Biol* *886*, 51–77.
- Trizzino, M., Park, Y., Holsbach-Beltrame, M., Aracena, K., Mika, K., Caliskan, M., Perry, G.H., Lynch, V.J., and Brown, C.D. (2017). Transposable elements are the primary source of novelty in primate gene regulation. *Genome Res.* *27*, 1623–1633.
- Trizzino, M., Kapusta, A., and Brown, C.D. (2018). Transposable elements generate regulatory novelty in a tissue-specific fashion. *BioRxiv* 268771.
- Tsurumi, A., and Li, W. (2012). Global heterochromatin loss. *Epigenetics* *7*, 680–688.
- Upton, K.R., Gerhardt, D.J., Jesuadian, J.S., Richardson, S.R., Sánchez-Luque, F.J., Bodea, G.O., Ewing, A.D., Salvador-Palomeque, C., van der Knaap, M.S., Brennan, P.M., et al. (2015). Ubiquitous L1 Mosaicism in Hippocampal Neurons. *Cell* *161*, 228–239.
- Vaags, A.K., Lionel, A.C., Sato, D., Goodenberger, M., Stein, Q.P., Curran, S., Ogilvie, C., Ahn, J.W., Drmic, I., Senman, L., et al. (2012). Rare deletions at the neurexin 3 locus in autism spectrum disorder. *Am. J. Hum. Genet.* *90*, 133–141.
- Van Meter, M., Kashyap, M., Rezazadeh, S., Geneva, A.J., Morello, T.D., Seluanov, A., and Gorbunova, V. (2014). SIRT6 represses LINE1 retrotransposons by ribosylating KAP1 but this repression fails with stress and age. *Nat Commun* *5*, 5011.
- Villeponteau, B. (1997). The heterochromatin loss model of aging. *Exp. Gerontol.* *32*, 383–394.
- Volkow, N.D., Fowler, J.S., Wang, G.-J., Swanson, J.M., and Telang, F. (2007). Dopamine in Drug Abuse and Addiction: Results of Imaging Studies and Treatment Implications. *Arch Neurol* *64*, 1575–1579.
- Vyjayanti, V.N., and Rao, K.S. (2006). DNA double strand break repair in brain: reduced NHEJ activity in aging rat neurons. *Neurosci. Lett.* *393*, 18–22.

- Wang, L., Jia, M., Yue, W., Tang, F., Qu, M., Ruan, Y., Lu, T., Zhang, H., Yan, H., Liu, J., et al. (2008). Association of the ENGRAILED 2 (EN2) gene with autism in Chinese Han population. *Am. J. Med. Genet. B Neuropsychiatr. Genet.* *147B*, 434–438.
- Winter, N., Kollwig, G., Zhang, S., and Kragler, F. (2007). MPB2C, a microtubule-associated protein, regulates non-cell-autonomy of the homeodomain protein KNOTTED1. *Plant Cell* *19*, 3001–3018.
- Wizenmann, A., Brunet, I., Lam, J., Sonnier, L., Beurdeley, M., Zarbalis, K., Weisenhorn-Vogt, D., Weinl, C., Dwivedy, A., Joliot, A., et al. (2009a). Extracellular Engrailed participates in the topographic guidance of retinal axons in vivo. *Neuron* *64*, 355–366.
- Wizenmann, A., Brunet, I., Lam, J., Sonnier, L., Beurdeley, M., Zarbalis, K., Weisenhorn-Vogt, D., Weinl, C., Dwivedy, A., Joliot, A., et al. (2009b). Extracellular Engrailed participates in the topographic guidance of retinal axons in vivo. *Neuron* *64*, 355–366.
- Wood, J.G., Jones, B.C., Jiang, N., Chang, C., Hosier, S., Wickremesinghe, P., Garcia, M., Hartnett, D.A., Burhenn, L., Neretti, N., et al. (2016). Chromatin-modifying genetic interventions suppress age-associated transposable element activation and extend life span in *Drosophila*. *Proc. Natl. Acad. Sci. U.S.A.* *113*, 11277–11282.
- Worman, H.J. (2012). Nuclear lamins and laminopathies. *The Journal of Pathology* *226*, 316–325.
- Wurst, W., and Bally-Cuif, L. (2001). Neural plate patterning: upstream and downstream of the isthmic organizer. *Nat. Rev. Neurosci.* *2*, 99–108.
- Wurst, W., Auerbach, A.B., and Joyner, A.L. (1994). Multiple developmental defects in Engrailed-1 mutant mice: an early mid-hindbrain deletion and patterning defects in forelimbs and sternum. *Development* *120*, 2065–2075.
- Yan, Z., Hu, H.Y., Jiang, X., Maierhofer, V., Neb, E., He, L., Hu, Y., Hu, H., Li, N., Chen, W., et al. (2011). Widespread expression of piRNA-like molecules in somatic tissues. *Nucleic Acids Res.* *39*, 6596–6607.
- Yang, F., and Wang, P.J. (2016). Multiple LINEs of retrotransposon silencing mechanisms in the mammalian germline. *Semin. Cell Dev. Biol.* *59*, 118–125.
- Yang, P., Lung, F.-W., Jong, Y.-J., Hsieh, H.-Y., Liang, C.-L., and Juo, S.-H.H. (2008). Association of the homeobox transcription factor gene ENGRAILED 2 with autistic disorder in Chinese children. *Neuropsychobiology* *57*, 3–8.
- Yoon, B.C., Jung, H., Dwivedy, A., O’Hare, C.M., Zivraj, K.H., and Holt, C.E. (2012). Local Translation of Extranuclear Lamin B Promotes Axon Maintenance. *Cell* *148*, 752–764.
- Zarei, S., Carr, K., Reiley, L., Diaz, K., Guerra, O., Altamirano, P.F., Pagani, W., Lodin, D., Orozco, G., and Chinaea, A. (2015). A comprehensive review of amyotrophic lateral sclerosis. *Surg Neurol Int* *6*.
- Zhao, K., Du, J., Han, X., Goodier, J.L., Li, P., Zhou, X., Wei, W., Evans, S.L., Li, L., Zhang, W., et al. (2013). Modulation of LINE-1 and Alu/SVA retrotransposition by Aicardi-Goutières syndrome-related SAMHD1. *Cell Rep* *4*, 1108–1115.

Zheng, J.-J., Li, W.-X., Liu, J.-Q., Guo, Y.-C., Wang, Q., Li, G.-H., Dai, S.-X., and Huang, J.-F. (2018). Low expression of aging-related NRXN3 is associated with Alzheimer disease. *Medicine (Baltimore)* 97.

ZHOU, C., HUANG, Y., and PRZEDBORSKI, S. (2008). Oxidative Stress in Parkinson's Disease: A Mechanism of Pathogenic and Therapeutic Significance. *Ann N Y Acad Sci* 1147, 93–104.

Zylka, M.J., Simon, J.M., and Philpot, B.D. (2015). Gene length matters in neurons. *Neuron* 86, 353–355.

An alternative splicing switch shapes neurexin repertoires in principal neurons versus interneurons in the mouse hippocampus | eLife.